

**ELUCIDATION OF UNDERLYING MOLECULAR  
MECHANISMS INVOLVED IN BISPHENOL A  
INDUCED CARDIOTOXICITY AND NEUROTOXICITY**



By

**AYESHA ISHTIAQ**

**Department of Biochemistry**

**Faculty of Biological Sciences**

**Quaid-i-Azam University**

**Islamabad, Pakistan**

**2024**

# **Elucidation of Underlying Molecular Mechanisms Involved in Bisphenol A Induced Cardiotoxicity and Neurotoxicity**



A dissertation submitted in the fulfillment of requirements for the

**Degree of Doctorate of Philosophy In  
Biochemistry/ Molecular Biology**

By

**Ayesha Ishtiaq**

Department of Biochemistry  
Faculty of Biological Sciences  
Quaid-i-Azam University  
Islamabad, Pakistan

2024

## **DECLARATION**

I hereby declare that the work presented in the following thesis is my own effort, except where otherwise acknowledged and that thesis is my own composition. No part of this thesis has been previously presented for any other degree.



**Ayesha Ishtiaq**

## **Author's Declaration**

I **Ayesha Ishtiaq** hereby state that my PhD thesis, *titled* **“Elucidation of Underlying Molecular Mechanisms Involved in Bisphenol A Induced Cardiotoxicity and Neurotoxicity”** is my own work and has not been submitted previously by me for taking any degree from **Department of Biochemistry, Faculty of Biological Sciences, Quaid-i-Azam University, Islamabad, Pakistan.**

Or anywhere else in the country/world.

At any time if my statement is found to be incorrect even after my graduation, the University has the right to withdraw my Ph.D degree.

Student/Author Signature:



**Ms. Ayesha Ishtiaq**  
**Date: August 1, 2024**

## Plagiarism Undertaking

I solemnly declare that research work presented in the PhD thesis, titled **“Elucidation of Underlying Molecular Mechanisms Involved in Bisphenol A Induced Cardiotoxicity and Neurotoxicity”** is solely my research work with no significant contribution from any other person. Small contribution/help wherever taken has been duly acknowledged and that complete thesis has been written by me.

I understand the zero-tolerance policy of the HEC and **Quaid-i-Azam University, Islamabad**, towards the plagiarism. Therefore, I as an Author of the above titled thesis declare that no portion of my thesis has been plagiarized and any material used as reference is properly referred/cited.

I undertake that if I am found guilty of any formal plagiarism in the above titled thesis even after award of PhD degree, the University reserves the right to withdraw/revoke my PhD degree and that HEC and the University has the right to publish my name on the HEC/University website on which names of students are placed who submitted plagiarized thesis.

Student/Author Signature: \_\_\_\_\_

  
**Ms. Ayesha Ishtiaq**  
**Date: August 1, 2024**

# Certificate of Approval

This is to certify that the research work presented in this thesis, entitled: “**Elucidation of Underlying Molecular Mechanisms Involved in Bisphenol A Induced Cardiotoxicity and Neurotoxicity**” was conducted by **Ms. Ayesha Ishtiaq** under the supervision of Prof. Dr. Iram Murtaza.

No part of this thesis has been submitted anywhere else for any other degree. This thesis is submitted to the Department of Biochemistry, Faculty of Biological Sciences, Quaid-i-Azam University, Islamabad, Pakistan in partial fulfillment of the requirements for the **Degree of Doctor of Philosophy** in the field of Biochemistry from Department of Biochemistry, Faculty of Biological Sciences, Quaid-i-Azam University, Islamabad, Pakistan.

**Ms. Ayesha Ishtiaq**

Signature: 

**Examination Committee:**


**1. External Examiner:**

**Prof. Dr. Shahid Mehmood Baig**  
Dean Life Sciences  
Health Services Academy,  
Ministry of Health Services  
Government of Pakistan Islamabad

Signature: 

**2. External Examiner:**

**Prof. Dr. Ishrat Jabeen**  
Research Center for Modeling and Simulation  
National University of Sciences and Technology  
(NUST), Islamabad

Signature: 

**3. Supervisor:**

**Prof. Dr. Iram Murtaza**

Signature: 

**4. Chairperson:**

**Prof. Dr. Iram Murtaza**

Signature: 

**Dated:**

**01-08-2024**

بِسْمِ اللَّهِ الرَّحْمَنِ الرَّحِيمِ

*Dedicated to my Loving  
Parents*



---

**TABLE OF CONTENTS**

ACKNOWLEDGEMENTS.....	i
LIST OF ABBREVIATIONS.....	iii
LIST OF TABLES.....	vii
LIST OF FIGURES.....	viii
ABSTRACT.....	xvi
1.INTRODUCTION.....	1
1.1. BPA as Environmental Toxicant.....	2
1.2. BPA: Characteristic and Metabolism.....	2
1.3. BPA toxicity.....	5
1.3.1. Cardiotoxicity.....	6
1.3.2. Neurotoxicity.....	9
1.4. BPA role in Oxidative stress.....	10
1.5. Stress responsive factors.....	11
1.5.1. p53.....	11
1.5.2. p53-upregulated modulator of apoptosis.....	12
1.5.3. Dynamin-related protein 1.....	12
1.5.4. Ubc13.....	13
1.5.5. USP7.....	14
1.5.6. CDIP1.....	16
1.5.7. BNIP3.....	17
1.5.8. PKC- $\delta$ .....	18
1.5.9. B cell lymphoma 2.....	18
1.5.10. Mitofusin 2.....	18
1.5.11. Regulation of Bcl2 and Mfn2.....	20
1.6. Micro-RNAs.....	21
1.6.1 Micro RNAs Biogenesis and Mechanism of Action.....	21
1.6.2 Role of miRNA in Different Pathologies.....	23
1.6.3 Role of miRNAs in cardiovascular disease.....	25
1.6.4 miRNA-15a-5p.....	26
1.6.5. miRNA-214-3p.....	27
1.7. Therapeutic Strategies.....	27
1.8. Antioxidant therapies.....	28
1.8.1 Antioxidant Therapy by Melatonin.....	28

---

1.8.2 Antioxidant Therapy by N-acetyl cystine .....	31
1.9 Tetra-aniline based Synthetic polymers .....	32
1.10 <i>Pistacia integerrima</i> .....	33
1.10.1. Ethnobotany .....	34
1.10.2. Biological Activities of <i>Pistacia integerrima</i> .....	34
1.11 Cancer .....	36
1.12 Breast Cancer .....	36
1.13 Worldwide Prevalence of Breast Cancer .....	37
1.14 Global Breast Cancer Related Mortality .....	37
1.15 Breast Cancer Prevalence in Pakistan .....	37
1.16 Categories of Breast Cancer .....	38
1.17 Risk Factors for Breast Cancer .....	38
1.18 BPA and Risk of Breast Cancer .....	39
1.19 Cross-talk between Tp53, WNT1 and ZEB1 Signaling Pathways .....	39
AIMS AND OBJECTIVES .....	41
2.1 Plant collection and identification .....	42
2.1.1 Preparation of methanolic extract of <i>Pistacia integerrima</i> galls .....	42
2.2 Ethical Consideration for Animal Model .....	42
2.3 Study Design .....	42
2.3 Dissection and tissue collection .....	44
2.4 Ethical Approval for human sample collection .....	44
2.5 Human Sample Collection and storage .....	44
2.6 Tissue homogenization .....	45
2.6.1 RIPA Lysis Buffer .....	45
2.7 mRNA/miRNA expression analysis .....	45
2.7.1 RNA extraction .....	45
2.7.2 cDNA synthesis .....	46
2.7.3 Primer Designing .....	47
2.7.4 Quantitative real-time PCR analysis .....	50
2.8 Protein quantification assay .....	51
2.9 Western blotting .....	52
2.9.1 Casting of SDS-PAGE gel .....	52
2.9.2 SDS-PAGE .....	53
2.9.3 Staining of gel .....	55
2.9.4 Gel transfer to nitrocellulose membrane .....	55

---

2.9.5 Blocking.....	56
2.9.6 Incubation with antibodies.....	56
2.9.7 Band detection .....	57
2.10 Oxidative profile .....	57
2.10.1 Reactive oxygen species (ROS) assay .....	57
2.10.2 Thiobarbituric acid reactive substances (TBARs) assay .....	59
2.11 Anti-Oxidative Profile .....	60
2.11.1 Super oxide dismutase (SOD) assay .....	60
2.11.2 Catalase activity (CAT) assay.....	60
2.11.3 Peroxidase (POD) assay.....	61
2.11.4 Ascorbate peroxidase assay .....	62
2.11.5 Reduced glutathione assay .....	62
2.12 Lipid profile analysis .....	63
2.12.1 Cholesterol assay .....	63
2.12.2 Triglycerides assay.....	64
2.13 Liver function analysis.....	64
2.13.1 Alanine aminotransferase (ALT) assay .....	64
2.13.2 Aspartate aminotransferase (AST) assay .....	65
2.14 Histological analysis .....	66
2.14.1 Microtomy.....	66
2.14.2 Microscopic Analysis.....	67
2.15 High performance liquid chromatography-UV (HPLC-UV) analysis.....	67
2.15.1 HPLC mobile phase buffer preparation .....	67
2.15.2 High performance liquid chromatography-UV (HPLC).....	67
2.16 Molecular docking .....	68
2.17 Molecular Dynamics simulation assay .....	68
2.18 Statistical analysis.....	70
3. RESULTS .....	71
3.1 Effect of <i>Pistacia integerrima</i> on baseline characteristics of experimental animals .....	71
3.2 Effect of <i>Pistacia integerrima</i> on cellular architecture .....	72
3.3 Effect of <i>Pistacia integerrima</i> on different biochemical parameters.....	74
3.3.1. Effect of <i>Pistacia integerrima</i> on oxidative profiling.....	74
3.3.2. Effect of <i>Pistacia Integerrima</i> on liver markers .....	76
3.3.3. Effect of <i>Pistacia integerrima</i> on lipid profile at blood peripheral level.....	76

---

3.3.4 Effect of <i>Pistacia integerrima</i> on Serum uric acid and kidney toxicity .....	77
3.3.5 Effect of <i>Pistacia integerrima</i> on serum glucose level.....	78
3.3.6 Antioxidant potential of <i>Pistacia integerrima</i> gall extract .....	79
3.4 Antiapoptotic potential of <i>Pistacia integerrima</i> ; effect on different apoptosis modulators in p53 mediated apoptosis.....	81
3.5 Baseline Characteristics of Experimental Groups .....	84
3.5.1 Dose Dependent Response of BPA on Body Weight .....	84
3.5.2 Dose Dependent Effect of BPA on Heart .....	85
3.6 Effect of <i>Pistacia integerrima</i> on the levels of different oxidative stress markers	86
3.6.1 Estimation of ROS level in serum, heart samples.....	86
3.6.2 Estimation of TBARs level in serum, and heart samples .....	87
3.6.3 Analysis of SOD Activity in serum, and heart samples.....	88
3.6.4 Evaluation of catalase activity in serum and heart tissue .....	88
3.6.5 Evaluation of Ascorbate peroxidase level in serum and heart tissues .....	89
3.7 Histological Analysis .....	90
3.8 Effect of <i>Pistacia integerrima</i> on the expression of p53 and its mediators in BPA-induced apoptosis.....	92
3.8.1 mRNA Expression Analysis of p53 in Heart Tissues.....	92
3.8.2 mRNA Expression Analysis of PUMA in Heart Tissues .....	93
3.8.3 mRNA Expression Analysis of Drp1 in Heart Tissues.....	94
3.8.4 Relative Expression of USP7 in Heart Tissue of Experimental Groups.....	94
3.8.5 mRNA Expression analysis of cytochrome c .....	95
3.9 Effect of <i>Pistacia integerrima</i> on the of miR-15a-5p and its target genes .....	95
3.9.1 Expression analysis of miRNA-15a-5p .....	96
3.9.2 Expression Analysis of mRNA of Bcl2 .....	97
3.9.3 Expression Analysis of mRNA of Mfn2.....	98
3.10 Effect of <i>Pistacia integerrima</i> on the expression of miRNA-214-3p and its target genes .....	99
3.10.1 Relative Expression of miRNA-214 in Heart Tissue.....	99
3.10.2 Relative Expression of CDIP1 in Heart Tissue of Experimental Groups...	100
3.10.3 mRNA Expression Analysis of BNIP3 in Heart Tissues.....	101
3.10.4 mRNA Expression Analysis of PKC- $\delta$ in Heart Tissues.....	102
3.11 Effect of <i>Pistacia integerrima</i> on p53 protein and its downstream targets .....	103
3.11.1 Expression of p53 Protein in Experimental Heart Tissues .....	103
3.11.2 Expression of P-p53 Protein in Experimental Heart Tissues.....	103
3.11.3 Expression of PUMA Protein in Experimental Heart Tissues.....	104

---

3.11.4 Expression of Drp1 Protein in Experimental Heart Tissues .....	104
3.11.5 Expression of Cytochrome C Protein in Experimental Heart Tissues .....	104
3.12 Effect of miRNA-15a-5p regulation on the protein expression of its target genes .....	107
EFFECT OF BPA ON NEUROTOXICITY .....	109
3.13 Experimental animal baseline characteristics .....	109
3.14 Melatonin alleviated BPA-induced cellular damage .....	110
3.15 Melatonin abolished BPA-induced oxidative stress .....	112
3.16 Melatonin reduced BPA-induced p53 activity.....	115
3.17 Melatonin alleviated BPA-induced toxicity <i>via</i> PUMA and Drp-1 signaling ...	116
3.18 Melatonin regulated BPA-induced expression of miRNA-214-3p and its target genes .....	122
3.19 Melatonin reduced expression of miRNA-15a-5p and its target genes .....	125
3.20 <i>Pistacia integerrima</i> regulated BPA-induced expression of miRNA-214-3p and its target genes.....	127
3.21 <i>Pistacia integerrima</i> normalized BPA-induced expression of miRNA-15a-5p and its target genes.....	130
3.22 Molecular docking studies of Es-37 and Ls-37 with proteins; Bcl-2, p53 and cytochrome c .....	132
3.23 Molecular dynamic simulation analysis.....	137
3.24 RMSD and RMSF analysis for stability and flexibility prediction.....	137
3.25 Es-37 and L-37 abolished BPA induced disturbed cellular architecture .....	139
3.26 Es-37 and L-37 abated BPA induced miRNA-15a-5p and target gene expression .....	140
3.27 Es-37 and L-37 alleviated the BPA induced p53 and cytochrome c expression	143
3.28 Es-37 and L-37 scavenged the BPA-generated free radicals.....	143
3.29 Es-37 and L-37 enhanced the antioxidant enzyme activities.....	146
3.30 Es-37 and L-37 normalized the BPA induced cellular damage markers .....	146
3.31 Demographic and clinical characters of breast cancer patients .....	151
3.32 Analysis of Bisphenol A (BPA) Concentration .....	153
3.33 Redox profiling of breast cancer samples .....	153
3.34 Expression analysis of p53 and linked markers in breast cancer samples.....	154
3.35 Histological Analysis of Breast Cancer Tissue Samples .....	154
4. DISCUSSION.....	158
Funding Source/Acknowledgments:.....	174
Publications.....	175

5. REFERENCES ..... 178

## ACKNOWLEDGEMENTS

Praise is to Allah, the Cherisher and Sustainer of the worlds, who showered His countless blessings upon us. **Almighty Allah** enabled me to compile my humble endeavors in the shape of this thesis. All respect goes to the **Holy Prophet Hazrat Muhammad (PBUH)** whose teachings strengthened our faith in Allah, who is the source of knowledge and wisdom for the entire humanity, who clarified that the pursuit of knowledge is a divine commandment.

I would like to extend my sincere gratitude my dignified and respectable supervisor and Chairperson, **Dr. Iram Murtaza**, for her affectionate supervision, inspiring attitude, masterly advice, and encouragement, and for providing me with all the privileges during my research work. Her expertise, valuable suggestions and patience added considerably to my experience and enabled me to complete this research project. I tender my thanks to **Dr. M. Ansar**, Ex-Chairperson, and all Honorable Teachers of the Department of Biochemistry, Quaid-i-Azam University, Islamabad for providing the research facilities of the department and guidance to accomplish this work.

I feel pride in extending my vehement sense of gratitude and sincere feelings of reverence and regard to **Dr. Hussain Mustatab Wahedi** for his continuous help, support, cooperation, guidance and advice throughout my experiment. His family-like support, care and scholarly suggestions can never be repaid.

I pay special thanks to my laboratory seniors and friends; specially Dr. Tahir Ali, Dr. Muhammad Ishtiaq Jan, Dr. Sobia Mushtaq, Dr. Iram Mushtaq, Khadam Hussain, Mehmand Khan, and all my lab juniors for their intense practical help and valuable suggestions throughout my research work. I will always cherish the sweetest memories and practical support from all my fellows and friends. Words can never express the company of my friends and colleagues for their kind support and guidance.

Words fail to express the intensity of my gratitude to my loving **Mama and Papa** whose prayers and inspiration gave me the courage to dream high and opened avenues for me to explore my abilities. My sweet and loving Mother like Aunt whose self-sacrificing love will always be cherished but can never be repaid. I wish to express my heartiest

and warmest thanks to my beloved Siblings **Ahsan Ishtiaq, Mahnoor Ishtiaq, and Mohsin Ishtiaq** for their unconditional love.

I would also like to acknowledge the clerical staff of the Department of Biochemistry, especially **Mr. Tariq, Mr. Shehzad** and **Mr. Fayaz** for their cooperation during my study. Lastly, I offer my regards and blessings to all who supported me in any respect during the completion of this thesis.

May Allah bless them all.

*Ayesha Ishtiaq*



**LIST OF ABBREVIATIONS**

<b>Abbreviations</b>	<b>Full name</b>
%	Percentage
µg	Micro gram
µl	Microliter
AMP	Adenosine monophosphate
ANOVA	Analysis of variance
APAF-1	Apoptosis peptidase activating factor 1
ARC	Activity-regulated cytoskeleton-associated protein
ATM	Ataxia-Telangiectasia mutated
BAK	Bcl-2-homologous antagonist/killer
Bax	BCL-2 associated X protein
BAX	Bcl-2 associated X protein
BBC3	Bcl-2 binding component 3
BCIP	5-Bromo-4-chloro-3-indolyl phosphate
Bcl-2	B-cell lymphoma 2
BNIP3	BCL-2 19 kDa interacting protein
bp	Base pair
BPA	Bisphenol A
BSA	Bovine serum albumin
Ca <sup>2+</sup>	Calcium ion
CAMK II	Calcium/calmodulin-dependent protein kinase II
CCl <sub>4</sub>	Carbon tetrachloride
CD95	Cluster of differentiation 95
cDNA	Complimentary deoxyribonucleic acid
Cyt c	Cytochrome c
DMSO	Dimethyl sulfoxide
DNA	Deoxyribonucleic acid
dNTPs	Deoxynucleotide triphosphates
Drp1	Dynamin related protein 1

DTNB	5,5'-dithiobis-2-nitrobenzoic acid
ERK	Extracellular-regulated protein kinase
ER $\alpha$	Estrogen receptor alpha
Fis1	Mitochondrial fission protein 1
GAPDH	Glyceraldehyde 3-phosphate dehydrogenase
GPER	G protein-coupled estrogen receptor
GSK3 $\beta$	Glycogen synthase kinase 3 beta
GTP	Guanosine triphosphate
HCl	Hydrochloric acid
HIF-1	Hypoxia inducing factor-1
IAP	Inhibitor of apoptosis
IgG	Immunoglobulin G
JNK	c-Jun N-terminal kinase
KCl	Potassium chloride
kg	Kilo gram
KH <sub>2</sub> PO <sub>4</sub>	Monopotassium phosphate
LC3 II	Light chain 3 II
MAPK	Mitogen activated protein kinase
Mff	Mitochondrial fission factor
Mfn2	Mitofusin
mg	Milligram
MgCl <sub>2</sub>	Magnesium chloride
MiD49	Mitochondrial dynamic protein 49
MiD51	Mitochondrial dynamic protein 51
miRNA	MicroRNA
Mix	Mixture
ml	Milliliter
mM	Millimolar
Mst-1	Macrophage-stimulating 1
Mel	Melatonin

---

MLT	Melatonin
MRM	Modified radical mastectomy
Na <sub>2</sub> HPO <sub>4</sub>	Disodium phosphate
NaN <sub>3</sub>	Sodium azide
NBT	Nitro blue tetrazolium
NMDA	N-methyl-D-aspartate
NO	Nitric oxide
NOXA	NADPH oxidase activator
°C	Degree centigrade
P.i	<i>Pistacia integerrima</i>
P38 MAPK	Protein kinases and the 38-kDa mitogen activated protein kinase
PBS	Phosphate buffer saline
PBST	Phosphate buffer saline-Tween
PCBs	Polychlorinated biphenyls
PCOS	Polycystic ovary syndrome
PCR	Polymerase chain reaction
PKA	Protein kinase A
PKC- $\delta$	Protein kinase C delta
PMSF	Phenyl methyl sulfonyl fluoride
PTEN	Phosphatase and tensin homolog
PUMA	The P53 upregulated modulator of apoptosis
<i>p-value</i>	Probability value
qRT-PCR	Quantitative real time polymerase chain reaction
Raf	Rapidly accelerated fibrosarcoma
Ras	Rat sarcoma
RNA	Ribonucleic acid
ROS	Reactive oxygen species
rpm	Revolutions per minute
RyR	Ryanodine receptor
SDS	Sodium dodecyl sulphate

SIRT1	Sirtuin 1
SR	Sarcoplasmic reticulum
TP53	Tumor protein 53
TNBC	Triple negative breast cancer
UV	Ultraviolet
WHO	World Health Organization
Wnt	Wingless/integrated
WWF	World Wide Fund for Nature
ZEB1	Zinc finger E-box binding protein 1

## **LIST OF TABLES**

S. No.	Title	Page No.
2.1	List of Primers	49
2.2	List of Antibodies	57
3.1	Effect of BPA on organ weights of different experimental	72
3.2	Binding Energies obtained from nine docking runs of L-37 and Es-37 oligomers with Bcl-2, cytochrome c, and p53	134
3.3	Bonding interactions of L-37 and Es-37 oligomers with amino acid residues of Bcl-2, cytochrome c, and p53	134
3.4	Demographical and clinical characters of breast cancer patients	152

## LIST OF FIGURES

Figure 1.1 Chemical structure of BPA (Midoro-Horiuti and Goldblum 2017).....	3
Figure.1.2. Production of ROS in mitochondria (Shirani, Alizadeh et al. 2019).....	3
Figure 1.3. BPA Metabolism in liver (Mattison, Karyakina et al. 2014) .....	4
Figure 1.4. Diseases caused by the BPA (Ryu, Rahman et al. 2017) .....	6
Figure 1.5. ROS mediated cardiomyocytes apoptosis (Iacobazzi, Suleiman et al. 2016) .....	7
Figure.1.6.BPA mediated neuro-apoptosis (Lee, Suk et al. 2008) .....	10
Figure 1.7. P53 induced apoptotic pathway (Chen et al., 2013).....	11
Figure 1.8. Mitochondrial fragmentation by Drp1 (Boland, Chourasia et al. 2013) ....	12
Figure 1.9. Possible Interactions between HAUSP, P53 and MDM2 adapted from (Brooks et al., 2007).....	15
Figure 1.10. Role of CDIP 1 in apoptosis adapted from (Namba, Tian et al. 2013) ...	16
Figure 1.11. BNIP3 induced mitochondrial apoptosis {Chinnadurai, 2008 #108) (Chinnadurai et al., 2009) .....	17
Figure 1.12. Mitochondrial fission and fusion (Sheridan and Martin 2010) .....	19
Figure 1.13. Biosynthesis of miRNA (Vrijens, Bollati et al. 2015).....	22
Figure 1.14. Role of miRNAs in different cellular processes (Cao, Yu et al. 2016) ...	24
Figure 1.15. Chemical structure of Melatonin (5-methoxy-N-acetyltryptamine) (Hardeland, Pandi-Perumal et al. 2006).....	28
Figure 1.16. Synthesis of Melatonin (Srinivasan, Zakaria et al. 2012) .....	29
Figure 1.17. Physiological function of Melatonin (Garrido, Terron et al. 2013) .....	30
Figure 1.18. Chemical Structure of Synthetic polymers.....	33
Figure 1.19. Gall of Pistacia integerrima (Shuaib, Ali et al. 2017) .....	33
Figure 1.20. Schematic diagram of biological activities of Pistacia integerrima (Bibi, Zia et al. 2015). .....	35
Figure 1.21. BPA modulated signaling pathways adapted from (Bouskine, Nebout et al. 2009) (Kumar, Sharma et al. 2015) .....	41
Figure 2.22 Schematic diagram of the study design .....	43
Figure 2. 23. Standard curve of BSA for protein quantification, x-axis and y-axis depict the different concentrations of BSA and absorbance respectively.....	52
Figure 2.24. Standard curve for ROS assay, the x-axis and y-axis depict the different concentrations of H <sub>2</sub> O <sub>2</sub> and absorbance respectively .....	58
Figure 3.25. Effect of Pistacia integerrima on cellular architecture a–f representative images of H&E staining of the heart tissues; a NS, b BPA, c P.I, d BPA + P.I, e Mel, f BPA + Mel, g–l representative images of H&E staining of the liver tissues; g NS, h BPA, i. P.I, j BPA + P.I, k Mel, l BPA + Mel, m–r representative images of H&E staining of the kidney tissues; m NS, n BPA, o P.I, p BPA + P.I, q Mel, r BPA + Mel, (red arrows are indicating normal cells, black arrows are indicating increased number of nuclei, whereas arrow heads are used to show abnormal cells, images taken at 40X, scale bar 100µm), s graphical representation of percentage abnormal cells in H&E stained heart, liver and kidney tissues. “***p < 0.001 in comparison to normal control (NS), #p < 0.01 in comparison to disease control (BPA)” .....	74
Figure 3.26. Effect of Pistacia integerrima on ROS level, “***p < 0.001, in comparison to normal control (NS), #p < 0.01 in comparison to disease control (BPA)” .....	75

Figure 3.27. Effect of Pistacia integerrima on TBARs level in heart, kidney and liver samples. “**p < 0.001, in comparison to normal control (NS), #p < 0.01 in comparison to disease control (BPA)”	75
Figure 3.28. Effect of Pistacia integerrima on liver markers Estimation of liver marker enzymes ALT, AST and ALP In serum samples of different experimental groups, “**p < 0.01, *p < 0.01 in comparison to normal control (NS)”	76
Figure 3.29. Effect of Pistacia integerrima on lipid profile Estimation of cholesterol, triglycerides and HDL in serum samples of different experimental groups. “**p < 0.001 in comparison to normal control (NS), #p < 0.01 in comparison to disease control (BPA)”	77
Figure 3.30. Estimation of uric acid levels in experimental groups. The data plotted as “mean ± SD, **p < 0.001 in comparison to normal control (NS), #p < 0.01 in comparison to disease control (BPA)”	78
Figure 3.31. Estimation of blood glucose levels in different experimental groups. The data plotted as “mean ± SD, **p < 0.001 in comparison to normal control (NS), #p < 0.01 in comparison to disease control (BPA)”	78
Figure 3.32. Antioxidant potential of Pistacia integerrima gall extract a Estimation of SOD activity in heart, liver and kidney homogenates of different experimental groups b Estimation of SOD activity in serum samples. “The data plotted as mean ± SD, **p < 0.001 in in comparison to NS, #p < 0.01 in comparison to disease control (BPA)”	79
Figure 3.33. Antioxidant potential of Pistacia integerrima gall extract, a Estimation of CAT activity in heart, liver and kidney tissues, b Estimation of APX activity in heart liver and kidney tissues c Estimation of GSH activity in heart, liver and kidney tissues, d Estimation of POD activity in heart, liver and kidney tissues, e Estimation of CAT, POD, APX and GSH activity in serum. “**p < 0.001 in comparison to normal control (NS), #p < 0.01 in comparison to disease control (BPA)”	80
Figure 3.34. Antiapoptotic potential of Pistacia integerrima gall extract a Estimation of relative RNA expression of Ubc-13, b Estimation of relative RNA expression of p53, c Estimation of relative RNA expression of Drp1, d Estimation of relative RNA expression of PUMA. GAPDH was used as the reference gene “*p < 0.01, **p < 0.001”	81
Figure 3.35. Evaluation of Antiapoptotic potential of Pistacia integerrima a Representative image of the western blot for Drp1, P-p53, PUMA, p53, cytochrome C (Cyto c), Ubc13 and GAPDH proteins in heart tissues, b Graphical representation of the densitometric analysis of Ubc13, normalized by GAPDH in heart tissues, g graphical representation of the densitometric analysis of P-p53, normalized by GAPDH in heart tissues, h graphical representation of the densitometric analysis of p53, normalized by GAPDH in heart tissues, i graphical representation of the densitometric analysis of Drp1, normalized by GAPDH in heart tissues, j graphical representation of the densitometric analysis of PUMA, normalized by GAPDH in heart tissues, k graphical representation of the densitometric analysis of cytochrome C (Cyto c), normalized by GAPDH in heart tissues. “The data plotted as mean ± SD, *p < 0.01 **p < 0.001”	83
Figure 3.36. Estimation of daily body weight of all experimental groups (* BPA 2 is significant in comparison to control, @ BPA 3 is significant in comparison to control,	

# BPA2+MLT and BPA3+MLT are significant in comparison to disease group, \$ BPA2+P.I and BPA3+P.I are significant in comparison to disease group).....	84
Figure 3.37. Estimation of change in body weight “**/## shows p value < 0.01”.....	85
Figure 3.38. Estimation of heart weight to body weight ratio “* shows p value < 0.05, **/## shows p value < 0.01”.....	86
Figure 3.39. Estimation of ROS levels in different experimental groups “**/## shows p value < 0.01, blue colour bars show serum and red colour show homogenate”.....	86
Figure 3.40 Graphical representation of TBARs level in different experimental groups “**/## shows p value < 0.01, blue colour bars show serum and red colour show homogenate”.....	87
Figure 3.41. Graphical representation of the relative SOD activity “**/## shows p value < 0.01, ***/### shows p value < 0.001, blue colour bars show serum and red colour show homogenate”.....	88
Figure 3.42. Graphical representation of the catalase activity “**/## shows p value < 0.01, ***/### shows p value < 0.001”.....	89
Figure 3.43. Estimation of APX level in serum and heart tissue samples “**/## shows p value < 0.01, *** shows p value < 0.001”.....	90
Figure 3.44. Effect of Pistacia integerrima on cellular architecture, Representative images of H&E staining of the heart tissues of the different experimental groups including control, BPA2, BPA3, Melatoin, BPA2+melatonin, BPA3+melatonin, P. integerrima, BPA2+ P. integerrima, BPA3+ P. integerrima, images taken at 40X scale bar 100µm.....	91
Figure 3.45. Graphical representation of percentage abnormal cells “*/# shows p value < 0.05, **/## shows p value < 0.01”.....	92
Figure 3.46. Estimation of RNA expression of p53 in different experimental groups “***/### shows p value < 0.001”.....	93
Figure 3.47. Relative Expression analysis of PUMA “**/## shows p value < 0.01”..	93
Figure 3.48. Estimation of relative mRNA level of Drp1 “**/## shows p value < 0.01”.....	94
Figure 3.49. Estimation of RNA expression of USP7 in experimental groups “***/### shows p value < 0.001”.....	95
Figure 3.50. Estimation of mRNA expression of cytochrome c “**/## shows p value < 0.01”.....	96
Figure 3.51. Binding site of miRNA-15a-5p to 3'UTR of Bcl-2 and Mfn2 (source TargetScan database).....	96
Figure 3.52. Estimation of relative expression of miRNA-15a-5p in cardiac tissues“# shows p value < 0.05, **/## shows p value < 0.01, *** shows p value < 0.001”.....	97
Figure 3.53. Estimation of relative RNA expression of Bcl-2 in cardiac tissues “***/### shows p value < 0.001”.....	98
Figure 3.54. Estimation of relative RNA expression of Mfn2 in cardiac tissues “* shows p value < 0.05, ## shows p value < 0.01, ***/### shows p value < 0.001”.....	99
Figure 3.55. Estimation of the relative expression of miRNA_214-3p in cardiac tissues “* shows p value < 0.05, **/## shows p value < 0.01, ### shows p value < 0.001”.....	100
Figure 3.56. Binding region of miRNA-214-3p with 3'UTR of target genes (source TargetScan database).....	100



Figure 3.57. Estimation of relative RNA expression of CDIP1 in cardiac tissues “**/## shows p value < 0.01, ***/### shows p value < 0.001” .....	101
Figure 3.58. Estimation of the relative RNA expression of BNIP3 in cardiac tissues “***/### shows p value < 0.001” .....	102
Figure 3.59. Estimation of relative RNA expression of PKC- $\delta$ in cardiac tissues “## shows p value < 0.01, ***/### shows p value < 0.001” .....	103
Figure 3.60. Effect of Pistacia integerrima on p53 and its downstream target proteins .....	105
Figure 3.61. Effect of Pistacia integerrima on p53 and its downstream target proteins a. Representative blot images of p53, p-p53, PUMA, cytochrome c and GAPDH, b. Graphical representation of relative p53 protein expression, c. Graphical representation of relative p- p53 protein expression, d. Graphical representation of relative PUMA protein expression, e. Graphical representation of relative Drp1 protein expression, f. Graphical representation of relative cytochrome c protein expression “**/## shows p value < 0.01” .....	107
Figure 3.62 Graphical Representation of the ratio of p-p53/p53 “**/## shows p value < 0.01” .....	107
Figure 3.63. Antiapoptotic potential of Melatonin via regulation of miRNA-15a-5p target genes in in cardiac tissues a. Representative blot images of Bcl-2, Bcl2-p, Mfn- 2, Bax and GAPDH, b. Graphical representation of relative Bcl2 protein expression, c. Graphical representation of relative Bcl2-p protein expression, d. Graphical representation of relative Mfn2 protein expression, e. Graphical representation of relative Bax protein expression, f. Graphical representation of the ratio of Bax to Bcl2 protein, g. Graphical representation of the ratio of Bcl2-p to Bcl2 protein “*shows p value < 0.05, ** shows p value < 0.01, ***shows p value < 0.001” .....	108
Figure 3.64. Estimation of brain weight to body weight ratio in different experimental groups “* shows p value < 0.05, **shows p value < 0.01” .....	110
Figure 3.65. Melatonin alleviated BPA induced cellular damage a: Representative images of H&E staining of brain tissues of experimental groups; Control, BPA1 (100 $\mu$ g/kgBW), BPA2 (1mg/kgBW), BPA3 (10mg/kgBW), MLT, BPA1+MLT, BPA2+MLT, BPA3+MLT (Images taken at 40X, scale bar 100 $\mu$ m); b: Graphical representation of the percentage abnormal cells “***shows p value < 0.001” .....	111
Figure 3.66. Estimation of the ROS level in brain tissues “*shows p value < 0.05, **shows p value < 0.01” .....	112
Figure 3.67. Estimation of the TBARs level in brain tissues “***shows p value < 0.01” .....	113
Figure 3.68. Effect of melatonin on antioxidant profile a: Estimation of SOD activity in brain tissues; b: Estimation of Catalase activity in brain tissues; c: Estimation of POD activity in brain tissues; d: Estimation of APX level in brain tissues; e: Estimation of GSH activity in brain tissues “***shows p value < 0.05, **shows p value < 0.01” .....	114
Figure 3.69. Representative bar graph showing p53 mRNA level in the brain tissues “***shows p value < 0.01” .....	116
Figure 3.70. Estimation of relative mRNA level of PUMA in brain tissues “***shows p value < 0.01” .....	117

Figure 3.71. Estimation of relative mRNA level of Drp1 in brain tissues “**shows p value < 0.01” .....	117
Figure 3.72. Effect of melatonin on p53 and its target proteins expression a: Representative western blots showing p-p53, p53, PUMA, Drp-1 expression. b: Graphical representation of the densitometric analysis of p-p53, c: Graphical representation of the densitometric analysis of p53, d: Graphical representation of the densitometric analysis of PUMA, e: Graphical representation of the densitometric analysis of Drp1 “**shows p value < 0.01” .....	119
Figure 3.73. Effect of melatonin on p53 and its target proteins expression a: Representative western blots showing p-p53, p53, PUMA, Drp-1 expression. b: Graphical representation of the densitometric analysis of p-p53, c: Graphical representation of the densitometric analysis of p53, d: Graphical representation of the densitometric analysis of PUMA, e: Graphical representation of the densitometric analysis of Drp1 “**shows p value < 0.01” .....	120
Figure 3.74. Effect of melatonin on p53 and its target proteins expression a: Representative western blots showing p-p53, p53, PUMA, Drp-1 expression. b: Graphical representation of the densitometric analysis of p-p53, c: Graphical representation of the densitometric analysis of p53, d: Graphical representation of the densitometric analysis of PUMA, e: Graphical representation of the densitometric analysis of Drp1 “**shows p value < 0.01” .....	121
Figure 3.75. Estimation of ratio of p-p53/p53 protein in brain tissues “**shows p value < 0.01” .....	122
Figure 3.76. Estimation of relative expression of miRNA-214-3p in brain tissues “**/## shows p value < 0.01” .....	123
Figure 3.77. Estimation of relative expression of cdip1 in brain tissues “**/## shows p value < 0.01” .....	123
Figure 3.78. Estimation of relative expression of BNIP3 in brain tissues “## shows p value < 0.01 in comparison to control, ***shows p value < 0.001 in comparison to disease” .....	124
Figure 3.79. Estimation of relative expression of PKC- $\delta$ in brain tissues “**/## shows p value < 0.01” .....	125
Figure 3.80. Estimation of relative expression of miRNA-15a-5p in brain tissues “**/## shows p value < 0.01” .....	126
Figure 3.81. Estimation of relative expression of Bcl2 in brain tissues “**/## shows p value < 0.01” .....	126
Figure 3.82. Estimation of relative expression of Mfn2 in brain tissues “**/## shows p value < 0.01” .....	127
Figure 3.83. Estimation of relative expression of miRNA-214-3p in brain tissues “**/## shows p value < 0.01” .....	128
Figure 3.84. Estimation of relative expression of cdip1 in brain tissues “**/## shows p value < 0.01” .....	128
Figure 3.85. Estimation of relative expression of BNIP3 in brain tissues “## shows p value < 0.01, ***shows p value < 0.001” .....	129
Figure 3.86. Estimation of relative expression of PKC- $\delta$ in brain tissues “**/## shows p value < 0.01” .....	129

Figure 3.87. Estimation of relative expression of miRNA-15a-5p in brain tissues “**/## shows p value < 0.01” .....	130
Figure 3.88. Estimation of relative expression of Bcl2 in brain tissues “**/## shows p value < 0.01” .....	131
Figure 3.89. Estimation of relative expression of Mfn2 in brain tissues “**/## shows p value < 0.01” .....	131
Figure 3.90 Molecular docking of L-37 with Bcl-2. (A) 3D structure of interactions of target protein Bcl-2 (PDB id: 5jsn) with L-37 oligomer (blue) (B) 2D Ligplot of Bcl-2 interactions with L-37 (C) Hydrogen bonding between Bcl-2 and L-37 (D) Other types of interaction between Bcl-2 and L-37 in the 2D Ligplot. The color bar in (C) indicates the strength of the H-bonds .....	134
Figure 3.91 Molecular docking of Es-37 with Bcl-2. (A) 3D structure of interactions of target protein Bcl-2 (PDB id: 5jsn) with Es-37 oligomer (green) (B) 2D Ligplot of Bcl-2 interactions with Es-37 (C) Hydrogen bonding between Bcl-2 and Es-37 (cyan) (D) 3D view of different type of interactions between Bcl-2 and Es-37 with corresponding distances .....	135
Figure 3.92 Molecular docking of L-37 with Cytochrome c. (A) 3D structure of interactions of target protein cytochrome c (PDB id: 5z62) with L-37 oligomer (blue) (B) 2D Ligplot of protein interactions with L-37 (C) Hydrogen bonding between cytochrome c and L-37 (D) Other types of interaction between cytochrome c and L-37 in the 2D Ligplot.....	135
Figure 3.93 Molecular docking of Es-37 with cytochrome c (A) 3D structure of interactions of target protein cytochrome c (PDB id: 5z62) with Es-37 oligomer (blue) (B) 2D Ligplot of protein interactions with Es-37 (C) Hydrogen bonding between cytochrome c and Es-37 (blue) (D) 3D view of different type of interactions between cytochrome c and Es-37 with corresponding distances .....	136
Figure 3.94 Molecular docking of L-37 with p53 (A) 3D structure of interactions of target protein p53 (PDB id: 4mzi) with L-37 oligomer (red) (B) 2D Ligplot of protein interactions with L-37 (C) Hydrogen bonding between p53 and L-37 (red) (D) Other types of interaction between p53 and L-37 in the 2D Ligplot.....	136
Figure 3.95 Molecular docking of Es-37 with p53 (A) 3D structure of interactions of target protein p53 (PDB id: 4mzi) with Es-37 oligomer (red) (B) 2D Ligplot of protein interactions with Es-37 (C) Hydrogen bonding between p53 and Es-37 (pink) (D) 3D view of different type of interactions between p53 and Es-37 with corresponding distances.....	137
Figure 3.96 Trajectories analysis. (A) C alpha root mean square deviation and root mean square fluctuations of selected proteins and ligands (Es-37, L-37) (B) superimposition of Bcl-2-L-37 snapshots extracted at 11, 60 and 72ns, respectively (C) superimposition of Bcl-2-Es-37 snapshots extracted at 11, 60 and 72 ns, respectively .....	139
Figure 3.97 Histological analysis and relative mRNA expression. A-H; H&E staining of heart tissues; (A) normal, (B) BPA, (C) NAC, (D) BPA+NAC, (E) Es-37, (F) BPA+Es-37, (G) L-37, (H) BPA+L-37 treated heart tissues (images taken at 40X, scale bar 100µm), (I) % abnormal cells of heart, (J) Graphical representation of the relative expression of miRNA 15a-5p, (K) Graphical representation of the relative expression of Bcl-2 mRNA, (L) Graphical representation of the relative expression of	

p53 mRNA, (M) Graphical representation of the relative expression of cytochrome c mRNA, (N) Binding region of miRNA-15a-5p to 3'UTR of Bcl-2 gene (source TargetScan database)., “(*) at p value < 0.05, (**) at p value < 0.01” .....	141
Figure 3.98 Collagen deposition analysis A-H; Representative images of Masson's Trichome staining of heart tissues; (A) normal, (B) BPA, (C) NAC, (D) BPA+NAC, (E) Es-37, (F) BPA+Es-37, (G) L-37, (H) BPA+L-37 treated heart tissues. (The light green colour depicts the collagen deposition). Images taken at 10X magnification, scale bar 100µm .....	142
Figure 3.99 Protein expression analysis (A) Western blot of p53 protein, (B) Graphical representation of the densitometric analysis of p53 protein, (C) Western blot of p-p53 protein, (D) Graphical representation of the densitometric analysis of p-p53 protein, (E) Western blot of cytochrome c protein, (F) Graphical representation of the densitometric analysis of cytochrome protein. GAPDH was used as loading control. “(*) at p value < 0.05, (**) at p value < 0.01” .....	144
Figure 3.100 Normality curves of p53 and target genes, A miRNA-15a-5p expression, B Bcl2 mRNA expression, C p53 mRNA expression, D Cyt c mRNA expression, E p53 protein expression, F Cytochrome c protein expression, G P-p53 protein expression .....	145
Figure 3. 101 Effect of Es-37 and L-37 on biochemical Profile (A) Estimation of ROS activity in heart and serum, (B) Estimation of TBARs level in heart and serum, (C) Estimation of SOD activity in heart and serum, (D) Estimation of CAT activity in heart and serum, (E) Estimation of GSH activity in heart and serum, (F) Estimation of APX in heart and serum, (G) Estimation of POD activity in heart and serum, (H) Estimation of liver markers ALT and AST in serum, (I) Estimation of lipid profile cholesterol and triglycerides in serum, (J) Estimation of kidney profile uric acid and creatinine in serum “(**) in comparison to normal control at p value < 0.01, (#) in comparison to disease control at p value < 0.01” .....	148
Figure 3.102 Normality curve analysis of oxidative stress markers, A Representative graph of ROS, B Normality curve of TBARs, C Normality plot of SOD, D Normality plot of CAT, E Normality plot of GSH, F Normality plot of APX, G Normality plot of POD.....	149
Figure 3.103 Normality curve analysis of toxicity markers, A Representative graph of normality curve of ALT, B Normality curve of AST, C Normality plot of Uric acid, D Normality plot of Creatinine, E Normality plot of Cholesterol, F Normality plot of Triglycerides .....	150
Figure 3.104. Representative images of Chromatograms; A: chromatogram of standard at 210nm; B: chromatogram of serum sample of normal individuals at 210nm .....	153
Figure 3.105 Graphical representation of BPA concentration in control and malignant breast tissue samples; B: Graphical representation of ROS activity in control and malignant breast tissue samples; C: Graphical representation of SOD activity in control and malignant breast tissue samples; D: Graphical representation of Catalase (CAT) activity in control and malignant breast tissue samples; E: Graphical representation of the relative fold activity change of p53 in control and malignant breast tissue samples; F: Graphical representation of the relative fold activity change of WNT1 in control and malignant breast tissue samples; G: Graphical representation	

---

of the relative fold activity change of ZEB1 in control and malignant breast tissue samples; H: Graphical representation of the densitometric analysis of p53 protein in malignant and control breast tissue samples; I: Blot image of p53 and actin in malignant and control breast tissue samples. “The data was considered significant at ** p-value $\leq$ 0.01 or ***p-value $\leq$ 0.001” .....	155
Figure 3.106 Histological analysis of breast tissue samples; A: Representative image of DCIS female breast tissue; B: Representative image of IDC female breast tissue; C: Representative image of IDC male breast tissue, (magnification: 40X, Scale bar 50 $\mu$ m).....	156
Figure 3.107. Representative images of receptor status of different breast tissue samples analysed by IHC (Magnification 40X, scale bar 50 $\mu$ m), B Graphical representation of the frequency distribution of receptor status of breast cancer tissue samples.....	157
Figure 4.108 Schematic illustration of therapeutic potential of <i>Pistacia integerrima</i>	167
Figure 4.109 Schematic diagram illustrating the therapeutic potential of synthetic compounds .....	171
Figure 4.110 Schematic illustration of role of BPA in breast cancer .....	173
Figure 4. 111 Schematic diagram of Bisphenol A induced oxidative stress linked apoptosis .....	174

**ABSTRACT**

Exposure to environmental toxicants such as Bisphenol A (BPA) has raised serious health issues globally particularly in developing countries. BPA an endocrine disruptor, is ubiquitously used in the manufacturing of canned food, feeding bottles and different daily life products. BPA-generated reactive oxygen species can lead to several diseases including cardiotoxicity. However, the endpoints stimulated in BPA induced cardiotoxicity and neurotoxicity yet need to be investigated. The current study aimed to investigate the underlying molecular pathways which may contribute in revealing the protective effects of *Pistacia integerrima* against BPA induced oxidative stress. Herein, adult Sprague Dawley rats were administrated (subcutaneously) with BPA (100 µg/kg BW, 1 mg/kg BW, and 10 mg/kg BW), 200mg/kgBW *P. integerrima*, and melatonin (4 mg/kg BW) for 16 days of BPA. Our results showed BPA exposure significantly increased the oxidative stress as demonstrated by increased free radicals (ROS), TBARs level, and decreased antioxidant enzymes including superoxide dismutase and catalase in heart, liver, kidney and brain tissues. Present results of western blotting and qRT-PCR showed the increased expression of p53, PUMA and Drp1, while downregulation of Ubc13 in heart and brain tissues of BPA treated groups whereas the levels were reversed upon treatment with *P. integerrima*. The role of BPA in tissue apoptosis was further confirmed by the increased level of P-p53, cytochrome c and disrupted cellular architecture whereas the *P. integerrima* has shown its ameliorative potential by mitigating the adverse effects of BPA. Moreover, the lipid, and liver markers profile has also revealed the therapeutic potential of *P. integerrima* by maintaining the levels in the normal range. However, melatonin has also manifested the normalized expression of apoptotic markers, biochemical markers, and tissue architecture. MicroRNAs are the key regulators in various cellular mechanisms and have the potential to develop new therapeutic strategies. Therefore, the study also sought to investigate the role of miRNA-15a-5p and miRNA-214-3p in BPA induced cardiotoxicity and neurotoxicity. Different bioinformatics tools including TargetScan database were used to find the putative target genes of the miRNAs. The qRT-PCR analysis showed the upregulation of miRNA-15a-5p in the BPA administered groups. However, the expression of the putative target genes Bcl-2 and Mfn-2 was significantly downregulated at both transcriptional and translational level in the disease groups. The significant downregulation of miRNA-214-3p and upregulation of its putative target genes, cdip1, BNIP3 and PKCD in the disease groups suggests the role of miRNA-214-3p in BPA

induced toxicity. However, the treatment with *P. Integerrima* and melatonin ameliorated the toxic effects of BPA. Conclusively, the data suggest that *P. Integerrima* may be a potential candidate for the treatment of BPA induced toxicity by neutralizing the oxidative stress through miRNA mediated p53/PUMA/Drp-1/Bcl-2 signalling pathway. The second aim of the present study was to elucidate the highly selective antioxidative potential of synthetic tetra aniline polymers Es-37 and L-37 against BPA-induced cardiac cellular impairments (toxicity). In our results, BPA administration significantly elevated ROS, altered p53, cytochrome c, Bcl-2, and particularly miRNA-15a-5p expression; however: these changes were notably averted and reversed by Es-37 and L-37 treatment. Additionally, molecular docking of synthetic polymers L-37 and Es-37 with three proteins (p53, Cytochrome c, and Bcl-2) validated that L-37 has a greater binding affinity with the target proteins compared to Es-37, with the highest binding values reported for the enzymatic protein cytochrome c. Thus, our findings suggest that both synthetic polymers Es-37 and L-37 have the potential to scavenge free radicals, boost-up antioxidant enzyme activities, and avert (BPA-induced) toxicity, thus, may serve as cardioprotective agents. Concurrently, our finding suggests that miRNA-15a-5p overexpression is associated with oxidative stress and coincides with cardiotoxicity; thus, it may be used as a diagnostic marker in BPA-mediated cardiac pathologies. Keeping in view the findings, our research provides a platform for the development of miRNA-based therapeutic and diagnostic strategies against BPA-induced toxicity. After the elucidation of the toxic effects of BPA in cardiac and brain tissues, the current study also aimed to investigate the effect of BPA in breast cancer progression. Breast cancer is an abnormal division of breast cells. BPA, an environmental toxicant, is identified as an emerging risk factor for breast cancer development. However, to the best of our knowledge, no previous study has investigated the BPA levels in breast cancer patients in Pakistan. The present study sought to explore the role of BPA in tumor growth among the Pakistani population. As an endocrine-disrupting chemical (EDC), BPA has more significant potential to initiate tumorigenic events in breast tissue by generating oxidative stress. The level of BPA in the serum samples of breast cancer patients was significantly higher than control. Histological analysis of breast cancer tissue samples revealed distinct subtypes of tumor, such as ductal carcinoma in situ (DCIS) and invasive ductal carcinoma (IDC). There was a significant increase in ROS level while a significant decrease in the levels of superoxide dismutase and catalase enzymes in malignant breast tissue samples as

compared to control tissue samples. We found upregulated expression of p53, ZEB1 and WNT1 genes at mRNA level in malignant breast tissue samples. p53 protein expression in malignant breast tissue samples was also enhanced at the translational level. Conclusively, the current findings suggest a relationship between BPA and the progression of breast cancer, which may open new horizons of research for the development of future therapeutic strategies.



## 1. INTRODUCTION

Exposure to environmental toxicants is an emerging concern affecting both developed and developing countries (Rajak, Raza et al. 2021). According to WHO (2022) report, approximately 7 million deaths are caused annually due to an unhealthy environment (2022). According to WHO this unintentional poisoning kills nearly 0.3 million people globally each year. Environmental toxicants are the toxic chemicals that can be man-made, naturally occurring or biologically produced, ubiquitously present in our environment like air, soil, food, water and consumer products (Moore 2019). These include a wide range of chemicals like pesticides, industrial chemicals, fuels, organic compounds, heavy metals and various carcinogens, endocrine disrupting chemicals and many others that are contaminating our environment. These environmental toxicants are the major contributing factors in the development of various health disorders including diabetes, asthma, obesity, hypertension, immune diseases, neurodegenerative diseases, cancer, psychiatric problems, infertility, allergy and cardiovascular diseases (Claus, Guillou et al. 2017, Posnack 2021, Rebolledo-Solleiro, Flores et al. 2021).

Among Environmental toxicants endocrine disrupting chemicals (EDCs) are elements which deviates normal homeostasis by interfering with the body's natural endocrine system *i.e.* hormone synthesis, secretion, transport and their metabolism (Guarnotta, Amodei et al. 2022). EDCs are elements found in environment, food, and consumer products. Exposure to EDCs can cause a wide range of adverse reproductive, cardiovascular, neurological, metabolic, immune and developmental abnormalities in humans (Schug, Janesick et al. 2011, Fu, Xu et al. 2020). EDCs may either be classified as synthetic or natural EDCs (Özen and Darcan 2011). Synthetic EDCs include a broad range of chemicals such as industrial solvents or lubricants and their byproducts. Whereas natural EDC are found in food of human and animal *e.g.* phytoestrogens, including coumestrol and genistein (Diamanti-Kandarakis, Bourguignon et al. 2009).

Human are exposed to endocrine disruptors directly through phytoestrogens in plants and pharmaceutical. Whereas Bisphenol A (BPA) treated food bags, fungicides and pesticides are some examples of indirect way of their exposure. When a tissue is

exposed to EDCs, they alter the gene expression profile of that tissue, as a result they cause toxicity (Yang, Kim et al. 2015, Guarnotta, Amodei et al. 2022).

Because of numerous industrial and manufacturing activities, various environmental EDCs are ubiquitous in our living ecosystem. They specifically bind to the estrogen receptors and have the ability to act either as agonists or antagonists. Bisphenol-A (BPA) is one of the major EDC (Wang, Fu et al. 2015, Guarnotta, Amodei et al. 2022).

### **1.1. BPA as Environmental Toxicant**

Bisphenol A (BPA) is known as 4,4'-(propane-2,2-diyl) diphenol. BPA is a man-made synthetic chemical which has a dihydroxyphenyl group. BPA is extensively used and ubiquitously produced synthetic organic compound since 1960. The high volume production of polycarbonates and epoxy resins by chemical industries increases its production rate constantly every year (Flint, Markle et al. 2012, Wang, Liu et al. 2020). Annually 13% average increasing rate of BPA is reported in Asia. Worldwide 3.8 million tons of BPA is produced which is 30% polymerized to epoxy resin and 65% is polymerized for the production of resistant polycarbonate and plastic production (Nosarka 2017, Huelsmann, Will et al. 2021). These polymeric plastic and epoxy resins are used in manufacturing of food packaging bottles, food cans, bottle tops, water pipes, lines and epoxy resins (Ellahi and ur Rashid 2017). In addition to this at home and workplace on a daily basis we are exposed to BPA due to the coating of electronic instruments, automobiles, CDs, DVDs, sports safety equipment, carbonless paper and recycled paper (Welshons, Nagel et al. 2006, Huelsmann, Will et al. 2021).

### **1.2. BPA: Characteristic and Metabolism**

*Physical characteristics:* It is an industrial chemical which exists in white crystalline form. It is insoluble in water but easily dissolves in alcoholic and alkaline solvents. Most used in manufacturing of polycarbonates, epoxy resins and plastic industry. Chemical structure of BPA is described in figure 1.1.

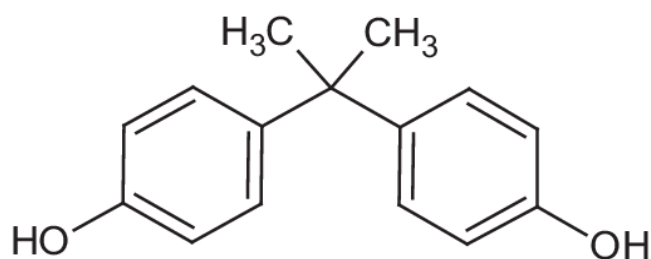


Figure 1.1 Chemical structure of BPA (Midoro-Horiuti and Goldblum 2017).

Previous studies have shown that BPA from epoxy resin and polycarbonates products can leach into foods and drinks as a result it is presumed to be in routine ingestion (Vandenberg, Hauser et al. 2007).

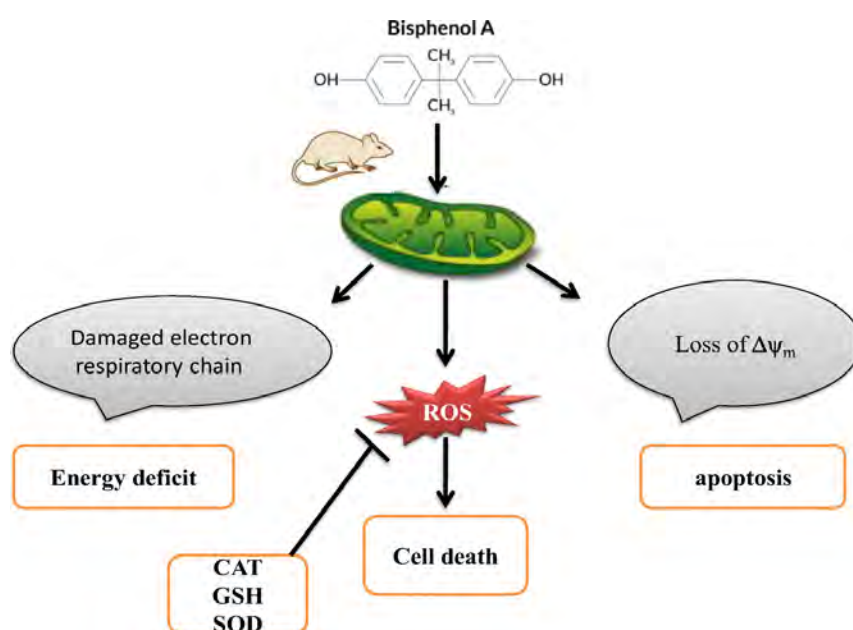


Figure 1.2. Production of ROS in mitochondria (Shirani, Alizadeh et al. 2019)

**Biological characteristics:** Bisphenol A is a synthetic estrogen, also known as xenoestrogen. It is well known endocrine disruptor. It has been reported that processed food contributes to 90% of BPA exposure and only 5% is by dust or direct dermal exposure (Geens, Aerts et al. 2012, Almeida, Raposo et al. 2018). Continuous exposure to BPA has adverse effects on animal and human life. At high concentration of BPA it has ability to produce fast cellular responses (Welshons, Nagel et al. 2006). Due to lipophilic properties it can easily interact with lipid content of cell membrane and initiate cellular signalling (Suthar, Verma et al. 2014, Almeida, Raposo et al. 2018).

BPA can bind with membrane associated estrogen receptors (ERs) and transduce estradiol like non-genomic steroid actions. BPA affinity for estrogen receptor is

approximately 1000-2000 times less than most active ligand  $17\beta$ -estradiol (Wetherill, Akingbemi et al. 2007, Bolli, Bulzomi et al. 2010). When BPA interacts with membrane receptor it causes mitochondrial disruption *via* increasing oxidative stress by generating ROS as described in given figure 1.2 (Ben-Jonathan 2019).

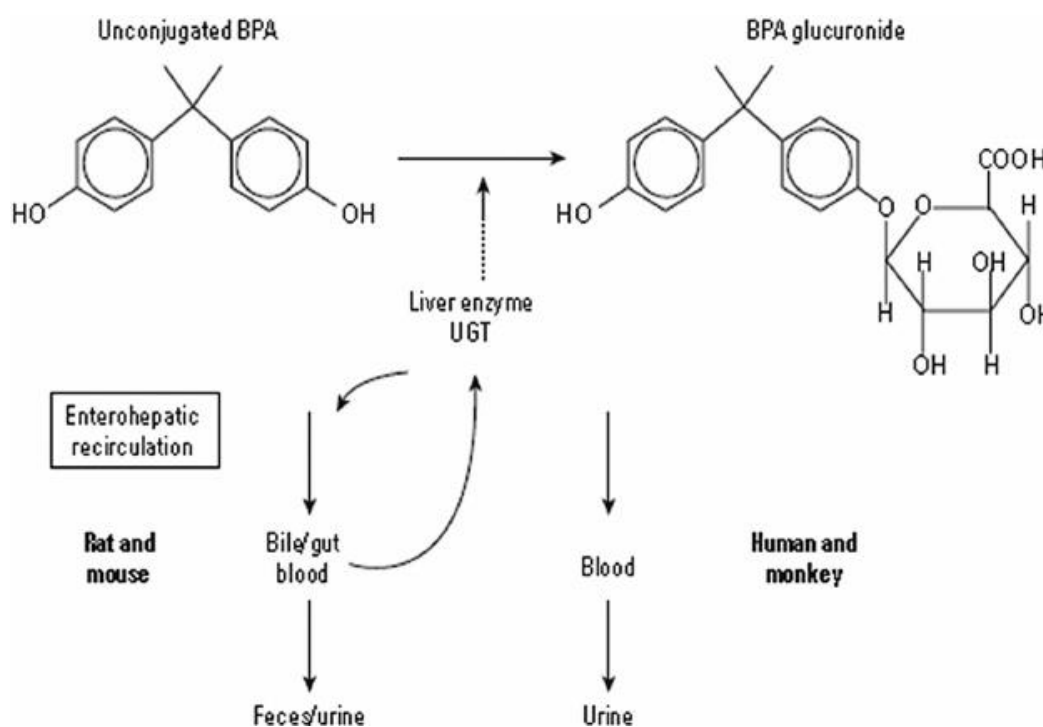


Figure 1.3. BPA Metabolism in liver (Mattison, Karyakina et al. 2014)

When BPA is given by oral administration it metabolizes into its conjugates BPA glucuronide and BPA sulfate by following glucuronidation and sulfation process respectively (Draganov, Markham et al. 2015). Enzymatic activity of UDP glucuronosyl transferase (UGT) converts BPA by primarily binding with glucuronic acid in gut and liver and convert it into the BPA glucuronide (BPA-G). BPA-G in human is completely excreted out from the body in urine (Strassburg, Strassburg et al. 2002, Hanioka, Naito et al. 2008). Very small amount of BPA remains unconjugated known as free BPA. BPA sulfate (BPA-S) is active metabolite which is produced by the sulfation (Atkinson and Roy 1995, Thayer, Doerge et al. 2015). These conjugated forms of BPA interacts with membrane estrogen receptor alpha and initiate cellular signalling cascade (Viñas, Goldblum et al. 2013). Minor concentration of monomeric BPA which is known as “aglycone” form is present in blood circulation and interrupts multiple signalling pathways that ultimately leads to pathophysiological conditions

(Völkel, Kiranoglu et al. 2008). A general description of BPA metabolism is given in figure 1.3 which illustrate the excretion of BPA in rats and human.

### 1.3. BPA toxicity

In human, numerous diseases and health complications are associated with increased level of BPA as shown in figure 1.4. BPA exposure can cause ROS production and due to oxidative stress, it can generate neuro, cardio, kidney and hepatic toxicities (Lang, Galloway et al. 2008, Rebolledo-Solleiro, Flores et al. 2021). It can alter the liver enzymes activities, rate of miscarriages and premature deliveries has also been increased due to BPA exposure (Lang, Galloway et al. 2008). Increased BPA exposure to human can lead to several cardiac complications (Rubin 2011, Bruno, Mathews et al. 2019).

In early 1930s, BPA was discovered as compound having estrogenic activities (Dodds and Lawson 1936, MacKay and Abizaid 2018). BPA can bind with ER $\alpha$  and ER $\beta$  receptors based on its structural similarity with beta-estradiol (E2). Although it has very less affinity for these receptors as compared to estrogen. BPA attains both agonist and antagonist properties upon interaction with ER- $\alpha$  and ER- $\beta$  (Peters, Ingman et al. 2011). Even at very low doses BPA has ability to induce effects like estrogen. Additionally, unlike estrogens BPA also has high affinity for the estrogen receptor-related receptor  $\gamma$  (ERR $\gamma$ ) (Okada, Tokunaga et al. 2007). Moreover BPA can also bind to the cells expressing the G-protein coupled receptor *i.e.* GPR30 or GPER (G-protein coupled estrogen receptor) there by it mimics the action of natural estrogen hormone 17 $\beta$ -estradiol (Alonso-Magdalena, Ropero et al. 2012). BPA can also show affinity for the membrane estrogen receptor (mER), which activates guanylyl cyclase and protein kinase G, which induce depolarized Ca<sup>2+</sup> flow into L-calcium channel, by turning off the ATP dependent K<sup>+</sup> channel. It also causes cAMP response element binding protein (CREB) phosphorylation by enhancing calcium signalling. It can also control the transcription of cAMP/Ca<sup>2+</sup> response elements (Alonso-Magdalena, Ropero et al. 2012, Jalal, Surendranath et al. 2018). Later on it was demonstrated that BPA exhibit anti-androgenic effects and can bind to androgen receptors (Lee, Chattopadhyay et al. 2003). Moreover, BPA can also antagonize thyroid hormones actions due to its ability to bind with thyroid hormones (Schönfelder, Wittfoht et al. 2002). Extensive studies have

documented that BPA exposure and various life threatening diseases such as obesity, cancer, disorders of the neuroendocrine, reproductive and immune system are potentially linked to each other (Zoeller, Brown et al. 2012, Bruno, Mathews et al. 2019, Rebolledo-Solleiro, Flores et al. 2021). Numerous evidences have proved that the cardiovascular system is a potential target of BPA. So BPA exposure may be consider a risk factor for a wide range of cardiovascular related abnormalities including cardiac arrhythmias and vascular diseases (Gao and Wang 2014).

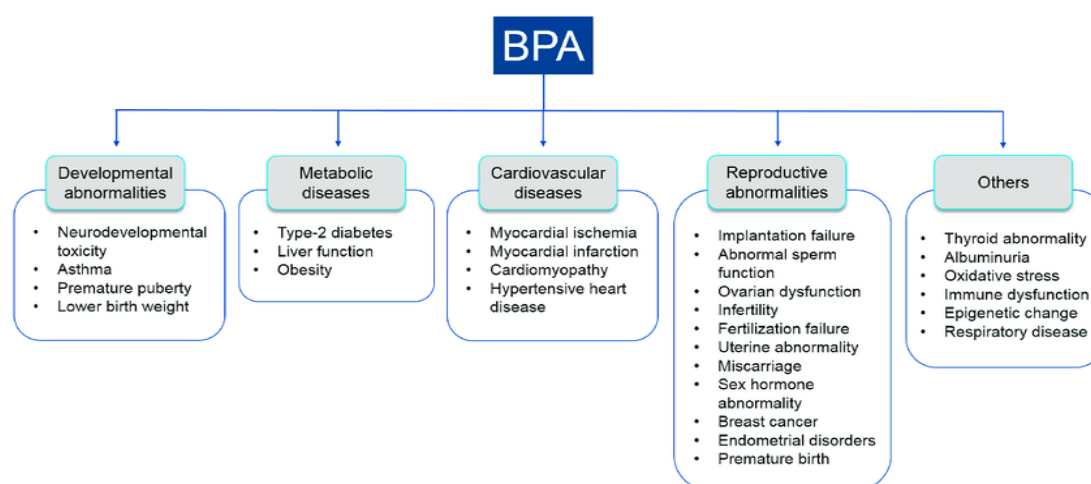


Figure 1.4. Diseases caused by the BPA (Ryu, Rahman et al. 2017)

### 1.3.1. Cardiotoxicity

Cardiovascular diseases (CVDs) are among one of the most significant health problems worldwide that contributes to the mortality and morbidity. Oxidative stress is one of the key factor in the development of cardiovascular pathologies (Dubois-Deruy, Peugnet et al. 2020). Studies have reported that BPA exposure in adult populations and increased risk of CVDs are associated with each other. It has been suggested that BPA exposure at very “low-dose” could alter the physiological functioning of cardiovascular system by promoting abnormal cardiovascular activities such as cardiac remodelling, altered blood pressure, atherosclerosis, and arrhythmias (Melzer, Osborne et al. 2012, Gao, Liang et al. 2013, Zhang, Shan et al. 2020). Basic molecular mechanisms behind BPA induced cardiotoxicity involve ion channel inhibition or activation, alteration of cardiac  $\text{Ca}^+$  handling  $\text{Ca}^{2+}$  handling proteins phosphorylation mechanism (Yan, Chen et al. 2011, Gao, Liang et al. 2013), oxidative stress, and modification of genome and

transcriptome. These evidences suggest that BPA environmental exposure is a contributing risk factor for CVDs (Gao and Wang 2014, Posnack 2021). Under normal physiological conditions, the toxic effects of ROS can be neutralized by scavenging enzymes such as superoxide dismutase (SOD), catalase and glutathione peroxidase (GSHPx) and by some other non-enzymatic antioxidants. However, when ROS generation exceeds the normal defense capacity of antioxidant, oxidative stress start showing its adverse effect on the structural integrity and functionality of biological tissues including heart (Trifunovic, Wredenberg et al. 2004, Tsutsui, Kinugawa et al. 2008). Major sources of cellular ROS generation within the heart include endothelial cells, cardiac myocytes, and neutrophils.

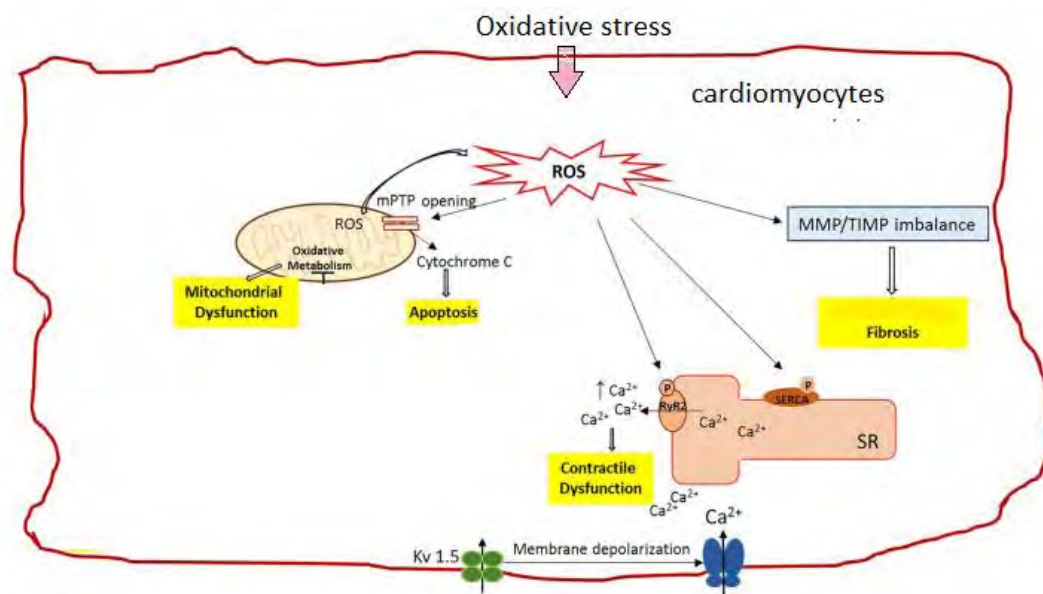


Figure 1.5. ROS mediated cardiomyocytes apoptosis (Iacobazzi, Suleiman et al. 2016)

There are several mechanisms through which ROS can be generated within cardiomyocytes such as mitochondrial electron transport, xanthine dehydrogenase/xanthine oxidase, NAD(P)H oxidase. Cardiac myocytes have the highest volume density of mitochondria for synthesis of ATP by oxidative metabolism. It has been reported that mitochondrial electron transport plays a significant role in ROS production and ultimately leads to heart failure. Mitochondria generate ROS through transport of a single electron to molecular oxygen in the respiratory chain (Tsutsui, Kinugawa et al. 2008, van der Pol, van Gilst et al. 2019). Other contributor of oxidative stress include enzymatic sources such as vascular endothelial cells in which xanthine

oxidase, NAD(P)H oxidase, and activated leukocytes produce ROS *via* NAD(P)H oxidase which are reported to be highly activated in cardiac failure (Bauersachs, Bouloumi. et al. 1999, van der Pol, van Gilst et al. 2019). In endothelium and vascular smooth muscle NAD(P)H oxidase is considered as a major source of ROS production (fig. 1.5). In human heart failure myocardial activity of NAD(P)H oxidase is increased (Heymes, Bendall et al. 2003, Yang and Lian 2020).

Many important functions of the heart are maintained by the ion channels such as electrical conduction and heart excitability *etc.* BPA has the adverse effects on the functioning of ion channels in the CV system. It has been documented that BPA high dose increase the conductance of Ca<sup>2+</sup>/voltage-sensitive K Maxi-K channels in human coronary artery smooth muscle cells (Asano, Tune et al. 2010, Soriano, Ripoll et al. 2016). Various studies have shown that BPA also have ability to block the heart sodium channels (O'Reilly, Eberhardt et al. 2012, Soriano, Ripoll et al. 2016). Inactivation steady state of sodium channels shifts to the hyperpolarized potentials state due to BPA exposure (Gao and Wang 2014). BPA also have inhibitory effect on L and T type calcium Ca<sup>2+</sup> channels. Similar result was observed on variety of voltage-gated Ca<sup>2+</sup> calcium channels such as N, P/Q type calcium channels in mouse ventricular myocyte (Deutschmann, Hans et al. 2013, Michaela, Mária et al. 2014).

In cardiac myocytes various metabolic changes occur which are associated with accumulation of ROS (Misra, Sarwat et al. 2009, Yang and Lian 2020). It can trigger crucial changes at the molecular and cellular level which lead to contractile dysfunction, fibrosis, insufficient energy production and cardiac apoptosis. Oxidative stress cause the activation of Ryanodine receptors (RyR2) and modification of sarcoplasmic membrane, which results in abnormalities of cardiac myocyte Ca<sup>2+</sup> transients and contractile functioning (Sharma and Kass 2014, Iacobazzi, Suleiman et al. 2016, Yang and Lian 2020). In addition, high ROS levels forms nitro tyrosine residues in tissue inhibitor of metalloproteinases (TIMPs) and releases active matrix metalloproteinases (MMPs), persuading fibrosis and ventricular remodelling (Qipshidze, Tyagi et al. 2011). Furthermore, ROS can behave as the secondary messengers for variety of signalling pathways involving MAPKs, PKC and Src within cardiomyocytes. Persistent ROS levels cause mitochondrial membrane depolarization. Therefore, more ROS are



formed, causing the release of cytochrome c from mitochondria which results in cellular apoptosis (Iacobazzi, Suleiman et al. 2016). Overall, increased ROS levels can lead to molecular, cellular and structural changes causing cardiac failure.

### 1.3.2. Neurotoxicity

It has been documented that BPA exposure generates oxidative stress and enhances lipid peroxidation in various organs *i.e.* liver, heart, kidney and brain. (Kabuto, Amakawa et al. 2004, Guarnotta, Amodei et al. 2022). Several studies have investigated the effects of BPA on brain development, and neuroendocrine signalling. BPA exposure causes over expression of ERs in different regions of brain in pregnant rats, mice and pups (Ramos, Varayoud et al. 2003). Whereas, BPA exposure decreases the number of dopamine containing neurons. However, low dose exposure of BPA reduces cell viability in case of neuronal cells (Lee, Seong et al. 2007). Studies in mice indicate that BPA exposure can cause abnormalities in synaptic plasticity and neuronal connectivity in brain (Kundakovic and Champagne 2011). It leaves severe consequences on brain function such as reflex action which results in decrease in learning ability (Luo, Wei et al. 2013, Zhou, Wang et al. 2017). ROS can also be generated via mitochondrial respiratory chain in neuronal cells. Where it inhibits respiratory complexes in brain resulting in life threatening disorders including Parkinson's, Alzheimer's and Huntington's diseases (Adam-Vizi 2005). BPA exposure causes anxiety and depression due to abnormalities in brain development. BPA generate ROS as it binds to GPER and this binding ultimately causes apoptosis (Lee, Suk et al. 2008, Cao, Ren et al. 2017). Elevation of apoptosis due to chronic BPA exposure can cause neuronal swelling which leads to the release of glutamate in spinal cord of rat. It also increase post synaptic processes, as a result it causes severe neuropathies (Nishio, Taniguchi et al. 2013). Imbalance in the intracellular ionic homeostasis are major contributors in BPA mediated neurotoxicity. It has been observed that BPA exposure can upregulate glutamate receptor interacting protein (GRIP) expression. As a result, it disturbs  $Ca^{2+}$  permeability *i.e.* More  $Ca^{2+}$  influx take place in the injured neurons (Bats, Groc et al. 2007). Increase in intracellular  $Ca^{2+}$  lead to the initiation of proapoptotic cascade (Hajnóczky, Csordás et al. 2006, Bahar, Kim et al. 2016). ROS generation can therefore increase the chances of cellular death and apoptosis. Overall brain

mitochondrial functions are fully compromised due to elevated level of BPA mediated neuronal apoptosis (Hajnóczky, Csordás et al. 2006, Son and Han 2018). Elevated level of BPA produces neurotoxicity *via* variety of signalling pathways *i.e.* Activating MAPK signalling pathway. Major members of MAPKs include ERK, JNK and p38 (Bindhumol, Chitra et al. 2003, Lee, Suk et al. 2008). MAPKs play vital role in regulating cell growth, differentiation, and apoptosis and are also associated to neuronal cell death and differentiation. BPA exposure can change the expression pattern of ERK, JNK and also inhibit the expression of cell survival mechanism done by NF-KB (Lee, Suk et al. 2008). Moreover, high dose BPA exposure can activate caspases 3 which is a key factor in neurological apoptosis (Sharif-Askari, Alam et al. 2001, Gao, Yang et al. 2015) as shown in figure 1.6.

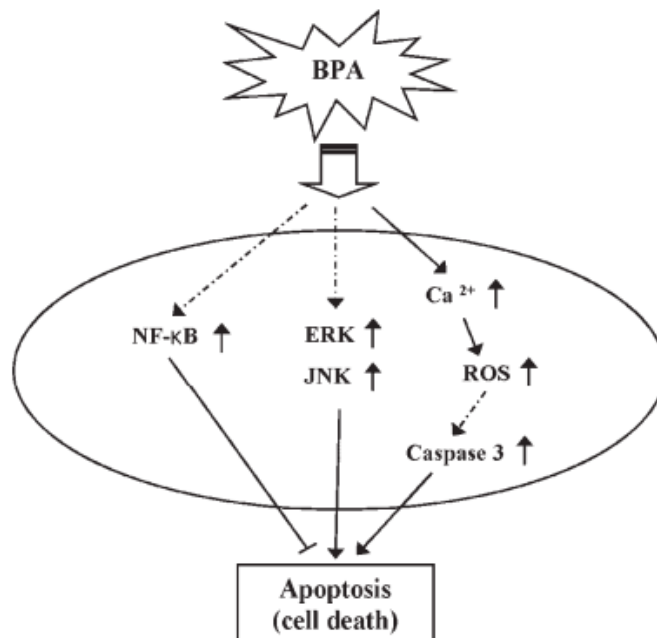


Figure.1.6. BPA mediated neuro-apoptosis (Lee, Suk et al. 2008)

#### 1.4. BPA role in Oxidative stress

BPA exposure causes the production of reactive oxygen species (ROS) and compromise the mitochondrial function in the heart (Aboul Ezz, Khadrawy et al. 2015). ROS impairs the contractile function and induces structural damage in the heart cells (Tsutsui, Kinugawa et al. 2009). In various cardiovascular pathologies increased ROS production causes peroxidation of lipids and proteins, DNA damage and cellular

dysfunction which can lead to cell death (Tsutsui, Kinugawa et al. 2011). ROS activates variety of transcription factors and signalling kinases in the heart and trigger apoptosis. ROS induce necrosis and apoptosis in cardiac cells by a variety of signalling pathways such as JNK, CaMKII, p38 MAPK, as well as mitochondrial cytochrome c release (Matsuzawa and Ichijo 2005, Zhang, Shan et al. 2020).

## 1.5. Stress responsive factors

### 1.5.1. p53

The p53 protein is tumor suppressor and also act as a transcription factor that regulate the expression of a number of genes involved in DNA repair, growth arrest and apoptosis in response to stressful stimuli (Li, Liu et al. 2016, Wen, Liu et al. 2019). It is activated by various kinases including ATM, JNK2 and MAPKs, and become activated under stressful conditions or DNA damage (Redza-Dutordoir and Averill-Bates 2016, Lu, Miao et al. 2017). The p53 mediate DNA repair, growth arrest and senescence at low stress while it regulates apoptosis on sever damage by the up-regulation of pro-apoptotic members like BAX, PUMA, NOXA and APAF-1 and down-regulation of anti-apoptotic proteins BCL-X , BCL2 and IAPs (Yoshida and Miki 2010). BAX and PUMA activated by p53 translocated into the mitochondria and causes its permeabilization resulting in the release of cytochrome c leading to mitochondrial apoptotic pathway (Chipuk and Green 2009, Pallepatti and Averill-Bates 2010) (Figure 1.7).

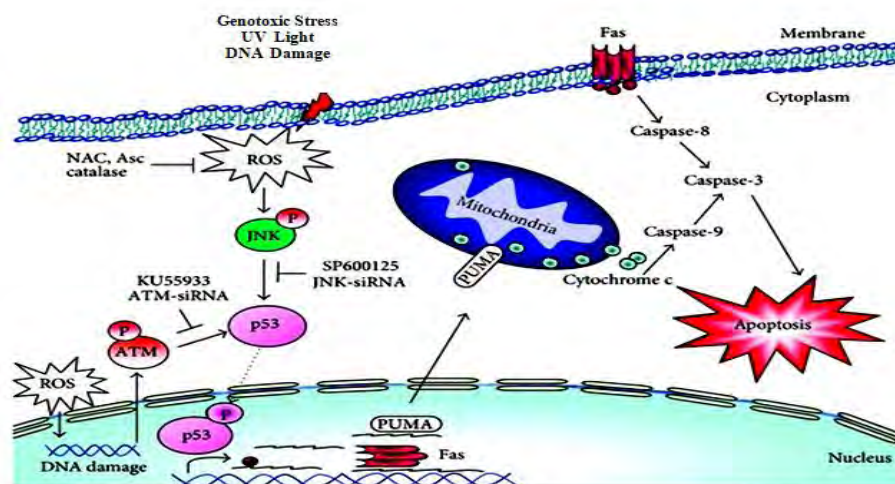


Figure 1.7. P53 induced apoptotic pathway (Chen et al., 2013)

### 1.5.2. p53-upregulated modulator of apoptosis

PUMA (p53-upregulated modulator of apoptosis) also called as BCL2-binding component 3 (BBC3). p53 upregulates the expression level of PUMA in the cell (Wang, Yu et al. 2007). This elevated level of PUMA then activates pro-apoptotic proteins like BAK and BAX resulting in the translocation of BAK and BAX to mitochondria causing mitochondrial dysfunction and induce apoptosis (Jeng, Inoue-Yamauchi et al. 2018). PUMA also increase the Drp-1 recruitment to mitochondria which causes mitochondrial fragmentation leading to apoptosis (Wang, Li et al. 2009). PUMA also induce apoptosis in p53-independent manner through various transcription factors such as E2F1, FOXO-3a, and p73 (Jeng, Inoue-Yamauchi et al. 2018).

### 1.5.3. Dynamin-related protein 1

Dynamin-related protein 1 (Drp1) is a GTPase regulating mitochondrial fission. Drp1 from cytosol is recruited onto the outer membrane of mitochondria *via* mitochondrial fission factor (Mff), mitochondrial fission protein 1 (Fis1) and mitochondrial dynamic proteins (MiD49 and MiD51) (Losón, Song et al. 2013) (Fig. 1.8).

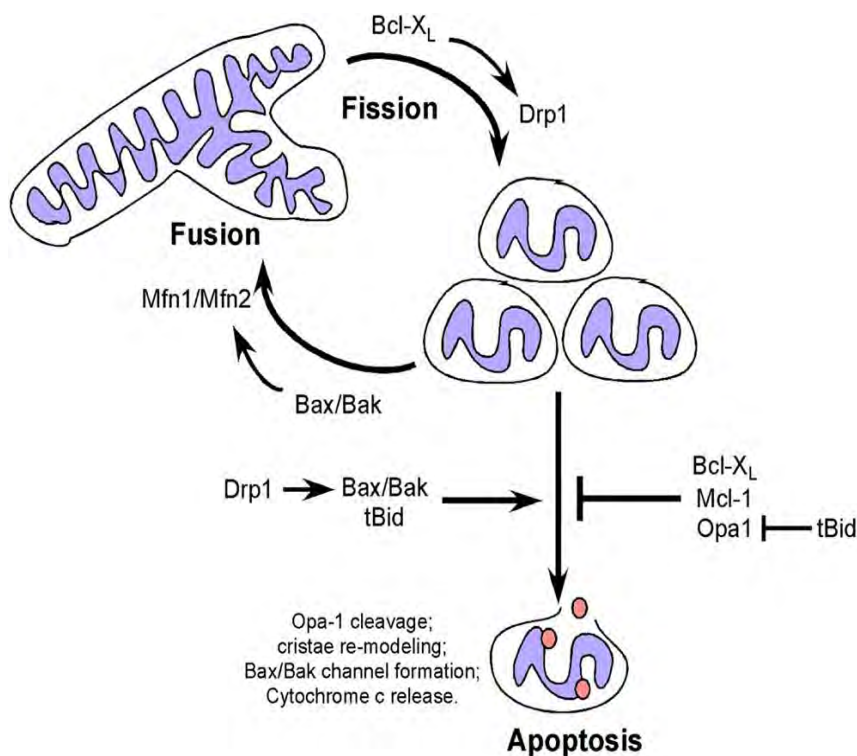


Figure 1.8. Mitochondrial fragmentation by Drp1 (Boland, Chourasia et al. 2013)

PUMA also enhance the Drp1 recruitment to mitochondria through translocation of Bax/Bad to mitochondria (Din, Mason et al. 2013). Drp1 form helical assembly around mitochondria and GTP hydrolysis causes constriction of mitochondrial tubule until lipids become depolarized resulting in the fragmentation of mitochondria (Din, Mason et al. 2013). Drp1 is also involved in release of cytochrome c from mitochondria and caspase cascade activation (Hall, Burke et al. 2014). Drp1 is also phosphorylated and activated by MAPKs through Ras/Raf signalling and by p53 transcriptionally resulting in mitochondrial dysfunction and apoptosis (Kashatus, Nascimento et al. 2015).

#### **1.5.4. Ubc13**

Ubc13 is the only identified E2 conjugating enzyme responsible for the catalyses of Lysine-K63 linked ubiquitination which is mainly occurs as a result of stress responses i.e. NFκB activation and DNA repair (Petroski, Zhou et al. 2007). Ubc13-Uev1a complex protein kinase activation and receptor-mediated signalling results in the NFκB activation via TNF associated factors 2 and 6 (TRAF2) and (TRAF6) which act as E3 ligases for Ubc13. While Ubc13-Mms2 complex formation results in DNA repair (Andersen, Zhou et al. 2005). Ubc13 is responsible for K63 polyubiquitin modification of TRAF2 and TRAF6 after stimulation of Tumor Necrosis Factor (TNF) receptors, Toll-like receptors, and several interleukin receptors which results in TAK1 (Transforming growth factor (TGF)β activated kinase) complex activation and ultimately causes the IKK (IkappaB kinase) activation (Wertz and Dixit 2008). IkappaB the inhibitor of NFκB is phosphorylated by IKK causing its proteasomal degradation by ubiquitination and allowing the NFκB to do transcriptional activation in nucleus (Wertz and Dixit 2008, Tokunaga, Sakata et al. 2009). Ubiquitination has not only role in proteasome mediated degradation but is also a crucial signalling factor in various processes. Proteasome independent ubiquitination of p53 also occurs by Ubc13 an E2 conjugating enzyme responsible for the lysine 63 linked polyubiquitination of p53 (Brooks and Gu 2011). In the normal cell condition p53 is kept at low level by HDM2 (homologue of MDM2) because of its proteasomal degradation and cytoplasmic localization by the process of poly and mono ubiquitination respectively (Lee and Gu 2010). Major E3 ligase for the p53 is HDM2. Mdm2 mediated proteasomal degradation of p53 is prevented by ubc13 which eventually translocate and stabilize p53 and increases its half-life. Ubc13 is the negative regulator of p53 transcriptional activity by

movement of p53 to the cytoplasm and increases its monomeric form of p53 by preventing its nuclear tetramerization (Topisirovic, Gutierrez et al. 2009). p53 tetramerization is important for its stability which is immediately occur after its translation on ribosome. Association of Ubc13 with the p53 on the polysome is responsible for monomeric form of p53 before its tetramer formation. Activated JNK by stress causes the dissociation of p53-Ubc13 complex via phosphorylation of p53 on Thr-81 residue (Laine, Topisirovic et al. 2006, Topisirovic, Gutierrez et al. 2009) which ultimately stabilize and activates the p53 transcriptional activity and induce apoptosis via PUMA, NADPH oxidase activator (NOXA), Bcl-2 Interacting Mediator of Cell Death (BIM) and BID. Apoptotic activity of p53 is performed by both transcriptional dependent and transcriptional independent manner. Cytoplasmic p53 inhibits its transcriptional activity and performs its function in transcriptional independent manner i.e. activating apoptosis through mitochondria (Lee and Gu 2010). Mitochondrial apoptosis occurs through extrinsic and intrinsic pathway. Extrinsic pathway activates pro-caspase 8 which ultimately activate the effector caspases and induce apoptosis (Zhao, Tang et al. 2016). Intrinsic pathway is regulated by anti-apoptotic (XIAP, BCL-2 and BCL-X1) and proapoptotic family of proteins (BAX, BAD, BID, SMAC and Diablo). In response to stress p53 is translocated to mitochondrial membrane and binds with antiapoptotic proteins and allow the proapoptotic proteins to be activated and formation of their oligomerization which eventually release the cytochrome c from inner mitochondrial space due to mitochondrial outer membrane permeabilization (MOMO) (Tomita, Marchenko et al. 2006). Cytochrome c causes APAF-1 mediated caspase 9 activation (Apoptosome formation) which in turn activate the effector caspases i.e caspase-3, caspase-6 and caspase-7 which ultimately causes cell death (Siu, Pun et al. 2008).

#### **1.5.5. USP7**

USP7 is a member of deubiquitinating enzymes (DUBs) i.e. enzymes involved in removing ubiquitin moiety from its target proteins i.e. p53 and Mdm2. It is also called as herpes associated ubiquitin-specific protease (HAUSP) (Komander, Clague et al. 2009). Many studies highlighted the role of USP7 in tumor biology because it maintains the levels of two important proteins *i.e.* murine double minute 2 protein (MDM2) a ubiquitin ligase and tumor protein (p53) (Brooks and Gu 2006). From in vivo and in

in vitro experiment it has been investigated that USP7 regulates p53 level by directly binding and removing ubiquitin moiety from p53. Therefore activation of USP7 maintains p53 level, triggers cell cycle arrest and stimulates apoptosis in a P53 dependent manner. Mdm2 and p53 are predominant targets for USP7 additionally several other proteins like FOXO4, histone 2B and PTEN have been identified as an important targets of USP7 and play critical role in different signaling pathways like oxidative stress induced signaling pathway (Van der Horst, de Vries-Smits et al. 2006, Song, Salmena et al. 2008) (Fig. 1.9).

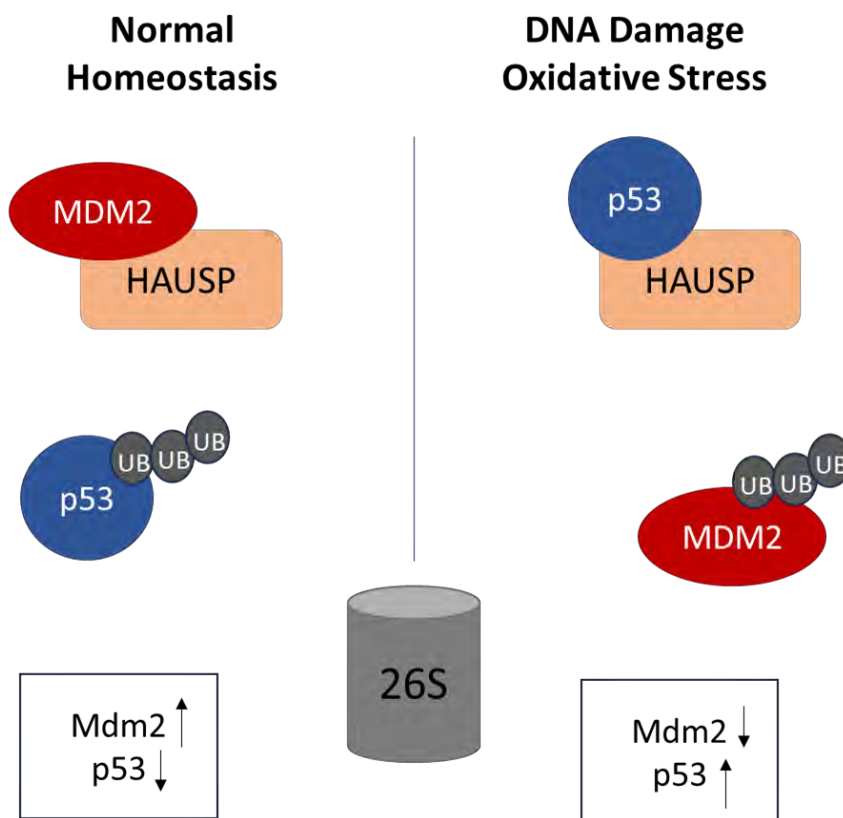


Figure 1.9. Possible Interactions between HAUSP, P53 and MDM2 adapted from (Brooks et al., 2007)

Under normal cellular conditions i.e. when cells are not exposed to any stress conditions, Mdm2 is considered as a major substrate for USP7 alternative to p53. USP7 thus regulates mdm2 levels by its deubiquitination likewise mdm2 stabilization and accordingly p53 ubiquitylation and degradation. Ubiquitylation of p53 is one of the main mechanisms for maintenance of p53 level within the cell (Brooks, Li et al. 2007). Recent studies show that mitochondrial deubiquitinase i.e. HAUSP is a crucial factor involved in apoptosis (Marchenko, Wolff et al. 2007). It has been highlighted that under

normal physiological condition, mdm2 is considered as a predominant partner of HAUSP. Mdm2, HAUSP and p53 are three major proteins required for maintenance of p53 level and mediating apoptosis in p53 dependent manner. Various cellular stress signals e.g. DNA damage blocks the interactions between USP7 and mdm2. There are numerous mechanisms that prevent USP7 and mdm2 interactions, one major is the induction of essential kinases e.g. ATM, its expression is induced in response to DNA damage. It destabilizes mdm2 and increase the level of free HAUSP. HAUSP then deubiquitinate and activate p53. p53 upon activation initiates apoptosis through induction of several of its downstream targets (Brooks, Li et al. 2007).

### 1.5.6. CDIP1

Cell Death Inducing p53 Target 1 (CDIP1) was analyzed as p53 target gene, also known as Cell Death Involved P53 target. Many studies have reported that its level raised upon DNA damage.

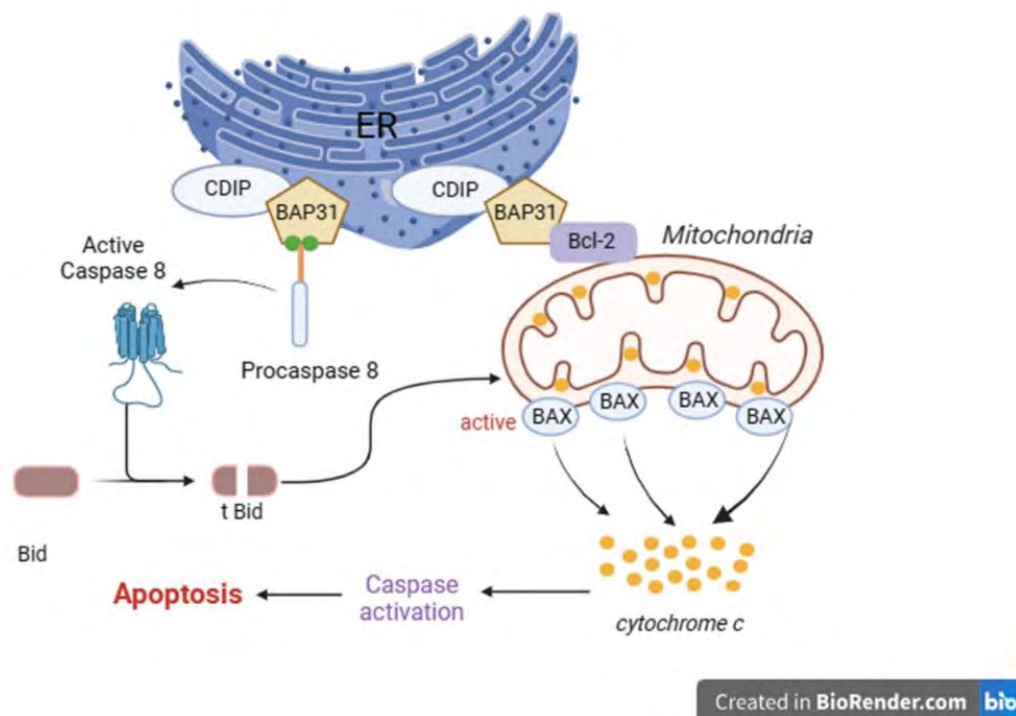


Figure 1.10. Role of CDIP1 in apoptosis adapted from (Namba, Tian et al. 2013)

Therefore, it is suggested that CDIP1 is the main downstream modulator of apoptosis which initiate apoptosis in a p53 dependent manner (Brown, Ongusaha et al. 2007). CDIP1 requires BAP31 for its proapoptotic activity. The interactions between CDIP1



and BAP31 results in BCL2 sequestration. Such interactions also trigger proapoptotic machinery (such as caspase 8 and bid activation) which results in Bax oligomerization and ultimately apoptosis (Fig. 1.10). CDIP1 and BAP31 associations therefore induce apoptosis through ER mediated stress and thus this strategy provides a positive mechanism for crosstalk between ER and mitochondria (Namba, Tian et al. 2013).

### 1.5.7. BNIP3

Bcl-2 19 kDa interacting protein (BNIP3) is a Bcl-2 protein family member which acts as a pro-apoptotic factor (He, Xiang et al. 2019). Expression level of BNIP3 can be increased by hypoxia inducing factor-1 (HIF-1) under stressful condition such as hypoxia (Burton and Gibson 2009, Ma, Chen et al. 2017). When expression of BNIP3 is induced then it is translocated to mitochondria and causes loss of mitochondrial membrane potential and enhances the production of reactive oxygen species (ROS) leading to cell death (Burton and Gibson 2009, Du, Li et al. 2017). BNIP3 induces apoptosis through JNK pathway by up-regulating Bax and down-regulating Bcl-2 and causes mitochondrial dysfunction leading to cell apoptosis (Jin, Li et al. 2018, He, Xiang et al. 2019). BNIP3 induces the translocation of Drp1 to mitochondria leading to mitochondrial fragmentation (Lee, Lee et al. 2011) (Fig. 1.11).

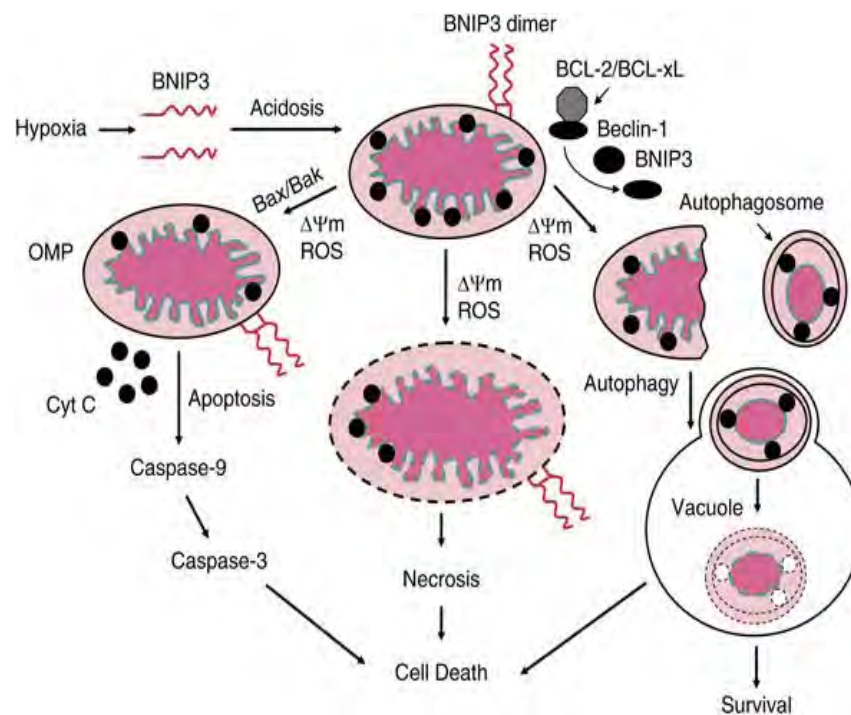


Figure 1.11. BNIP3 induced mitochondrial apoptosis (Lee, Lee et al. 2011)

### **1.5.8. PKC- $\delta$**

Protein Kinase C delta (or PKC- $\delta$ ) is a protein kinase C family member which act as a pro-apoptotic kinase. It is involved in various signaling pathways which regulate differentiation, growth and apoptosis in different cell types (Xu, Pan et al. 2019). PKC- $\delta$  is activated by various apoptotic stimuli including UV- radiations, DNA damaging agents and oxidative stress, and translocated to various subcellular organelles including mitochondria, nucleus, cell membrane, etc (Zhao, Xia et al. 2012). Its translocation to mitochondria induces apoptosis by the loss of mitochondrial membrane potential and activation of caspase-3 and -9 (White, Gao et al. 2010, Zhao, Xia et al. 2012, Xu, Pan et al. 2019). Under oxidative stress PKC- $\delta$  phosphorylate Drp1 and causes its translocation to mitochondria, promoting mitochondrial fragmentation leading to apoptosis. PKC- $\delta$  interacts with p53 and phosphorylate it and trigger p53-dependant apoptotic pathway (Lee, Kim et al. 2006). JNK pathway is also activated by PKC- $\delta$  through MAPKs in response to DNA damage indicating role of PKC- $\delta$  in apoptosis (Zhao, Xia et al. 2012).

### **1.5.9. B cell lymphoma 2**

Bcl2 (B cell lymphoma 2) has been identified as one of the important member of Bcl2 family of proteins that maintains apoptosis through vast mechanism. Previous studies have shown that BCL2 gene is the product of chromosome number 14 and 18 translocation and has been identified in B cell lymphoma 2 (Warren, Wong-Brown et al. 2019). Bcl2 acts as key player of apoptosis due to its interactions with numerous Bcl2 family members; it forms either heterodimers or homodimers with several proapoptotic and antiapoptotic members of Bcl2 family. Such interactions trigger proapoptotic machinery and ultimate result of which was apoptosis. Previous studies have shown that up-regulation of Bcl-2 can prevent apoptosis in cardiomyocytes by inhibiting the Bak/Bax association, enhance cell growth and improve heart function (Chen, Chua et al. 2001, Hardwick and Soane 2013).

### **1.5.10. Mitofusin 2**

Mitofusin 2 (Mfn2) gene encode the Mitofusin 2 protein which has GTPase activity and is located in outer mitochondrial membrane. Mfn2 is ubiquitous and highly expressed in heart and kidney (Chan 2006). It has a fundamental role in mitochondrial fusion and contribute to mitochondrial network maintenance. Mfn2 is also present in interfaces of

mitochondrial and endoplasmic reticulum and contributes to the release of calcium from ER to mitochondria for MPT (Pérez and Quintanilla 2017).

Mitochondria constantly undergo fusion and fission processes. Mitochondrial dynamics maintain the mitochondrial integrity and facilitating the merging of mitochondrial lipid bilayer membranes and DNA exchange in mitochondria (Chan 2006). Mfn2 is a major factor in oxidative stress mediated apoptosis and increased expression of mfn2 in cardiac cell leads to cardiomyocytes susceptibility to oxidative stress mediated apoptotic signal by inhibiting the activation of caspase-9 and Akt signalling (Shen, Zheng et al. 2007) (Fig. 1.12).

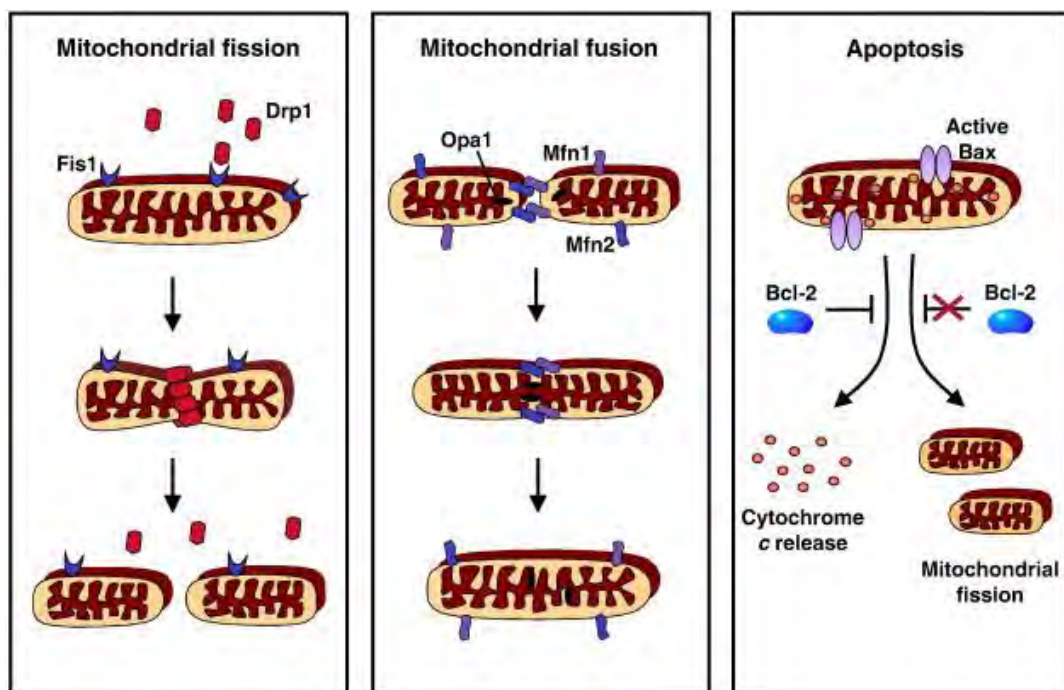


Figure 1.12. Mitochondrial fission and fusion (Sheridan and Martin 2010)

In normal cell Bak/Bax proteins are involved in mitochondrial fusion. Bax activate the GTPase assembly of mfn2 which leads to mitochondrial fusion (Karbowski, Norris et al. 2006). PGC-1 $\beta$  is peroxisome proliferator-activated receptor gamma coactivator-1  $\beta$ . It is positive regulator of normal expression of Mfn2 whereas PGC-1 $\alpha$  stimulate the expression of Mfn2 under the increased energy expenditure conditions (Soriano, Liesa et al. 2006, Liesa, Borda-d'Água et al. 2008). In cellular stress JNK and PTEN-induced putative kinase 1 (PINK1) phosphorylate mfn2, that eventually induce ubiquitylation of target Mfn2 for proteasomal degradation (Tanaka, Cleland et al. 2010, Chen and Dorn 2013).

Mfn2 deletion in cardiomyocytes reduces the ability for mitochondrial permeability transition (MPT) (Papanicolaou, Khairallah et al. 2011). MPT pores are activated by ROS and Calcium ion. MPT is regulated by MPTP (Mitochondrial permeability transition pore) and opening of MPTP cause depolarization and it is major determinant of myocytes loss (Pérez and Quintanilla 2017). These findings suggest that mfn2 regulates the calcium storage in intracellular environment which are involved in cardiac metabolic stress response, mitochondrial morphogenesis and programmed cell death (Papanicolaou, Khairallah et al. 2011). Mfn2 also inhibit the Bax and delays the apoptosis (Brooks, Wei et al. 2007).

#### **1.5.11. Regulation of Bcl2 and Mfn2**

Mitochondrial dynamics play a critical role in mitochondrial apoptotic signalling. Under stress condition cellular signalling pathways regulate the mitochondrial fusion and important for cell survival (Cervený, Tamura et al. 2007). In normal cell Bcl-2 and Bax positively regulate mitochondrial fusion process (Karbowski, Norris et al. 2006). During oxidative stress ROS causes the mitochondrial disruption (Peng, Rao et al. 2015). Peng *et al* demonstrated that upregulation of Mfn2 modulate the Bcl2/Bax ratio which plays a vital role in apoptosis induction. Downregulation of Bax and increased expression of Bcl2 prevent release of cytochrome c from mitochondria which ultimately block the activation of caspase 3 and procaspase 9. Mfn2 beyond its mitochondrial fusion also play a part in regulation of programmed cell death (Peng, Rao et al. 2015). Mfn2, Bcl2 and Bak are localized in outer membrane of mitochondria, interact with each other and modulate cellular signalling pathways. In previous studies it has been suggested that mfn2 interact with antiapoptotic Bcl2 family member which are important player of mitochondrial mediated apoptosis (Anilkumar and Prehn 2014). These interactions may lead to alterations in the mitochondrial membrane structure, block the MPT opening and activate the signalling cascade to inhibit release of proapoptotic proteins into the cytoplasm (Galloway, Lee et al. 2012).

Mfn2 and Bcl-2 are downregulated during oxidative stress conditions. There are certain regulatory molecules which are involved in downregulation of gene expression and translational repression by degrading the mRNA. Among multiple regulatory molecules, small microRNAs and small silencing RNAs have emerging role in negative

regulation of gene expression (Wu and Belasco 2008). In this study role of small microRNAs have been described.

## 1.6. Micro-RNAs

In 1993 discovery of miRNAs give a new dimension in the field of gene regulation in living organisms. These miRNAs belong to class of non-coding small RNA which do not translate into a protein. These are small RNA molecules comprising of 22 nucleotide strand and regulate gene expression by blocking the translation (Lam, Chow et al. 2015, Riffo-Campos, Riquelme et al. 2016). miRNAs targets the mRNAs, as seed sequence of miRNA at their 5' end of miRNAs binds with 3'UTR of mRNA to repress the expression at post transcriptional level (Nielsen, Shomron et al. 2007).

These small RNAs have changed the past views of biological landscape that defines gene regulation and play significant roles in physiological and pathophysiological processes. miRNAs regulate the biological processes ranging from embryonic to neoplastic developments (Bhaskaran and Mohan 2014). These miRNAs play significant role in several biological process such as apoptosis, tumorigenesis, differentiation, development, neural patterning, proliferation, immune responses and cell fate determination by up and down regulation of various genes. Dysregulation of these RNA molecules lead to several disorders such as cardiovascular diseases, diabetes, cancer and kidney disease etc. (Paul, Chakraborty et al. 2018). Therefore, miRNA can be a novel therapeutic approach in many diseases.

### 1.6.1 Micro RNAs Biogenesis and Mechanism of Action

The small non-coding miRNA ( 22 to 24nt in length) is transcribed from miRNA gene into primary miRNA (pri-miRNA) of several hundred nucleotide long transcript by RNA polymerase II (Bhaskaran and Mohan 2014). Primary microRNA transcripts are transcribed from either coding or non-coding region and are further processed by a multiprotein complex named as microprocessor to yield pre-miRNA (precursor miRNA) ~70- to 120- nucleotide long. Microprocessor complex contains highly conserved proteins drosha and pasha which have RNase III and double strand RNA (dsRNA) binding protein respectively (Fig. 1.13). It forms a functionally active complex. Precursor miRNA is transported into the cytoplasm with 5' end overhangs by exportin 5. Exportin 5 are Ran dependent nuclear receptors proteins (Lund, Güttinger

et al. 2004). In cytoplasm Dicer-1 RNase III enzyme act on pre-miRNA and process this transcript into ~18- to 23 nucleotide long mature miRNA. Two strands of miRNA are separated with the assistance of double stranded RNA binding proteins, kinase activators and transactivation response of RNA binding proteins (Lee, Feinbaum et al. 1993, Denli, Tops et al. 2004).

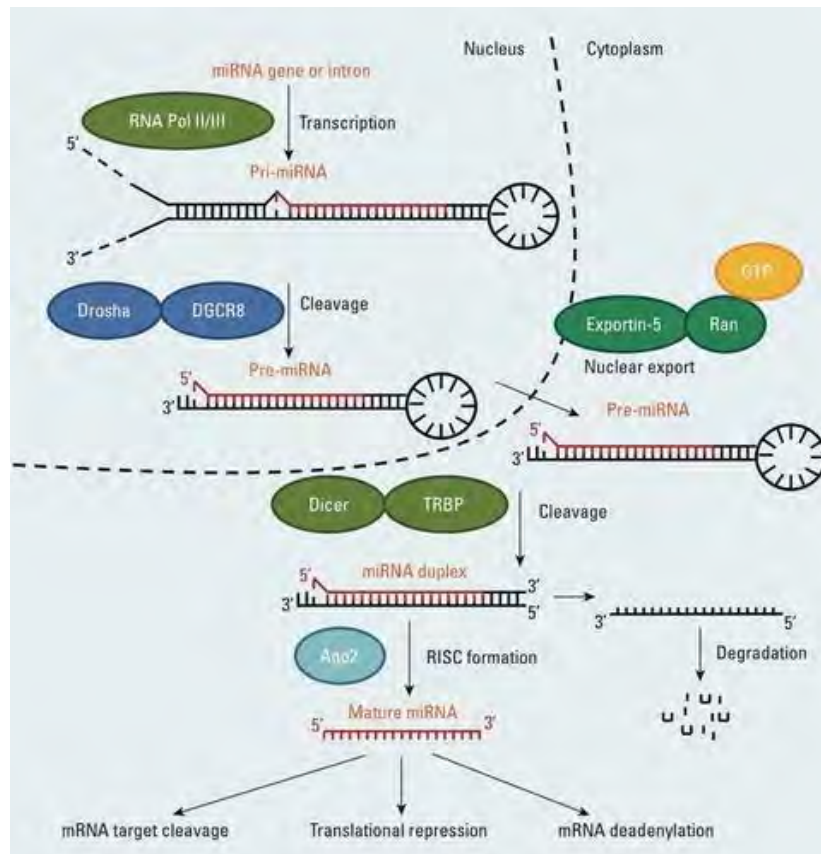


Figure 1.13. Biosynthesis of miRNA (Vrijens, Bollati et al. 2015)

. One of two strands is called as guide strand and other is passengers or miRNA strand. Guide strand is associated with argonaute proteins and directs miRNA towards the target messenger RNA (mRNA) (Castilla-Llorente, Spraggon et al. 2012).

The mechanism in which miRNA acts on mRNA is associated with RNA binding proteins which form a microribonuclear proteins (miRNP) complex. This complex is involved in the formation of RNA-induced silencing complex (RISC) (Schwarz, Hutvagner et al. 2003). Guide strand leads the complex to the mRNA by its complementary sequence binding and carries out the translation repression by degrading target mRNA. Argonaute proteins bound with miRNA with their target mRNA are thought to be stored as cytoplasmic bodies or also named as processing

bodies (P-bodies) for degradation or translational repression (Castilla-Llorente, Spraggon et al. 2012).

### **1.6.2 Role of miRNA in Different Pathologies**

In mammalian genome approximately 2200 miRNAs have been reported. One third of total human genome is regulated by the small micro RNAs (Urbich, Kuehbacher et al. 2008). These micro RNAs are transcribed from the exons, introns of coding and non-coding regions (Baskerville and Bartel 2005). These are involved in many cellular processes i.e. growth, metabolism, apoptosis, cell proliferation, differentiation and development (Berezikov and Plasterk 2005, Bilen, Liu et al. 2006). Micro RNAs seems to be expressed tissue-cell specific which illustrate their unique nature in physiological functions. MicroRNAs have potential to play role in development of various disease such as cancer, cardiovascular diseases, diabetes mellitus, neurodegenerative diseases, inflammatory diseases, liver and skin diseases. Figure 1.14 shows miRNAs are involved in multiple processes.

It has been reported that expression of micro-RNAs is altered in cancer. Several reports have revealed that most of miRNA encoding regions are located in cancer associated genomic sites (Reddy 2015). Over expression of miRNA acts as oncogenes and regulate the cell differentiation and apoptosis in cancer cells (Zhang, Pan et al. 2007). Micro RNAs profiling elaborate their role in several types of cancers such as colon cancer, blood cancer, hematological cancer, ovarian cancer, breast cancer, lungs and adenoma carcinomas. Wide ranges of miRNAs involvements in cancers reflect that these can be used in diagnosis and treatment for the cancer. Angiogenesis promote the cell proliferation in cancer cells and endothelial cells (Cao, Yu et al. 2016).

In past studies miRNA-16, miRNA-23a, miRNA-29, miRNA-21, miRNA-100, miRNA-221 and miRNA-222 dysregulated expression patterns was documented in endothelial cells in cancers (Poliseno, Tuccoli et al. 2006, Suárez, Fernández-Hernando et al. 2007).

In liver various types of cells are present and each type has different miRNAs expression profile. The most abundant miRNA in liver is miRNA-122 and has emerging role in liver diseases with liver inflammation, fibrosis and cirrhosis. Circulating forms

of miRNAs have great significance in diagnosing liver damage. They can serve as early biomarkers for liver disease and liver carcinoma (Szabo and Bala 2013).

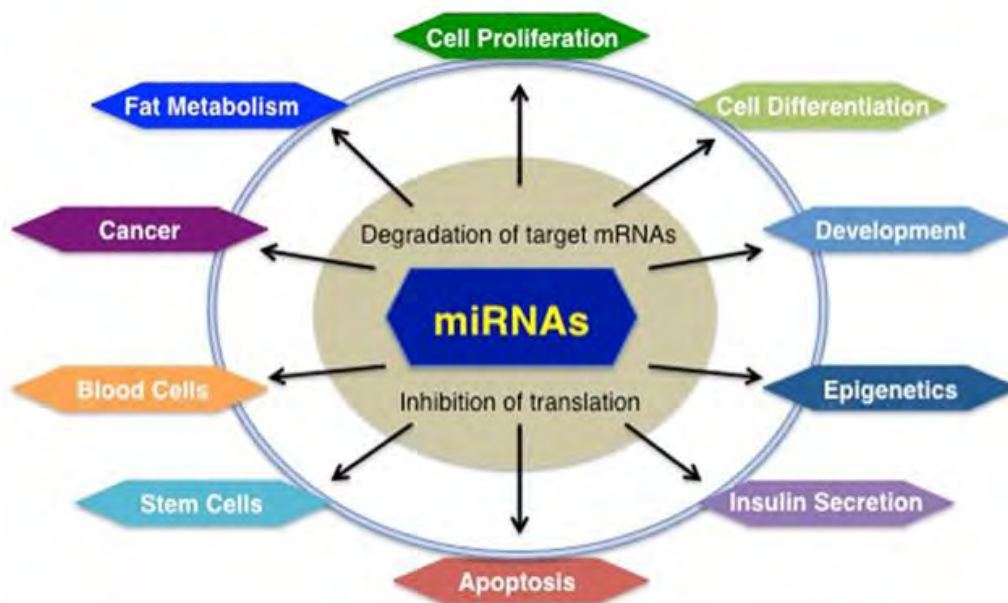


Figure 1.14. Role of miRNAs in different cellular processes (Cao, Yu et al. 2016)

MicroRNAs are also involved in hair follicle morphogenesis, autoimmune disease and other skin diseases (Zavadil, Narasimhan et al. 2007). Micro RNAs such as miR-146a, miR-203, miR-125b and miR-21 have potential to regulate the skin inflammatory diseases (Bostjancic and Glavac 2008). Micro RNAs have also significant importance in abnormal healing sequence and wound angiogenesis in chronic wounds (Shilo, Roy et al. 2007).

Formers studies have shown the miRNAs involvement in regulation of muscles development and muscles specific miRNAs including miR-206, miR-1 and miR-133 (McCarthy and Esser 2007). Duchenne muscular dystrophy and facioscapulohumeral muscular dystrophy (FSHD) have different expression of miRNA-382 and miRNA-381 (Eisenberg, Eran et al. 2007). Certain other documented studies have shown the significant increase in the expression of miRNAs-100, miRNAs-107 and miRNAs-103 in myopathies (Eisenberg, Alexander et al. 2009).

Discovery of miRNAs give a new dimension in diabetes and its associated complications. Micro RNAs are potentially involved in regulation of beta cell differentiation, insulin production, insulin secretion, lipid and glucose metabolism. Chronic hyperglycemia and diabetes may leads to change the expression of miRNAs in



certain types of muscles as, liver, kidney, heart and pancreatic tissues (Tang, Tang et al. 2008). MicroRNA-21, miR-29, miR-377, miR-216a, miR-200 and miR-192 targets the multiple genes which are involved in diabetic neuropathy (Kantharidis, Wang et al. 2011).

### **1.6.3 Role of miRNAs in cardiovascular disease**

Heart disease is the leading cause of morbidity and mortality of human in the world. These miRNAs are emerging therapeutics targets in wide ranges of cardiac pathologies. Several previous studies demonstrated the critical roles of miRNAs in heart diseases. These miRNAs get altered their expression and target the multiple genes which cause cell damage and cell death. Micro RNA has potential to target mRNA these can be used a novel therapeutic approach in many disease (Hu, Ma et al. 2016). Several types of miRNAs are reported in cardiovascular studies. Some of these are discussed here.

*Myocardial miRNAs:* Micro RNA-1 is highly expressed in cardiac and skeletal muscles and regulates the growth of cardiomyocytes in heart (Zhao, Samal et al. 2005). Both miRNA-133 and miRNA-1 are transcribed from the same loci of chromosomes and promote the myoblast proliferation (Chen, Mandel et al. 2006). These two miRNAs are oppositely regulated in cardiac hypertrophy. These miRNAs also assist in cardiac size and function (Care, Catalucci et al. 2007). During oxidative stress miRNA-1 promote apoptosis and miRNA-133 has anti-apoptotic effect and overcome the caspase-9 expression (Xu, Lu et al. 2007). Expression of miRNA-21 is increased in ischemic heart and its expression is downregulated during apoptosis (Ye, Perez-Polo et al. 2011).

*Cardiomyopathies:* miRNA-1 and miRNA-206 play a significant role in cardiac physiology and cardiogenesis (Shan, Lin et al. 2010). The upregulation of miRNA-133 in diabetic heart promote the expression of serum response factor (SRF) which may leads to the development of cardiac hypertrophy (Care, Catalucci et al. 2007). Cardiac hypertrophy is regulated by miRNA-22 by targeting Hdac4 and Sirt1 genes expression (Gupta, Halley et al. 2013).

*Heart failure:* Various types of miRNAs are reported in heart failure patients such as miR-122, miR-423p, miR-210, miR-622 and miR-499 (Ye, Perez-Polo et al. 2011). Micro RNA-499 is upregulated in acute heart failure (Corsten, Dennert et al. 2010).

*Coronary artery diseases (CAD):* Micro-RNAs are potential biomarkers in coronary artery disease. Fichtlscherer and his groups deliberated the expression profile of miRNAs in CAD patients. In their study the level of miRNA-133 and miRNA-208a were significantly increased in plasma of coronary artery disease patients. Whereas expression of miRNA-17, miRNA-126 and miRNA-92a, miRNA-155 and miRNA-145 were decreased in the plasma of diseased group (Fichtlscherer, De Rosa et al. 2010).

*Myocardial ischemia:* Cardiac ischemia and reperfusion is characterized by lack of blood and oxygen supply to heart. He *et al* studied the expression of miRNAs involved in cardiac ischemia. He reported 16 miRNAs which show the alteration in expression. Among these 16, 10 miRNAs showed increased expression whereas 6 were downregulated (He, Xiao et al. 2011). Micro RNA-499 is highly expressed in heart and its expression is downregulated during heart I/R injury (Lorenzen, Batkai et al. 2013). Change in expression of miRNAs in early phase of reperfusion injury is cause the myocardial apoptosis and oxidative stress. There expressional and functional analysis of miRNAs can illustrate the mechanism of reperfusion injury and myocardial infarction (Choi, Cha et al. 2014).

#### **1.6.4 miRNA-15a-5p**

Micro RNAs are highly conserved regulatory molecules. Micro RNA-15/107 family is highly conserved family of miRNAs. It has been transcribed from chromosomes 13q14 (Lendeckel). This family has comprised of ten family members including miRNA-16-5p, miRNA-103a, miRNA-646, miRNA-195-5p, miRNA-503-5p, miRNA-497-5p, miRNA-424-5p, miRNA-107, miRNA-15b-5p and miRNA-15a-5p (Finnerty, Wang et al. 2010). These mature miRNAs are highly expressed in eleven human tissues including heart, liver, lungs, kidney, thalamus, cerebral cortex, primary visual cortex, frontal cortex, spleen, skeletal muscles and stomach (Wang, Danaher et al. 2014). Potential overlapping between these members with each other is the similar seed sequence “AGCAGC” for binding to their target genes. Previous documented data has been shown that different members of miRNA-15/107 family are involved in cancers, osteoarthritis, benign and malignant tumors and cardiac diseases (Huang, Liu et al. 2015).

MiRNA-15a-5p negatively regulate cell survival and promote apoptosis (Chen, Wu et al. 2017). It is the member of miRNA-15/107 family. In this study database TargetScan was used to find the target genes of miRNA-15a-5p ([http://www.targetscan.org/vert\\_72/](http://www.targetscan.org/vert_72/)).

### **1.6.5. miRNA-214-3p**

miRNA-214 was first recognized for its role in apoptosis of tumor cells (Cheng, Byrom et al. 2005). miR-214 has been found dysregulated in various disorders including cancer, ischemic stroke and cardiovascular diseases (Jan, Khan et al. 2017). Role of miR-214 has been considered as multifunctional. Over expression of miRNA-214 decrease neuronal apoptosis significantly by reducing Bax protein, increasing expression of Bcl2, consequently decreases the release of cytochrome c from mitochondria and caspase cascade inactivation leading to ischemic stroke (Gao, Zhang et al. 2017). It has cardioprotective effects on cardiomyocytes by decreasing PTEN expression (Wang, Ha et al. 2016).

### **1.7. Therapeutic Strategies**

Major cause of oxidative stress is the elevated level of reactive oxygen species in our body. Researchers have introduced numerous strategies to neutralize the continuous production of ROS. Naturally, neutralizing molecules in our body are called as antioxidants. Antioxidants have the ability to scavenge the oxidants species in our body to regulate the normal physiological conditions. There are various naturally occurring antioxidant molecules in our body including Catalase, Glutathione, Peroxidases and Superoxide Dismutase which have enzymatic activity. Non enzymatic antioxidants in our body includes vitamin A, C, E, flavonoids, carotenoids, melatonin and N-acetyl cysteine (NAC) (Kabuto, Hasuike et al. 2003). Many natural and synthetic chemicals are used as a therapeutic agent. In this study melatonin is used as therapeutic agent which is a naturally occurring hormone in living organisms (Nair, Suresh et al. 2018).

Different strategies have been employed to cure neuro and cardiovascular disorders. Nano medicine is one of the emerging field in which nanomaterials are employed for the detection, treatment and prevention of numerous disorders including neurological disorders (Modi, Pillay et al. 2010). Other novel strategies include drug designing, neurogenesis, stem cell transplant and clinical pharmacology. Targeting an antioxidant

to mitochondria is another strategy against cardiac pathologies (Adlam, Harrison et al. 2005). Induction with heat shock proteins and treatment with micro RNA are some other therapeutic strategies against oxidative stress (Kalmar and Greensmith 2009, Ali, Mushtaq et al. 2019).

## 1.8. Antioxidant therapies

Antioxidants are the stable molecules that play role in reducing cellular damage by neutralizing free radicals (Lobo, Patil et al. 2010). They have ability to scavenge free radicals. Antioxidants which are produced during normal body metabolism include glutathione and ascorbic acids (Shi, Noguchi et al. 1999). Antioxidative defense mechanism comprise of enzymatic and non-enzymatic mechanisms (Rice-Evans and Diplock 1993, Augustyniak, Bartosz et al. 2010). In enzymatic mechanism antioxidant enzymes detoxify ROS through enzymatic cascade leading to detoxification (ČIPAK GAŠPAROVIĆ, Lovaković et al. 2010). It is a chain breaking mechanism by which it donates electron to free radical. Non-enzymatic system is considered as a first line of defense. It involves removal of ROS by quenching initiator catalyst. Vitamin E ( $\alpha$ -tocopherol), vitamin C (ascorbic acid), and B-carotene are the examples of non-enzymatic antioxidants. There is a need of new compounds having antioxidative potential, to treat stress mediated pathologies. The use of antioxidant polymer as a treatment is another strategy to resolve this issue. Oxidative stress due to BPA can be combat by using antioxidative compound, melatonin, as a therapeutic agent (Anjum, Rahman et al. 2011).

### 1.8.1 Antioxidant Therapy by Melatonin

Melatonin is natural hormones, in 1956 it was identified and isolated from pineal gland of cow (Lerner, Case et al. 1959) (fig 1.15). It is an indoleamine known as 5-methoxy-N-acetyltryptamine (Hardeland, Pandi-Perumal et al. 2006).

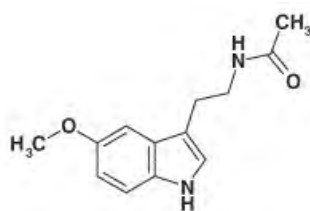


Figure 1.15. Chemical structure of Melatonin (5-methoxy-N-acetyltryptamine) (Hardeland, Pandi-Perumal et al. 2006)

Primary source of melatonin synthesis is pineal gland. Other organs also synthesize small amount of melatonin i.e. retina, immune cells, reproductive tract, skin and gastrointestinal tract (GI) (Acuña-Castroviejo, Escames et al. 2014). Melatonin is synthesized from essential amino acid tryptophan by four enzymatic steps. L-tryptophan is converted into the melatonin by following hydroxylation, decarboxylation, acetylation and methylation reaction respectively (Wang, Erlandsen et al. 2002). Synthesis of melatonin is described in figure 1.16.

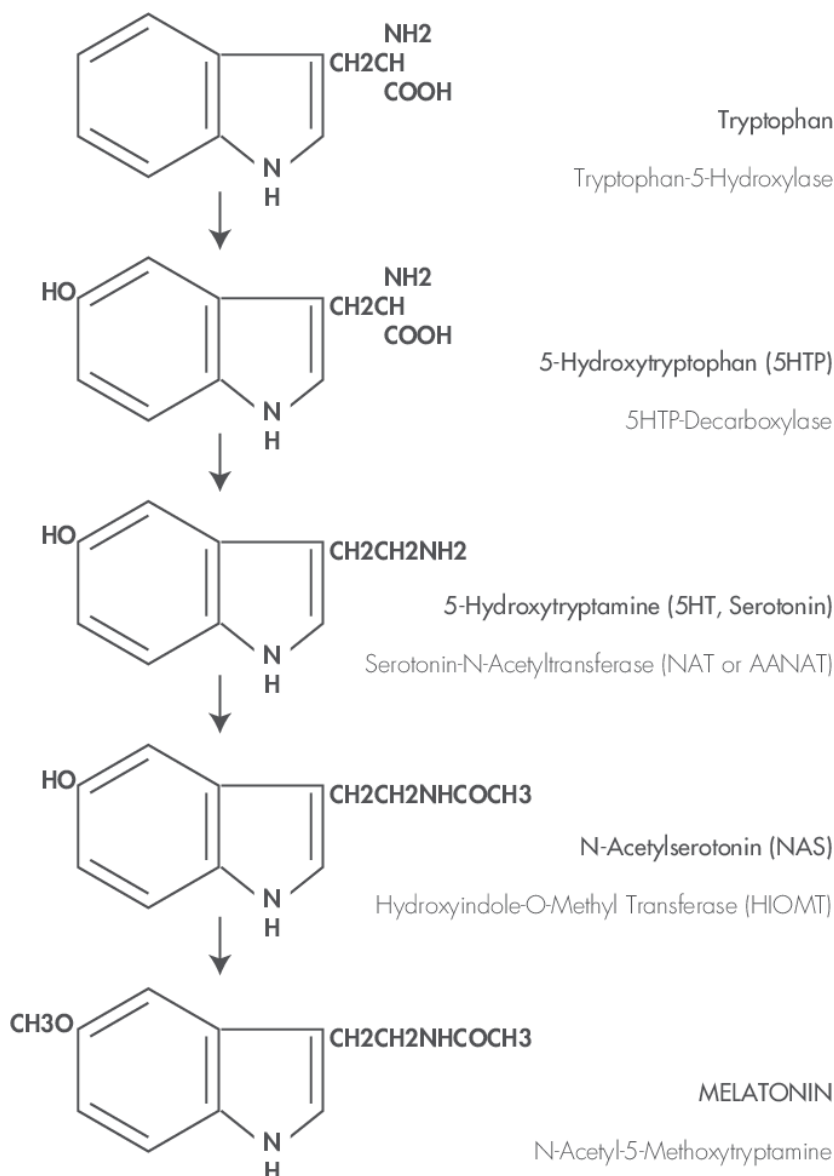


Figure 1.16. Synthesis of Melatonin (Srinivasan, Zakaria et al. 2012)

In 1993 melatonin has been reported as strong free radical scavenger (Tan 1993). It has ability to upregulate antioxidant signalling of enzymes and downregulation of pro-

oxidant enzymes. Melatonin on remarkable basis produce protective metabolites for detoxification of free radicals and also known as non-enzymatic antioxidant (Hardeland 2005). Melatonin also plays physiological roles in regulation of circadian and endocrine rhythm, anti-inflammation, regulation of sleep, immune responses, retinal physiology, fibrosis, thermo regulation and antioxidant activity (Hu, Ma et al. 2016, Majidinia, Reiter et al. 2018, Ali, Mushtaq et al. 2019). Physiological functions of MiRNAs are shown in figure 1.17.

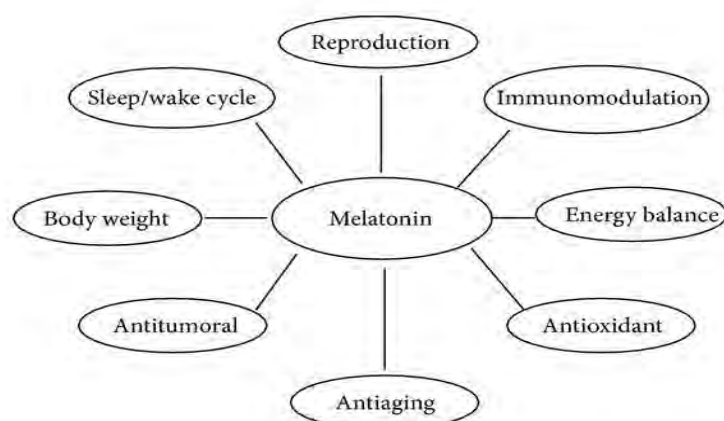


Figure 1.17. Physiological function of Melatonin (Garrido, Terron et al. 2013)

Various studies have been reported that melatonin activities are associated with G-protein couple receptors in the cell membranes of animals (Reiter, Mayo et al. 2016). These receptors are known as melatonin receptor type 1 (MT1), melatonin receptor type 2 (MT2) and melatonin receptors type 3 (MT3). MT3 is also called as quinine reductase 2 and reported in rabbit and hamsters but it is not yet reported in human being (Nosjean, Ferro et al. 2000, Benleulmi-Chaachoua, Chen et al. 2016, Jockers, Delagrangé et al. 2016). Melatonin through MT1 and MT2 receptors activation negatively regulates adenylyl cyclase and inhibits cyclic adenosine monophosphate (cAMP) signalling and triggers the phospholipase C signalling which in turn increases the calcium level in cell and activates downstream signalling events (Tarocco, Carocchia et al. 2019).

There has been reported that these signalling events upregulate the transcriptional activities of antioxidant and downregulate the pro-oxidant enzymatic activities. MT2 receptor activation hinders the guanylyl cyclase and inhibits cyclic guanosine monophosphate (cGMP) formation and stimulate phospholipase C activity (Reiter, Mayo et al. 2016, Tarocco, Carocchia et al. 2019).

### 1.8.2 Antioxidant Therapy by N-acetyl cystine

N-acetyl cystine is an acetylated cystine compound having nitrogen atom bounded by an acetyl group. It is a derivative of naturally occurring amino acid L-cystine. It is well tolerated, inexpensive and safe medication available commercially since long time (Mokhtari, Afsharian et al. 2017). Although it is not a naturally occurring antioxidant, but it possesses most of the characteristics of natural antioxidant. It is involved in playing role as a precursor of glutathione a naturally occurring antioxidant (Elgindy, El-Huseiny et al. 2010). It has wide range applications *e.g.* it is involved in biogenesis of glutathione. In our current study we employed NAC because, it is a direct scavenger of ROS and free radicals generated by BPA. Therefore, it has potential to act as an adjuvant therapy in combination with some other predictable therapies against most dreadful diseases generated by the ROS which include cardio and neuro disorders, hepatic toxicity *etc.* (Shahin, Hassanin et al. 2009, Bavarsad Shahripour, Harrigan et al. 2014, Tardiolo, Bramanti et al. 2018). The most striking property of NAC is, it promotes detoxification. Therefore, it helps to prevent against oxidative stress related toxicities and ultimately cause apoptosis. It reduces mitochondrial membrane depolarization as well as it increases the intracellular level of glutathione (Amin, Shaaban et al. 2008).

In cellular system NAC plays a protecting role *via*  $\text{Na}^+$  dependent alanine-serine-cystine (ASC) pathway (Ishige, Tanaka et al. 2005, Bavarsad Shahripour, Harrigan et al. 2014). NAC can enter the cell without the assistance of any membrane transporter. As it is a membrane permeable cystine precursor. When it enters to the cell, NAC is hydrolyzed and releases cystine to the cell. Synthesis of GSH takes place by a reaction which is co-catalyzed by the action of two enzymes GSH synthetase and  $\gamma$ -glutamyl cystine synthetase. The synthesis is highly dependent on the availability of limiting reagent, in this case cystine is a limiting precursor. So, GSH inhibits the enzyme  $\gamma$ -glutamyl synthetase via feedback from the product of GSH (Bavarsad Shahripour, Harrigan et al. 2014). GSH reductase along with NADPH is required for maintaining of intracellular GSH in its thiol form. GSH functions to protect against oxidative stress generated by ROS.

### 1.9 Tetra-aniline based Synthetic polymers

The use of antioxidant polymer as a treatment is another strategy to neutralize the ROS generated pathological issues. They have a broad range of applications *e.g.* they can be used in regenerative medicine, drug delivery or tissue engineering *etc.* (Chen, Qin et al. 2018). They are incorporated with small antioxidant molecule *i.e.* vitamin E or vitamin C and delivered to a specific tissue site (van Lith and Ameer 2016). Among antioxidant polymers phenolic polymers are reported to have ROS scavenging properties (Jabeen, Janjua et al. 2017). They can attenuate oxidative stress mediated pathologies. In the present study Es-37 and L-37 compounds have been used as a treatment against cardiotoxicity. It is synthesized *via* poly condensation reaction between PEG and TANI (tetra aniline) along with the dropwise addition of fumaryl chloride and tri ethyl amine in DCM at 0°C. These polymers are well characterized by using different techniques. These are composed of tetra aniline and polyethylene glycol (PEG). Tetra aniline due to its electroactive nature gives the compound antioxidant property where as PEG is well known for its biocompatibility. It has known to be involved in cardiac repair. It also protects against mitochondrial dysfunction, oxidative stress and apoptosis and ultimately plays role in cell survival. PEG is also involved in prevention against neuronal apoptosis *i.e.* it inhibits release of cytochrome c and caspase activation (Kitchens, Konkle et al. 2013). It gives the polymer hydrophilicity and increase the circulation time of adhered drug (Sheikhpour, Barani et al. 2017). Whereas fumarate moiety makes Es-37 a biodegradable as well as make it able to cross link (Manavitehrani, Fathi et al. 2016). Together these moieties make Es-37 and L-37 nontoxic, biodegradable and electroactive terpolymers which show antioxidant potential. Therefore, Es-37 and L-37 (Fig. 1.18) can be used as a potential treatment to combat ROS generation in stress mediated pathologies.



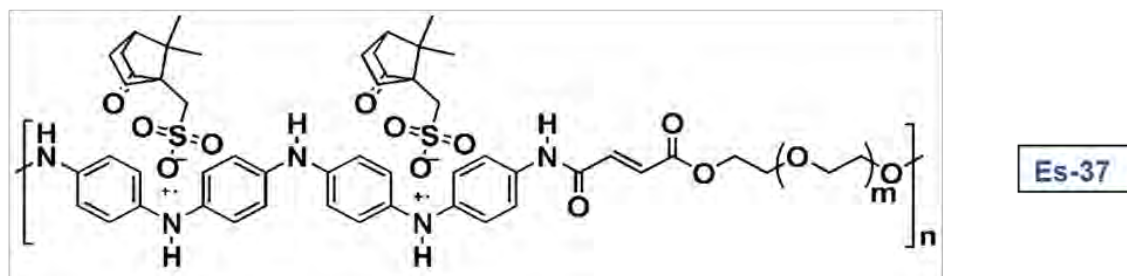
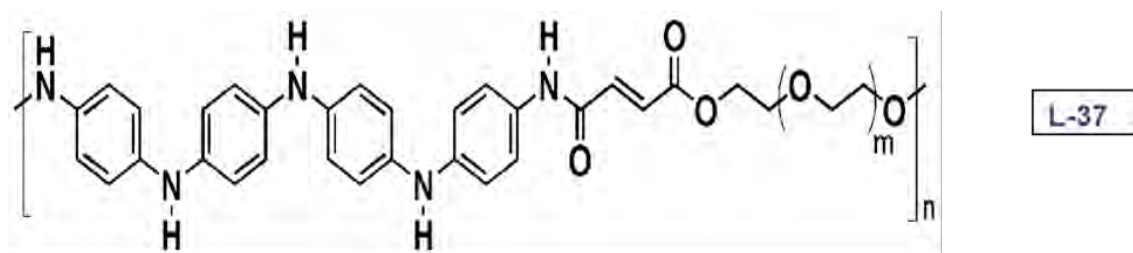


Figure 1.18. Chemical Structure of Synthetic polymers

### 1.10 *Pistacia integerrima*

*Pistacia integerrima* (P.I) is a dioecious tree which belongs to *Anacardiaceae* family. It is widely distributed in Asia, commonly found in Pakistan, East Afghanistan and Himalaya from Indus to Kumaon (Pant and Samant 2010) (Fig. 1.19).



Figure 1.19. Gall of *Pistacia integerrima* (Shuaib, Ali et al. 2017)

This plant is commonly known as zebrawood and Crab's claw while in Pakistan commonly called as Shnai, Thoak and Khanjar (Orwa, Mutua et al. 2009). *Pistacia*

*integerrima* is well identified due to galls present on the plant leaves and petioles formed by the attack of insect ‘aphis’ of Pemphigus species (Bibi, Zia et al. 2015). The infestation of plant leaves and petioles by this insect change them into hard, rugose, horn-shaped, hollow and pale greenish brown galls which are crucial for traditional medicines as they are the storage sites for secondary metabolites (Ullah, Mehmood et al. 2012).

### 1.10.1. Ethnobotany

*Pistacia integerrima* is a medicinal plant traditionally used for the treatment of various diseases including cough, vomiting, appetite, asthma, phthisis, jaundice, dysentery and liver disorders (Mamoon, Mir et al. 2011, Ullah, Mehmood et al. 2012). Galls of *Pistacia integerrima* are aromatic in nature, have terebinthine odour and slightly bitter taste (Ahmad, Waheed et al. 2010). They have expectorant, antiemetic, antirheumatic, appetizer, bronchodilator and diuretic effects (Jamil, Ahmad et al. 2002, Ahmad, Waheed et al. 2010). They are used as remedy for phthisis, cough, asthma, chronic bronchitis, hiccough, dysentery, vomiting, fever, psoriasis, skin diseases, to increase the appetite, diarrhoea, hepatitis and liver disorders (Ahmad, Waheed et al. 2010, Uddin, Rauf et al. 2011). Galls together with other drugs are also used to treat scorpion sting and bite of snake. Bark extract of *Pistacia integerrima* is used for the treatment of hepatitis as well as jaundice (Islam, Ahmad et al. 2006). Resins of stem of *Pistacia integerrima* can be used for wound healing. Fruits of *Pistacia integerrima* are used to cure liver diseases (Mamoon, Mir et al. 2011). Stems and branches of this plant can be used as ornamental wood, fuel wood and construction while the leaves as cattle fodder (Hussain, Shah et al. 2007).

### 1.10.2. Biological Activities of *Pistacia integerrima*

*Pistacia integerrima* has a wide range of biological activities including antioxidant, antimicrobial, anticancer, anti-inflammatory, analgesic, hypouricemic and radical scavenging activities (Ahmad, Farman et al. 2008). *Pistacia integerrima* shows a significant antioxidant activity because of its phenolic constituents and play an important role in reducing oxidative stress (Naseem Saud, Muhammad et al. 2006, Bibi, Zia et al. 2015) (Fig. 1.20).

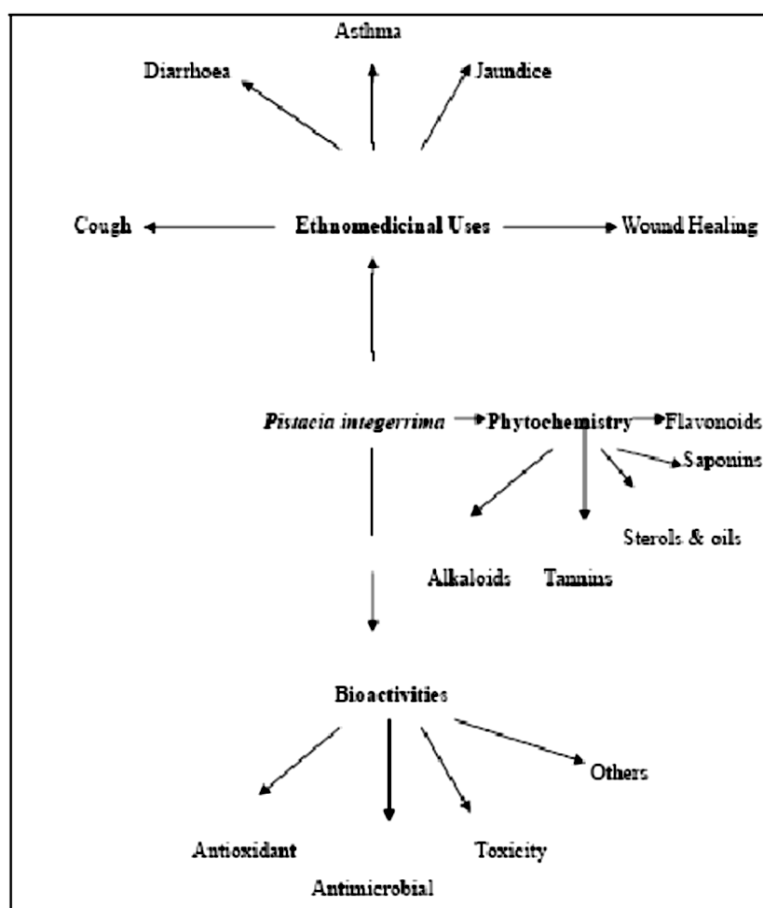


Figure 1.20. Schematic diagram of biological activities of *Pistacia integerrima* (Bibi, Zia et al. 2015).

Gall and leaf extract of *Pistacia integerrima* have significant antioxidant activity. Leaves of *Pistacia integerrima* show high xanthine oxidase inhibitory activity due to the presence of polyphenols, tannins and flavonoids. Due to its xanthine inhibitory activity it plays an important role in suppressing uric acid in case of hyperuricemia (Naseem Saud, Muhammad et al. 2006, Ahmad, Farman et al. 2008). *Pistacia integerrima* exhibit antifungal and antibacterial activities. Stem extract of *Pistacia integerrima* shows anti-bacterial activities against various types of pathogenic bacteria including *Salmonella Setubal*, *Pseudomonas picketti*, *Bacillus subtilis* and *Staphylococcus aureus* (Bibi, Zia et al. 2015). Methanolic bark extract also shows excellent antimicrobial activity. *Pistacia integerrima* has proved to have anticancer and antitumor activities. Stem extract of *Pistacia integerrima* is cytotoxic against breast cancer. Gall and bark extract of *Pistacia integerrima* have significant anti-inflammatory and analgesic activities. *Pistacia integerrima* extracts were also found effective to treat the hepatic injury in the rats treated with CCl<sub>4</sub>. Leaves and galls extract

of *Pistacia integerrima* also show anti-nociceptive and analgesic activities (Ahmad, Waheed et al. 2010, Ullah, Mehmood et al. 2012, Bibi, Zia et al. 2015). Extracts of bark possess anti gastrointestinal motility activity. Leaf extracts were also observed to have free radical scavenging activity (Ahmad, Farman et al. 2008, Shafiq, Muhammad et al. 2011).

*Pistacia integerrima* has been found to have a wide range of phytochemicals such as alkaloids, flavonoids, terpenoids, carotenoids, catechins, sterols, tannins, saponins and essential oils so it can serve as a candidate for synthetic drugs (Ahmad, Waheed et al. 2010, Uddin, Rauf et al. 2011).

### **1.11 Cancer**

Cancer is a genetic disorder that appears when the instruction in cellular DNA is altered, the leading process of alteration is through the irregular patterns of gene expression leading towards abnormal multiplication of cells. Different internal and external factors are involved in the deregulation of the cell signaling pathways, that have fundamental role in cell growth and decide its fate (Bild, Yao et al. 2006). Cancer can be either malignant or benign. In benign form, cells divide aberrantly but they do not invade other organs of the body. While in malignant form, cancerous cells have potential to proliferate beyond their site of origin (Fayyad, Piatetsky-Shapiro et al. 1996).

### **1.12 Breast Cancer**

Breast cancer (BC) is classified as irregular proliferation and multiplication of cells in the breast tissue (Khuwaja and Abu-Rezq 2004). The inner lining of milk ducts and breast lobules (distribute milk to milk ducts) are generally affected by breast cancer known as ductal carcinoma and lobular carcinoma respectively (Sharma, Dave et al. 2010). The disorder may be developed either as a result of hereditary factors or environmental factors (Mieszkowski 2006). In women, breast cancer (BC) is nearly 100 times more common than men (Sharma, Dave et al. 2010). In men breast carcinoma is an unusual disorder with a frequency of 1 case per 100,000 people in Europe (Eggemann, Ignatov et al. 2013). Breast cancer in male covers less than 1% of all cancers in men (Korde, Zujewski et al. 2010). Although, the prevalence of breast cancer in male is constantly rising (Giordano, Cohen et al. 2004).

### **1.13 Worldwide Prevalence of Breast Cancer**

Globally, the second most widespread and familiar cancer in women is breast cancer as compared to all other cancers. Breast cancer prevalence is at peak in Western Europe and United States however it is now expanding abruptly in Africa, Asia and Latin America. Approximately, 1.1 million new cases of breast cancer have been reported in the year 2004 (Chaurasia, Pal et al. 2018). Annually, about 1.7 million fresh cases of breast cancer are being diagnosed worldwide (Siegel, Miller et al. 2015). In 2017, approximately 252,710 women with invasive breast cancer and about 2,470 men were identified with breast cancer in United States only (Bahar, Kim et al. 2016). In 2018, about 2,088,849 new patients of breast cancer were diagnosed and around, 626,679 people died of breast cancer globally (Bray, Ferlay et al. 2018). By 2030, the number of breast cancer patients can be increased up to 3.2 million annually (Ginsburg, Bray et al. 2017).

### **1.14 Global Breast Cancer Related Mortality**

Breast cancer is second leading factor of cancer related deaths among women worldwide with poor prognosis and about 521,900 people died in the year 2012 only. About 60% of cancer related deaths occur in under developed regions of world compared to cancer deaths worldwide (Siegel, Miller et al. 2015). Metastasis of cancer cells is considered to be the prime cause of breast cancer related mortality (Weigelt, Glas et al. 2004). Annually, about 45,000 women died of distant metastasis of breast cancer cells in United States only (Parker and Sukumar 2003).

### **1.15 Breast Cancer Prevalence in Pakistan**

In comparison to Western population breast cancer is one of the most familiar disorder among Pakistani population (Mahmood, Rana et al. 2006). One out of every nine women in Pakistan experiences breast cancer that is of utmost prevalence in Asia (Sohail and Alam 2007). The prevalence of breast cancer in Pakistani female patients is about 46.8%, according to the data declared by Shaukat Khanum Memorial Cancer Hospital & Research Centre' (Annual Cancer Registry Report). Frequency of spreading breast cancer is abnormally rising in Pakistani women. On the basis of molecular classification, luminal B subtype (ER+ PR+ HER2+) of breast cancer is more commonly diagnosed among young Pakistani women which is highly aggressive form and has poor prognosis as compared to luminal A subtype (ER+PR+HER2-) and is the

main source of breast cancer related deaths among Pakistani population (Hashmi, Aijaz et al. 2018). In Pakistan, approximately 90,000 victims of breast cancer have been recorded but unfortunately, there was no proper detection of cancer types due to the unavailability of the proper markers. Breast cancer accounts for 38.5% of all cancers in Pakistan. Approximately 10% of breast cancer cases were recognized and cured while about 75% breast cancer patients could not take any treatment and died within a time period of five years. Survival rate of breast cancer patients improves up to 90% by early diagnosis (Spurdle, Couch et al. 2014).

### **1.16 Categories of Breast Cancer**

Breast cancer types are usually described by region in which it develop and its confinement within specific cell. Different classes of tumors may originate within distinct regions of the breast. Mostly, breast tumors occur due to benign (non-cancerous) variations within breast tissue. For instance, fibrocystic variation in the breast tissue is a non- cancerous (benign) process which triggers the development of cysts (aggregated masses of fluid), fibrosis (formation of damage connective tissue), granular areas and breast pain in women (Sharma, Dave et al. 2010). About 50-75% of breast cancers develop in the milk ducts, between 10-15% develop in the lobules (milk producing glands) and a few develop in other breast tissues (SJ 2000).

### **1.17 Risk Factors for Breast Cancer**

Several factors are involved in breast cancer development such as age, obesity, menstrual history i.e. delay menopause and premature menarche, delay first full-term pregnancy, nulliparity, no breast feeding (Biswas and Kapoor 2005). Hormonal replacement therapy, contraceptive pills, alcohol consumption, lack of exercise, radiation exposure, excessive dietary intake, sedentary way of living, prolonged exposure to estrogen can also contribute in breast cancer development (Sharma et al., 2010). Genetic irregularity such as mutation and abnormality of BRCA1 and BRCA2 (tumor suppressor genes) is main factor of breast cancer development. Women with BRCA1 mutation have increase chance of breast cancer development at young age (Chandira, Prabakaran et al. 2019). Xenoestrogen such as Bisphenol A (BPA) (synthetic estrogen) is present abundantly in the environment and prolonged exposure to this chemical is main factor of breast cancer development (Olsen, Meussen-Elholm et al. 2003).

### 1.18 BPA and Risk of Breast Cancer

BPA is recognized as xenoestrogen (mimicking endogenous estrogen) and reported as endocrine disrupting chemical (EDC) by US Environmental Protection Agency (EPA) and World Wide Fund for Nature (WWF) and declared as a social, environmental and universal problem (Mohapatra, Brar et al. 2010). EDCs are natural or synthetic compounds, abundantly present in the environment and main cause of derailment of endocrine system by interacting with natural hormones in the body (Gore, Chappell et al. 2015). BPA is involved in the development of hormone-dependent cancers like prostate cancer, breast cancer and ovarian cancer. Polycystic ovary syndrome (PCOS) which is metabolic disorder, diabetes and heart diseases are also developed by BPA due to its estrogen-like activity (Liu, Yu et al. 2013). Low-dose of BPA, is prime source of breast cancer development in females especially during crucial phase of breast growth as breast tissue is not well-organized at that stage (Birnbaum and Fenton 2003). Exposure of human breast cancer cell line to BPA, causes cellular multiplication and oxidative stress (Wetherill, Akingbemi et al. 2007). BPA is also capable of generating neoplastic modifications in human breast epithelial cells *in vitro* (Fernandez and Russo 2010). BPA has potential to alter the development of mammary gland at fetal stage and is the leading cause of gynecomastia (enlarged male breast tissue) development in men (Nakao, Akiyama et al. 2015). A large number of genes are associated with breast cancer development either by mutation, downregulation or overexpression. The present study aims to investigate the expression of certain breast cancer genes which are dysregulated by BPA.

### 1.19 Cross-talk between Tp53, WNT1 and ZEB1 Signaling Pathways

TP53 gene encodes the protein p53, and the first tumor suppressor gene to be identified in 1979 (Vogelstein, Lane et al. 2000). Approximately, 50% of all human cancers have mutated TP53 gene expression (Sigal and Rotter 2000). p53 sustains genomic integrity by protecting the cell from tumorigenesis and *via* halting the proliferation of cells within damaged DNA that's why known as 'the guardian of the genome' (Lane 1992). Li-Fraumeni syndrome occurs in the individuals having germ-line p53 mutation which increases the risk of breast cancer progression. About 20% of all breast cancer cases contain p53 mutation (Malkin, Li et al. 1990). Many factors are required for p53

activation as UV-radiations, x-rays, oncogenic signals, cellular stress like oxidative stress and hypoxia.

Wnt1 gene is identified as mammary oncogene in 1980, while conducting breast cancer research on mouse models. In mouse it is designated with small letters (wnt1) (Nusse and Varmus 1982). WNT1 is also involved in breast cancer development in humans and designated with capital letters (WNT1). WNT1 gene contains instructions for the production of a cysteine-rich glycoprotein, and it is a member of 19 genes superfamily (Van Amerongen 2012, Constantinou, Pace et al. 2016).

ZEB1 (zinc finger E-box binding protein 1) is a familiar transcription factor that initiates EMT (epithelial to mesenchymal transition) process equally important for physiological and pathological mechanisms (Eger, Aigner et al. 2005, Zhang, Sun et al. 2015). Overexpression of ZEB1 induces EMT mechanism in breast cancer by reducing expression of E-cadherin protein (cell adhesion protein) gives metastatic properties to cancerous cells and associated with poor prognosis (Chu, Hu et al. 2013, Jang, Kim et al. 2015, Ye and Weinberg 2015).

BPA causes the activation of WNT4 gene necessary for breast cancer development, similarly BPA may also involve in the activation of WNT1 gene (cousin of WNT4) and lead towards breast cancer development through the activation of  $\beta$ -catenin dependent (canonical) pathway (Faivre and Lange 2007, Ayyanan, Laribi et al. 2011). BPA initiates the activation of Akt/Pi3k and mTOR pathways by binding to GPR30 (G protein-coupled receptor for estrogen) lead towards multiplication and migration of cancer cells (Bouskine, Nebout et al. 2009). Activated Akt/Pi3k is involved in the phosphorylation of MDM2 (murine double minute 2) gene causing overexpression of MDM2 mRNA and higher accumulation of MDM2 protein within cell, overexpressed MDM2 protein then translocated to the nucleus where it directly attacks on p53 by binding to transactivation domain of p53 which ultimately suppress or downregulate the p53 expression in breast cancer and generates anti-apoptotic signals involve in the proliferation of cancer cells (Iwakuma and Lozano 2003, Wade, Li et al. 2013). Mutated p53 is involved in the stability of  $\beta$ -catenin within cell and this cross-talk causes the growth and survival of breast cancer cells as shown in figure 1.21.



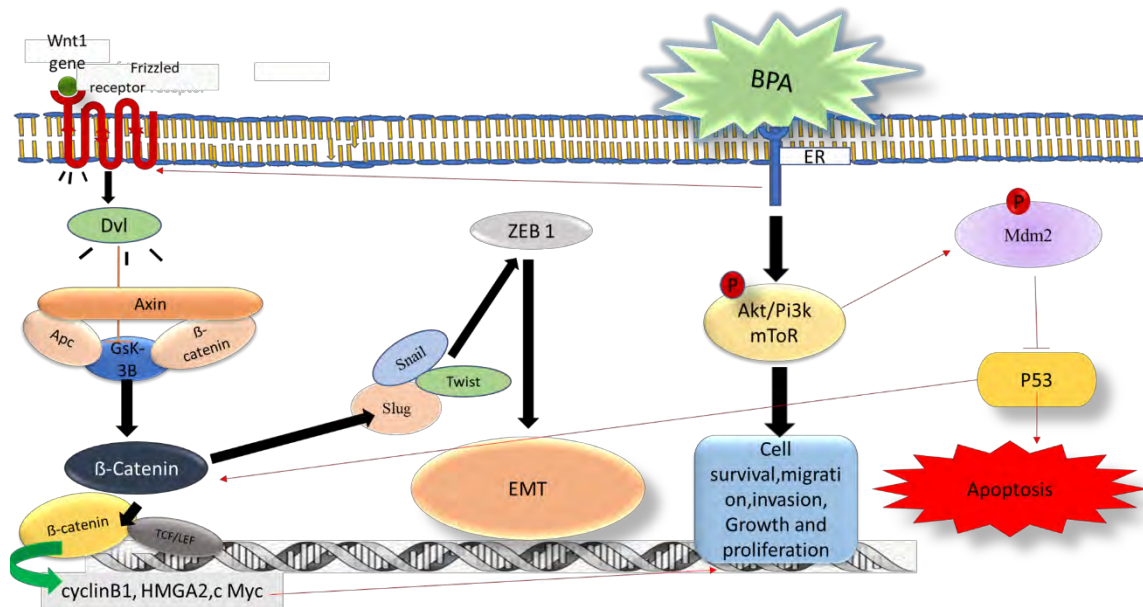


Figure 1.21. BPA modulated signaling pathways adapted from (Bouskine, Nebout et al. 2009) (Kumar, Sharma et al. 2015)

## AIMS AND OBJECTIVES

The aim and objective of the study are:

- To analyze the role of BPA in generation of oxidative stress leading to cardiotoxicity and neurotoxicity
- To elucidate the therapeutic potential of the *P. integerrima* in the post transcriptional and post translational regulation of p53 signaling nexus in BPA induced mitochondria-linked apoptosis
- To analyse the role of BPA in breast cancer progression

## **MATERIALS AND METHODS**

### **2.1 Plant collection and identification**

*Pistacia integerrima* galls (Voucher No G.H 04708) were collected in September 2017 from village Salhad District Abbottabad KPK, Pakistan. The coordinates of the area are 34.130978, 73.201076. It was identified by Dr. Abdul Majid, Plant Taxonomist at Hazara University, Mansehra, Pakistan.

#### **2.1.1 Preparation of methanolic extract of *Pistacia integerrima* galls**

Plant galls were washed and air-dried in the shade. Dried galls were ground to a fine powder and soaked in methanol for three days with constant stirring. The extract was filtered and subjected to a rotary evaporator under vacuum at 40 °C to allow the evaporation of methanol. The process of extraction was repeated thrice for complete extraction (Liu, Zhao et al. 2008). The gummy mass was stored at room temperature. 0.5 % dimethyl sulfoxide (DMSO) was used as a vehicle for extract. Measured amount of extract was dissolved in DMSO, shaken well and syringe filtered before use.

### **2.2 Ethical Consideration for Animal Model**

Sprague Dawley rats of both sexes (1:1) weighing 120-200g (7-10 weeks) were selected for the experimental trials. The study was approved by the Ethical Committee of Quaid-i-Azam University, Islamabad (BEC-FBS-QAU2018-76). Experiments involving animals were carried out according to the guidelines of National Institute of Health (NIH guidelines Islamabad, Pakistan) as per the considerations of U.K. Animals (Scientific Procedures) Act, 1986. All animals were treated kindly and with regard for reduction of suffering. To analyse the toxic effects of BPA on general population, rats of both sexes were selected in this study. Rats were provided with standard laboratory feed and drinking water in glass bottles to minimize the risk of BPA that could confound the results of the study.

### **2.3 Study Design**

Animals were randomly divided into groups with six rats each. Bisphenol A was used to induce toxicity in rats while melatonin and plant extract (*Pistacia integerrima*) were used as treatment. All groups received their respective doses daily for 16 days. The animals were divided into groups (nine rats in each group) as normal control group

which was administered with normal saline (NS), disease control; BPA was given at three multiple doses, 100 µg/kg BW, 1mg/kgBW and 10mg/kgBW of body weight prepared in olive oil (Batista, Alonso-Magdalenal et al. 2012), Antioxidant group; Melatonin was used as a standard antioxidant in this study and was given at a dose of 4 mg/kg BW in normal saline. The dose was selected based on three different studies as previously our research group has reported the therapeutic potential of melatonin in cardiac tissues oxidative stress by using the lower dose of melatonin that was 2.5 mg/kg BW (Ali, Mushtaq et al. 2019). Dakshayani et al. have reported the higher dose of melatonin i.e. 5 mg/kg BW whereas another study by Sewerynek et al. has shown the antioxidant potential of melatonin by using 4 mg/kg BW (Sewerynek, Abe et al. 1995, Dakshayani, Subramanian et al. 2005). The plant extract control group was given *P. integerrima* at a dose of 200 mg/kg BW in 0.5% DMSO (Ahmad, Waheed et al. 2010). The melatonin treatment group, in which both melatonin and BPA were administered and the plant extract treatment group, which was treated with both *P. integerrima* and BPA. All doses were administered subcutaneously (Fig. 2.22).



Figure 2.22 Schematic diagram of the study design

To analyze the therapeutic potential of tetra-aniline based terpolymers in BPA toxicity model. The Bisphenol A was given at a dosage of (1 mg/Kg) of body weight, BPA was dissolved in olive oil (Batista, Alonso-Magdalenal et al. 2012). NAC was given at a dosage of (50 mg/Kg) in normal injection water. The Es-37 and L-37 were given at a dosage of (1 mg/Kg) in normal injection water. Our research group has previously shortlisted dose regimen to L-37 and Es-37 *in vitro*. NAC and BPA were administered through subcutaneous route while synthetic polymers were administered through intraperitoneal route.

### **2.3 Dissection and tissue collection**

After completion of sixteen days dosing, rats body weight was measured and then anesthetized by chloroform to proceed dissection. Rats were dissected from their ventral side and their heart, liver, brain and kidney were collected. Organs were washed with phosphate buffer saline. Heart and brain tissues were divided into parts. One part for RNA extraction and other was for expression analysis as in western blotting. Tissues were also fixed in 10% formalin solution for histological analysis.

### **2.4 Ethical Approval for human sample collection**

Tissue and blood samples were collected from 50 patients that have undergone breast surgery at Holy Family Hospital Rawalpindi, Punjab, Pakistan. The Institutional Ethics and Clinical Research Committee of Holy Family Hospital Rawalpindi, Punjab Pakistan approved the current study. In this study, informed written consent was taken from the breast cancer given to patients prior to participation. However, the privacy rights of human subjects were carefully observed. In human subject studies, research was conducted in accordance with the 1975 Helsinki Declaration. Breast cancer patients of both sexes and age above fifteen years were included in the study. However, the patients having any other type of cancer along with breast cancer were not included in the study. Blood samples collected from control (healthy) individuals of the same sex and age and a region of tissue which was 3cm away from the tumor site were used as a control in our study. Data related to several demographic demographical and clinical parameters such as age, ethnic group, weight, matrimonial status, occupational status, family history, educational status, stage of breast cancer, breast cancer treatment and link of breast cancer and other diseases, tumor size, Ki67 (cell proliferation marker) index score value and ER, PR, HER2, E-cadherin status was recorded.

### **2.5 Human Sample Collection and storage**

Serum samples were collected in gel tube (Atlas-labovac, Italiano), centrifugation was done at 6000 rpm for 10 minutes and samples were stored at -20°C for the evaluation of bisphenol A (BPA) level through high performance liquid chromatography-UV (HPLC-UV, Agilent 1100 series, USA). Fresh biopsy samples were classified into Normal group (control) and Malignant group. Samples were further proceeded for RNA extraction, western blot analysis and immunohistochemistry.

## 2.6 Tissue homogenization

It is the most employed technique used for the cell lysis to purify intracellular proteins. Rat tissues were homogenized by using electric homogenizer (Biogen series Pro200; Pro scientific, USA) in RIPA lysis buffer.

### 2.6.1 RIPA Lysis Buffer

Following chemicals were required for the preparation of extraction buffer.

#### Reagents required for RIPA Lysis buffer

Sr. No	Chemicals	Concentrations
1.	Tris-HCl	10mM PH-7.4
2.	EDTA	5Mm PH-8.0
3.	NaCl	0.15M
4.	Triton X-100	1%
5.	DTT	5M (1:1000)
6.	PMSF in isopropanol	100mM (1:1000)

Tissue was collected and 100mg section was weighed. Tissues were homogenized in 500ul lysis buffer with electric homogenizer. Lysate were centrifuged at 13000rpm, 4°C for 10minutes. The supernatant was stored at -20 °C for further analysis.

## 2.7 mRNA/miRNA expression analysis

### 2.7.1 RNA extraction

RNA extraction was performed by following the protocol of (Jan, Khan et al. 2017).

#### RNA Extraction Requirement reagents

Sr. No.	Reagents	Concentrations
1.	TRIzol	500ul
2.	Chloroform	50ul
3.	Isopropanol	150ul
4.	Glycogen	1ul
5.	DEPC treated water	20ul
6.	70% ethanol	500ul

For mRNA/miRNA extraction, the area was decontaminated with ethanol swab. The tissue was minced in TRIzol Reagent (Thermo Scientific, USA). The 50ul chloroform was added and vortexed for about 15 secs for chloroform penetration. The samples were

incubated for 5 min and centrifuged at 13500rpm for 15 min at 4°C. Centrifugation separates samples in 3 layers. RNA is present specifically in the upper clear layer. The RNA containing upper aqueous phase was transferred into a fresh eppendorf, carefully without disturbing the interphase. To the upper clear layer add 150µl isopropyl alcohol and keep at room temperature for 5 min. The samples were shifted on ice for 5 min and centrifuged at 13500rpm for 15 min at 4°C to precipitate RNA. A visible white pellet is obtained. The supernatant was removed and the pellet was washed with 500µl of 70% absolute ethanol. It was vortexed gently and recentrifuged at 13500rpm for 15 min 4°C. The supernatant was discarded and the pellet was air-dried for 10 min. The RNA pellet was resuspended in 20µl DEPC treated water and vortexed thoroughly. Then RNA concentration, purity and absorbance were measured *via* U/VIS NanoDrop-1000™ (Nanodrop, V3.7, Thermo Fisher Scientific, USA). The 260/280 ratio was recorded to check the RNA concentration and then proceeded for cDNA synthesis. RNA samples were kept at -80°C.

### 2.7.2 cDNA synthesis

cDNA synthesis was accomplished through “Revert Aid First Strand cDNA Synthesis Kit” (Thermo Fisher).

#### **Reagents Required**

The reagents required for cDNA synthesis are:

PCR water	
RNA samples	1µg/µl
Random hexamer primer	1µl
0.5X reaction buffer	4.5µl
10nM dNTP mix	2µl
Ribolock RNase inhibitor	0.5µl
Revert aid RT	1µl

RNA sample and PCR water were combined on ice according to the calculated readings. 1µl random hexamer primer was added. The samples were incubated at 65°C for 5min. Samples were spun briefly and promptly shifted on the ice. Then the following components were added:

0.5X reaction buffer = 4.5 $\mu$ l

10nM dNTP mix = 2 $\mu$ l

Ribolock RNase inhibitor = 0.5 $\mu$ l

Revert aid RT = 1 $\mu$ l

The 20 $\mu$ l reaction mixture of each sample was incubated in the thermocycler machine programmed as 42°C for 60mins and stored at -80°C.

### **2.7.3 Primer Designing**

Specific gene and miRNA primers were designed and validated from [http://www.targetscan.org/cgi-bin/targetscan/vert\\_72/](http://www.targetscan.org/cgi-bin/targetscan/vert_72/), IDT SciTools software and OligoAnalyzer 3.0. The primers were purchased from BJI, China (Table. 2.1).

Table 2.1. List of Primers

S. No.	Gene	Forward Primer	Reverse Primer	Amplicon Size
1	<b>Ubc-13</b>	5'.....AGCAGAACCAGATGAGAGCA.....3'	5'.....GTTCGGATCTGCAGTGCTG.....3'	137
2	<b>PUMA</b>	5'.....AAGAAGAGCAACATCGACAC.....3'	5'.....CTAGTTGGGCTCCATTTCTG.....3'	165
3	<b>DRP1</b>	5'.....TCAGATTGTCGTAGTGGGAAC.....3'	5'.....TGGACCAGCTGCAGAATAAG.....3'	129
4	<b>GAPDH</b>	5'.....TTCAACAGCAACTCCCATT..... 3'	5'.....CACCACCCTGTTGCTGTA .....3'	120
5	<b>p53</b>	5'.....CTACCCGAAGACCAAGAAGG.....3'	5'.....GCAGAGGCTGTCAGTCTGAG ..... 3'	92
6	<b>Cytochrome c</b>	5'..... CTGGGGAGAGGATACCCT..... 3'	5'..... TTAGGTCTGCCCTTTCTCC .....3'	110
7	<b>BNIP3</b>	5'.....TCTGTTAGCCATTGGATTGG ..... 3'	5'.....TCACAGCTCAGCGTGAATC .....3'	121
8	<b>CDIP1</b>	5'.....CCTGCCTCATCAATGACTTC..... 3'	5'...ATGGGGAGCAAAGCACA.....3'	145
9	<b>USP7</b>	5'.....GGGCTTGACCACTTCAAC ..... 3'	5'... ACACACCCACGCACTGT.....3'	121
10	<b>PRKC-<math>\delta</math></b>	5'.....AACCCCAACTTTCCTTCAGT ..... 3'	5'..... AAAGCAGGTCTGGGAGCT.....3'	127
11	<b>Bcl2</b>	5'.....TTGATTTCTCCTGGCTGTCTC ..... 3'	5'...TGTTTGGGGCAGGTCTG .....3'	115
12	<b>Mitofusin 2</b>	5..'TCAAGACCGTGAACCAGC.. 3'	5..'AGAAGTGGACACTTGGAGTTG.. 3'	103
13	<b>miRNA-214-3p</b>	5'.....GACAGCAGGCACAGACA.....3'	5'.....GTGCAGGGTCCGAGGT.....3'	
14	<b>miRNA-15a-5p</b>	5'.....GGGTAGCAGCACATAATGG.....3'	5'.....GTGCAGGGTCCGAGGT.....3'	



15	<b>U6</b>	5'.....GCTTCGGCAGCACATATACTAA.....3'	5'.....AACGCTTCACGAATTTGCGT.....3'	
16	<b>TP53 (Human)</b>	5'.....TGCTACTTGACTTACGATGGTG.....3'	5'.....CCTGGGCATCCTTGAGTTC.....3'	129
17	<b>ZEB1(Human)</b>	5'..... AGAGAAGGGAATGCTAAGAAGT.....3'	5'..... TGCATCTGACTCGCATTTCATC.....3'	129
18	<b>WNT1(Human)</b>	5'..... CTGCACGAGTGTCTGTGAG.....3'	5'..... AGTGTGACTGGAGGTACTCG.....3'	129
19	<b>GAPDH (Human)</b>	5'..... TGACAGAACTAGCAGAACGTG.....3'	5'..... TTGATCGCCACTGAGAACC.....3'	129

### 2.7.4 Quantitative real-time PCR analysis

qRT-PCR was performed to determine the quantitative gene/miRNA expression analysis involved in pathophysiological processes by using the SYBR Green Master Mix (Thermo-fisher scientific, USA), according to the protocol of (Jan, Khan et al. 2017).

#### **Equipment**

My GO PRO PCR (IS-IT Life Sciences Limited, Republic of Ireland)

#### **Reagents Required**

cDNA samples

Nuclease-free water

SYBR green Master Mix (Thermo Fisher Scientific, USA)

Forward and Reverse Primers

#### **Procedure**

Two master mix was prepared to run the samples in duplicate.

Master Mix 1 Composition	
cDNA	0.5µl
Nuclease-free H <sub>2</sub> O	4µl

Master Mix 2 Composition	
SYBR Green Dye Master Mix	5µl
Forward Primer	0.25µl
Reverse Primer	0.25µl

According to the samples, an additional amount of both master mixes was prepared separately on ice and SYBR green dye was added.

Gene-specific forward and reverse primer pair was used to target specific gene expression. From master mix 1 and 2 4.5 $\mu$ l and 5.5 $\mu$ l was picked respectively and carefully aliquot in each PCR tube making the final volume up to 10 $\mu$ l. The whole reaction was performed over ice. Samples were tapped to remove any bubbles present and then run in the RT-PCR machine upon setting the software to analyze the data accordingly. The Ct values were recorded and the relative expression was measured through REST tool (Pfaffl, Horgan et al. 2002, Ali, Waheed et al. 2015).

### **2.8 Protein quantification assay**

Quantification of protein was performed by using Bradford Assay. Protein quantification of tissue homogenates was carried out by making serial dilutions of Bovine Serum Albumin (BSA) and create a standard curve of absorbance measured by MultiScanGo Microplate spectrophotometer (Thermo Fischer Scientific, USA spectrophotometer) at 595nm wavelength.

#### **Procedure**

Working solution of Bradford assay was prepared in 1:4 ratio of Bradford reagent (Roti Quant Carl Roth Germany) in water. To generate standard curve, serial dilutions of BSA were prepared from 10M stock solution of BSA and poured 200ul of working solutions and 5ul of BSA dilutions into microtiter plate. For Protein quantification, 5ul of protein samples (tissue lysate) and 200ul of working solution was poured in the microtiter plate. Dilutions and samples in microtiter plate were incubated at room temperature for half hour. Then absorbance was measured at 595nm wavelength on spectrophotometer. Then standard curve by following linear line equation was plotted. (Absorbance vs protein concentration). Trend line was a straight line that represented the data on scatter graph (Fig. 2.23). This data was used for protein quantification in protein samples.

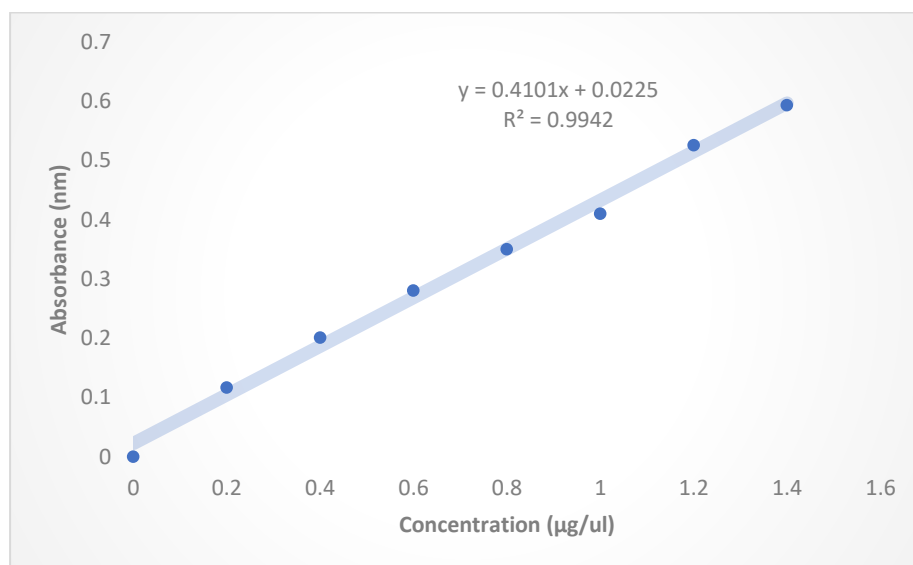


Figure 2. 23. Standard curve of BSA for protein quantification, x-axis and y-axis depict the different concentrations of BSA and absorbance respectively

## 2.9 Western blotting

Western blotting is a technique used for the analysis of proteins expression. It was performed by following the protocol of Ali *et al* (Ali, Mushtaq et al. 2019) by using the western blotting apparatus of Bio-Rad USA.

Following steps were involved in western blotting.

- Casting of SDS-PAGE gel
- Gel electrophoresis
- Gel staining
- Gel transfer to nitrocellulose membrane
- Blocking
  - Primary antibody incubation
  - Secondary antibody incubation
- Detection

### 2.9.1 Casting of SDS-PAGE gel

#### Required reagents for SDS-PAGE

Sr. No.	Reagents	Separating gel concentrations (12%)	Stacking gel concentrations (4%)
1.	Distilled Water	1647.5ul	1437.5ul

2.	Tri-HCl	1250ul	625ul
3.	SDS-10%	50ul	25ul
4.	Bis Acrylamide (30%)	2000ul	412.5ul
5.	AP	50ul	25ul
6.	TEMED	2.6ul	2.5ul

### Procedure

To make SDS-PAGE, glass plates were arranged and assembled in the casting frame. First master mix of separating gel was prepared by adding all required chemicals, shortly vortex and immediately poured in space between the glass plates. Master mix was filled up to the 0.7cm below from the inserting comb. Then isopropanol was added onto the gel surface to linearize the gel level and remove the air bubbles. When gel was polymerized after 40-60 minutes. Isopropanol was removed by using filter paper and gel was washed with sterilized water. For making the stacking gel master mix of required chemicals was prepared. Master mix of stacking gel was poured onto the separating gel. Then comb was inserted for well formation. When the gel was solidified, gel plates were removed from casting frame.

### 2.9.2 SDS-PAGE

It is a commonly used technique that is used to separate proteins according to their molecular weight by applying electric field on the gel. To carry out gel electrophoresis following fundamental steps were performed.

- Sample preparation
- Sample loading
- Gel running

### Sample Preparation

For sample preparation 7ul loading dye, sample according to the graph plotted by BSA dilutions and sterilize water were added in an eppendorf to make total volume up to 15ul. Then samples were heated on hot plate at 95°C for 10 minutes for protein denaturation. Protein samples were centrifuge for 1 minute at 2000rpm.

Sr. No	Chemicals	Concentrations
1.	Sample (lysate)	30ug protein

2.	Loading dye	7ul
3.	Sterilize water	Depending upon sample concentration

### Sample loading and gel running:

SDS-PAGE was placed into the electrode assembly and fixed into the gel electrophoresis tank. Running buffer was poured into the casting frame, gel electrophoresis tank was occupied with running buffer up to the filling mark.

Protein samples were carefully loaded into the each well and 5ul protein ladder was loaded in the very first well. Gel was run and 90V of voltage was applied for 45 minutes and then 120V for 40 minutes.

### Chemicals preparation

1X SDS running buffer was prepared.

#### Required reagents for SDS Buffer

Sr. No.	Chemicals	Concentrations
1.	Tris	125mM
2.	Glycine	1.25M
3.	SDS	0.5%

#### Required reagents for Fixing solution

Sr. No.	Chemicals	Concentration
1.	Methanol	50%
2.	Glacial acetic acid	10%
3.	Distilled water	a/c required volume

#### Required reagents for staining solution

Sr. No.	Chemicals	Concentration
1.	Coomassie brilliant blue	0.1%
2.	Methanol	50%
3.	Glacial acetic acid	10%
4.	Distilled water	a/c required volume

**Required reagents for Distaining Solution**

Sr. No.	Chemicals	Concentrations
1.	Methanol	40%
2.	Glacial acetic acid	10%
3.	Distilled water	a/c required volume

**2.9.3 Staining of gel**

To check initial pattern of gel running and optimization of protein assay, gel staining was done. During protein transfer this step was not performed and proteins were directly transfer on nitrocellulose membrane. When the gel ran successfully, it was removed from the gel tank. Carefully removed the gel from glass plates and placed into the fixing solution. Gel in fixing solution was incubated at room temperature for overnight. Gel was removed and stained the gel for 30-45minutes. Afterward gel was destained and protein bands were visualized.

**2.9.4 Gel transfer to nitrocellulose membrane**

Following western blotting solutions were used

Reagents required for Transfer buffer

Sr. No.	Chemicals	Concentration
1.	Tris-base	48mM
2.	Glycine	39mM
3.	Methanol	0.04%
4.	SDS	20%
5.	Distilled water	a/c required volume

**Reagents required for TBST**

Sr. No.	Chemicals	Concentration
1.	Tris Base	1M
2.	NaCl	3M
3.	Distilled water	a/c required volume

1M Tris base was dissolved into distilled water and adjusted the PH 8.0 then poured the 3M NaCl and attained the total volume of solution up to 1000ml.

**Reagents required for Blocking solution**

Sr. No.	Chemicals	Concentration
1.	Non-Fat milk	5%
2.	TBST	100ml

**Procedure**

Proteins were transferred to the Nitrocellulose membrane (NC). Protein was transferred on NC by using semi-dry method by BIO-RAD Trans-Blot SD cell (BIO-RAD, USA). For protein transfer SDS-PAGE, NC and filter paper were soaked in transfer buffer. Transfer sandwich assembly was made by placing six filter paper on Trans-Blot and then NC was placed on it which was follow the placement of polyacrylamide gel and six filter paper on that. Gently air bubbles were removed from the transfer sandwich. Any bubbles present between the gel and NC can affect the protein transfer to the membrane. Set the voltage of power supply at 10V for 40 minutes.

**2.9.5 Blocking**

After successful protein transfer, nitrocellulose membrane (NC) was carefully removed and washed with TBST. For surface blocking NC was dipped into the blocking solution for 1 hour and placed on shaker at room temperature to prevent the nonspecific binding. Blocking solution was removed and washing of NC was carried out with TBST three times for 5 minutes each.

**2.9.6 Incubation with antibodies**

Nitrocellulose membrane was incubated at 4°C for overnight with primary antibody. Then nitrocellulose membrane was washed with TBST three times for 5 minutes each. In table 2.2 primary antibodies are mentioned which were used in experiment.

**Table 2.2. List of Antibodies**

Sr. No.	Primary Antibody	Catalogue number	Dilutions (ul)
1.	GAPDH	K00027	1:1000
2.	p53	sc-393031	1:1000
3.	P-p53	sc-51690	1:1000
4.	Drp1	sc-271583	1:1000



5.	PUMA	sc-374223	1:1000
6.	Cytochrome c	sc-13560	1:1000
7.	Ubc-13	sc-376470	1:1000
8.	P-Bcl2	sc-377554	1:1000
9.	Bcl2	sc-492	1:1000
10.	Mfn2	sc-515647	1:1000

### Incubation with Secondary Antibody

Nitrocellulose membrane was incubated with secondary antibody (Anti Rabbit-31460 Thermo scientific, Goat-antimouse ab-97020) for 2 hours at room temperature. NC was washed with final washing buffer for 5 minutes on the shaker.

### 2.9.7 Band detection

Chromogenic detection method was used in this protocol. For the detection of the signal, 5-bromo-4-chloro-3-indolylphosphate (BCIP) / Nitro Blue Tetrazolium (NBT) was used as a substrate. Nitrocellulose membrane was treated with 1 mL of NBT substrate followed by 30 minutes of incubation in dark. After that, bands were observed, and photographs were taken. Densitometric analysis was done by using ImageJ software.

### 2.10 Oxidative profile

To analyze the oxidative stress in the serum as well as in tissue lysates of experimental rats, ROS and TBARs assays were performed.

#### 2.10.1 Reactive oxygen species (ROS) assay

ROS assay was performed according to the protocol described in (Hayashi, Morishita et al. 2007). This assay was performed on both serum and homogenized tissue samples.

#### Principle

Reagents required for this assay are mentioned below along with their concentrations.

Reagents	Concentration	Volume
Sample		6.6µl

Sodium Acetate Buffer, pH 4.8	0.1M	133.3 $\mu$ l
R1: N, N-Diethyl para- phenyl diamine (DEPPD)	1mg/ml	1/25
R2: FeSO <sub>4</sub>	0.5%	24/25

### Procedure

Firstly, reagent 1 and reagent 2 were prepared by dissolving DEPPD and ferrous sulfate in acetate buffer respectively, according to the previously developed protocol. Next the reagent mixture was prepared by mixing 1 volume of R1 and 24 volumes of R2 followed by 2 minutes of incubation in dark. Hydrogen peroxide dilutions of 1M to 10M were prepared in order to generate standard curve. 6.6 $\mu$ l of distilled water/H<sub>2</sub>O<sub>2</sub> dilutions(1M-10M)/sample was added in separate wells of microtiter plate. To each well 133.3 $\mu$ l of acetate buffer and 186 $\mu$ l of reagent mix was added. Mixture was incubated for 1 minute and absorbance was measured at 505nm. Three readings were taken after every 15 minutes by multiskan GO (Thermo-Fischer scientific, USA) spectrophotometer. Linear line equation was used to generate standard curve shown below (Fig. 2.24).

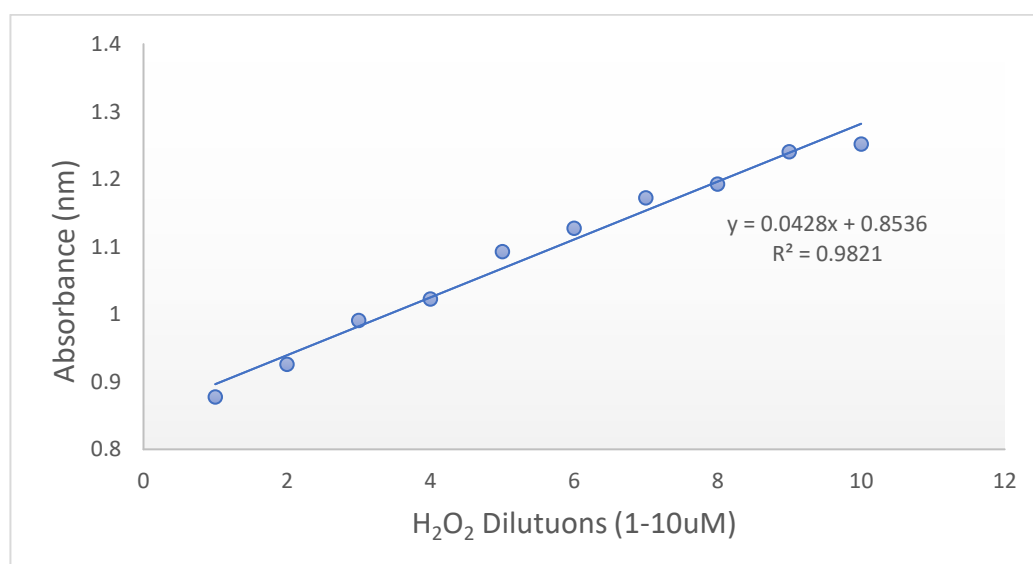


Figure 2.24. Standard curve for ROS assay, the x-axis and y-axis depict the different concentrations of H<sub>2</sub>O<sub>2</sub> and absorbance respectively

### 2.10.2 Thiobarbituric acid reactive substances (TBARs) assay

TBARs activity was measured in samples according to the instructions provided by the protocol described in (Tsai, Chang et al. 2014).

Reagents required for TBARs assay are as follows:

Reagents	Concentration	Volume
Sample		20µl
Tris -HCL	150mM	8.3µl
Ferrous sulphate	1mM	8.33µl
Trichloroacetic acid	10%	83.3µl
Thiobarbituric acid	0.375%	83.3µl
Ascorbic acid	1.5mM	8.33µl
Distilled water		50µl

#### Procedure

8.33µl of sample was added in an eppendorf followed by addition of Tris HCL (8.33µl), FeSO<sub>4</sub> (8.33µl) and ascorbic acid (8.33µl), respectively. 50µl of distilled water was also added and the mixture was incubated at room temperature for 15 min. After the incubation time was completed, 83.3µl of TCA was added to the eppendorf followed by the addition of 83.3µl TBA. Mixture was then boiled in hot water for 15 min and then centrifuged for 10 minutes at 3000rpm. From each centrifuged sample, 250µl of supernatant was collected and shifted to each well of the plate. Absorbance of the samples were measured by multiskan GO (Thermo-Fischer scientific, USA) spectrophotometer at 532nm three times and levels of lipid peroxidation were calculated by the given formula

$$\text{TBARS (nM/mg of protein)} = \text{O.D} * \text{Total volume} \times 1.56 \times 10^5 \times \text{protein in mg / ml.}$$

## 2.11 Anti-Oxidative Profile

### 2.11.1 Super oxide dismutase (SOD) assay

Anti-oxidative profiling was done by measuring SOD activity according to protocol described in (Ali, Waheed et al. 2015). Reagents required for SOD assay are as follows:

Reagents	Concentration	Volume
Sample		5µl
Phosphate buffer saline, pH 7.8	50mM	26.75ml
L-Methionine	9.9µM	1.5ml
NBT	57µM	1ml
Triton X-100	0.025%	750µl
Riboflavin	0.9 µM	3µl

### Procedure

1.5ml L-Methionine, 750µl Triton x-100 and 1ml NBT.2HCL were mixed together to prepare 3.25ml of reagent mixture followed by addition of 26.75ml of buffer resulting in 30ml reagent mix. In each well of the microtiter plate containing 5µl of serum sample, 250µl of the reagent mixture was added. Fluorescent light was given to illuminate the microtiter plate at room temperature for 7 minutes followed by 5 minutes of incubation at 37°C. After that, 3µl of riboflavin was added to each well followed by 8min incubation at 40 °C. After incubating the mixture, absorbance was recorded three times at 560nm (each reading/min) by multiskan GO (Thermo-Fischer scientific, USA) spectrophotometer. NBT inhibition value was calculated as

$$(\text{Abs. Blank} - \text{Abs. sample}) / (\text{Abs. Blank}) * 100$$

### 2.11.2 Catalase activity (CAT) assay

CAT assay was performed to measure free H<sub>2</sub>O<sub>2</sub> present in the sample according to the protocol described in (Ali et al., 2015).

Reagents required for CAT assay are as follows:

Reagents	Concentration	Volume
Samples		8.09 $\mu$ l
Potassium phosphate buffer, pH 7	50mM	161 $\mu$ l
H <sub>2</sub> O <sub>2</sub>	5.9mM	80.90 $\mu$ l

### Procedure

CAT assay was performed in 96-well microtiter plate. In each well of the microtiter plate, 161 $\mu$ l of buffer, 80.90 $\mu$ l of H<sub>2</sub>O<sub>2</sub> and 8.09 $\mu$ l of sample were added. Mixture of all reagents were taken as blank except sample. Absorbance at 570nm was measured by multiskan GO (Thermo-Fischer scientific, USA) spectrophotometer. Three readings were taken with the gap of 30 seconds.

### 2.11.3 Peroxidase (POD) assay

Peroxidase enzyme converts H<sub>2</sub>O<sub>2</sub> into water and oxygen. Reagents required for POD assay are as follows (Ishtiaq et al., 2020):

Reagents	Concentration	Volume
Samples		8.33 $\mu$ l
Phosphate buffer, pH 5.0	50mM	208.3 $\mu$ l
Guaiacol	20mM	8.33 $\mu$ l
H <sub>2</sub> O <sub>2</sub>	40mM	25 $\mu$ l

### Procedure

208.3µl of buffer, 8.33µl of guaiacol and 8.33µl of sample were added in each well and stirred. 25µl of H<sub>2</sub>O<sub>2</sub> was added at the end and absorbance was measured at 420nm. Three readings were taken with the gap of 1 minute by multiskan GO (Thermo-Fischer scientific, USA) spectrophotometer.

#### 2.11.4 Ascorbate peroxidase assay

Hydrogen peroxide is reduced to water by the action of ascorbate peroxidase, which uses ascorbic acid as its substrate. Reagents required for APX assay are as follows (Ali et al., 2015):

Reagents	Concentration	Volume
Sample		25µl
Potassium phosphate buffer, pH 7	50mM	175µl in blank, 150µl in samples
EDTA	1mM	25µl
Ascorbate	5mM	25µl
H <sub>2</sub> O <sub>2</sub>	1mM	25µl

#### Procedure

Assay was performed in microtiter plate. 175µl of Potassium phosphate buffer along with 25µl of Ascorbate, 25µl of EDTA and 25µl H<sub>2</sub>O<sub>2</sub> were added in one of the wells of the microtiter plate which is considered as blank. In all other wells, 25µl of sample was also added along with 25µl of Ascorbate, 25µl of EDTA, 25µl H<sub>2</sub>O<sub>2</sub> and 150µl of buffer. Absorbance was measured at 290nm by multiskan GO (Thermo-Fischer scientific, USA) spectrophotometer. Three readings were taken and the levels of the enzyme was calculated by using formula

**Ascorbate activity = Absorbance \* Extinction Co-efficient of Ascorbate .**

#### 2.11.5 Reduced glutathione assay

Reagents required to perform GSH assay are as follows (Ishtiaq et al., 2020)

Reagents	Concentration	volume
DTNB (5,5'-dithiobis-2-nitrobenzoic acid)	0.4%	78.12 $\mu$ l
Sodium Phosphate buffer	0.4M	156.25 $\mu$ l
Serum sample		15.62 $\mu$ l

### Procedure

Assay was performed in a microtiter plate. 15.62 $\mu$ l serum sample was added in each well followed by addition of 156.25 $\mu$ l of buffer and 78.12 $\mu$ l of DTNB. DTNB also known as Ellman's reagent, is commonly used in biochemical assays to detect the presence of free sulfhydryl groups (-SH) in proteins. This reagent reacts with sulfhydryl groups to form a yellow-colored product, 5-thio-2-nitrobenzoic acid (TNB), which can be quantified spectrophotometrically at 412 nm. Appearance of the yellow color was an indication that GSH was present in the sample. Absorbance at 412nm was measured by multiskan GO (Thermo-Fischer scientific, USA) spectrophotometer.

## 2.12 Lipid profile analysis

Lipid profiling was done by performing cholesterol and triglycerides assays.

### 2.12.1 Cholesterol assay

AMP diagnostic Kit protocol was used to perform cholesterol assay.

Reagents	Volume
Sample	2 $\mu$ l
Reagent	200 $\mu$ l
Standard	2 $\mu$ l

### Procedure

2 $\mu$ l sample was added in each microtiter well and 2 $\mu$ l of standard was also added in a separate well. 200 $\mu$ l of reagent was added in both standard as well as sample wells. Incubation of 5 minutes was given to the mixture at room temperature. Absorbance of both standard and sample were measured at 500nm. Three readings were taken by using

multiskan GO (Thermo-Fischer scientific, USA) spectrophotometer and the amount of total cholesterol was calculated by using formula given below

$$\text{Cholesterol (mg/dL)} = \text{Sample}_{\text{abs}} / \text{Standard}_{\text{abs}} \times \text{Conc. of standard}$$

### 2.12.2 Triglycerides assay

Levels of triglycerides were measured by following the protocol given in AMP diagnostic Kit and reagents used are as follows:

Reagents	Volume
Triglyceride reagent	200 $\mu$ l
Standard	2 $\mu$ l
Sample	2 $\mu$ l

#### Procedure

2 $\mu$ l sample was added in each well and 2 $\mu$ l of standard was also added in a separate well. 200 $\mu$ l of reagent was added in both standard as well as sample containing wells. Incubation of 5 minutes was given to the mixture at room temperature. Absorbance of both standard and sample were measured at 500nm. Three readings were taken by using multiskan GO (Thermo-Fischer scientific, USA) spectrophotometer and the amount of total triglycerides was calculated by using formula given below:

$$\text{Total triglyceride (mg/dL)} = \text{Sample}_{\text{abs}} / \text{Standard}_{\text{abs}} \times \text{concentration}$$

### 2.13 Liver function analysis

Alanine Aminotransferase (ALT) and Aspartate Aminotransferase (AST) enzymes are the important markers to check either the liver is functioning properly or not, ALT and AST assays were performed to measure the levels of these enzymes.

#### 2.13.1 Alanine aminotransferase (ALT) assay

To check the levels of ALT enzymes in serum samples, protocol given by AMP diagnostic Kit was followed.



Reagents used in this protocol are as follows:

Reagents	Concentrations	Volume
Serum sample		10 $\mu$ l
Reagent 1 (Tris-buffer, PH 7.3, L-Alanine, Lactate dehydrogenase)	150mM , 750mM/L > 1.350 U/L	4 parts of total volume
Reagent 2 (NADH, 2-Oxoglutarate, Biocides)	1.3mM, 75mM	1 part of total volume

### Procedure

Reagents from the kit were mixed to prepare reagent mixture. 4 volumes of R1 were mixed with 1 volume of R2 depending on the number of samples. 10 $\mu$ l sample was added in each well followed by addition of 200 $\mu$ l of reagent mixture. Mixture was incubated at room temperature for 1 min and absorbance was measured by multiskan GO (Thermo-Fischer scientific, USA) spectrophotometer at 340nm. Three readings were taken with the gap of 60seconds and ALT level in samples was calculated according to kit formula:

$$\Delta A / \text{min} * 3333 = \text{ALT activity (unit/ L) at 37}$$

### 2.13.2 Aspartate aminotransferase (AST) assay

AMP diagnostic kit method was used to check AST levels in serum samples.

Reagents	Concentrations	Volume
Sample		10 $\mu$ l
Reagent 1 (Tris-buffer, PH 7.8 , L-aspartate, MDH, LDH)	121mM, 362mM/L, > 460 U/L, >600 U/L	4 parts of total volume

Reagent 2 (NADH, 2-Oxoglutarate, Biocides)	1.3mM/L, 75mM/L	1 part of total volume
--	-----------------	------------------------

### Procedure

Reagent 1 and reagent 2 from the kit were mixed at the ratio of 4:1 depending on the number of samples. In each well of microtiter plate 10 $\mu$ l sample and 200 $\mu$ l of reagent mixture were added. Plate was incubated at room temperature for 60seconds and absorbance was measured three times by multiskan GO spectrophotometer at 340nm. AST level in samples was calculated according to the formula given below:

$$\Delta A / \text{min} \times 3333 = \text{Activity of AST (unit/ L)}.$$

### 2.14 Histological analysis

Histopathological analysis of heart tissue was performed by following the protocol described in (Cardiff, Miller et al. 2014). For microscopic analysis heart tissue was placed in fixative solution and then tissue was dehydrated. This dehydrated tissue was treated with cedar wood oil until it become transparent. This treatment was done at room temperature. Transparent tissue was transferred into the liquid wax and removed the bubble for appropriate solidification of wax. Tissue was embedded in paraffin wax which was trimmed by using sterilize blade. Heart tissue was mounted on paraffin wax block for sectioning.

#### Fixative solution recipe

Sr. No.	Chemicals	Concentrations
1.	Formaldehyde	30%
2.	Absolute alcohol	60%
3.	Acetic acid	10%

#### 2.14.1 Microtomy

Paraffin embedded tissue was censored into the 5um thin pieces by microtome which gave them smooth texture. These thin sections of tissues were incubated at 60°C and glass slides for tissue fixation were incubated in oven at 65 °C for overnight. At the end tissue on slide was stained with hematoxylin.

### 2.14.2 Microscopic Analysis

Microscopic analysis of tissue slides was carried out by using light microscope at 40X magnification microscope (Olympus Microscope; Life Sciences Solutions, Tokyo Japan). Tissue slides of all experimental groups were analyzed, and photograph were taken, and cell surface area was measured.

### 2.15 High performance liquid chromatography-UV (HPLC-UV) analysis

Bisphenol A (BPA) level in the serum samples of healthy individuals was estimated by high performance liquid chromatography-UV (HPLC-UV, Agilent 1100 Series, USA) method.

#### List of HPLC chemicals

No.	Chemicals
1.	Bisphenol A (BPA)
2.	Acetonitrile
3.	HPLC water
4.	n-hexane
5.	Blood samples of healthy individuals

#### 2.15.1 HPLC mobile phase buffer preparation

Mobile phase buffer for HPLC was prepared by mixing HPLC water and acetonitrile in the ratio of 40:60 respectively. Sonication of mobile phase buffer was done for 15 minutes before use (Aristiawan, Aryana et al. 2015).

#### 2.15.2 High performance liquid chromatography-UV (HPLC)

Standard and sample for HPLC were prepared by the protocol of (Aristiawan, Aryana et al. 2015). Sample was prepared by mixing 300 µl of blood serum with 300 µl of n-hexane and shaken for 1 minute. 2000 µl of acetonitrile was added into mixture and again shaken for 1 minute. Centrifugation was done at 2500 rpm for 15 minutes. Two layers were formed after centrifugation lower phase containing acetonitrile was transferred into new eppendorf. tube mixture was filtered by using 0.2 µm PTFE

(Whatman) filter paper before use. Sample was run according to the protocol of (Aristiawan, Aryana et al. 2015).

### **2.16 Molecular docking**

Molecular docking is a reliable tool used to study the incorporation of the drug molecule in the target-specific DNA or proteins to study their interactions. This facile method is commonly employed to investigate the most favourable binding sites and the types of interactions based on the distance between the atoms in the amino acid and the ligand molecule. Although there is minimal literature on the docking of polymers due to their macromolecular nature, we have attempted to study the interactions of two synthetic terpolymers using small oligomers with three different proteins in this study. For this purpose, oligomeric structures of L-37 and Es-37 were optimized quantum chemically in the TURBOMOLE software package at the B3LYP/TZVP level of density functional theory (Balasubramani, Chen et al. 2020). The structures of the proteins were obtained from the Protein Data Bank of RCSB, and docking simulations were carried out in Autodock Vina using AutoDockTools-1.5.6. Autodock Vina is an Broyden-Fletcher-Goldfarb-Shanno algorithm-based docking program with significant improvements in accuracy compared to the earlier AutoDock 4.0. The target protein receptors were prepared for docking by eliminating water molecules and assigning Kollman charges. This was followed by the addition of hydrogen atoms and subsequent energy minimization. The pdbqt files of the three proteins Bcl-2 (PDB id: 5jsn), Cytochrome c (PDB id: 5z62), p53 (PDB id: 4mzi) and the ligands were generated. The active sites were obtained using the Site Finder tool using default parameters and torsion roots were identified. A grid box with XYZ dimensions of 60x60x60 was adopted for the receptor proteins and nine docking runs were executed. The lowest energy conformation was selected for further analysis. The binding interactions between protein and docked complexes were observed through 2D representative ligplots obtained by BIOVIA Discovery Studio Visualizer (BIOVIA, San Diego: Dassault Systemes, 2017) and LigPlot plus software (Laskowski and Swindells 2011)

### **2.17 Molecular Dynamics simulation assay**

The top-ranked complexes were subsequently subjected to a production run of 100-ns. The significance of this assay is to decode the binding affinity of Es-37 and L-37 with respect to p53, Bcl-2, and cytochrome c versus time. MD simulation was performed in

three stages: preparation of systems followed by pre-processing and production run. The aforementioned stages were completed using the Assistant model building with Energy Refinement 18 (Amber18) (Case, Cerutti et al. 2016). During the first phase, systems parameters and topology features for Es-37 and L-37 and targeted proteins p53, Bcl-2, and cytochrome c were generated with an antechamber program (Wang, Wang et al. 2006). The acquired complexes were later submerged in a TIP3P solvation box having a size of 12 Å using a Leap program (Feller, Zhang et al. 1995). The intermolecular forces of the systems were described using the force field ff14SB (Maier, Martinez et al. 2015). The neutralization of complexes was accomplished by adding 25 sodium ion (Na<sup>+</sup>). During the second phase, systems were prepared for the production run. Initially, the energy content of the systems was conserved sequentially as follows: energy minimization of hydrogen atoms as well as water box, with restraint on rest of the systems, entire systems atoms minimization with restraint on alpha carbon atoms, and lastly, the minimization of non-heavy atoms while restraining the rest of the systems. Later, systems were subjected to gradual heating up to 300 K (input time step of 2 femtoseconds, restraint of 5 kcal/mol – Å<sup>2</sup> on C $\alpha$  atoms, time duration of 20 picoseconds). Langevin dynamics (Izaguirre, Catarella et al. 2001) was employed to apply constant temperature (gamma value, 1.0). Restraint on hydrogen bonds was maintained through SHAKE algorithm, and implementation of NVT ensemble was made for heating the system. The complex system was subjected to equilibration for 100-ps and the time step was considered of 2-fs. NPT ensemble was used with a constraint on C $\alpha$  atoms of 5 kcal/mol – Å<sup>2</sup> to accomplish pressure equilibrium. This step was then followed by an extended time of 50-ps with the implementation of the same factors except for the reduction of constraint by 1 kcal/mol – Å<sup>2</sup> on carbon atoms after every 10-ps. During the equilibrium phase of the system, it was allowed to balance itself for 1 nanosecond. During the last phase, the generation of simulation trajectories for 100-ns and a time of 2-fs was done. Berendsen algorithm (Lemak and Balabaev 1994) was used for the production of the complex system with NVT ensemble. A reference value of 8.0 Å was used to characterize the un-bounded forces and for the hydrogen bonds SHAKE algorithm was used. Statistical analysis of simulated trajectories was performed using a CPPTRAJ module (Roe and Cheatham III 2013) of (Sanchez and Sharma) while the stability of the systems was investigated by evaluation

of numerous structural features. UCSF Chimera was opted for the visual analysis of the trajectories of system (Pettersen, Goddard et al. 2004).

### **2.18 Statistical analysis**

Statistical examination of all study was performed (analysis of variance) by means of one-way ANOVA. For multiple comparison Tukey's Test was applied. Using IBM SPSS (Statistical Program for Social Science) results were calculated, and statistics was calculated, significant at *p value* < 0.01 or < 0.05. GraphPad Prism 8 software was used for graphical representation of the data.

### 3. RESULTS

#### 3.1. Effect of *Pistacia integerrima* on baseline characteristics of experimental animals

The toxicity was induced in the experimental animal model by the administration of BPA which resulted in oxidative stress by altering the ROS and antioxidants enzymes level. Baseline characteristics including body weight and organ weights were measured and analysed. Organ (liver) weight to body weight ratio was found to be remarkably increased in the case of BPA as compared to normal control. The kidney to body weight ratio was slightly increased whereas no significant variation was observed in case of heart weight to body weight ratio (Table 3.1). However, in case of treatment groups (BPA+P.I and BPA+ Mel) the organ weight (heart, liver, and kidney) was comparable to normal control.

**Table. 3.1 Effect of BPA on organ weights of different experimental groups**

<b>Groups</b>	<b>Heart Weight / Body Weight</b>	<b>Liver Weight / Body Weight</b>	<b>Kidney Weight / Body Weight</b>
NS	0.0033±0.00017	0.033±0.0012	0.0076±4.06E-05
BPA	0.0029±0.000248	0.042±0.0019	0.0079±0.000359
P.I	0.0024± 0.00048	0.030±0.00115	0.0072±0.000287
BPA+P.I	0.0031±0.000233	0.027±0.00287	0.0082±0.00061
Mel	0.0027±0.00039	0.036±0.0013	0.0066±0.00123
BPA+Mel	0.0028±8.485E-05	0.037±0.00152	0.0052±0.000895

### 3.2. Effect of *Pistacia integerrima* on cellular architecture

Cytoprotective effect of *Pistacia integerrima* against BPA induced toxicity was assessed by histological analysis of tissues (heart, liver, and kidney). In case of BPA treated heart tissues H and E staining showed increased number of nuclei, disruption of cellular membrane, the increased surface area of the cell and disturbed nucleus to cytoplasm ratio, all these features are hallmarks of apoptosis in the cardiomyocytes. However, the NS, P.I and Mel showed normal cellular organization (intact cell membrane, normal nuclear number and nucleus to cytoplasm ratio (Fig. 3.25 a, b, c, e), Moreover, the treatment groups (BPA+P.I and BPA+Mel) depicted the decreased number of nuclei and intact cellular architecture (Fig. 3.25 d, f, a). The percentage abnormal cells was significantly increased in BPA treated heart tissues as compared to normal control (NS), while in treatment groups (BPA+P.I and BPA+Mel) the percentage abnormal cells was significantly reduced.

The histology of the BPA treated liver tissues showed the shrinkage of hepatocytes with hyper-eosinophilic cytoplasm and increased percentage of abnormal cells. Moreover, the small cluster of cells was also observed in BPA treated liver tissues (Fig. 3.25 g, h). However, in P.I, Mel and treatment groups (BPA+P.I and BPA+Mel) the morphology of hepatocytes was very close to normal architecture with less percentage of abnormal cells (Fig. 3.25 i, j, k, l, b).



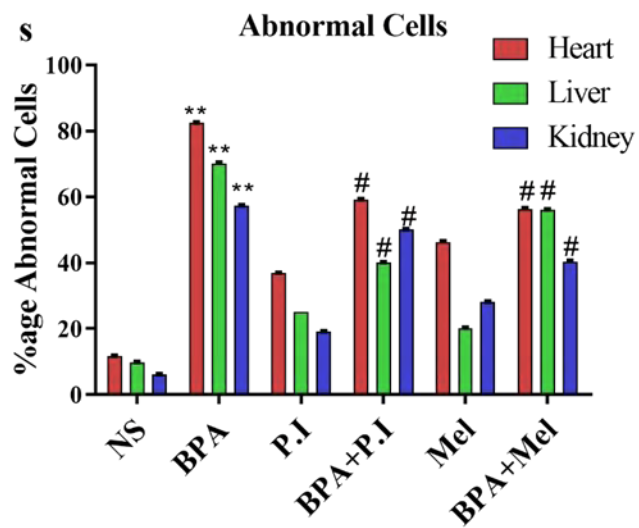
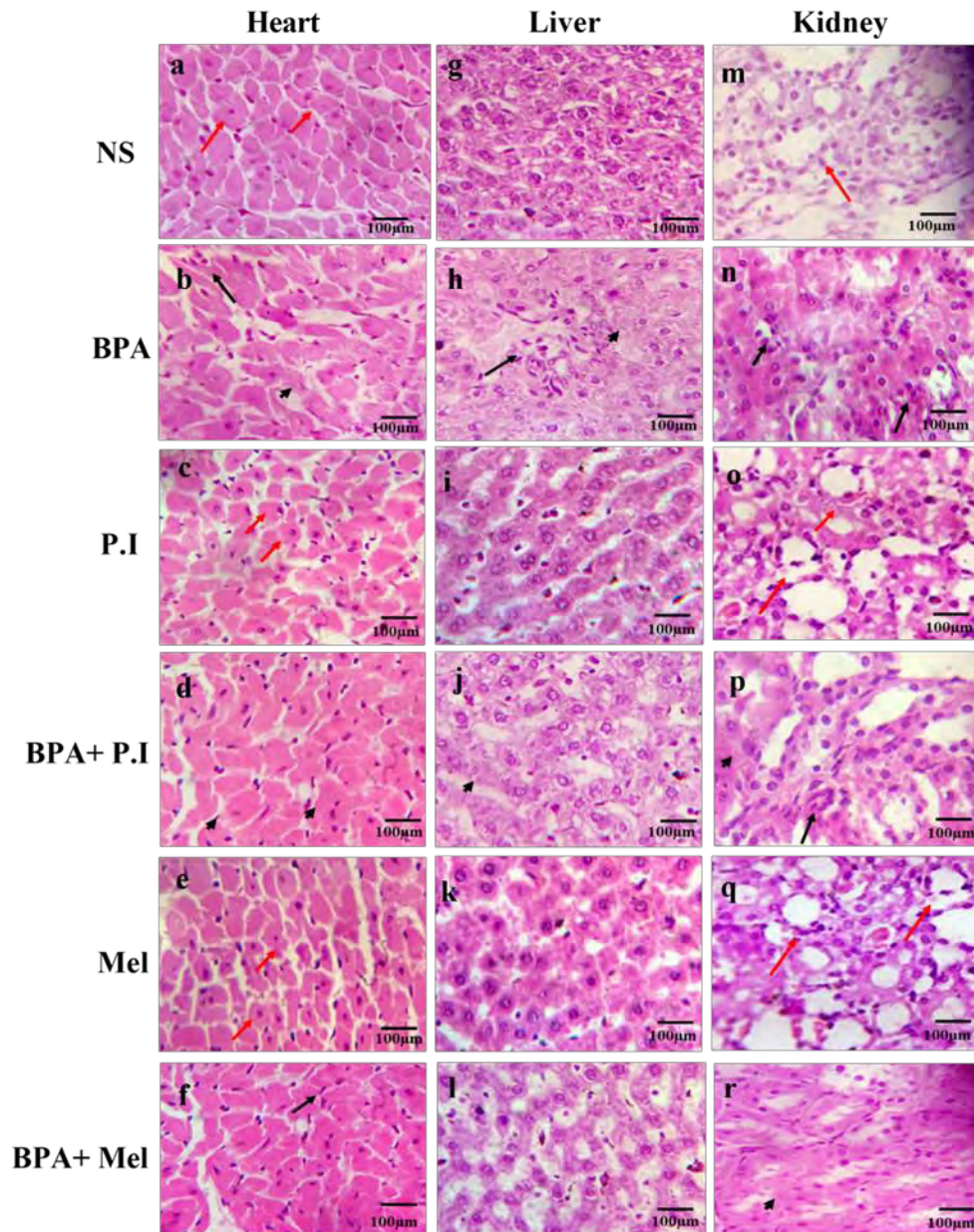


Figure 3.25. Effect of *Pistacia integerrima* on cellular architecture a–f representative images of H&E staining of the heart tissues; a NS, b BPA, c P.I, d BPA + P.I, e Mel, f BPA + Mel, g–l representative images of H&E staining of the liver tissues; g NS, h BPA, i. P.I, j BPA + P.I, k Mel, l BPA + Mel, m–r representative images of H&E staining of the kidney tissues; m NS, n BPA, o P.I, p BPA + P.I, q Mel, r BPA + Mel, (red arrows are indicating normal cells, black arrows are indicating increased number of nuclei, whereas arrow heads are used to show abnormal cells, images taken at 40X, scale bar 100 $\mu$ m), s graphical representation of percentage abnormal cells in H&E stained heart, liver and kidney tissues. “\*\* $p < 0.001$  in comparison to normal control (NS), # $p < 0.01$  in comparison to disease control (BPA)”

Kidney tissues of BPA treated rats showed the disruption of the kidney tubules with increased abnormal cells. In addition, BPA has also resulted in the loss of cellular architecture, the amorphous appearance of the area and joined cells showed extensive nuclear pyknosis and condensed shrunken morphology with more apoptotic bodies as compared to the histological outcomes of normal tissues (Fig. 3.25 m, n). The cellular architecture of both P.I and Mel groups were comparable to normal control (Fig. 3.25 o, q). The treatment with plant extract (BPA+P.I) and the melatonin (BPA+Mel) manifested the analeptic effects by reducing the number of abnormal cells and apoptotic bodies. The cellular architecture was restored to normal upon treatment with P.I (BPA+P.I) and melatonin (BPA+Mel) (Fig. 3.25 p, r, a, b).

### 3.3. Effect of *Pistacia integerrima* on different biochemical parameters

#### 3.3.1. Effect of *Pistacia integerrima* on oxidative profiling

BPA while acting as pro-oxidant plays a key role in the development and progression of the toxicity. Herein, to evaluate the status of toxicity the level of reactive oxygen species was analysed. Increased production of ROS in both serum and tissues (heart, liver, and kidney) was observed in BPA treated rat models as compared to normal control (NS). While the ROS level of Mel and P.I group was comparable to NS however in the presence of potent antioxidant, melatonin (BPA+Mel) a significant decrease in ROS level was detected. Similarly, ROS level was significantly reduced in plant extract treated rats (BPA+P.I) as compared to diseased group (Fig. 3.26). Further, oxidative stress was also confirmed through lipid peroxidation (TBARs) assay where significantly increased TBARs level was detected at tissue level (heart, liver kidney) in BPA treated rats as compared to normal control (NS). The increase in ROS can lead to the activation of JNK ultimately causing the activation of p53 which leads to

apoptosis. However, the protective role of *Pistacia integerrima* gall extract against BPA

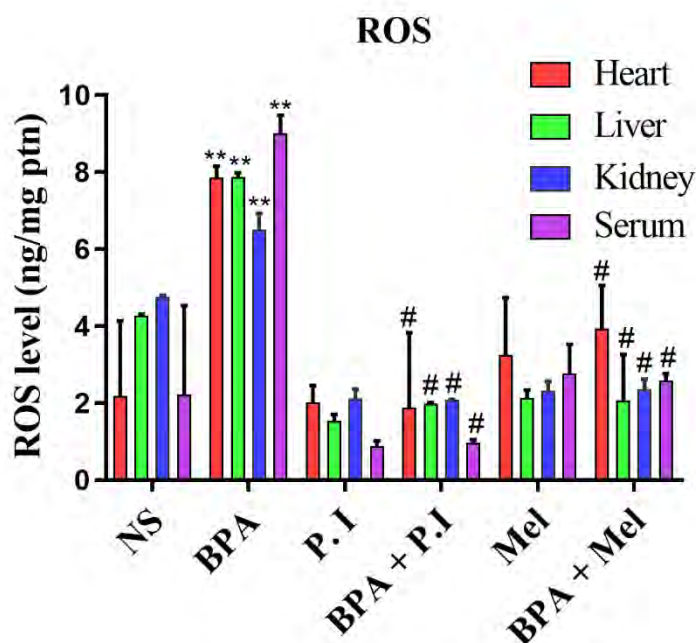


Figure 3.26. Effect of *Pistacia integerrima* on ROS level, “\*\*\* $p < 0.001$ , in comparison to normal control (NS), # $p < 0.01$  in comparison to disease control (BPA)”

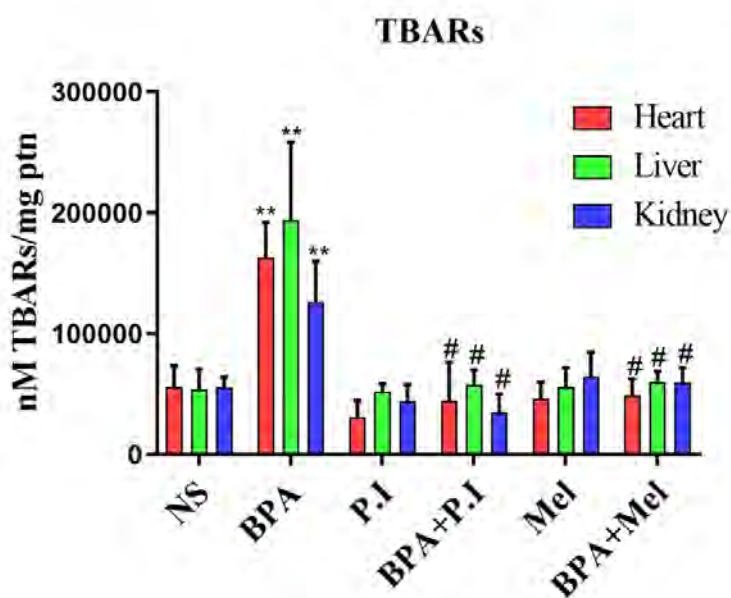


Figure 3.27. Effect of *Pistacia integerrima* on TBARs level in heart, kidney and liver samples. “\*\*\* $p < 0.001$ , in comparison to normal control (NS), # $p < 0.01$  in comparison to disease control (BPA)”

induced toxicity via treatment with melatonin (BPA+Mel) and plant extract (BPA+P.I) significantly decreased the TBARs level as compared to disease control (Fig. 3.27). Thus, suggesting the protective role of *Pistacia integerrima* gall extract against BPA induced toxicity via free radical scavenging potential.

### 3.3.2. Effect of *Pistacia Integerrima* on liver markers

In our present study, the level of liver marker enzymes was analysed to evaluate the effect of therapeutic compounds on the liver. The ALT, ALP and AST were greatly enhanced in rats treated with BPA indicating liver damage. Whereas, upon treatment with melatonin (BPA+Mel) and Plant extract (BPA+P.I) the level of these enzymes was significantly reduced as compared to BPA treated rats (Fig. 3.28) which suggests the hepato-protective potential of plant extract.

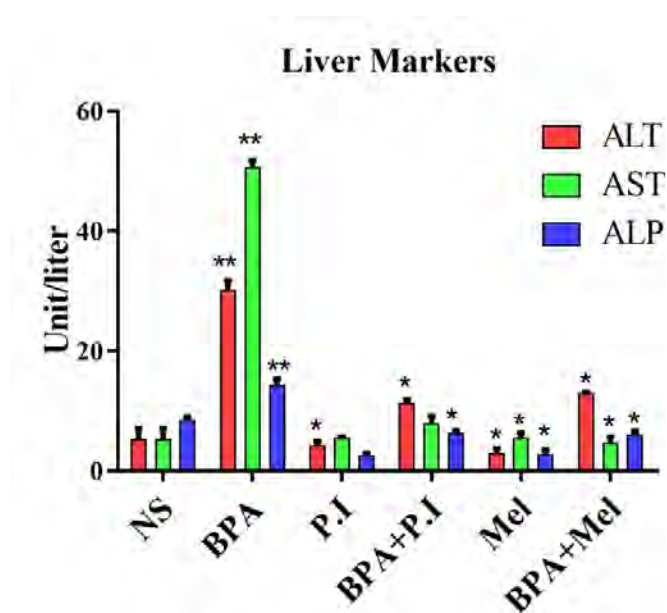


Figure 3.28. Effect of *Pistacia integerrima* on liver markers Estimation of liver marker enzymes ALT, AST and ALP In serum samples of different experimental groups, “\*\* $p < 0.01$ , \* $p < 0.01$  in comparison to normal control (NS)”

### 3.3.3. Effect of *Pistacia integerrima* on lipid profile at blood peripheral level

Development of various pathologies cause disturbance in the lipid metabolism. Serum cholesterol and triglycerides levels were significantly increased in BPA treated rats as compared to normal control (NS). Whereas these levels were significantly decreased

upon treatment with melatonin (BPA+Mel) and *Pistacia integerrima* (BPA+P.I). Serum HDL was reduced in case of BPA administered rats as compared to normal control however, the increased level of HDL was observed in plant extract treated group (BPA+P.I) as compared to the disease control (Fig. 3.29).

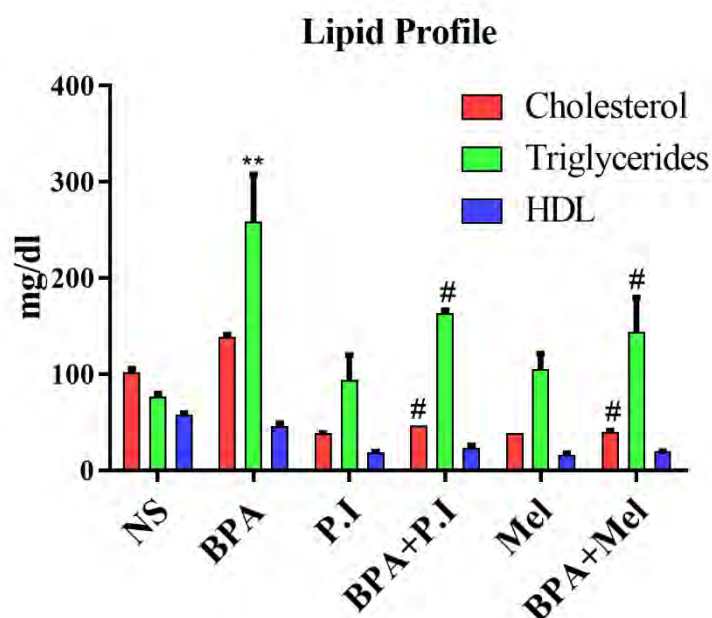


Figure 3.29. Effect of *Pistacia integerrima* on lipid profile Estimation of cholesterol, triglycerides and HDL in serum samples of different experimental groups. “\*\* $p < 0.001$  in comparison to normal control (NS), # $p < 0.01$  in comparison to disease control (BPA)”

#### 3.3.4. Effect of *Pistacia integerrima* on Serum uric acid and kidney toxicity

In current study the uric acid levels were significantly enhanced indicating kidney toxicity of BPA as compared to normal control (NS). Whereas upon treatment with *Pistacia integerrima* (BPA+P.I) and melatonin (BPA+Mel) serum uric acid level was significantly decreased as compared to disease control (Fig. 3.30).

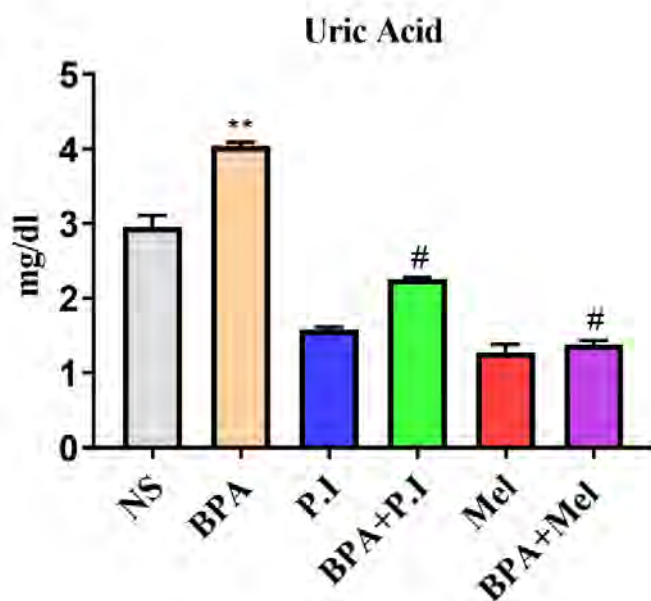


Figure 3.30. Estimation of uric acid levels in experimental groups. The data plotted as “mean  $\pm$  SD, \*\* $p < 0.001$  in comparison to normal control (NS), # $p < 0.01$  in comparison to disease control (BPA)”

### 3.3.5. Effect of *Pistacia integrerrima* on serum glucose level

The glucose levels are kept within a narrow range by body’s homeostatic mechanism, in which the key player is hormonal regulation.

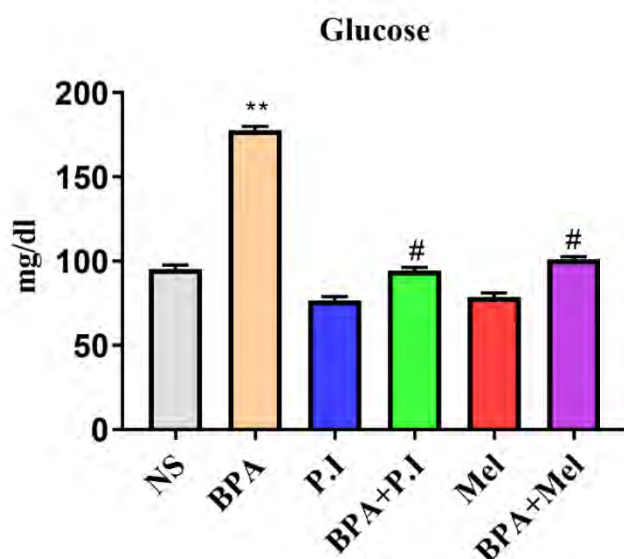


Figure 3.31. Estimation of blood glucose levels in different experimental groups. The data plotted as “mean  $\pm$  SD, \*\* $p < 0.001$  in comparison to normal control (NS), # $p < 0.01$  in comparison to disease control (BPA)”

Herein, the glucose level was significantly increased when BPA was administered to the rats for 16 days however increasing the BPA exposure time suggests a possible link of BPA to hyperglycemia. Whereas in plant extract treated rats (BPA+P.I), significant decrease in the serum glucose level was observed as compared to disease control (Fig. 3.31). Similar results were observed in case of melatonin treatment (BPA+Mel) group.

### 3.3.6. Antioxidant potential of *Pistacia integerrima* gall extract

Antioxidant enzymes prevent the cellular damage caused by ROS by catalysing the decomposition of damaging peroxide into neutral compounds. The antioxidant profiling was done to confirm the therapeutic potential of *P. integerrima*.

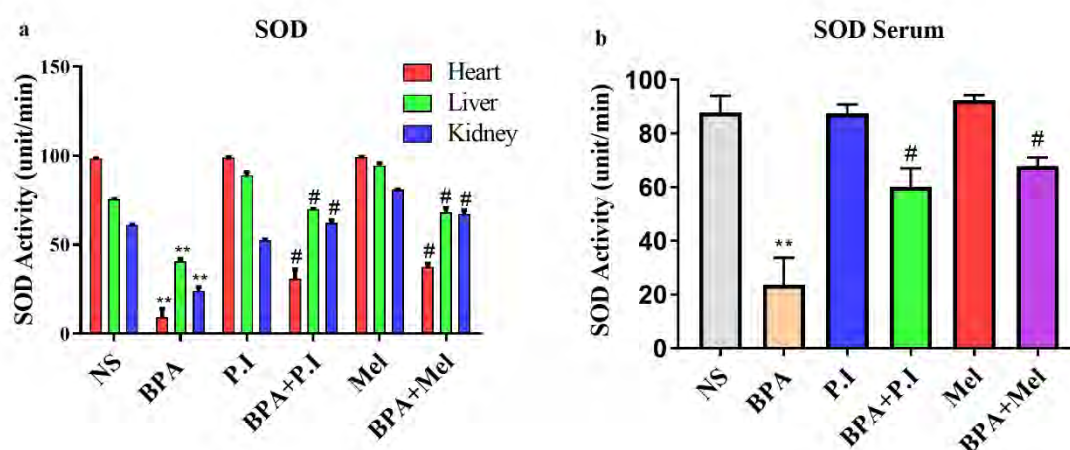


Figure 3.32. Antioxidant potential of *Pistacia integerrima* gall extract a Estimation of SOD activity in heart, liver and kidney homogenates of different experimental groups b Estimation of SOD activity in serum samples. “The data plotted as mean  $\pm$  SD, \*\* $p < 0.001$  in comparison to NS, # $p < 0.01$  in comparison to disease control (BPA)””

The antioxidant enzymes activities (SOD, CAT, APX, GSH and POD) were significantly reduced in BPA treated rat model as compared to normal control (NS) in case of both serum and tissues (heart, liver, kidney) (Fig. 3.32 a, b). While the antioxidant enzymes level (SOD, CAT, APX, GSH and POD) of Mel and P.I group were comparable to normal control (NS). However, the decreased antioxidant enzymes

activities were elevated upon treatment with melatonin (BPA+Mel) in both serum and tissues (heart, liver, kidney). Nearly two-fold increase in the SOD activity was observed

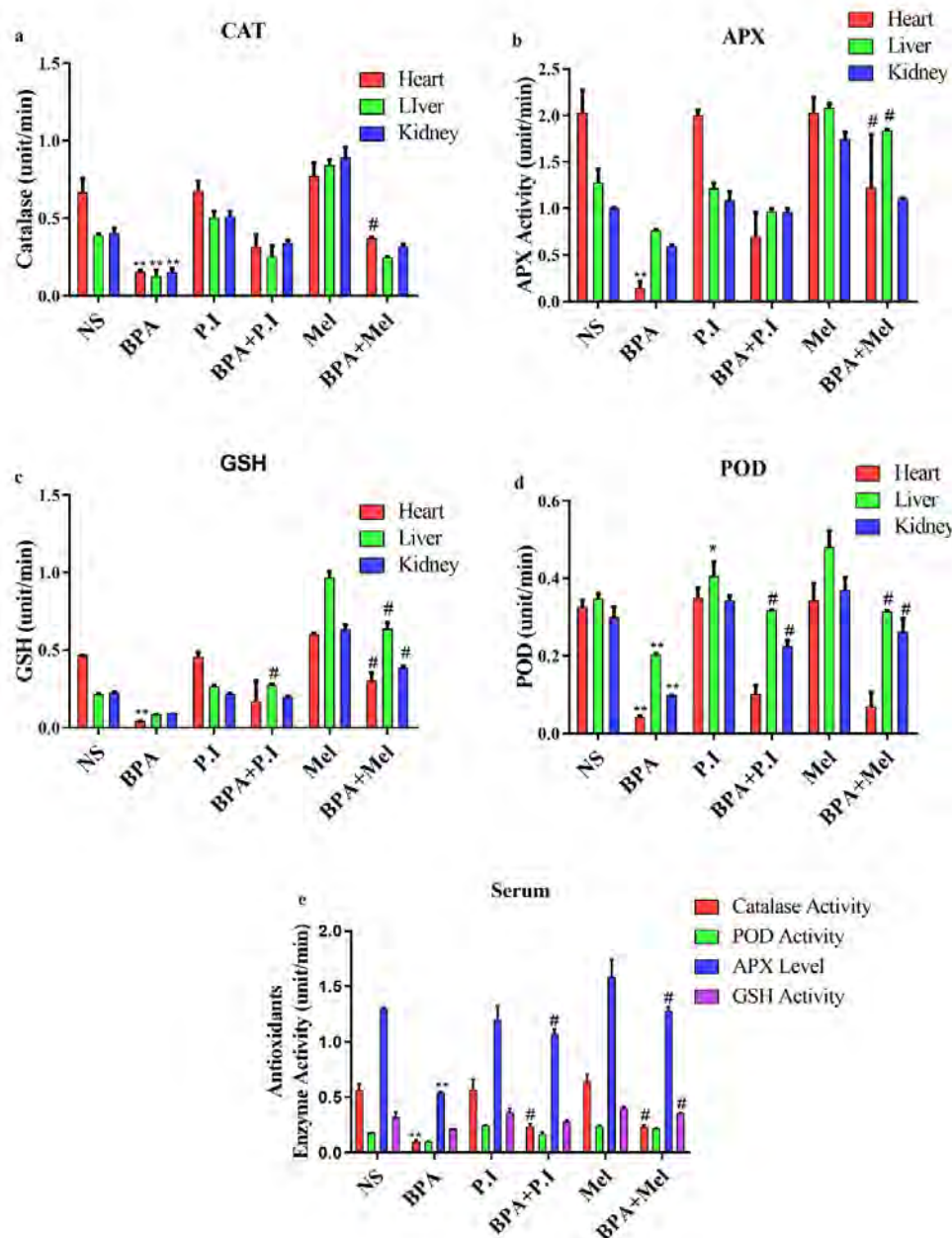


Figure 3.33. Antioxidant potential of *Pistacia integerrima* gall extract, a Estimation of CAT activity in heart, liver and kidney tissues, b Estimation of APX activity in heart liver and kidney tissues c Estimation of GSH activity in heart, liver and kidney tissues, d Estimation of POD activity in heart, liver and kidney tissues, e Estimation of CAT, POD, APX and GSH activity in serum. “\*\* $p < 0.001$  in comparison to normal control (NS), # $p < 0.01$  in comparison to disease control (BPA)”



in *P. integerrima* treated group (BPA+P.I). The *Pistacia integerrima* treatment (BPA+P.I) also resulted in increased antioxidants levels (CAT, APX, GSH and POD) as compared to disease control (BPA) suggesting the antioxidant boosting potential of *P. Integerrima* (Fig. 3.33 a, b, c, d, e).

### 3.4. Antiapoptotic potential of *Pistacia integerrima*; effect on different apoptosis modulators in p53 mediated apoptosis

Altered expression of the apoptosis related genes play crucial role in cardiotoxicity. In current study, the RNA expression level of the key player of apoptosis, the transcription factor p53 was significantly increased conversely the Ubc13 was significantly downregulated in heart tissues of BPA treated rats.

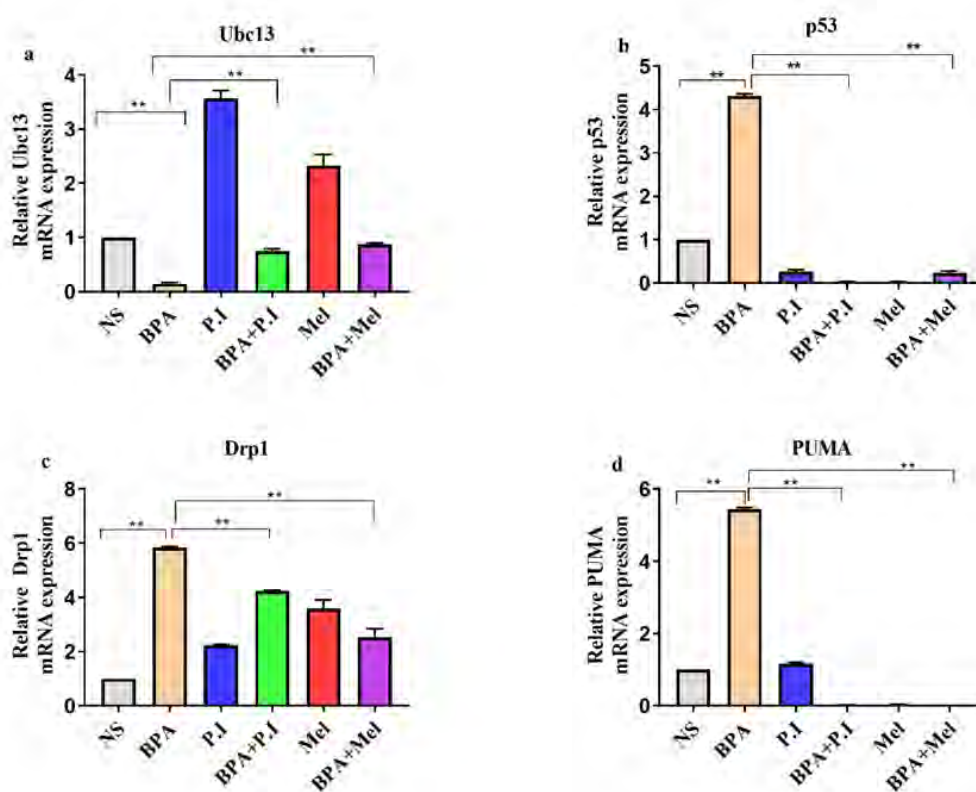


Figure 3.34. Antiapoptotic potential of *Pistacia integerrima* gall extract a Estimation of relative RNA expression of Ubc-13, b Estimation of relative RNA expression of p53, c Estimation of relative RNA expression of Drp1, d Estimation of relative RNA expression of PUMA. GAPDH was used as the reference gene “\* $p < 0.01$ , \*\* $p < 0.001$ ”

On treatment with plant extract (BPA+P.I) and melatonin (BPA+Mel) the levels of p53 were decreased along with the upregulated levels of Ubc13 (Fig. 3.34 a, b). The mitochondrial membrane potential regulatory genes PUMA and Drp1 were upregulated at RNA level in BPA treated group however the decreased expression was observed in extract treatment groups (BPA+P.I) which suggests the p53 mediated mitochondrial linked apoptosis (Fig. 3.34 c, d). BPA+Mel also showed significantly downregulated expression of PUMA and Drp1.

The RNA expression results were further confirmed by the protein expression analysis through western blotting. Reduced expression of Ubc13 and high expression of apoptotic genes, such as the transcription factor p53 serve as the marker of apoptosis. Our results showed decreased expression level of Ubc13 in heart tissues of BPA treated model whereas melatonin and plant extract treated groups (BPA+P.I and BPA+Mel) the protein level of Ubc13 was comparable to normal (Fig. 3.35 a, b). The increased expression of both phospho-p53 and p53 in BPA administered rats revealed the role of BPA in triggering heart tissues apoptosis whereas the levels were comparatively less in the treatment groups (BPA+Mel and BPA+P.I) (Fig. 3.35 a, c, d). Whereas in the case of mitochondrial apoptosis regulatory proteins, PUMA and Drp1 there was significant increase in BPA treated group and the expression levels were downregulated in the *Pistacia integerrima* (BPA+P.I) and melatonin treated (BPA+Mel) groups (Fig. 3.35 a, e, f, g).

To further confirm the role of p53 in BPA induced apoptosis we have analysed the expression level of cytoplasmic cytochrome c. As the release of cytochrome c to the cytoplasm is considered as the key indicator of apoptosis. The expression of cytochrome c was significantly increased in BPA treated rats as compared to normal control (NS), while the expression level of cytochrome C in P.I and Mel groups was comparable to NS. Moreover, in treatment groups, BPA+P.I and BPA+Mel, the expression level was significantly decreased suggesting the antiapoptotic potential of P.I against BPA induced cardiotoxicity.

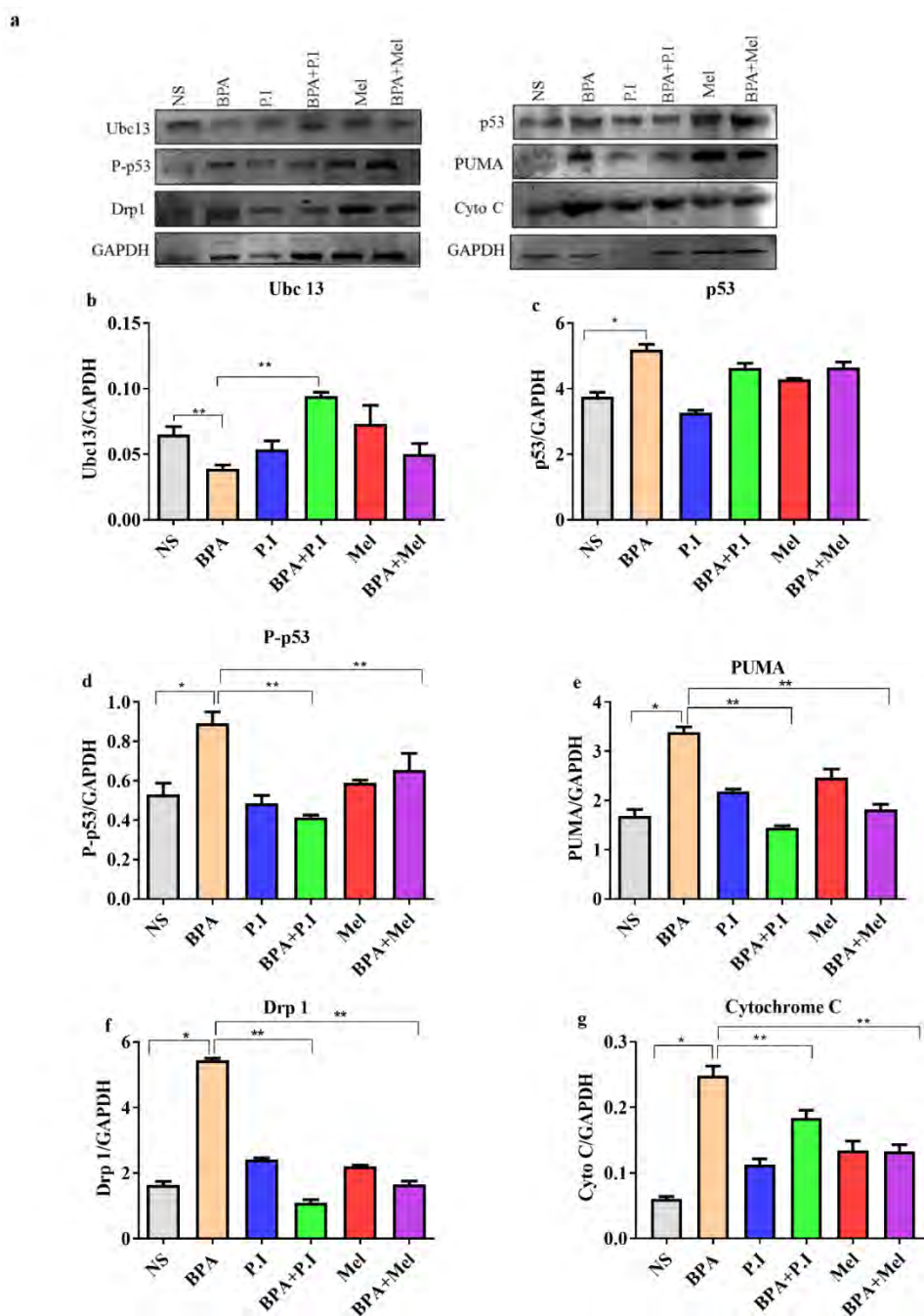


Figure 3.35. Evaluation of Antiapoptotic potential of *Pistacia integerrima* a Representative image of the western blot for Drp1, P-p53, PUMA, p53, cytochrome C (Cyto c), Ubc13 and GAPDH proteins in heart tissues, b Graphical representation of the densitometric analysis of Ubc13, normalized by GAPDH in heart tissues, g graphical representation of the densitometric analysis of P-p53, normalized by GAPDH in heart tissues, h graphical representation of the densitometric analysis of p53, normalized by GAPDH in heart tissues, i graphical representation of the densitometric analysis of Drp1, normalized by GAPDH in heart tissues, j graphical representation of the densitometric analysis of PUMA, normalized by GAPDH in heart tissues, k graphical representation of the densitometric analysis of cytochrome C (Cyto c), normalized by GAPDH in heart tissues. “The data plotted as mean  $\pm$  SD, \* $p < 0.01$  \*\* $p < 0.001$ ”

### 3.5 Baseline Characteristics of Experimental Groups

#### 3.5.1 Dose Dependent Response of BPA on Body Weight

BPA is an environmental toxicant, act as a xenoestrogen. Body of all the rats was recorded daily. The figure 3.36 represents the average daily body weight of all the experimental groups. In addition, change in body weight of different experimental groups was also calculated. Figure 3.12 comprises of the data of change in body weight in different experimental groups. Body weights of the BPA2 and BPA3 groups were significantly increased in comparison with the control group. Whereas in the treatment groups (BPA2+MLT and BPA3+MLT) body weight was significantly reduced as compared to the respective disease group. Statistical analysis of these group was done by using one-way ANOVA followed by Tukey's test, significance was calculated at  $p$  value  $< 0.01$ . Graphical representation of change in body weight is shown in figure 3.37.

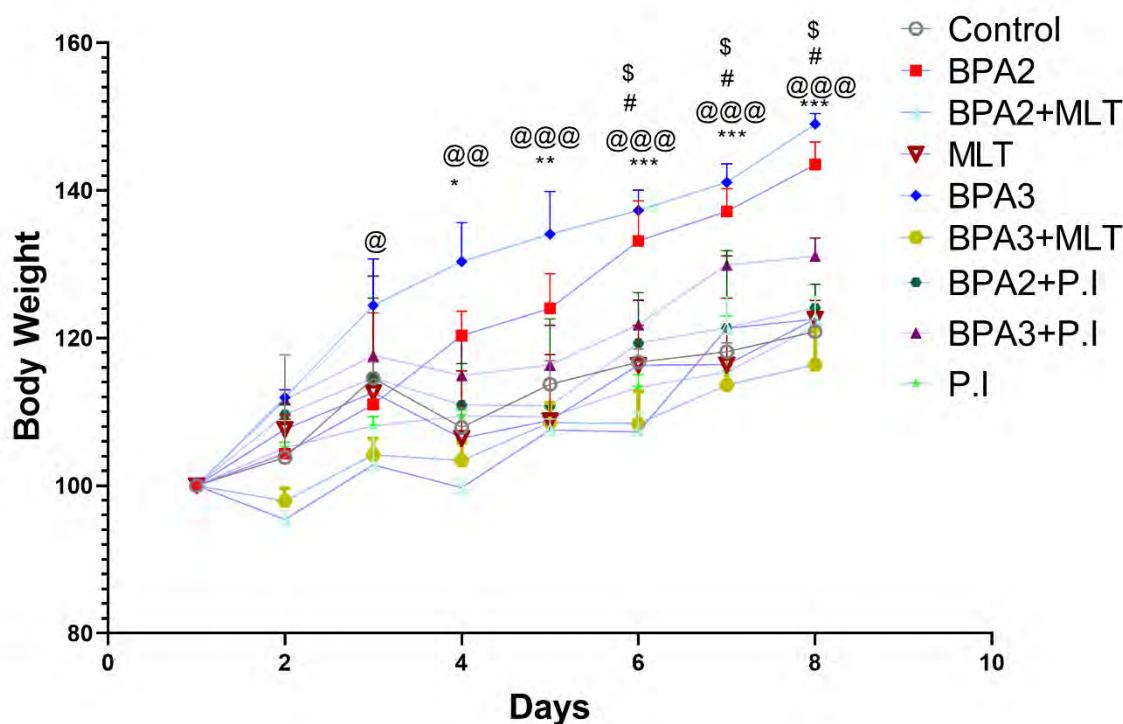


Figure 3.36. Estimation of daily body weight of all experimental groups (\* BPA 2 is significant in comparison to control, @ BPA 3 is significant in comparison to control, # BPA2+MLT and BPA3+MLT are significant in comparison to disease group, \$ BPA2+P.I and BPA3+P.I are significant in comparison to disease group)

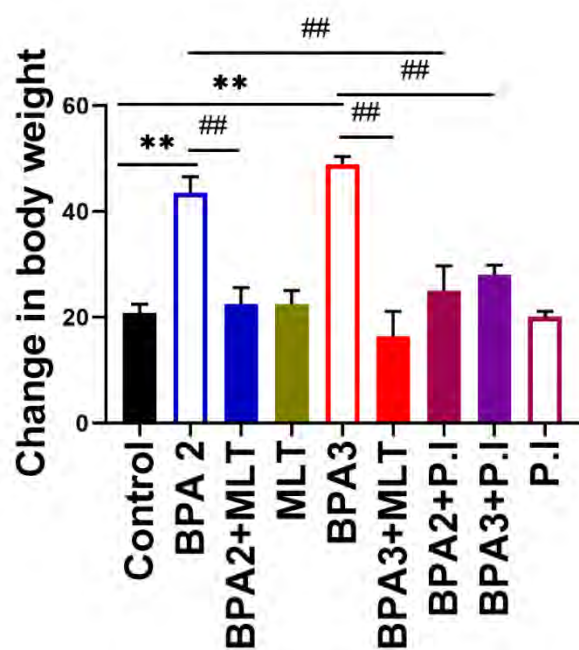


Figure 3.37. Estimation of change in body weight “\*\*/## shows  $p$  value  $< 0.01$ ”

### 3.5.2 Dose Dependent Effect of BPA on Heart

Effect of BPA on heart weight was analyzed by calculating the heart weight to body weight ratio (HW/BW). Figure 3.38 describe the relative index of HW/BW ratio. HW/BW ratio was significantly upregulated in BPA2 and BP3 group as compared to normal group. In treatment group B2+MLT and B3+MLT HW/BW ratio was normalized as compared to disease group. Moreover, the treatment with plant extract also showed the HW/BW comparable to the control group.

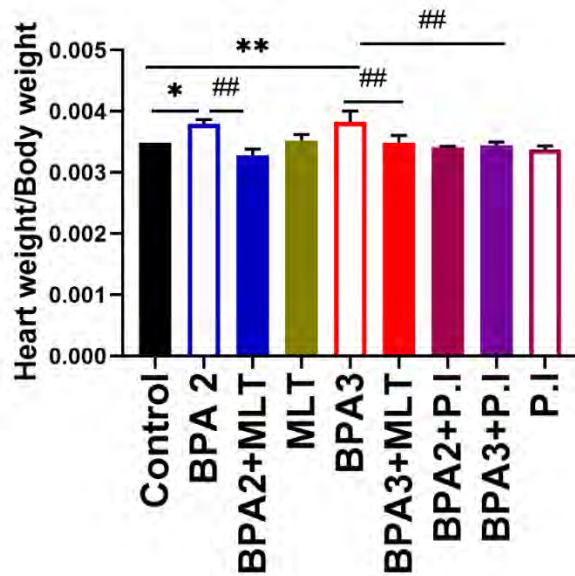


Figure 3.38. Estimation of heart weight to body weight ratio “\* shows  $p$  value  $< 0.05$ , \*\*/## shows  $p$  value  $< 0.01$ ”

### 3.6 Effect of *Pistacia integerrima* on the levels of different oxidative stress markers

#### 3.6.1 Estimation of ROS level in serum, heart samples

BPA causes oxidative stress by generating ROS. In current study ROS levels were analyzed in both serum and heart tissue lysates to estimate the BPA toxicity.

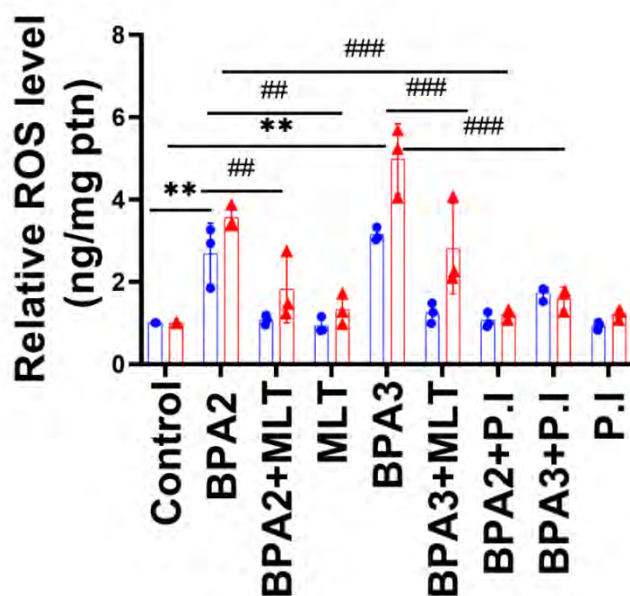


Figure 3.39. Estimation of ROS levels in different experimental groups “\*\*/## shows  $p$  value  $< 0.01$ , blue colour bars show serum and red colour show homogenate”

ROS levels were significantly increased in BPA administered groups (BPA2 and BPA3) in both serum and heart tissue as compared to the control group (Fig. 3.39). However, the treatment with *Pistacia integerrima* significantly reduced the levels of ROS in treatment groups (BPA2+P.I and BPA3+P.I) in both serum and heart tissues. In addition to plant extract the melatonin administered groups also showed significantly decreased ROS levels as compared to the disease groups (BPA2 and BPA3). Both P.I and MLT showed comparable results with respect to the control.

### 3.6.2 Estimation of TBARs level in serum, and heart samples

ROS leads to the lipid damage therefore to further confirm the oxidative stress TBARs levels were analyzed. TBARs level in BPA administered groups (BPA2 and BPA3) was

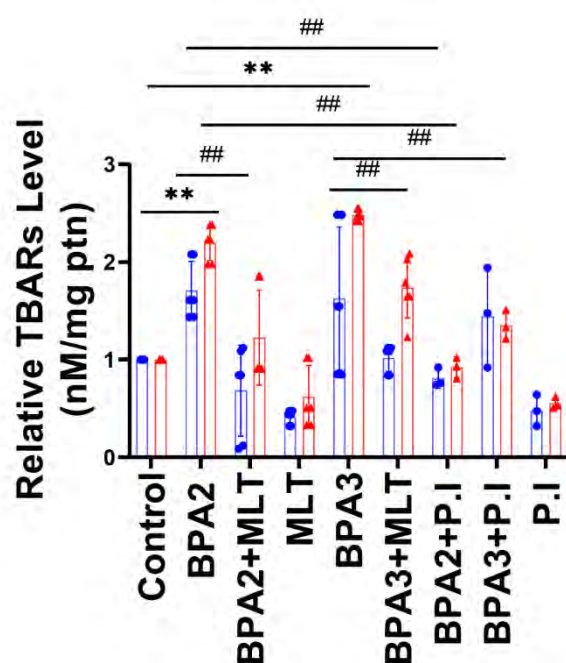


Figure 3.40 Graphical representation of TBARs level in different experimental groups “\*\*/## shows  $p$  value  $< 0.01$ , blue colour bars show serum and red colour show homogenate”

significantly increased as compared to the control in both serum and heart tissue samples (Fig. 3.40). TBARs levels were significantly decreased in both BPA2+P.I and BPA3+P.I treated groups as compared to the disease group. In addition, treatment with melatonin showed significantly decreased levels of TBARs in both serum and heart tissues.

### 3.6.3 Analysis of SOD Activity in serum, and heart samples

A significant decrease in SOD activity of both serum and heart tissue sample was observed in disease groups (BPA2 and BPA3) as compared to the control, as shown in figure 3.41. Whereas the SOD activity was significantly elevated in the case of both plant extract treatment groups, BPA2+P.I and BPA3+P.I as compared to BPA administered group (BPA2 and BPA3). In addition, a significant increase in SOD activity was observed in BPA2+MLT and BPA3+MLT. The P.I group showed SOD activity comparable to the control suggesting the nontoxic potential of the plant extract.

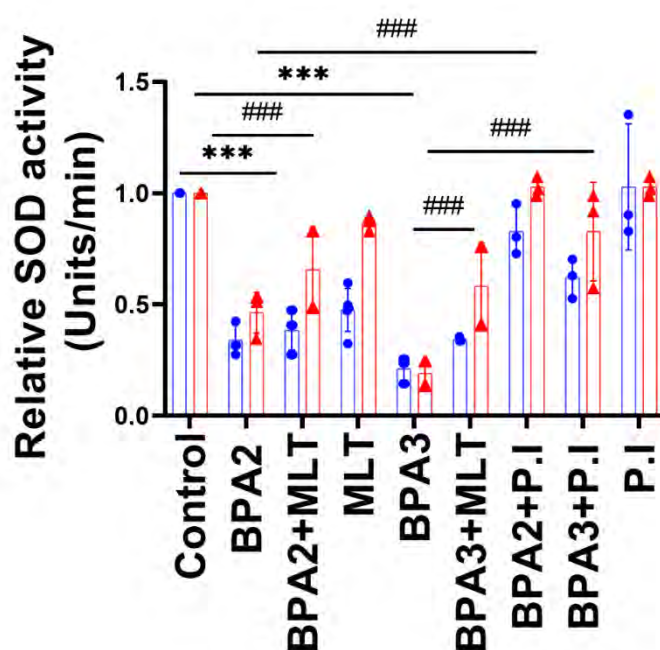


Figure 3.41. Graphical representation of the relative SOD activity “\*\*/# shows  $p$  value < 0.01, \*\*\*/### shows  $p$  value < 0.001, blue colour bars show serum and red colour show homogenate”

### 3.6.4 Evaluation of catalase activity in serum and heart tissue

Serum catalase activity was significantly reduced in disease group (BPA1 and BPA2) as compared to the control. In case of melatonin treatment group (BPA2+MLT and



BPA3+MLT), catalase activity was significantly increased as compared to the diseased group, (Fig. 3.42). Catalase activity in heart tissues was significantly decreased in BPA administered groups (BPA2 and BPA3) as compared to the control. Treatment with plant extract showed significantly increased catalase activity in both serum and heart tissue samples as compared to the disease group, suggesting the antioxidant boosting potential of plant extract.

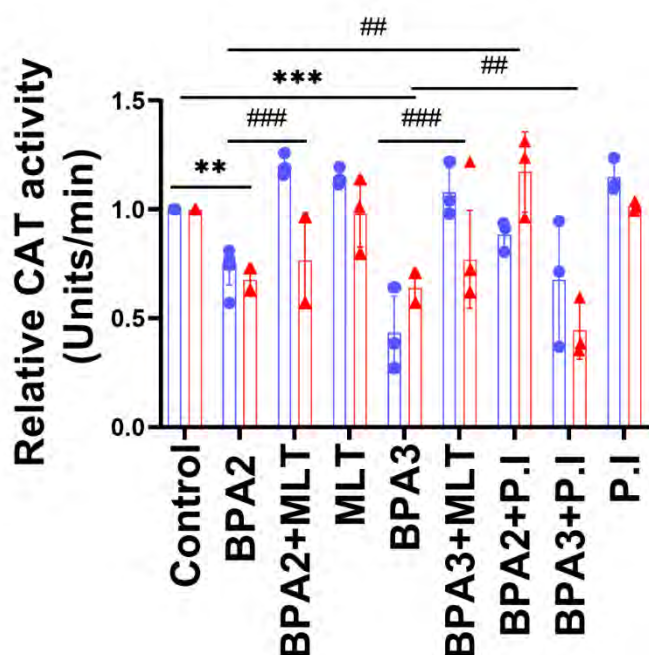


Figure 3.42. Graphical representation of the catalase activity “\*\*/## shows  $p$  value < 0.01, \*\*\*/### shows  $p$  value < 0.001”

### 3.6.5 Evaluation of Ascorbate peroxidase level in serum and heart tissues

Ascorbate per oxidase (APX) level was significantly reduced in both serum and samples of BPA administered groups (BPA2 and BPA3) as compared to the control. APX level was significantly increased in treatment groups (BPA2+P.I and BPA3+P.I) as compared to disease group (Fig. 3.43). In addition to plant extract, melatonin also showed its antioxidant potential by significantly reducing the APX level in both serum

and heart tissues. P.I and MLT administered groups showed APX level comparable to the control.

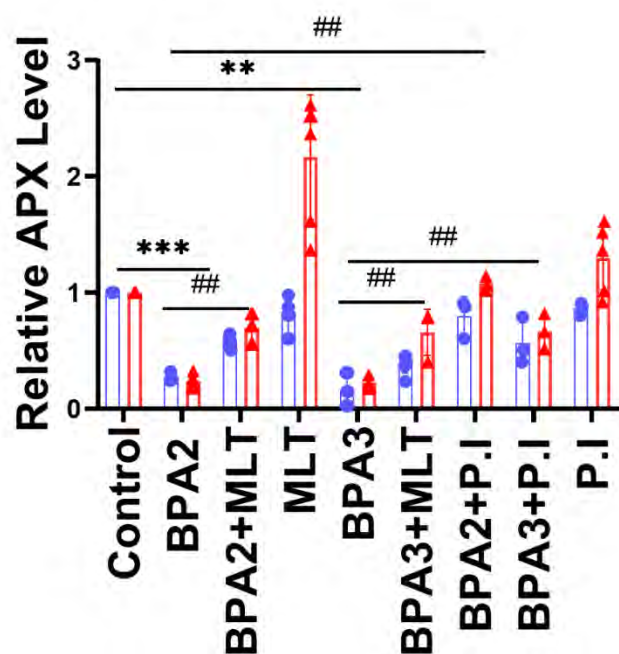


Figure 3.43. Estimation of APX level in serum and heart tissue samples “\*\*/# shows  $p$  value  $< 0.01$ , \*\*\* shows  $p$  value  $< 0.001$ ”

### 3.7 Histological Analysis

Histological analysis was performed to analyze the cellular damages induced by BPA. BPA disrupt the cardiac cell physiology as shown in figure 3.44. Hematoxylin and eosin staining (H & E) showed the increased number of nuclei, disrupted nucleus to cytoplasm ratio, increased cell surface area and loss of cellular architecture in diseased groups (BPA2 and BPA3) as compared to normal group. All these changes are characteristics of cellular damage caused by necrosis and apoptosis in cardiomyocytes. Whereas plant extract and melatonin groups showed the intact cellular structure and well-defined nuclei. However, melatonin (B2+MLT and B3+MLT) and plant extract (B2+P.I and B3+P.I) treatment groups showed the reduced number of cellular nuclei as compared to disease groups BPA2 and BPA3.

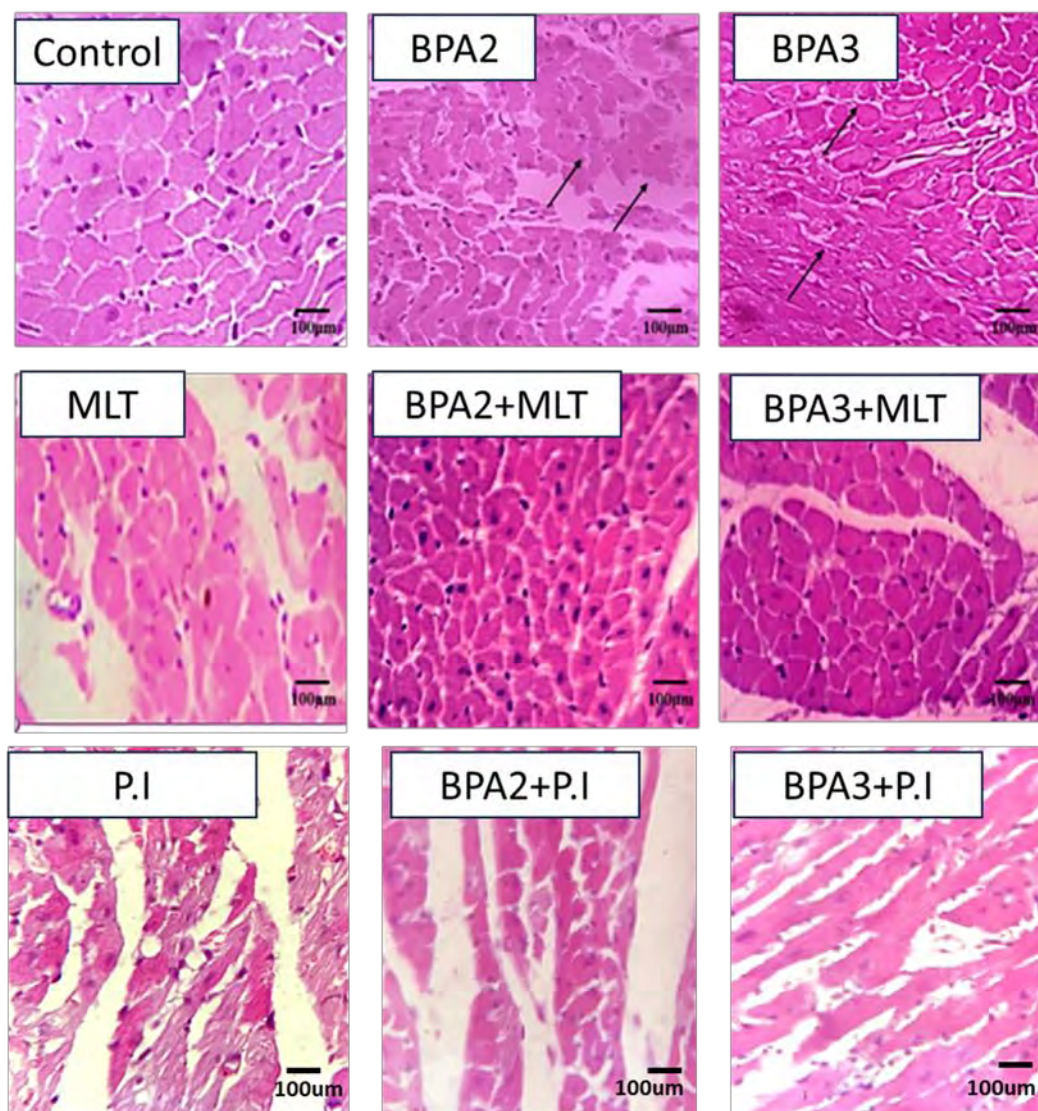


Figure 3.44. Effect of *Pistacia integerrima* on cellular architecture, Representative images of H&E staining of the heart tissues of the different experimental groups including control, BPA2, BPA3, Melatonin, BPA2+melatonin, BPA3+melatonin, *P. integerrima*, BPA2+ *P. integerrima*, BPA3+ *P. integerrima*, images taken at 40X scale bar 100µm

Percentage abnormal cells was also measured. The number of abnormal cells were high in BPA2 and BPA3 groups (Fig. 3.45). Whereas, the number of abnormal cells in melatonin and *Pistacia integerrima* control groups was comparable. Plant extract in treatment groups tried to overcome the effect of BPA and showed a reduced number of abnormal cells in heart tissues. Graphical representation of abnormal cells percentage is shown in figure 3.40.

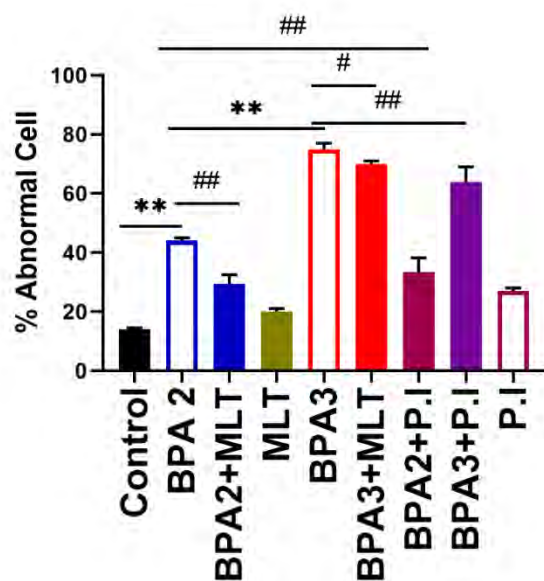


Figure 3.45. Graphical representation of percentage abnormal cells “\*/# shows  $p$  value  $< 0.05$ , \*\*/## shows  $p$  value  $< 0.01$ ”

### 3.8 Effect of *Pistacia integerrima* on the expression of p53 and its mediators in BPA-induced apoptosis

#### 3.8.1 mRNA Expression Analysis of p53 in Heart Tissues

p53 is a tumor suppressor involved in DNA repair, growth arrest, and apoptosis in response to stressful stimuli. Real-time PCR was performed to analyze the expression level of p53 in heart tissues. RNA expression of all experimental groups was normalized by GAPDH (Fig. 3.46). p53 expression level was significantly elevated in disease groups (BPA2 and BPA3) as compared to the normal control. Its expression was significantly suppressed in *Pistacia integerrima* treated rats (BPA2+ P.I) and (BPA3+P.I) as compared with disease group. The plant extract treatment has significantly decreased the expression of p53 even in the higher dose of BPA which suggests its antiapoptotic potential.

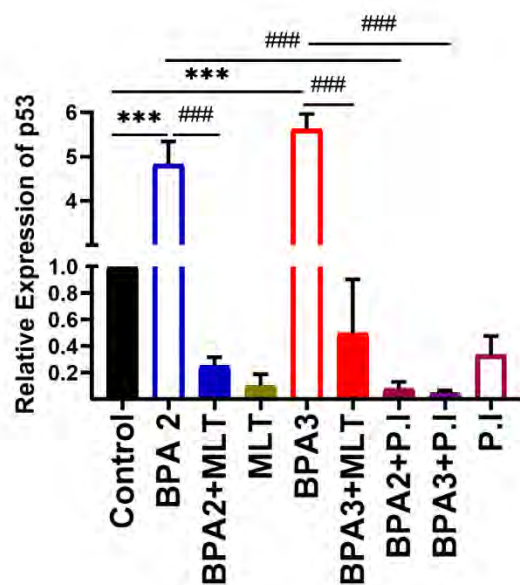


Figure 3.46. Estimation of RNA expression of p53 in different experimental groups “\*\*\*/### shows  $p$  value  $< 0.001$ ”

### 3.8.2 mRNA Expression Analysis of PUMA in Heart Tissues

The expression level of PUMA was significantly elevated in disease groups (BPA2 and BPA3) as compared to control.

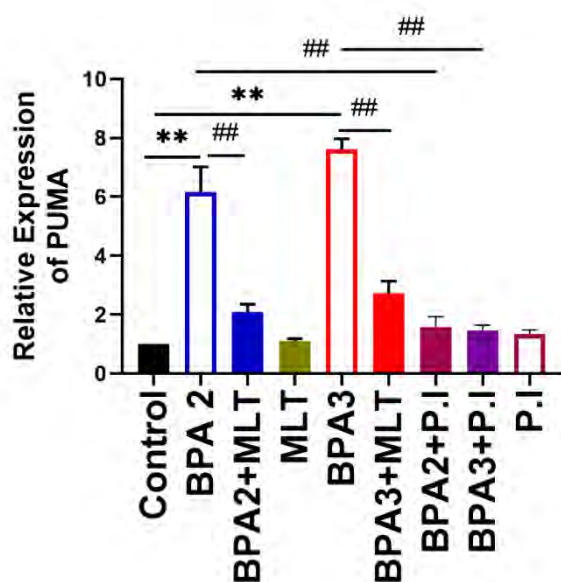


Figure 3.47. Relative Expression analysis of PUMA “\*\*/# shows  $p$  value  $< 0.01$ ”

Melatonin treatment showed significant downregulation in the expression of PUMA in case of both doses of BPA (BPA2+MLT and BPA3+MLT) (Fig. 3.47). Expression

level of PUMA was significantly decreased in *Pistacia integerrima* treated rats (BPA2+ P.I) and (BPA3+P.I) as compared with the disease group. The plant extract treatment has significantly decreased the expression of PUMA even in the higher dose of BPA, which suggests its antiapoptotic potential.

### 3.8.3 mRNA Expression Analysis of Drp1 in Heart Tissues

The Drp1 expression level was significantly elevated in BPA administered groups (BPA2 and BPA3) as compared to normal control (Fig. 3. 48). Its expression was significantly decreased in *Pistacia integerrima* treated groups (BPA2+ P.I) and (BPA3+P.I) as compared with the disease group, suggesting the plant extract's analeptic potential. The plant extract treatment has significantly decreased the expression of Drp-1 even in the higher dose of BPA, which suggests its antiapoptotic potential.

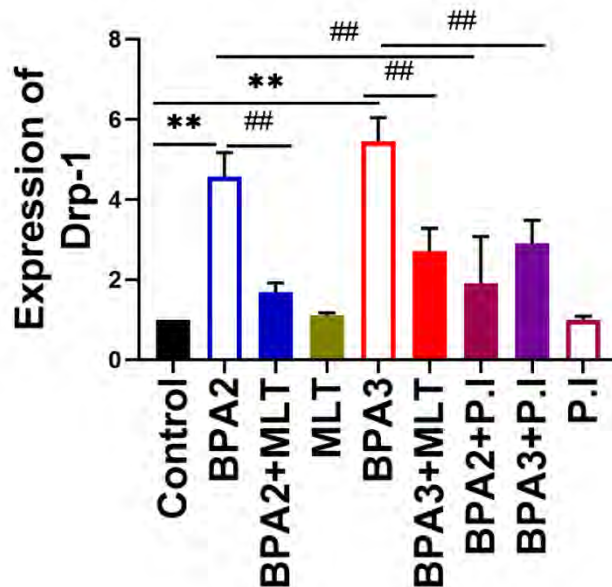


Figure 3.48. Estimation of relative mRNA level of Drp1 “\*\*/# shows p value < 0.01”

### 3.8.4 Relative Expression of USP7 in Heart Tissue of Experimental Groups

Usp7 is an important deubiquitinating enzyme that regulates p53 levels. BPA administration (BPA2 and BPA3) significantly reduced the levels of USP7 in disease group as compared to the control group. Significantly increased expression of USP7 in

case of BPA2+ P.I and BPA3+P.I was observed in contrast to disease group. GAPDH was used as an internal control. The graphical representation of USP7 expression is shown in figure 3.49.

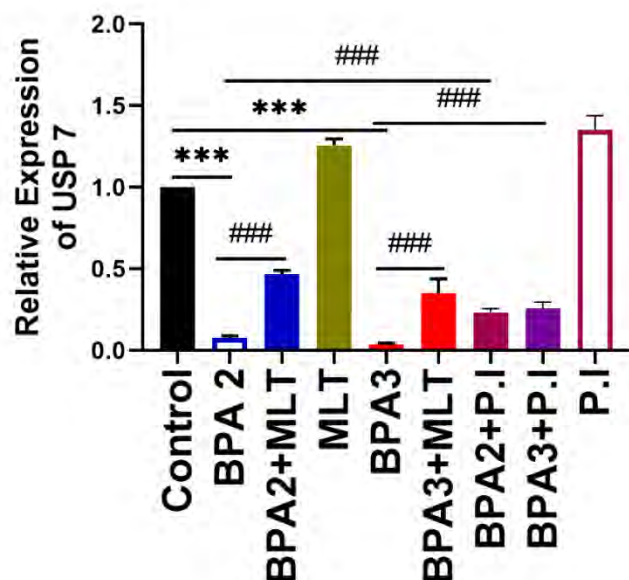


Figure 3.49. Estimation of RNA expression of USP7 in experimental groups “\*\*\*/### shows  $p$  value  $< 0.001$ ”

### 3.8.5 mRNA Expression analysis of cytochrome c

BPA administration at both doses (BPA2 and BPA3) significantly reduced the levels of cytochrome c in disease groups as compared to the control group. Significantly increased expression of cytochrome c in case of BPA2+ P.I and BPA3+P.I was observed in contrast to disease group. GAPDH was used as an internal control. The graphical representation of cytochrome c expression is shown in figure 3.50.

### 3.9 Effect of Pistacia integerrima on the of miR-15a-5p and its target genes

MiRNA-15a-5p negatively regulate cell survival and promote apoptosis. By using the TargetScan software we found that Bcl2 and Mfn2 are putative target genes of miR-15a-5p ([http://www.targetscan.org/vert\\_72/](http://www.targetscan.org/vert_72/)). MiR-15a-5p bind with highly conserved 8 mer sequence of 3UTR of mRNA of Bcl2 and Mfn2. The binding sequences of target genes Bcl2 and Mfn2 are shown in figure 3.51.

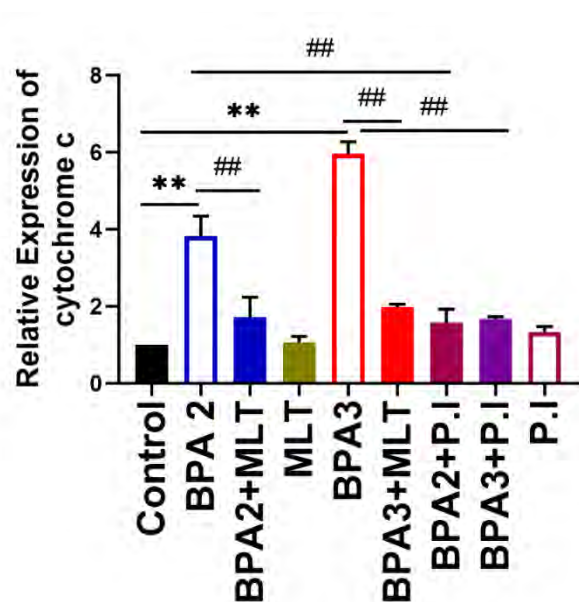


Figure 3.50. Estimation of mRNA expression of cytochrome c “\*\*/# shows p value < 0.01”

Position 2449-2456 of BCL2 3' UTR	5' ...GAAUGACAAACGCCGUGCUGCUA...	8mer
mo-miR-15a-5p	3' UUUGGUAUUACACGACGAU	
Position 1531-1538 of MFN2 3' UTR	5' ...AGCACUUUAGUUUCUUGCUGCUA...	8mer
mo-miR-15a-5p	3' UUUGGUAUUACACGACGAU	

Figure 3.51. Binding site of miRNA-15a-5p to 3'UTR of Bcl-2 and Mfn2 (source TargetScan database)

### 3.9.1 Expression analysis of miRNA-15a-5p

In this study miRNA-15a-5p expression was analyzed by qRT-PCR. Its expression analysis described that miRNA-15a-5p was significantly increased in BPA2 and BPA3 diseased group as compared to control group. Interestingly its expression was significantly downregulated in BPA2+P.I and BPA3+P.I as compared to BPA2 and BPA3 disease group respectively. miRNA-15a-5p expression was also significantly downregulated in melatonin treatment groups. U6 was used as an internal control. The figure 3.52 is given below shows the relative expression of miRNA-15a-5p in heart tissue samples.



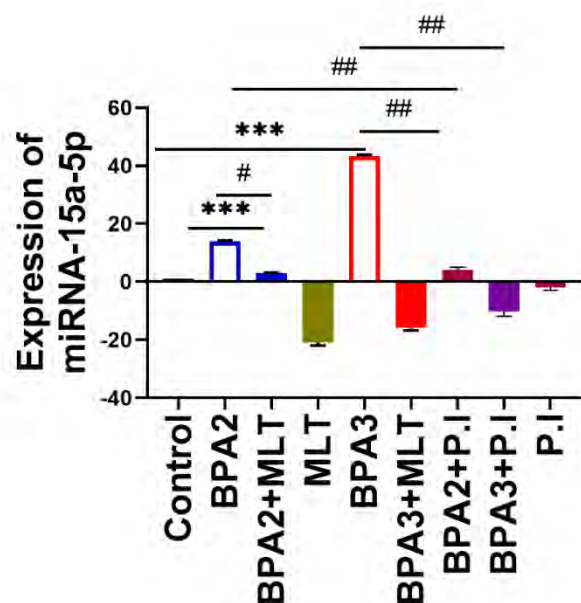


Figure 3.52. Estimation of relative expression of miRNA-15a-5p in cardiac tissues “# shows  $p$  value  $< 0.05$ , \*\*/### shows  $p$  value  $< 0.01$ , \*\*\* shows  $p$  value  $< 0.001$ ”

### 3.9.2 Expression Analysis of mRNA of Bcl2

Bcl2 protein is involved in inhibition of proapoptotic member of Bcl2 family of proteins and regulates apoptosis in the cell. In the current study expression of Bcl2 was significantly decrease in BPA2 (1mg/kg) and BPA3 (10mg/kg) treated groups as compared to control group. Statistical analysis of these group was calculated by using one-way ANOVA followed by Tukey’s test at  $p$  value  $< 0.01$ . Whereas the gene expression of Bcl2 was significantly increased in melatonin treated groups BPA2+MLT and BPA3+MLT. Interestingly the treatment with plant extract showed significantly upregulated expression of Bcl2 in both treatment groups (BPA2+P.I, BPA3+P.I) as compared to the diseased group (Fig. 3.53). GAPDH was used to normalize the expression of the gene.

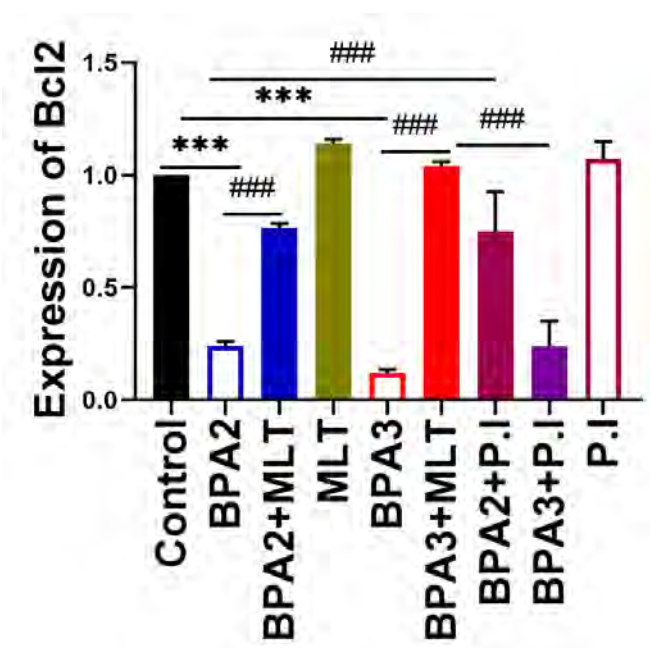


Figure 3.53. Estimation of relative RNA expression of Bcl-2 in cardiac tissues “\*\*\*/### shows p value < 0.001”

### 3.9.3 Expression Analysis of mRNA of Mfn2

Mfn2 is mitochondrial outer membrane GTPase that play a central role in mitochondrial fusion process and its activation is also associated with mitochondrial mediated apoptosis. In this study expression of Mitofusin 2 was assessed and it was found that the expression of Mfn2 was not changed significantly in BPA2 disease group as related to control group (Fig. 3.54). Whereas its expression was significantly reduced in BPA3 disease group as compared to the control group. In melatonin treatment groups (BPA2+MLT and BPA3+MLT) Mfn2 expression was significantly upregulated as compared to disease groups BPA2 and BPA3, respectively. The treatment with plant extract (BPA2+P.I and BPA3+P.I) showed significantly upregulated expression of Mfn2 as compared to control suggesting the role of *P. integerrima* in mitigating the miRNA-15a-5p induced apoptosis.

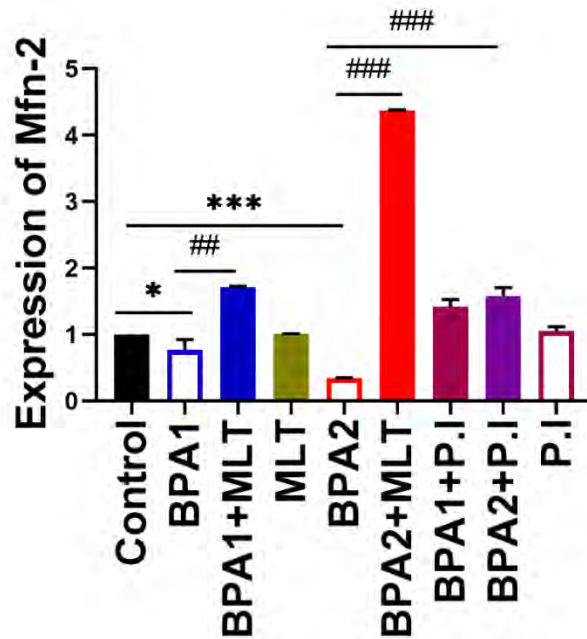


Figure 3.54. Estimation of relative RNA expression of *Mfn2* in cardiac tissues “\* shows  $p$  value < 0.05, ## shows  $p$  value < 0.01, \*\*\*/### shows  $p$  value < 0.001”

### 3.10 Effect of *Pistacia integerrima* on the expression of miRNA-214-3p and its target genes

#### 3.10.1 Relative Expression of miRNA-214 in Heart Tissue

The miRNA-214-3p is a bifunctional micro-RNA; in our study BPA administration (BPA2 and BPA3) significantly downregulated the miRNA-214-3p expression in heart tissue. The expression of miRNA-214-3p was significantly upregulated in treatment groups as compared to diseased group. Moreover, the expression of P.I and melatonin was comparable to the control group. U6 was used as an internal control. The graphical representation of miRNA-214-3p expression is shown in figure 3.55.

MiRNA-214-3p regulate cell survival and reduce apoptosis. By using the TargetScan software we find that PKCD, BNIP3 and Cdipl are putative target genes of miR-214-3p ([http://www.targetscan.org/vert\\_72/](http://www.targetscan.org/vert_72/)). miRNA-214-3p binds with highly conserved sequence of 3’UTR of mRNA of the respective target genes. The binding sequences of target genes Bcl2 and Mfn2 are shown in figure 3.56.

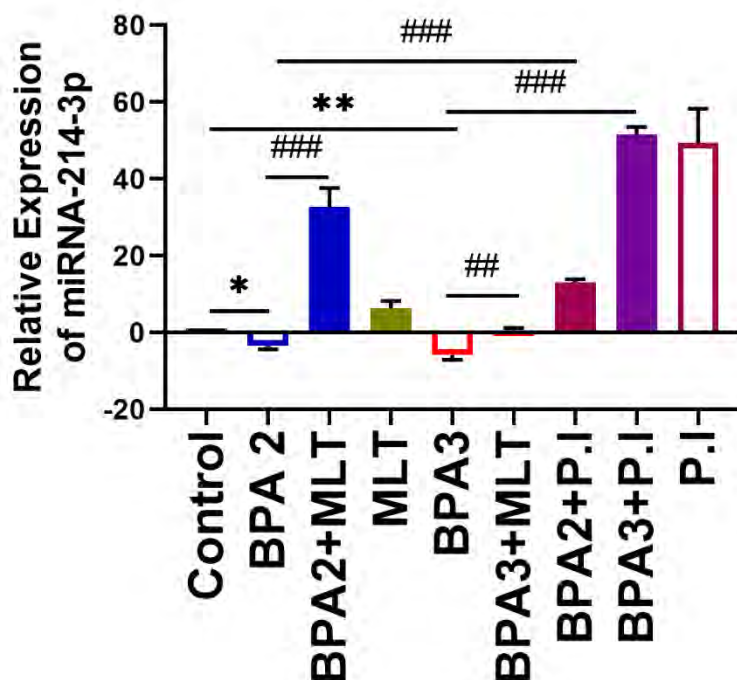


Figure 3.55. Estimation of the relative expression of miRNA\_214-3p in cardiac tissues “\* shows  $p$  value  $< 0.05$ , \*\*/### shows  $p$  value  $< 0.01$ , ### shows  $p$  value  $< 0.001$ ”

	Predicted consequential pairing of target region (top) and miRNA (bottom)	Site type	Context++ score	Context++ score percentile
Position 97-103 of PRKCD 3' UTR	5' ...GGGUGACUGGUAUCCUGCUGC... rno-miR-214-3p 3' GACGGACAGACACGGACGACA	7mer-m8	-0.24	95
Position 1693-1699 of CDIP1 3' UTR	5' ...GUCUUUUUGAGUUCCUGCUGU... rno-miR-214-3p 3' GACGGACAGACACGGACGACA	7mer-m8	-0.30	97
Position 614-620 of BNIP3 3' UTR	5' ...UACGCCUUUAUCUCUCUGCUGAG... rno-miR-214-3p 3' GACGGACAGACACGGACGACA	7mer-A1	-0.19	91

Figure 3.56. Binding region of miRNA-214-3p with 3'UTR of target genes (source TargetScan database)

### 3.10.2 Relative Expression of CDIP1 in Heart Tissue of Experimental Groups

CDIP1 was analyzed as miRNA-214-3p putative target gene, and its expression was significantly reduced in response to BPA induced oxidative stress. In case of BPA2 and BPA3, the expression was significantly upregulated which corresponds to the downregulated levels of the miRNA-214-3p. CDIP1 expression was significantly reduced in plant extract treated groups (BPA2+P.I and BPA3+P.I) as compared to disease group. Moreover, expression of CDIP1 was significantly reduced in melatonin-

treated groups as compared to the disease group. The graphical representation of CDIP1 expression is shown in figure (3.57).

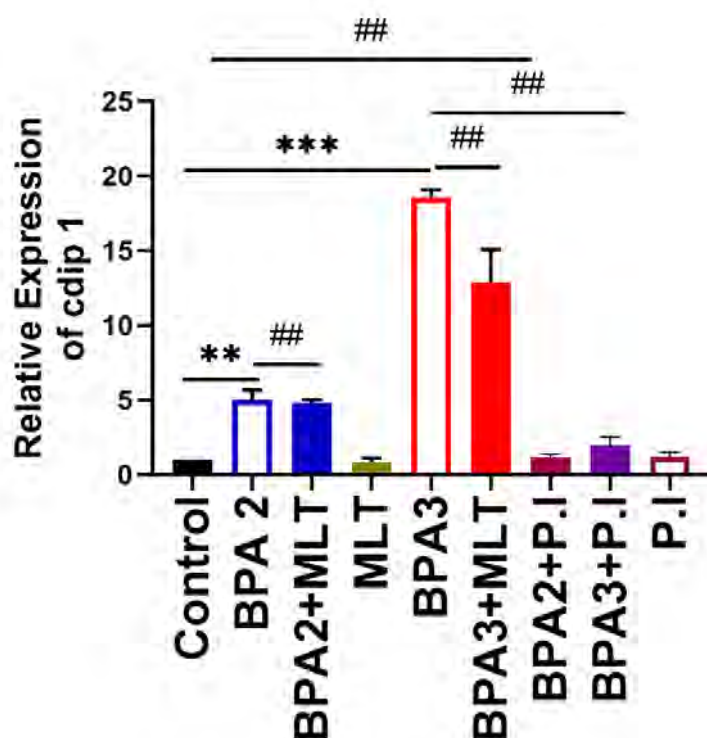


Figure 3.57. Estimation of relative RNA expression of CDIP1 in cardiac tissues “\*\*/# shows  $p$  value < 0.01, \*\*\*/### shows  $p$  value < 0.001”

### 3.10.3 mRNA Expression Analysis of BNIP3 in Heart Tissues

BNIP3, a Bcl2 interacting protein which induce apoptosis. The bioinformatics analysis confirmed BNIP3 as the target gene of miRNA-214-3p. BNIP3 expression of all experimental groups was normalized by GAPDH. Relative expression level of BNIP3 was significantly elevated in BPA treated groups (BPA2 and BPA3) as compared to the control, however, it was significantly reduced in BPA2+P.I and BPA3 +P.I groups compared to disease suggesting that *Pistacia integerrima* may serve as a therapeutic agent against BPA. BNIP3 expression was comparable to the control group in *Pistacia integerrima* and melatonin groups (Figure 3.58).

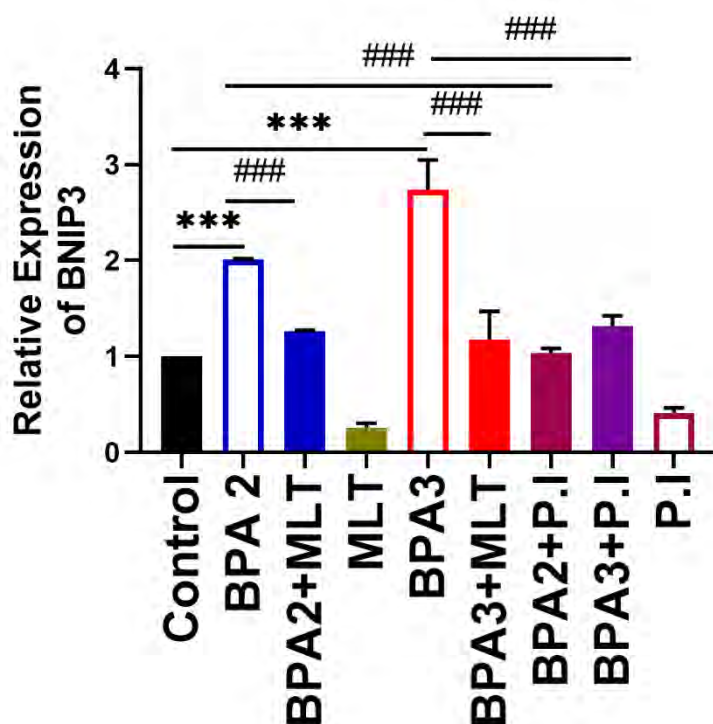


Figure 3.58. Estimation of the relative RNA expression of BNIP3 in cardiac tissues “\*\*\*/### shows  $p$  value  $< 0.001$ ”

#### 3.10.4 mRNA Expression Analysis of PKC- $\delta$ in Heart Tissues

PKC- $\delta$  is a protein kinase which acts as a pro-apoptotic kinase. The TargetScan analysis confirmed PKC- $\delta$  as the putative target of miRNA-214-3p. RNA expression of PKC- $\delta$  was significantly up-regulated in BPA administered group (BPA2 and BPA 3) as compared to the control. PKC- $\delta$  expression was significantly reduced in *P. integerrima* treatment groups (BPA2+P.I and BPA3+P.I) as compared to disease. The *P. integerrima* treatment was able to normalize the expression of PKC- $\delta$  at higher dose of BPA (10mg/kg), suggesting its analeptic potential (Figure 3.59).

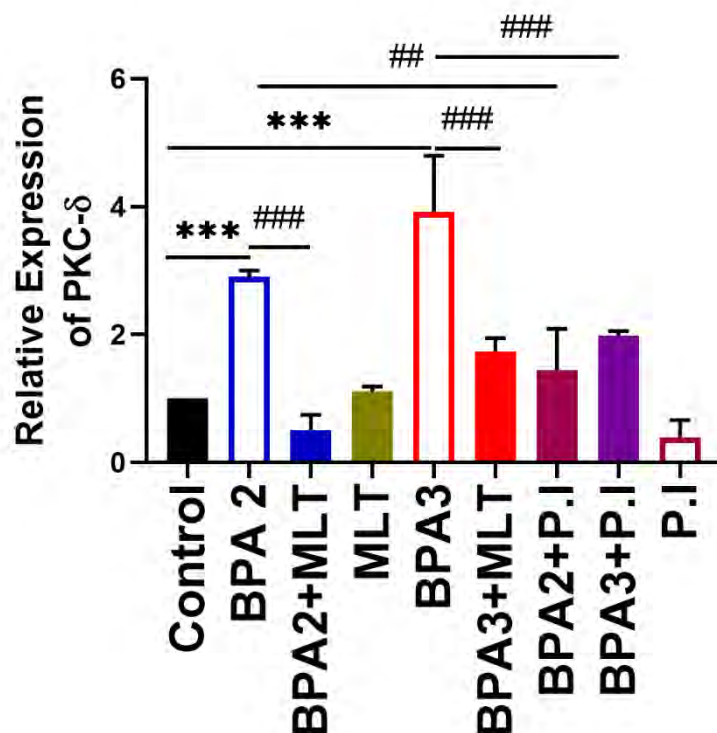


Figure 3.59. Estimation of relative RNA expression of PKC- $\delta$  in cardiac tissues “### shows  $p$  value < 0.01, \*\*\*/### shows  $p$  value < 0.001”

### 3.11 Effect of *Pistacia integerrima* on p53 protein and its downstream targets

#### 3.11.1 Expression of p53 Protein in Experimental Heart Tissues

p53 is an important transcription factor which regulates cellular homeostasis and also shows important role in mitochondrial dependent apoptotic pathway. BPA administration causes cellular toxicity and increases the expression of p53 protein. In our study BPA administration has increased the expression of p53 as compared to control group. The expression of p53 was significantly reduced in BPA2+P.I and BPA3+P.I group as compared to disease group. Same effect was also observed in BPA+melatonin group. Likewise, the expression of p53 in P.I and Melatonin group was comparable to the control group (figure 3. 60 a, b, 3.61 a, b). GAPDH was used as a loading control.

#### 3.11.2 Expression of P-p53 Protein in Experimental Heart Tissues

In current study, BPA administration (BPA2 and BPA3) increased the expression of P-p53 in disease group as compared to the control group. The expression of P-p53 was significantly reduced in both plant extract treatment groups (BPA2+P.I and BPA3+P.I)

as compared to disease group. The expression of P-p53 in *Pistacia integerrima* and melatonin group was comparable to control group (figure 3.60 a, c, 3.61 a,c). In addition, the melatonin, the antioxidant, treatment groups BPA2+MLT and BPA3+MLT showed significantly downregulated expression of P-p53 as compared to control. GAPDH was used as a loading control. Moreover, the ratio of p-p53 to p-53 was significantly increased in both disease groups (BPA2 and BPA3) as compared to control. However, the treatment with *Pistacia integerrima* and melatonin group showed significantly ratio of p-p53 to p53 (figure 3.62).

### 3.11.3 Expression of PUMA Protein in Experimental Heart Tissues

PUMA is a proapoptotic protein and its expression is elevated upon stress conditions. In our study BPA administration (BPA1 and BPA2) significantly increased the expression of PUMA as compared to the control group. The expression of PUMA was significantly reduced in BPA1+ P.I and BPA2+P.I group as compared to disease group. The same effect was also observed in the melatonin treatment groups (figure 3.60 a, d 3.61 a,d).

### 3.11.4 Expression of Drp1 Protein in Experimental Heart Tissues

Drp1, proapoptotic protein, is the downstream target of PUMA which regulates mitochondrial morphology and also plays important role in mitochondrial dependent apoptotic pathway. As shown in (figure 3.60 a, e, 3.61 a,e). expression of Drp1 was significantly increased in BPA (BPA2 and BPA3) group as compared to the control group. Significantly decreased expression of Drp1 protein was observed in plant extract treatment groups as compared to the disease group. GAPDH was used as a loading control.

### 3.11.5 Expression of Cytochrome C Protein in Experimental Heart Tissues

Cytochrome c is a proapoptotic protein located between the inner and outer mitochondrial membrane. Oxidative stress induced by BPA, causes its translocation from mitochondria into cytosol. In our study BPA administration (BPA2 and BPA3) depicted significantly increased expression of cytochrome c as compared to the control group. The expression of cytochrome c in P. I and Melatonin group was comparable to



control group. However, the expression of cytochrome c was significantly decreased in treatment groups BPA2+ P.I and BPA3+P.I as compared to disease group (figure 3.55a, f, 3.56a,f).

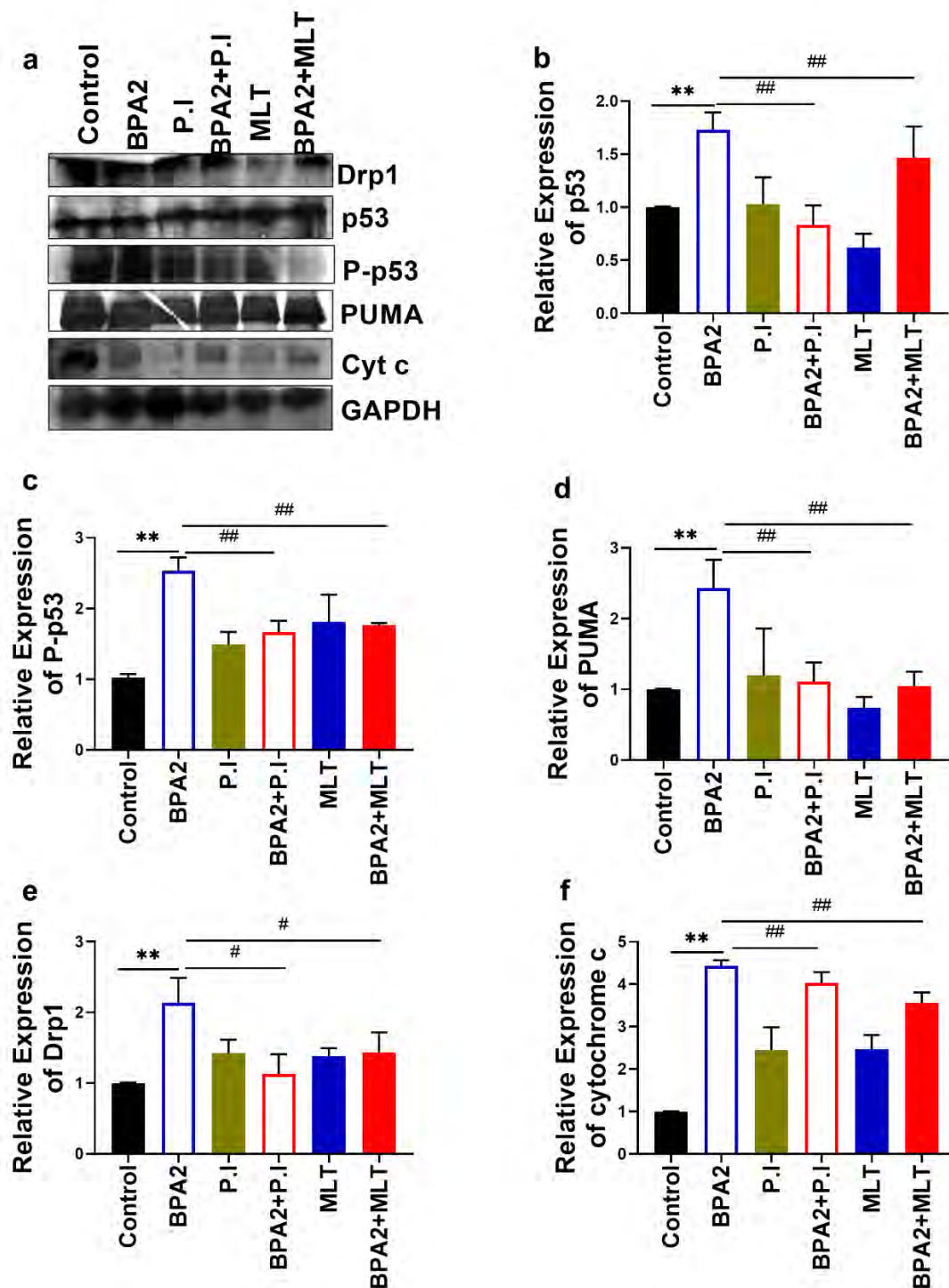


Figure 3.60. Effect of *Pistacia integerrima* on p53 and its downstream target proteins

a. Representative blot images of p53, p-p53, PUMA, cytochrome c and GAPDH, b. Graphical representation of relative p53 protein expression, c. Graphical representation of relative p-p53 protein expression, d. Graphical representation of relative PUMA protein expression, e. Graphical representation of relative Drp1 protein expression, f. Graphical representation of relative cytochrome c protein expression “\*/ # shows p value < 0.05, \*\*/## shows p value < 0.01”

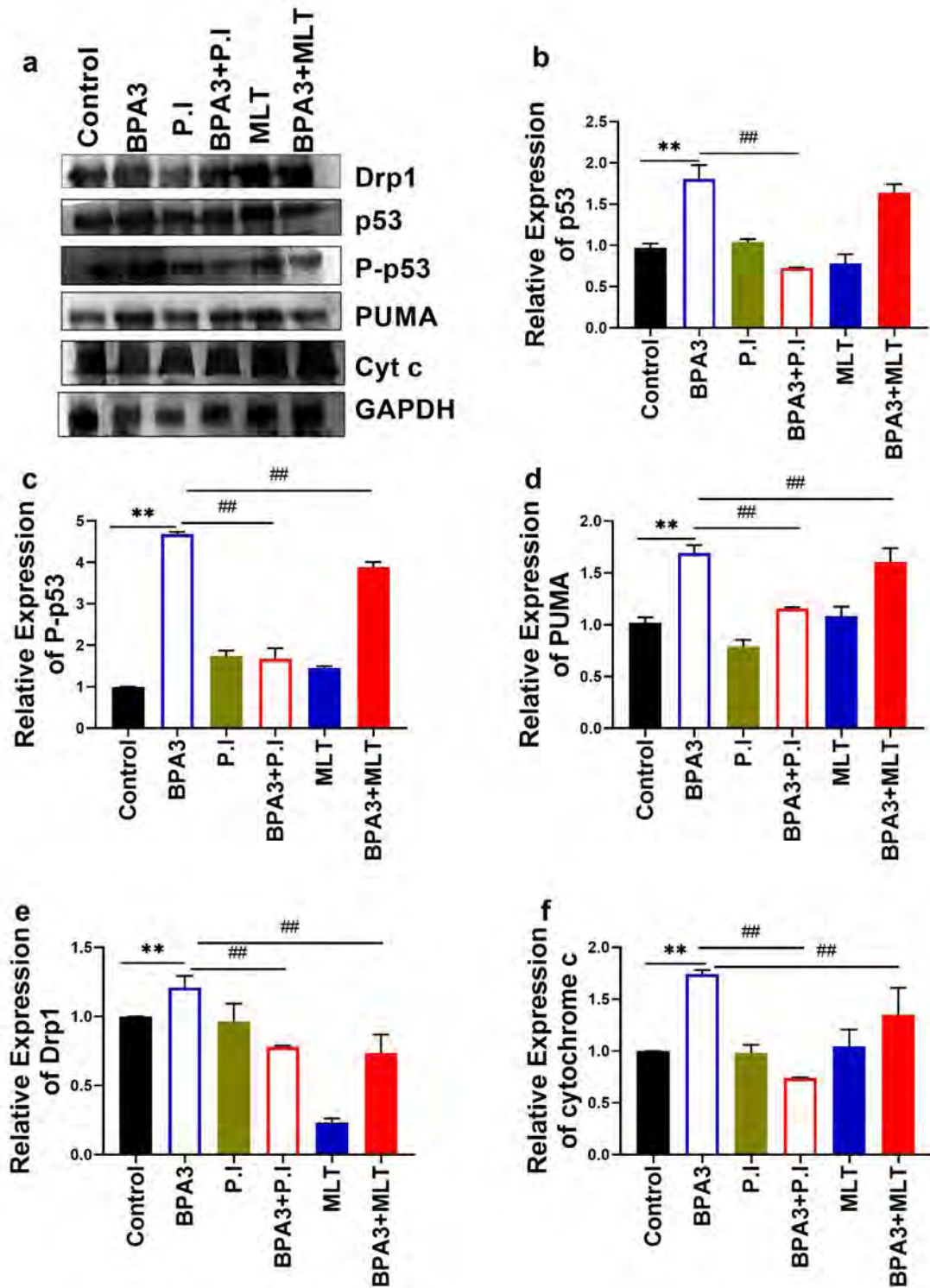


Figure 3.61. Effect of *Pistacia integerrima* on p53 and its downstream target proteins a. Representative blot images of p53, p-p53, PUMA, cytochrome c and GAPDH, b. Graphical representation of relative p53 protein expression, c. Graphical representation of relative p-p53 protein expression, d. Graphical representation of relative PUMA protein expression, e. Graphical representation of relative Drp1 protein expression, f. Graphical representation of relative cytochrome c protein expression “\*\*/## shows p value < 0.01”

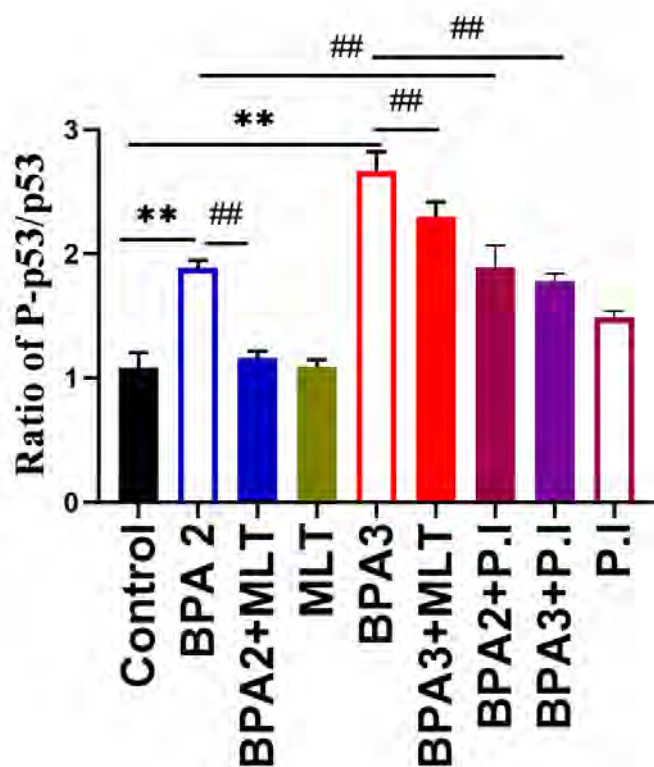
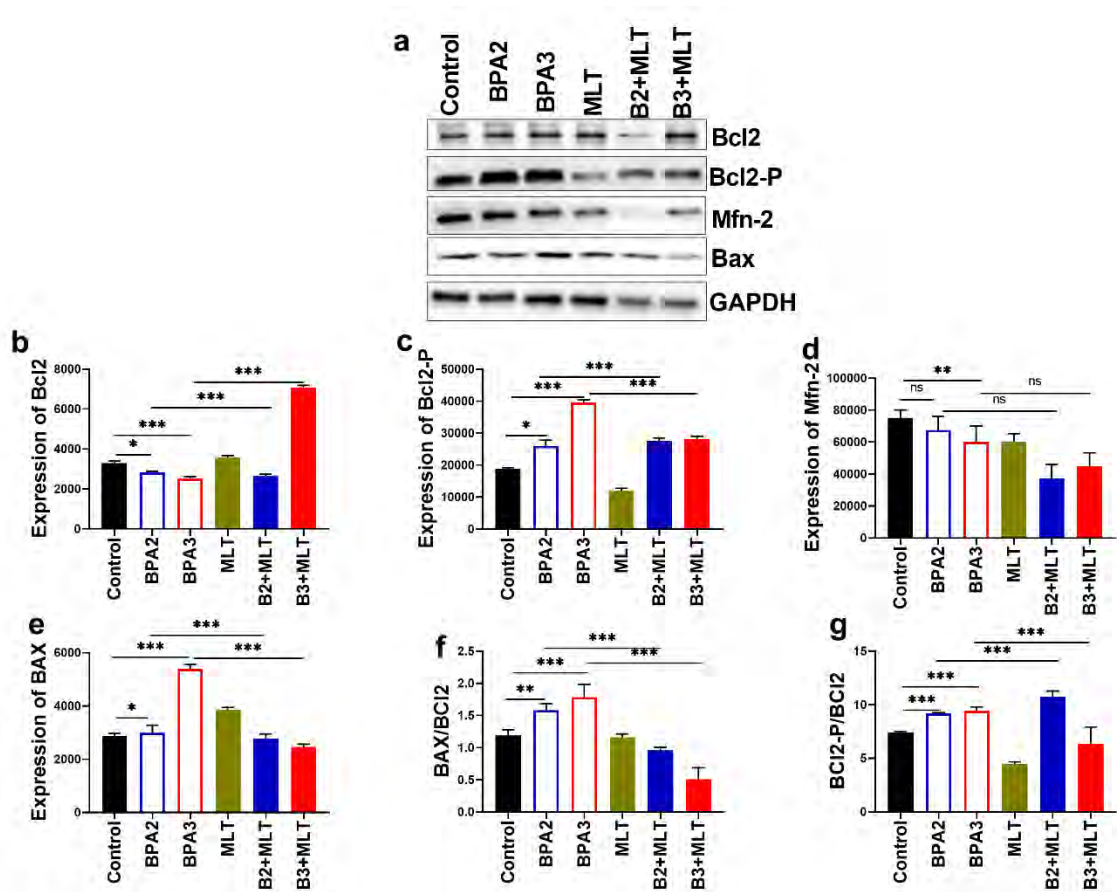


Figure 3.62 Graphical Representation of the ratio of p-p53/p53 “\*\*/## shows p value < 0.01”

### 3.12 Effect of miRNA-15a-5p regulation on the protein expression of its target genes

Bcl2 is an antiapoptotic protein and during oxidative stress expression of Bcl2 protein is downregulated. In BPA disease groups (BPA2 and BPA3) the expression of Bcl2 protein was significantly downregulated as compared to control. Melatonin treatment gets back their expression in low BPA dose (BPA2+MLT). However, the expression was also upregulated in treatment group of high dose of BPA2 (BPA2+MLT). Western blot of Bcl2 is shown in figure 3.63 a, b. To further confirm the activity of Bcl2 the phosphorylated Bcl2 expression was also analyzed. The expression of P-Bcl2 was significantly upregulated in BPA administered groups (BPA2 and BPA3) as compared

to the control, however, the treatment groups (BPA1+MLT and BPA2+MLT) showed significantly downregulated expression of P-Bcl2 fig. 3.63 a, c.



*Figure 3.63. Antiapoptotic potential of Melatonin via regulation of miRNA-15a-5p target genes in cardiac tissues a. Representative blot images of Bcl-2, Bcl2-p, Mfn-2, Bax and GAPDH, b. Graphical representation of relative Bcl2 protein expression, c. Graphical representation of relative Bcl2-p protein expression, d. Graphical representation of relative Mfn2 protein expression, e. Graphical representation of relative Bax protein expression, f. Graphical representation of the ratio of Bax to Bcl2 protein, g. Graphical representation of the ratio of Bcl2-p to Bcl2 protein “\*shows p value < 0.05, \*\* shows p value < 0.01, \*\*\*shows p value < 0.001”*

Mfn2 proteins play a fundamental role in mitochondrial fusion and during oxidative stress expression of Mfn2 is downregulated. In BPA disease groups (BPA2 and BPA3) the expression of Mfn2 was significantly downregulated as compared to control. Whereas, melatonin treatment normalize the expression of Mfn2 in low dose (BPA2+MLT) and high dose of BPA (BPA3+MLT) as compare to disease control.

Western blot of Mfn2 is shown in figure 3.63 a, d. The Bax protein is also one of the key players of apoptosis. The expression of Bax protein was significantly upregulated in high dose of BPA (BPA3) as compared to control, however, the treatment with melatonin significantly downregulated the expression of Bax as compared to the disease group fig. 3.63 a, e. The ratio of Bax to Bcl2 and P-Bcl2 to Bcl2 are the apoptosis index. The BPA groups (BPA2 and BPA3) showed a significantly increased ratio of Bax/Bcl2 and P-Bcl2/Bcl2 which confirms the BPA induced apoptosis *via* oxidative stress (fig. 3.63 f, g). Interestingly, the treatment with melatonin significantly reduced the ratios mitigating the toxic effects of BPA.

## **EFFECT OF BPA ON NEUROTOXICITY**

### **3.13 Experimental animal baseline characteristics**

To highlight the neurotoxic effects of BPA on baseline characteristics of animals body weight, and brain weight to body weight ratio was measured and analyzed. BPA treatment increased the animal body weight in a dose-dependent manner however, melatonin administration abolished BPA effects on body weights. As, the organ to body weight ratio is used to measure the harmful effect of the compound in toxicology studies. Herein, the brain weight to body weight ratio was found to be significantly decreased in all the three doses of BPA (BPA1, BPA2, BPA3), however, these changes were reversed by melatonin treatment, suggesting the ameliorative potential of melatonin in combating the toxic effects of BPA (Fig. 3.64). The brain weight to body weight ratio was comparable to normal in MLT group suggesting its therapeutic potential.

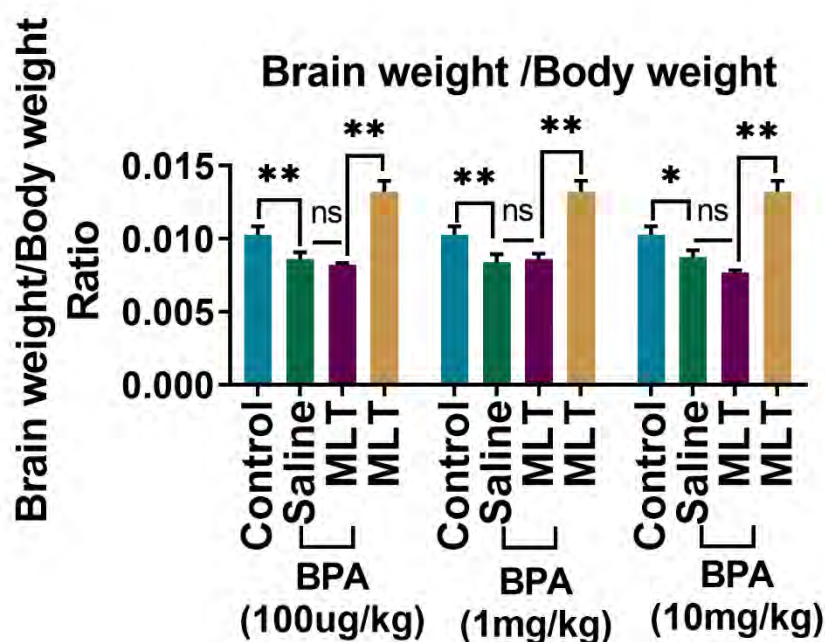


Figure 3.64. Estimation of brain weight to body weight ratio in different experimental groups  
 “\* shows  $p$  value  $< 0.05$ , \*\*shows  $p$  value  $< 0.01$ ”

### 3.14 Melatonin alleviated BPA-induced cellular damage

To evaluate the effect of melatonin on cellular architecture of brain tissues histological analysis was performed. BPA treatment showed increased disruption of cell, cell shrinkage, nuclear pyknosis and karyorrhexis in a dose dependent manner (Fig.3.65 a). However, melatonin treatment reversed these changes in all treatment groups (BPA1+MLT, BPA2+MLT and BPA3+MLT). While MLT group showed normalized cellular architecture. Increased percentage of abnormal cells was observed in BPA1 (nearly 2 fold), BPA2 (nearly 3 fold) and BPA3 (nearly 4 fold) in comparison to control whereas melatonin treatment significantly reduced the abnormal cell percentage as compared to disease group (Fig. 3.65 b). In MLT group the cellular morphology was very close to normal architecture with less percentage abnormal cells.

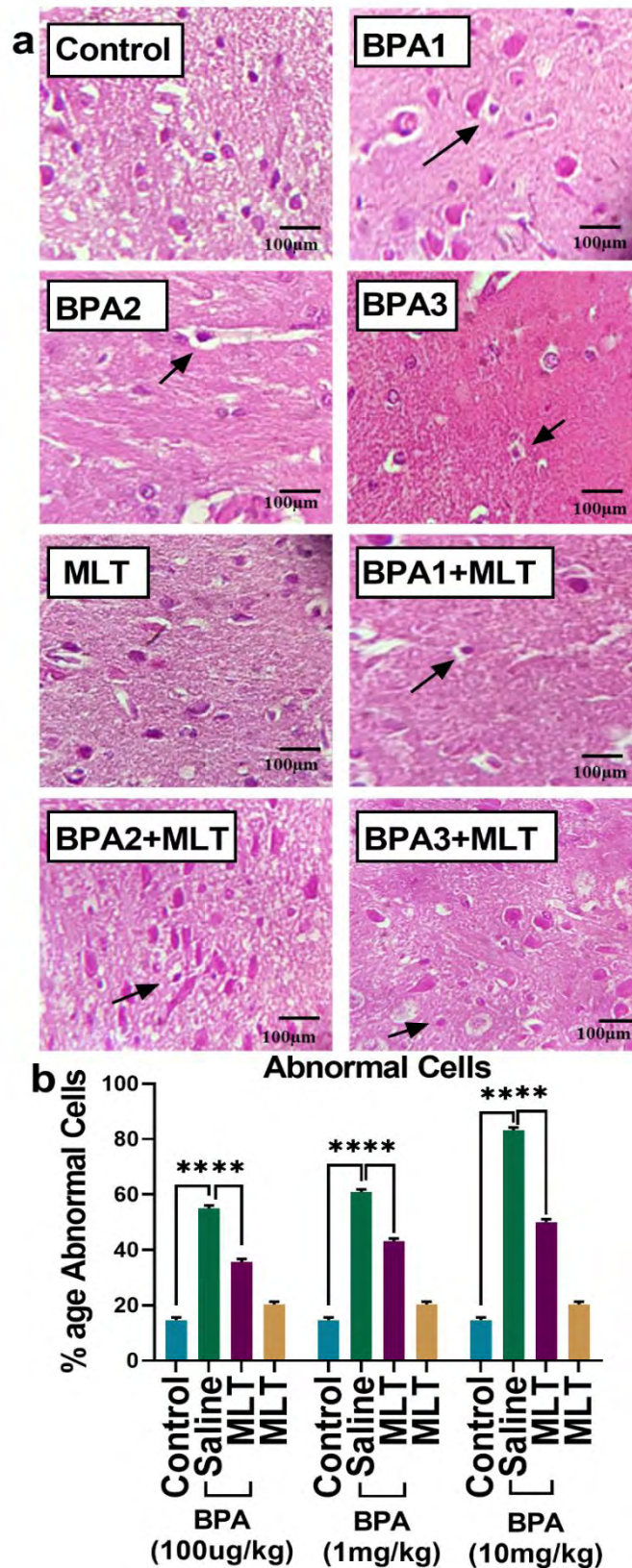


Figure 3.65. Melatonin alleviated BPA induced cellular damage a: Representative images of H&E staining of brain tissues of experimental groups; Control, BPA1 (100µg/kgBW), BPA2

(1mg/kgBW), BPA3 (10mg/kgBW), MLT, BPA1+MLT, BPA2+MLT, BPA3+MLT (Images taken at 40X, scale bar 100 $\mu$ m); b: Graphical representation of the percentage abnormal cells “\*\*\*shows  $p$  value < 0.001”

### 3.15 Melatonin abolished BPA-induced oxidative stress

Herein, the status of oxidative stress was evaluated by measuring ROS and TBARs level. BPA-treatment resulted in continuously accelerated ROS production. Notably, BPA-induced ROS production was dose-dependent, as nearly three times higher ROS levels (424% increase in comparison to control) were detected in 10 mg/kg BW BPA treated rats compared to the 1 mg/kg (173% increase in comparison to control) and 100 $\mu$ g/kg BW (164% increase in comparison to control) (Fig. 3.66).

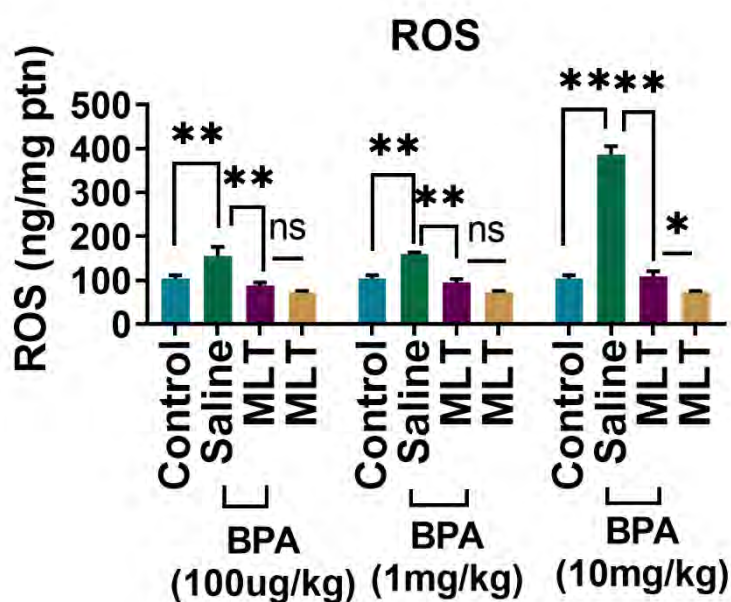


Figure 3.66. Estimation of the ROS level in brain tissues “\*shows  $p$  value < 0.05, \*\*shows  $p$  value < 0.01”

Further, oxidative stress was also confirmed through lipid peroxidation (TBARs) assay. Similar to the ROS level, increased TBARs level was detected in all three doses of BPA treated rats as compared to normal control, however, the results were nearly six fold high (10 mg/kg) dose of BPA treated animals. While both ROS and TBARs level of the MLT group were comparable to the control. Interestingly, melatonin treatment significantly reversed BPA-induced effects by reducing ROS and TBARs level, indicating its antioxidant potential against BPA induced oxidative stress (Fig. 3.67).



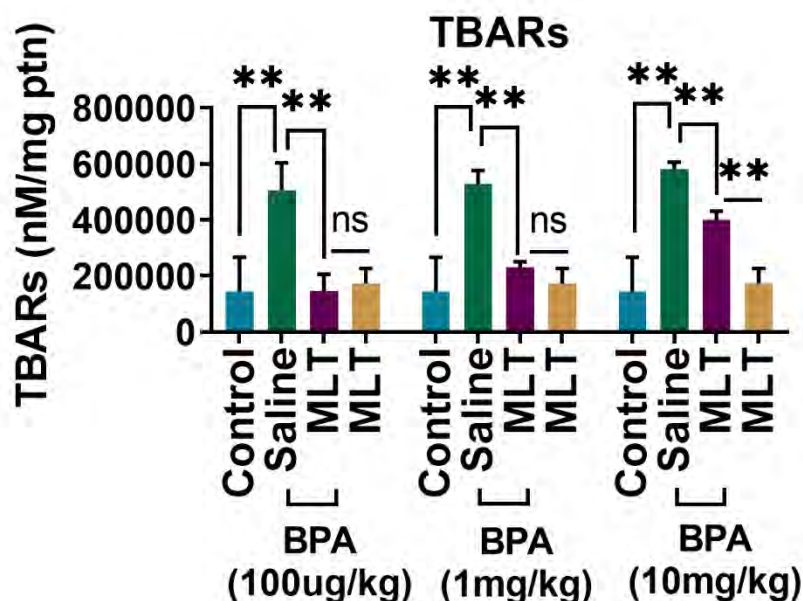


Figure 3.67. Estimation of the TBARs level in brain tissues “\*\*shows  $p$  value  $< 0.01$ ”

Moreover, to confirm the protective effects of melatonin different antioxidant enzymes activities were measured. Our result showed nearly two fold reduced SOD activity in lower doses of BPA (100 $\mu$ g/kg, 1mg/kg), whereas nearly three fold reduction in SOD activity in case of higher dose of BPA (10mg/kg). However, melatonin treatment (BPA1+MLT, BPA2+MLT, BPA3+MLT) significantly increased the SOD activity in comparison to disease group (Fig. 3.68a). The SOD activity was comparable to the control in MLT treated group. The CAT activity was found to be significantly reduced in 100 $\mu$ g/kg (nearly two fold), 1mg/kg (nearly three fold), and 10mg/kg (nearly three fold) doses of BPA, whereas the melatonin treatment showed significantly increased activity of CAT in all the treatment groups (BPA1+MLT, BPA2+MLT, BPA3+MLT) in comparison to disease group (Fig. 3.68b). The CAT activity was comparable to control in MLT treated group. Nearly two fold decreased POD activity was observed in BPA treated groups (100 $\mu$ g/kg, 1mg/kg) while the POD activity was found to be nearly three fold reduced in higher dose of BPA (10mg/kg) (Fig. 3.68c).

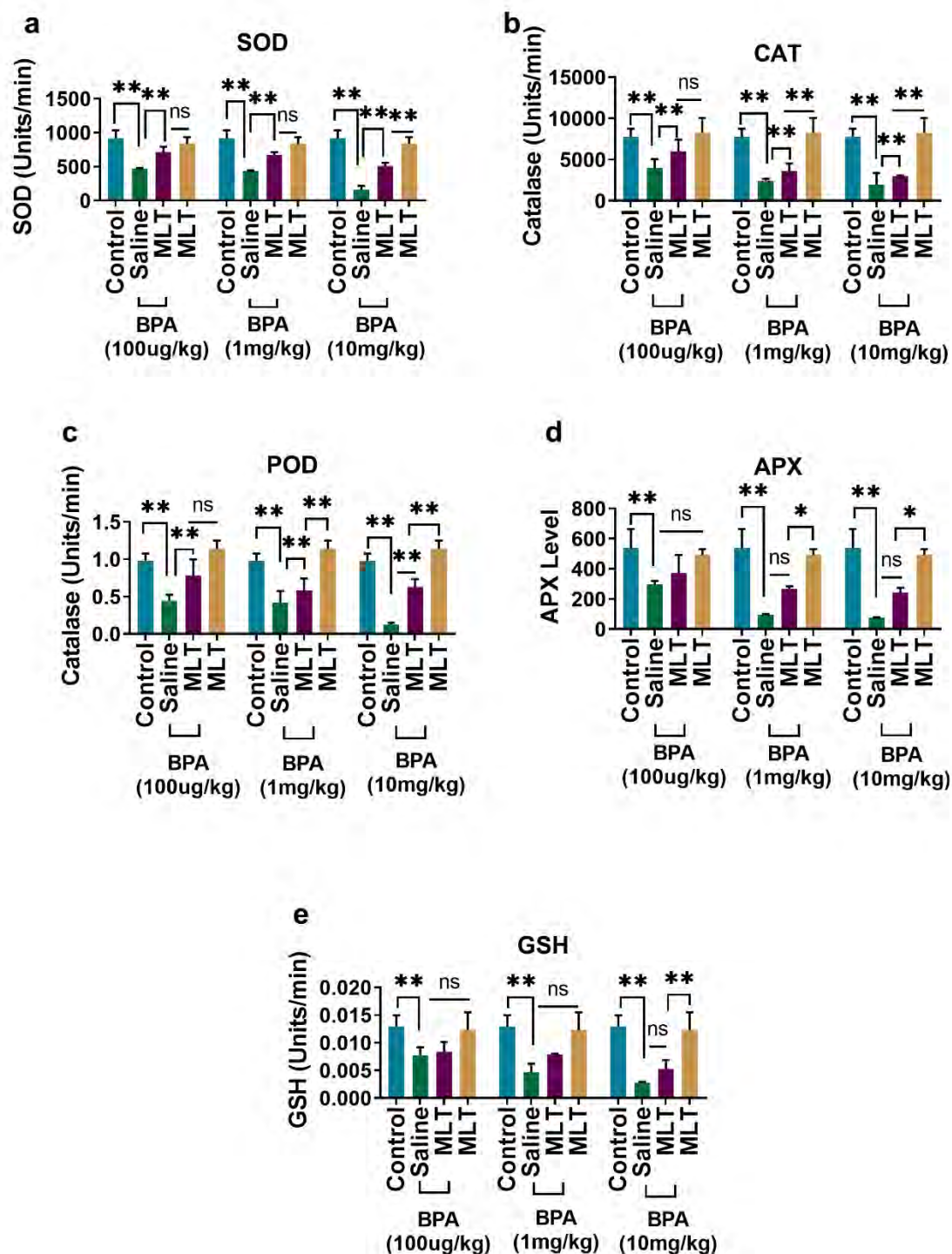


Figure 3.68. Effect of melatonin on antioxidant profile a: Estimation of SOD activity in brain tissues; b: Estimation of Catalase activity in brain tissues; c: Estimation of POD activity in brain tissues; d: Estimation of APX level in brain tissues; e: Estimation of GSH activity in brain tissues “\*shows p value < 0.05, \*\*shows p value < 0.01”

Whereas, melatonin treatment resulted in increased POD activity in all treatment groups (BPA1+MLT, BPA2+MLT, BPA3+MLT) in comparison to disease group. However,

the POD activity was found to be comparable to control in MLT. Our results showed that BPA dose (100µg/kg) significantly decreased APX activity to nearly two fold whereas the higher doses of BPA (1mg/kg, and 10mg/kg) decreased the APX activity by nearly three fold in comparison to control, however, melatonin treatment significantly improved the BPA-suppressed antioxidants activities in comparison to disease group (Fig. 3.68 d). The APX activity of the MLT group was comparable to the control. The GSH levels were significantly reduced in BPA treated rat model (100µg/kg nearly 1.5 fold, 1mg/kg nearly 3 fold, and 10mg/kg nearly 3 fold) as compared to control. While the GSH level of MLT group was comparable to control. However, the decreased GSH levels were elevated upon treatment with melatonin (BPA1+MLT, BPA2+MLT, BPA3+MLT) (Fig. 3.68 e). These findings suggest that along with its free radical scavenging potential melatonin could boost antioxidants to counterbalance oxidative stress and its consequences.

### **3.16 Melatonin reduced BPA-induced p53 activity**

In the present study, the expression and activity of p53 were measured to analyze the protective role of melatonin in combating the BPA induced p53 mediated apoptosis. BPA-treatment significantly enhanced the p53 mRNA in all three doses (100µg/kg nearly 6 log ratio increase, 1mg/kg nearly 12 log ratio increase, and 10mg/kg nearly 13 log ratio increase) (Fig. 3.69) as well as protein level in comparison to control however, the effects were reversed by melatonin treatment. While the level of both protein and mRNA level of p53 in MLT group was comparable to control (Fig. 3.72 a, b, 3.73 a, b, 3.74 a, b). Further, p53 phosphorylation is important for its stability, DNA binding, and as well as its apoptotic activity. Herein, we measured p53 phosphorylation at Ser392 which confirms the apoptotic role of p53. The increased expression of p-p53 was found in all the three doses of BPA (100µg/kg nearly 1.5 fold, 1mg/kg nearly 2 fold, and 10mg/kg nearly 2 fold) in comparison to control. Melatonin treatment significantly reduced the p53 activity by reducing its phosphorylation (Fig. 3.72 a, c, 3.73 a, c, 3.74 a, c). The expression level of phosphorylated p53 was comparable to control in MLT group.

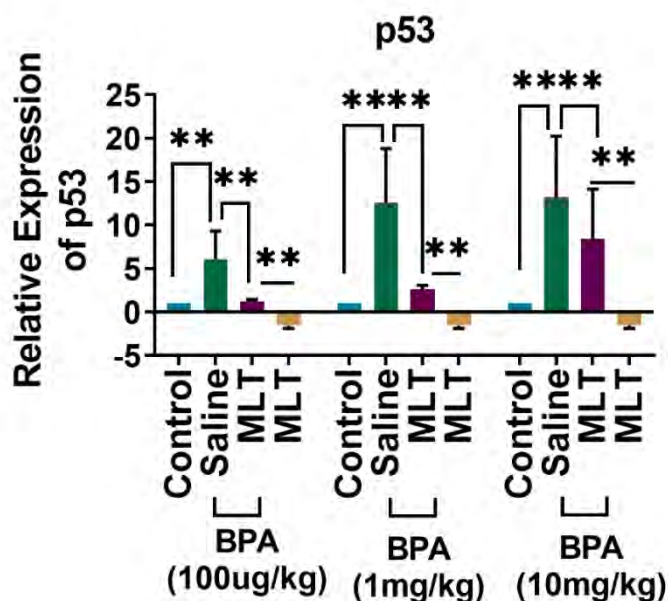


Figure 3.69. Representative bar graph showing p53 mRNA level in the brain tissues “\*\*\*shows p value < 0.01”

### 3.17 Melatonin alleviated BPA-induced toxicity *via* PUMA and Drp-1 signaling

PUMA is localized in the mitochondria and initiates mitochondrial dysfunction mediated apoptosis and apoptotic response to p53 (Yu, Wang et al. 2003, Ming, Wang et al. 2006). PUMA manifests its apoptotic role *via* a key player of mitochondrial dynamics, Drp-1. Therefore, to evaluate the protective role of melatonin in p53 linked mitochondrial dysfunction arbitrated apoptosis the expression of PUMA and Drp-1 was analyzed. PUMA mRNA levels were significantly increased in BPA treated models (100µg/kg nearly 6 log ratio increase, 1mg/kg nearly 14 log ratio increase, and 10mg/kg nearly 35 log ratio increase) whereas the levels were comparatively less in the treatment groups (Fig. 3.70). Moreover the expression level of Drp-1 mRNA was also found to be significantly

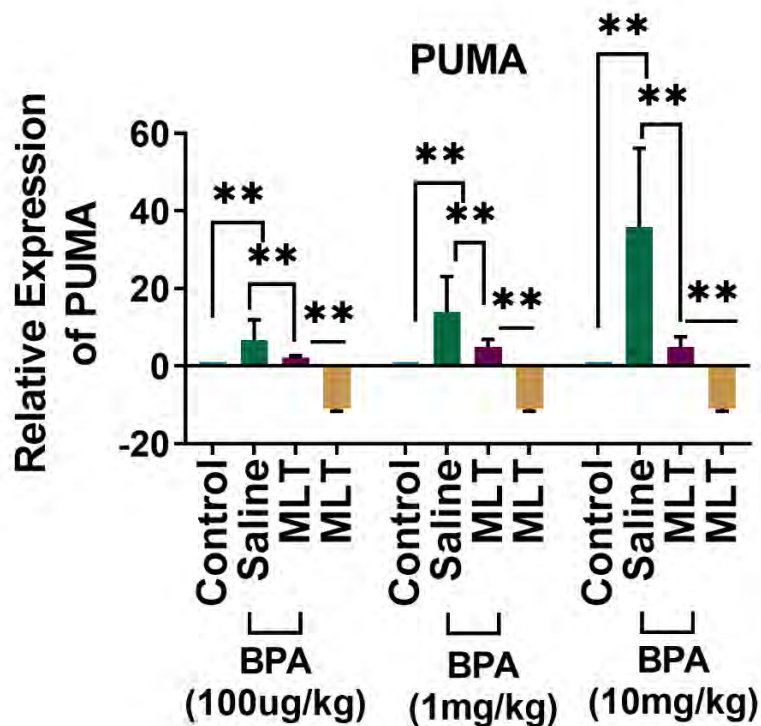


Figure 3.70. Estimation of relative mRNA level of PUMA in brain tissues “\*\*shows p value < 0.01”

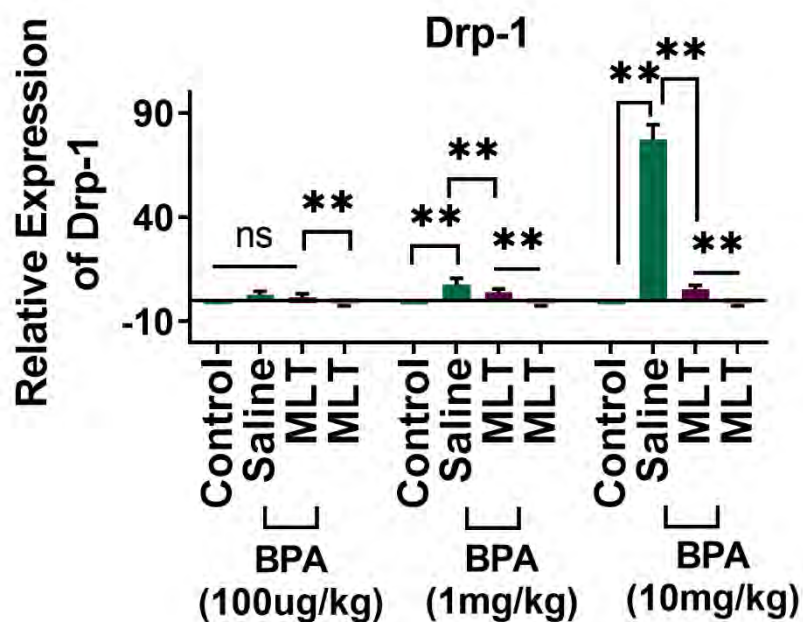


Figure 3.71. Estimation of relative mRNA level of Drp1 in brain tissues “\*\*shows p value < 0.01”

increased in all three doses of BPA ((100 $\mu$ g/kg nearly 2 log ratio increase, 1mg/kg nearly 7 log ratio increase, and 10mg/kg nearly 77 log ratio increase) in comparison to control however the melatonin treatment showed significantly downregulated expression as compared to disease (Fig. 3.71). While the level of both PUMA and Drp-1 mRNA level in MLT group was comparable to control. The RNA expression results were further confirmed by the protein analysis via immunoblotting. Our results showed that BPA administration significantly enhanced both PUMA and Drp-1 expression in the brain of the rats (Fig. 3.72 a, d, e, 3.73 a, d, e 3.74 a, d, e). which indicated the toxic potential of BPA. Notably, MLT group showed comparable to control expression of PUMA and Drp-1. Further, in case of treatment groups (BPA doses 100 $\mu$ g/kg, 1mg/kg and 10mg/kg). Melatonin treatment downregulated the RNA and protein expression of all the apoptotic markers in comparison to disease group suggesting its therapeutic potential.

Thus, suggesting the antiapoptotic role of melatonin by downregulation of phosphorylated p53. The activity of p53 was further evaluated by determining the ratio of phosphorylated p53 to p53 expression and interestingly we found significantly

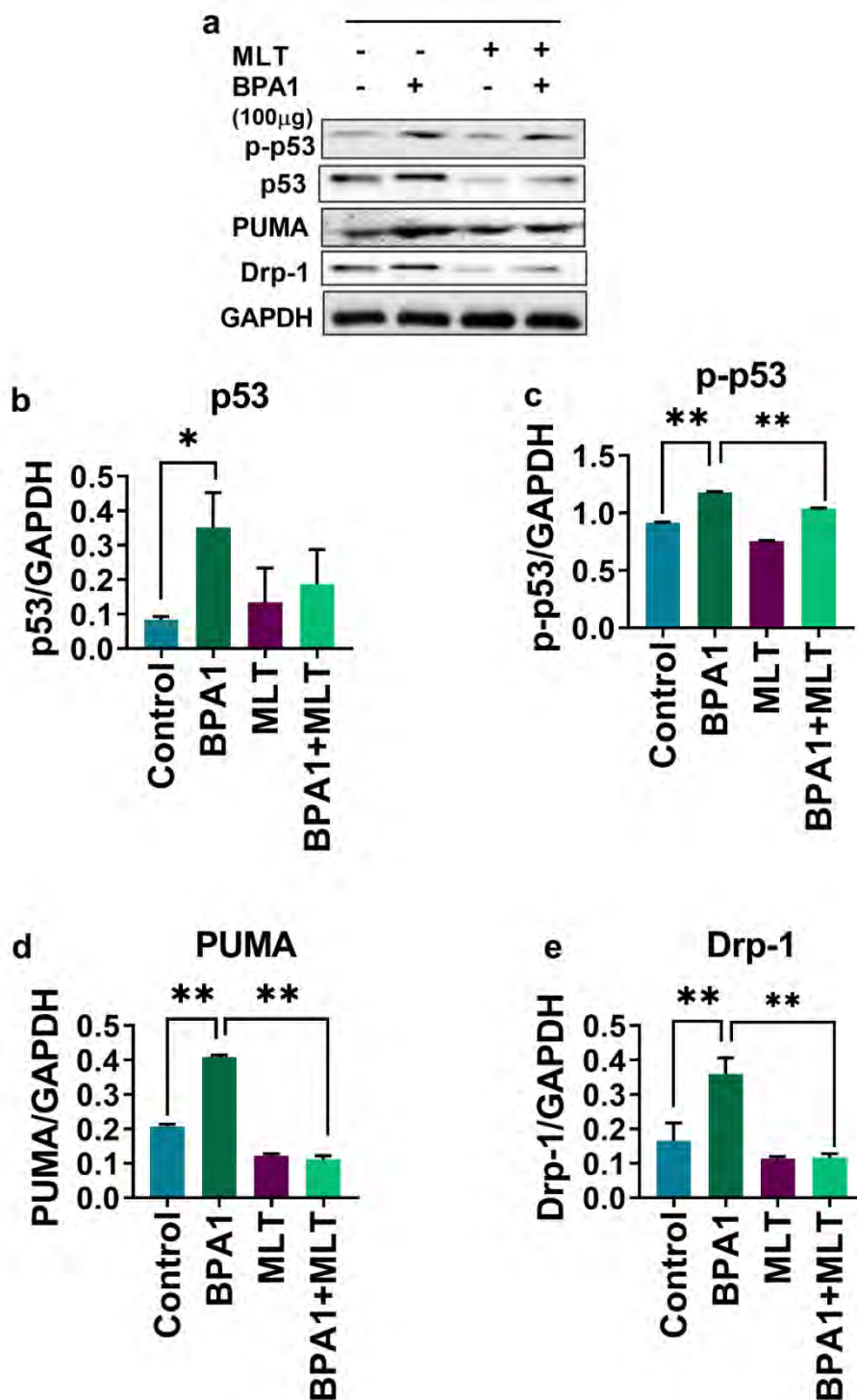


Figure 3.72. Effect of melatonin on p53 and its target proteins expression a: Representative western blots showing p-p53, p53, PUMA, Drp-1 expression. b: Graphical representation of the densitometric analysis of p-p53, c: Graphical representation of the densitometric analysis of p53, d: Graphical representation of the densitometric analysis of PUMA, e: Graphical representation of the densitometric analysis of Drp1 “\*\*shows p value < 0.01”

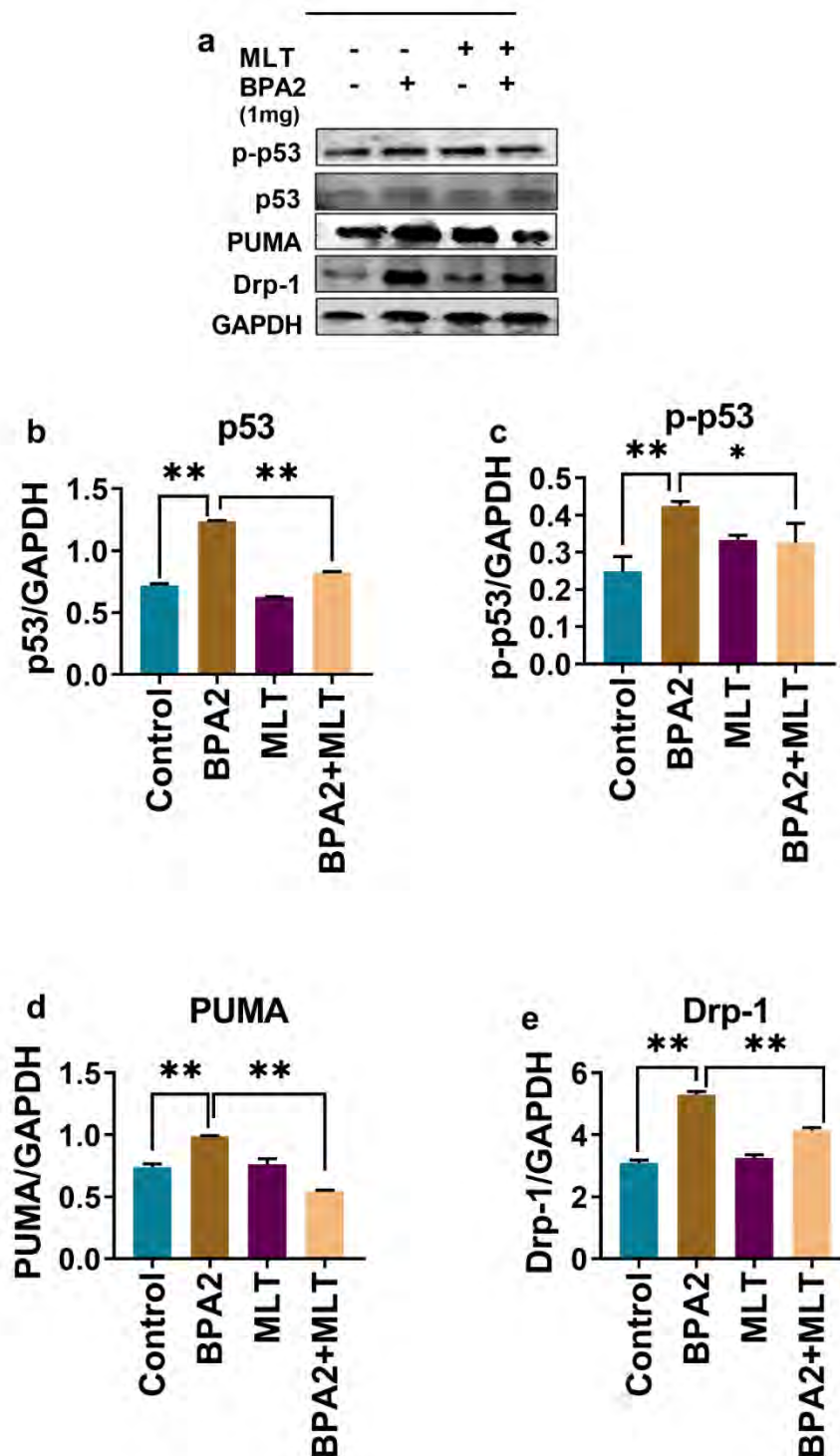


Figure 3.73. Effect of melatonin on p53 and its target proteins expression a: Representative western blots showing p-p53, p53, PUMA, Drp-1 expression. b: Graphical representation of the densitometric analysis of p-p53, c: Graphical representation of the densitometric analysis of p53, d: Graphical representation of the densitometric analysis of PUMA, e: Graphical representation of the densitometric analysis of Drp1 “\*\*shows p value < 0.01”



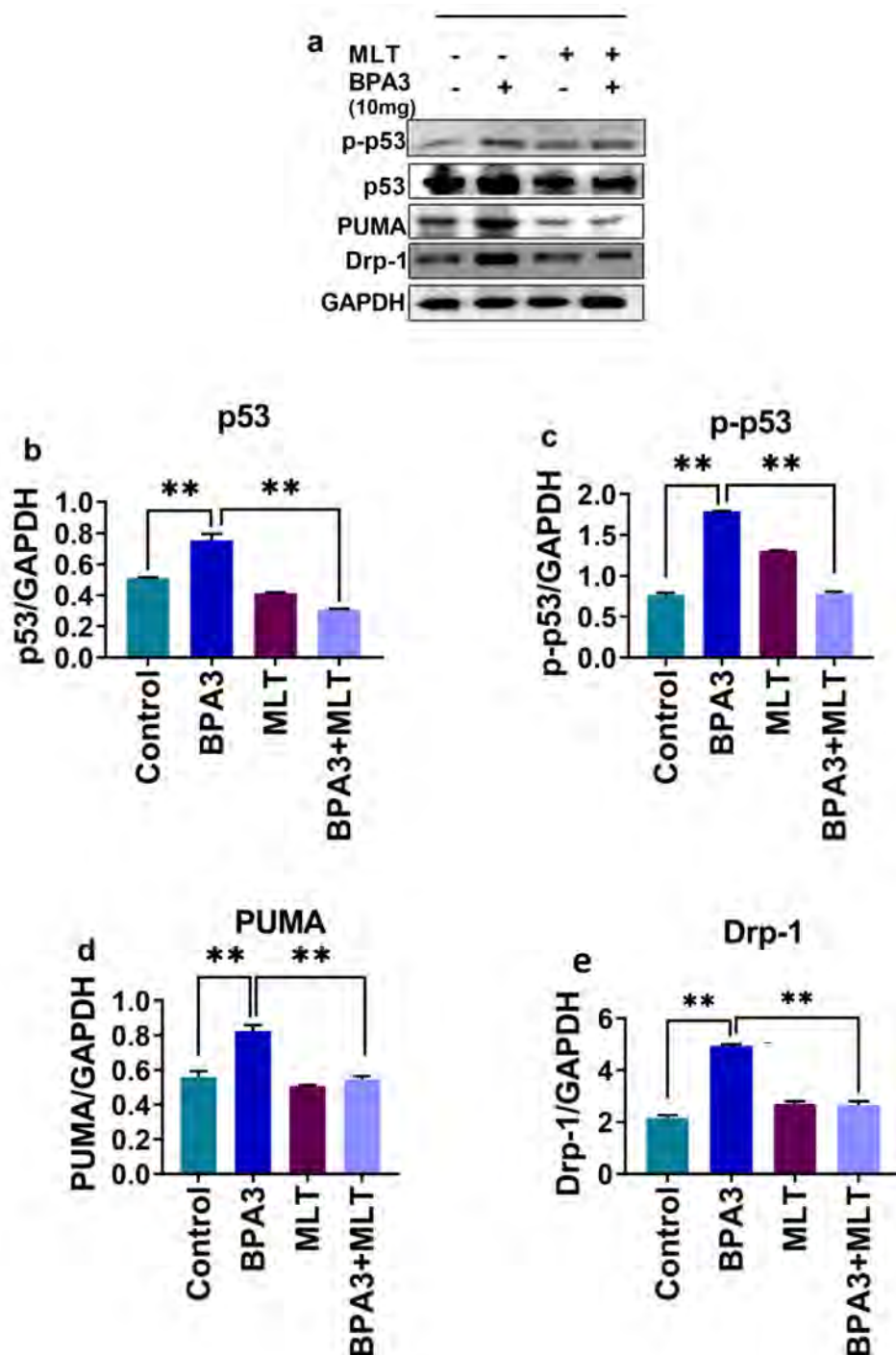


Figure 3.74. Effect of melatonin on p53 and its target proteins expression a: Representative western blots showing p-p53, p53, PUMA, Drp-1 expression. b: Graphical representation of the densitometric analysis of p-p53, c: Graphical representation of the densitometric analysis of p53, d: Graphical representation of the densitometric analysis of PUMA, e: Graphical representation of the densitometric analysis of Drp1 “\*\*shows p value < 0.01”

increased p-p53 to p53 ratio in all three doses of BPA. The dose-dependent increase of p-p53/p53 ratio suggests the positive correlation between p53 activity and dose of BPA.

However, the treatment with melatonin significantly reduced the ratio of p-p53/p53 (Fig. 3.75) indicating the therapeutic potential of melatonin.

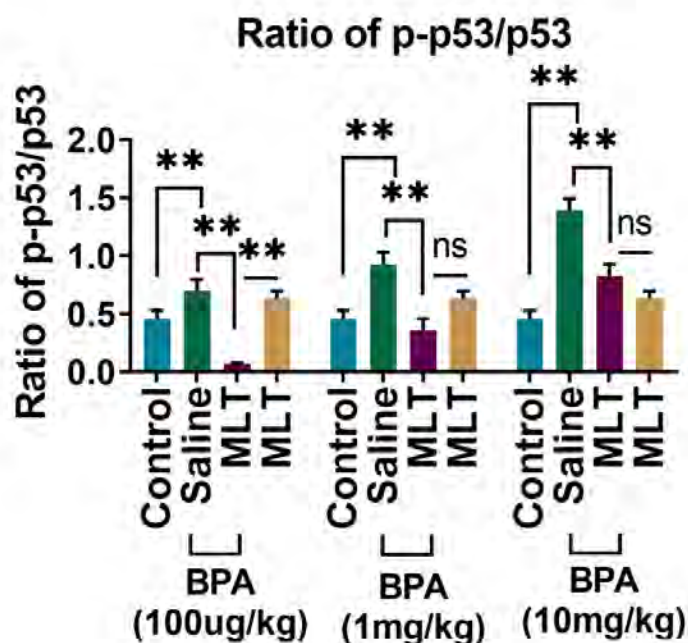


Figure 3.75. Estimation of ratio of p-p53/p53 protein in brain tissues “\*\*shows p value < 0.01”

### 3.18 Melatonin regulated BPA-induced expression of miRNA-214-3p and its target genes

The expression of miRNA-214-3p was analyzed in the brain tissues to evaluate the role in BPA induced apoptosis. The relative expression level of miRNA-214-3p was significantly downregulated upon BPA administration (BPA2 and BPA3) as compared to control. The expression of miRNA-214-3p was significantly upregulated in treatment groups (BPA2+MLT and BPA3+MLT) as compared to diseased group. Moreover, the expression in melatonin administered group was comparable to the control group. U6 was used as an internal control. The graphical representation of miRNA-214-3p expression is shown in figure 3.76. MiRNA-214-3p regulate apoptosis by targeting different genes involved in cell survival. By using the TargetScan software we found

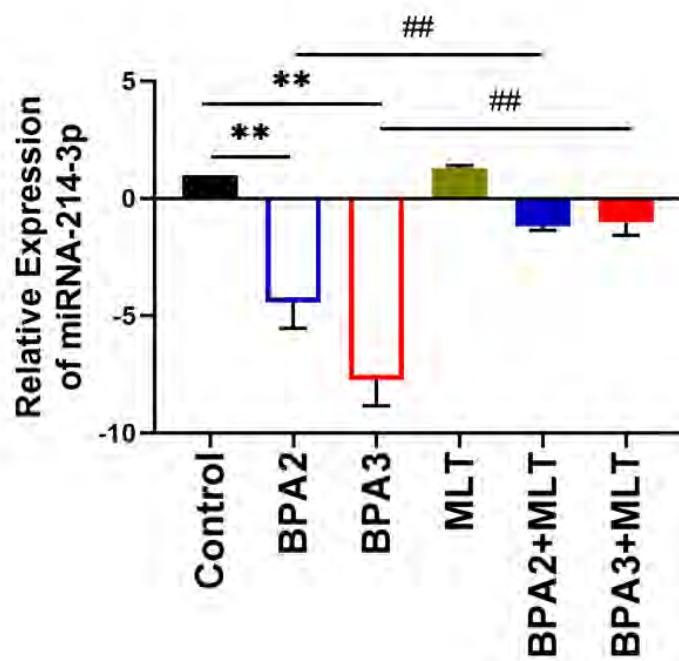


Figure 3.76. Estimation of relative expression of miRNA-214-3p in brain tissues “\*\*/## shows p value < 0.01”

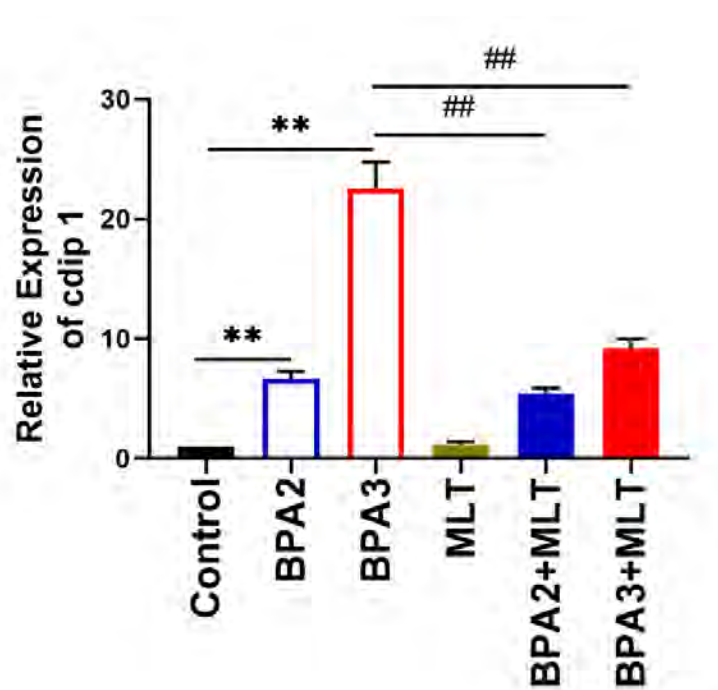


Figure 3.77. Estimation of relative expression of cdipl1 in brain tissues “\*\*/## shows p value < 0.01”

PKCD, BNIP3 and Cdipl are target genes of miR-214-3p ([http://www.targetscan.org/vert\\_72/](http://www.targetscan.org/vert_72/)). miRNA-214-3p binds with highly conserved sequence of 3'UTR of mRNA of the respective target genes. The relative expression of CDIP1 was analyzed as a putative target gene of miRNA-214-3p. In BPA administered group (BPA2 and BPA3), the expression was significantly upregulated which corresponds to the downregulated levels of the miRNA-214-3p. CDIP1 expression was significantly reduced in melatonin treated groups (BPA2+MLT and BPA3+MLT) as compared to disease group. The graphical representation of relative expression level of CDIP1 is shown in figure 3.77.

Another target gene of miRNA-214-3p, BNIP3 was analyzed to confirm the role of miRNA-214-3p in BPA induced apoptosis. The expression level of BNIP3 was significantly upregulated in BPA group (BPA2 and BPA3) as compared to the control, however, it was significantly reduced in the antioxidant treatment groups BPA2+MLT and BPA3 +MLT as compared to disease (Fig. 3.78).

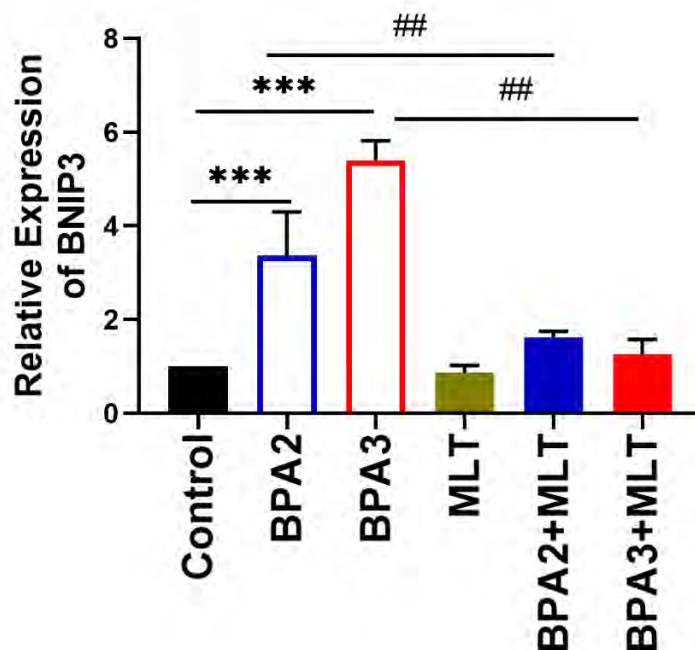


Figure 3.78. Estimation of relative expression of BNIP3 in brain tissues “## shows  $p$  value < 0.01 in comparison to control, \*\*\*shows  $p$  value < 0.001 in comparison to disease”

PKC- $\delta$  is also the putative target gene of miRNA-214-3p. Relative mRNA expression of PKC- $\delta$  was significantly up-regulated in BPA administered group (BPA2 and BPA

3) as compared to the control. PKC- $\delta$  expression was significantly reduced in melatonin treatment groups (BPA2+MLT and BPA3+MLT) as compared to disease (Fig. 3.79).

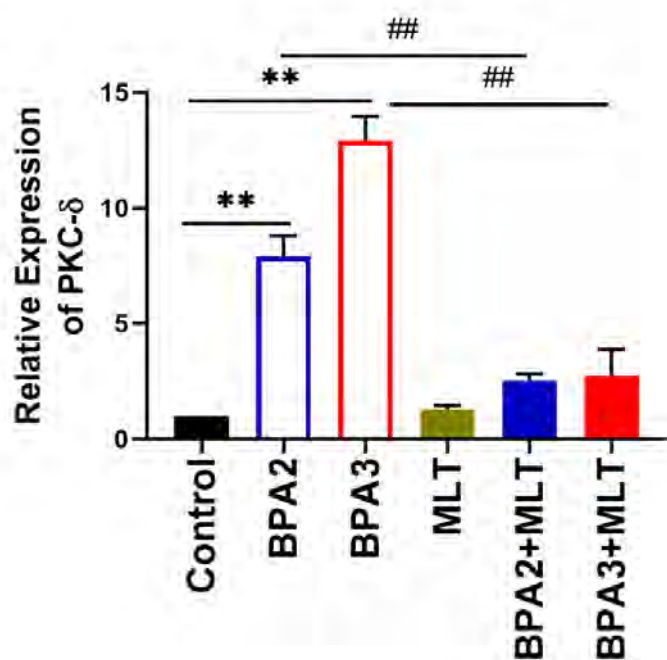


Figure 3.79. Estimation of relative expression of PKC- $\delta$  in brain tissues “\*\*/# shows  $p$  value < 0.01”

### 3.19 Melatonin reduced expression of miRNA-15a-5p and its target genes

In current study miRNA-15a-5p expression was significantly upregulated in BPA2 and BPA3 diseased group as compared to control group. Interestingly its expression was significantly downregulated in BPA2+MLT and BPA3+MLT as compared to BPA2 and BPA3 disease group respectively. miRNA-15a-5p expression was also significantly downregulated in melatonin administered group. U6 was used as an internal control (Fig. 3.80).

MiRNA-15a-5p negatively regulate cell survival and promote apoptosis. By using the TargetScan software we find that Bcl-2 and Mfn2 are putative target genes of miR-15a-5p ([http://www.targetscan.org/vert\\_72/](http://www.targetscan.org/vert_72/)). MiR-15a-5p bind with highly conserved 8 mer sequence of 3UTR of mRNA of Bcl-2 and Mfn2. Bcl-2, target of miRNA-15a-5p, regulates apoptosis in the cell. In the current study expression of Bcl-2 was significantly

decrease in both doses of BPA, BPA2(1mg/kg) and BPA3 (10mg/kg) treated groups as compared to control group.

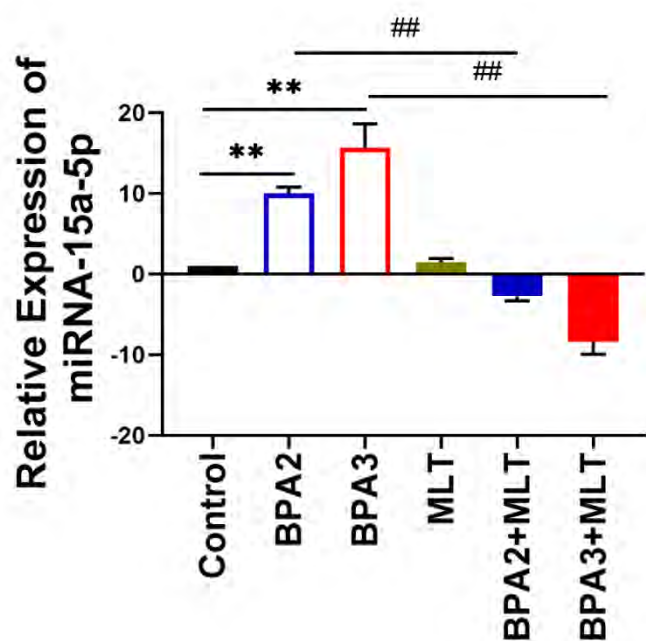


Figure 3.80. Estimation of relative expression of miRNA-15a-5p in brain tissues “\*\*/# shows  $p$  value  $< 0.01$ ”

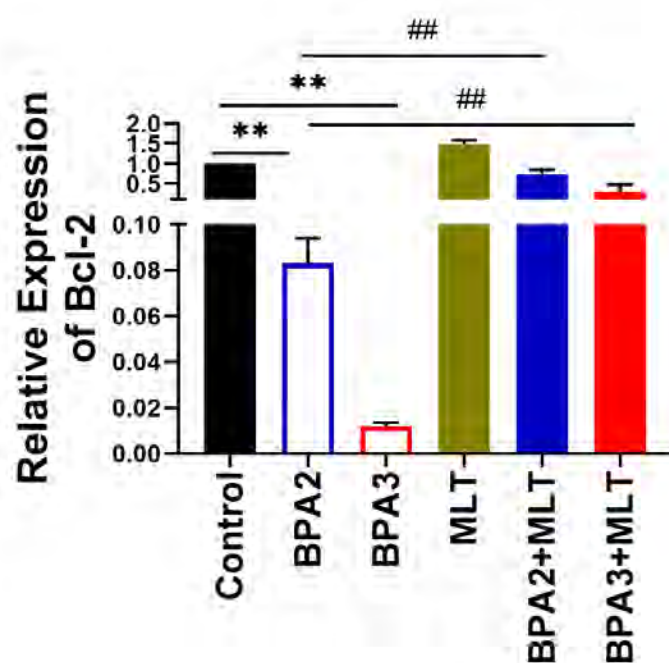


Figure 3.81. Estimation of relative expression of Bcl2 in brain tissues “\*\*/# shows  $p$  value  $< 0.01$ ”

Whereas the gene expression of Bcl-2 was significantly increased in Melatonin treated groups BPA2+MLT and BPA3+MLT. GAPDH was used to normalize the expression of the gene (Fig. 3.81).

In this study expression of Mitofusin 2 was assessed and it was found that the expression of Mfn2 was significantly reduced in disease group (BPA2 and BPA3) as compared to control group. Whereas its expression was significantly increased upon melatonin treatment (BPA2+MLT and BPA3+MLT) as compared to disease groups BPA2 and BPA3 respectively (Fig. 3.82).

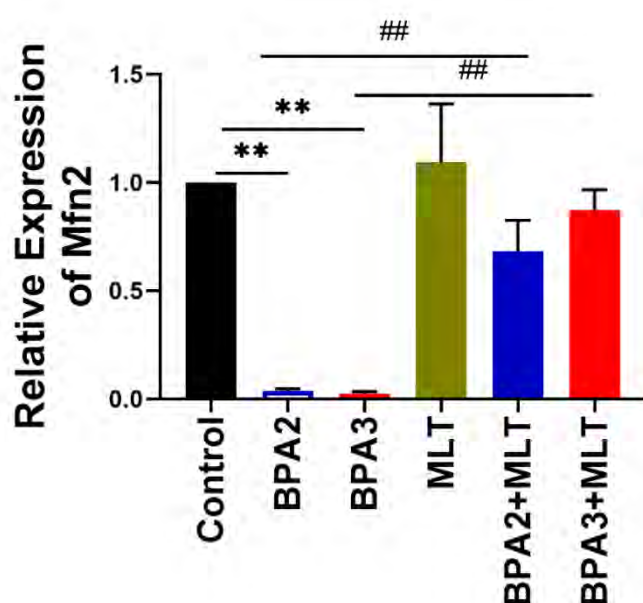


Figure 3.82. Estimation of relative expression of Mfn2 in brain tissues “\*\*/# shows  $p$  value < 0.01”

### 3.20 *Pistacia integerrima* regulated BPA-induced expression of miRNA-214-3p and its target genes

The relative expression level of miRNA-214-3p was significantly downregulated in BPA administered groups (BPA2 and BPA3) as compared to control. The expression of miRNA-214-3p was significantly upregulated in treatment groups (BPA2+P.I and BPA3+P.I) as compared to diseased group. Moreover, the expression in melatonin administered group was comparable to the control group. U6 was used as an internal control (Fig. 3.83). The relative expression level of CDIP1 was significantly

upregulated in disease group (BPA2 and BPA3) as compared to control. CDIP1 expression was significantly reduced in plant extract treated groups (BPA2+P.I and BPA3+P.I) as compared to disease group (Fig. 3.84).

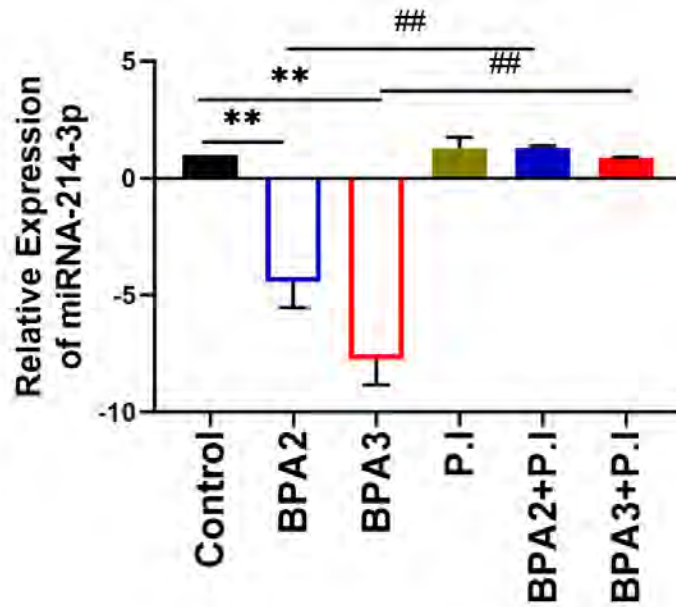


Figure 3.83. Estimation of relative expression of miRNA-214-3p in brain tissues “\*\*/# shows p value < 0.01”

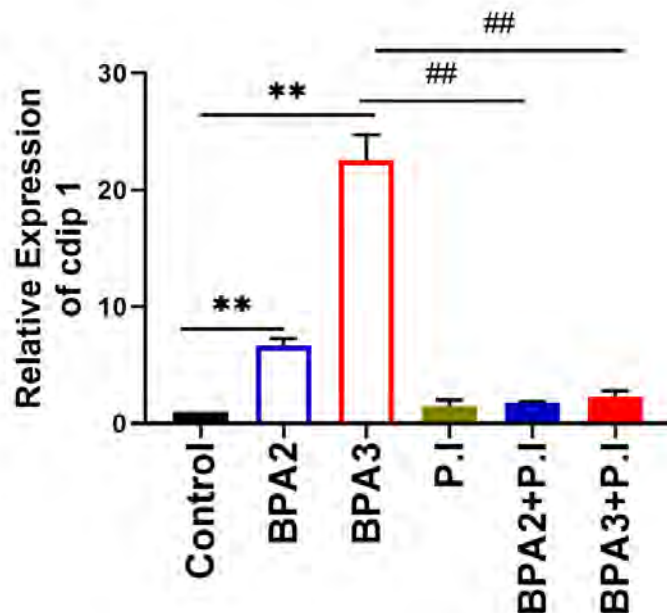


Figure 3.84. Estimation of relative expression of cdip1 in brain tissues “\*\*/# shows p value < 0.01”



Relative expression level of BNIP3 and PKC- $\delta$  was significantly elevated in BPA treated groups (BPA2 and BPA3) as compared to the control, however, it was significantly reduced in BPA2+P.I and BPA3+P.I groups compared to disease group (Fig. 3.85, 3.86). However, upon treatment with plant extract, *P. Integerrima*, the expression was significantly reduced.

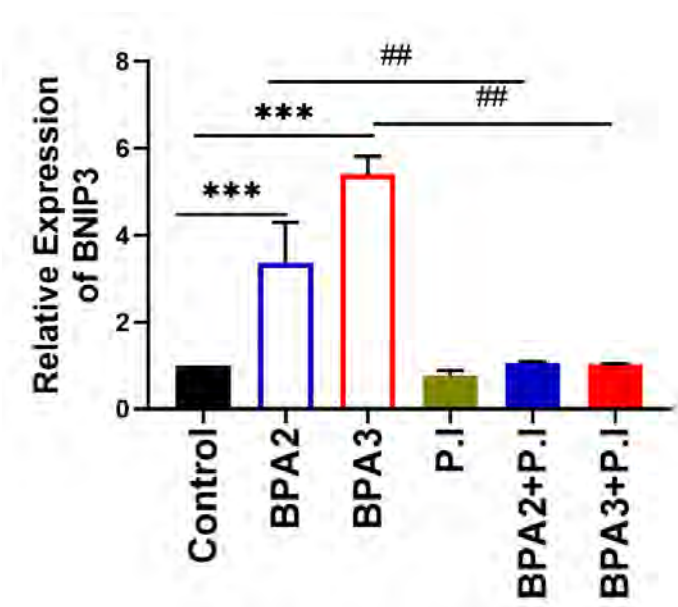


Figure 3.85. Estimation of relative expression of BNIP3 in brain tissues “## shows p value < 0.01, \*\*\*shows p value < 0.001”

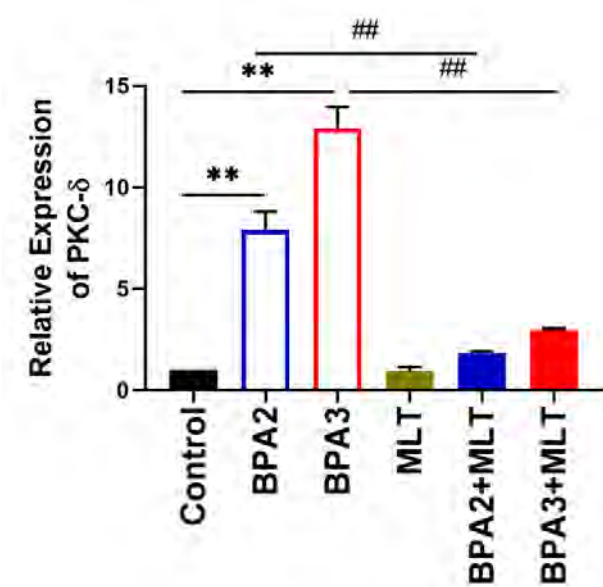


Figure 3.86. Estimation of relative expression of PKC- $\delta$  in brain tissues “\*\*/# shows p value < 0.01”

### 3.21 *Pistacia integerrima* normalized BPA-induced expression of miRNA-15a-5p and its target genes

In current study miRNA-15a-5p expression was significantly elevated in BPA2 and BPA3 diseased group as compared to control group. Interestingly its expression was significantly downregulated in BPA2+P.I and BPA3+P.I as compared to BPA2 and BPA3 disease group respectively. U6 was used as an internal control (Fig. 3.87).

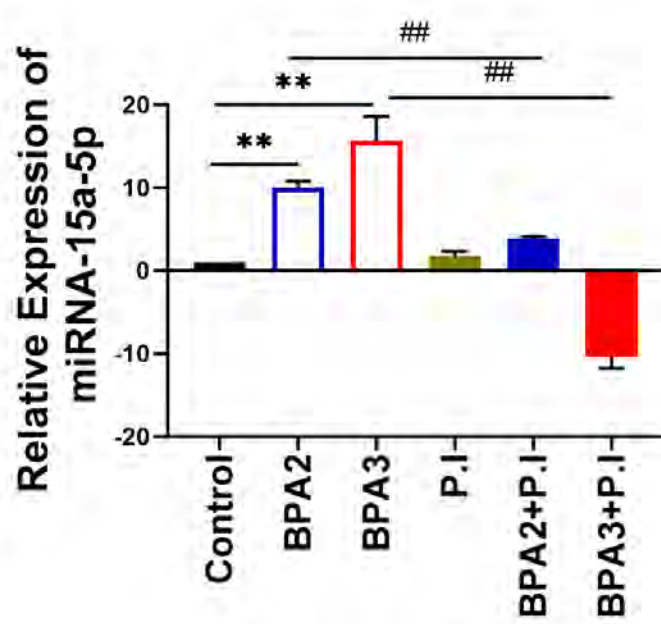


Figure 3.87. Estimation of relative expression of miRNA-15a-5p in brain tissues “\*\*/# shows p value < 0.01”

Bcl-2 protein is antiapoptotic member of Bcl-2 family of proteins and regulates apoptosis in the cell. In the current study expression of Bcl-2 was significantly decrease in BPA2 (1mg/kg) and BPA3 (10mg/kg) treated groups as compared to control group. Whereas the mRNA expression of Bcl-2 was significantly increased in plant extract treated groups BPA2+P.I and BPA3+P.I. GAPDH was used to normalize the expression of the gene (Fig. 3.88). In this study expression of Mitofusin 2 was assessed and it was found that the expression of Mfn2 significantly downregulated in BPA2 and BPA 3 diseased groups as compared to control group. Whereas the treatment with plant extract (BPA2+P.I and BPA3+P.I) showed significantly upregulated expression of Mfn2 as

compared to control suggesting the role of *P. integerrima* in mitigating the miRNA-15a-5p induced apoptosis (Fig. 3.89).

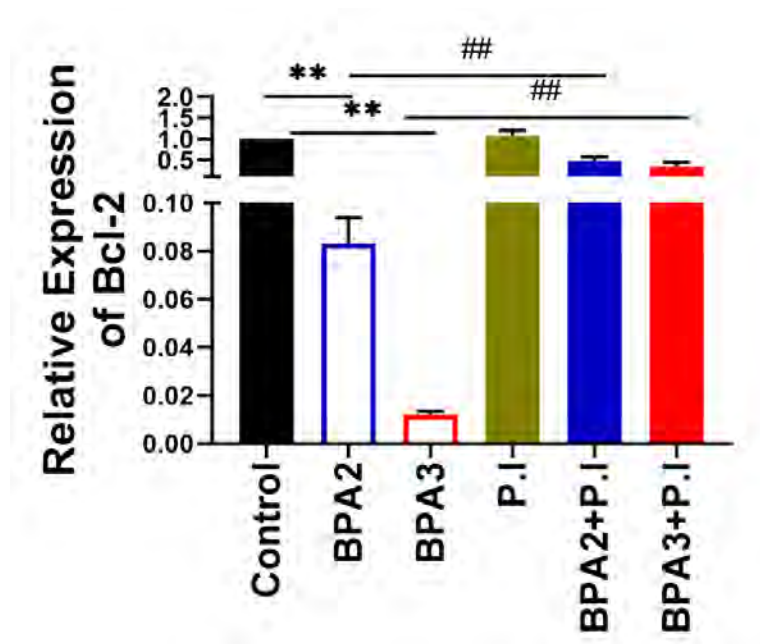


Figure 3.88. Estimation of relative expression of *Bcl2* in brain tissues “\*\*/# shows  $p$  value < 0.01”

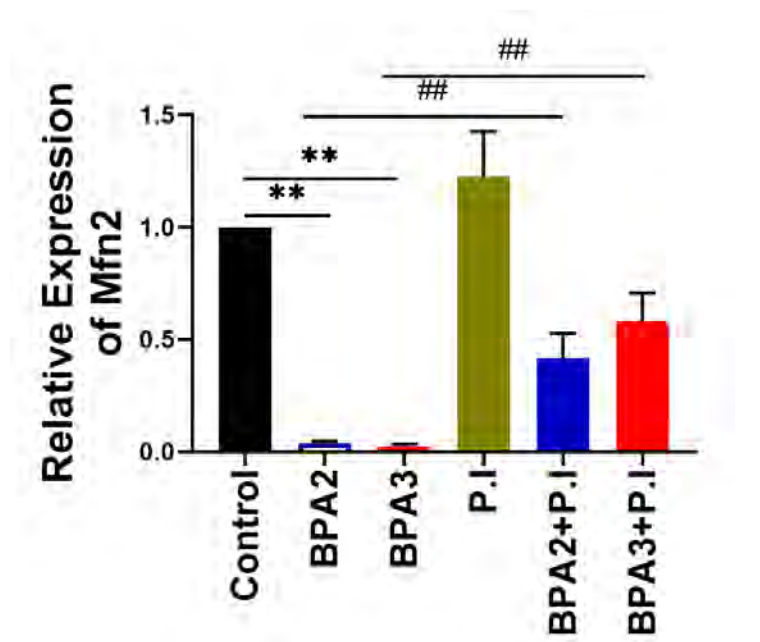


Figure 3.89. Estimation of relative expression of *Mfn2* in brain tissues “\*\*/# shows  $p$  value < 0.01”

### 3.22 Molecular docking studies of Es-37 and Ls-37 with proteins; Bcl-2, p53 and cytochrome c

Initially, we performed the docking of P53, Bcl-2, and cytochrome with oligomers of Es-37 and L-37 to confirm their possible modes of interaction and favourable binding sites. The optimized geometries of oligomers of L-37 and Es-37 used in the docking procedure are presented in Figure S2 in the supplementary section. The binding energies obtained from nine molecular docking runs of Bcl-2, cytochrome c, and p53 with L-37 and Es-37 in kcal/mol are shown in Table 3.2. The best confirmation of the docked complex is based on minimized energy and is selected for further analysis. Additionally, the distance between the oligomers and atoms in the amino acids can indicate the nature of interactions between them; these are listed in Table 3.3. The grid parameters adopted in the simulations covered the complete area encompassing receptor-binding amino acids of proteins, leaving enough space for the flexible ligand to explore conformations. Results indicate that L-37 has enhanced binding affinity towards the receptor protein cytochrome c with a binding affinity of -9.4 kcal/mol, compared to Es-37 (lower binding energy of -7.8 kcal/mol). The synthetic polymers, L-37 and Es-37 show large binding affinity values with the other enzymatic proteins Bcl-2 and p53 in the range of -5.9 to -7.8 kcal/mol, with L-37 oligomers always showing a greater binding tendency. The significant negative values indicate that the studied oligomers show low binding energy due to their enhanced affinity with the protein residues (Masouri et al. 2021). Cytochrome c appears to be the best enzymatic protein to interact with the synthetic polymers showing the most negative value of binding energy (-9.4 kcal/mol) for L-37.

The docked complexes of the oligomers (L-37 and Es-37) with the three proteins are shown in Figures 1-6 (A). The majority of interactions (within 5 Å range) between the oligomers of Es-37 and L-37 with the three proteins (p53, Bcl-2 and cytochrome c) comprise of hydrogen bonding, L-37 shows a total of fourteen bonding interactions with cytochrome c as compared to eleven with Bcl-2 and eight for p53 protein residues. Out of these, L-37 shows three H-bonds with Bcl-2 while the rest are  $\pi$ - $\pi$  interactions (Figure 3.90 A, B, C, D). In contrast, the oligomer Es-37 shows a total of eleven types of interaction with Bcl-2 (Figure 3.91 A, B, C, D), out of which four are conventional hydrogen bonds, one is a carbon-H bond and the rest are  $\pi$ - cation and  $\pi$ -anion.

**Table. 3.2 Binding Energies obtained from nine docking runs of L-37 and Es-37 oligomers with Bcl-2, cytochrome c, and p53**

Modes of Binding	Binding Energy of Bcl2 (kcal.mol)		Binding Energy of Cytochrome c (kcal.mol)		Binding Energy of p53 (kcal.mol)	
	L-37	Es-37	L-37	Es-37	L-37	Es-37
1	<u>-7.8</u>	<u>-7.2</u>	<u>-9.4</u>	<u>-7.8</u>	<u>-5.8</u>	<u>-6.0</u>
2	<u>-7.8</u>	<u>-7.2</u>	<u>-9.4</u>	<u>-7.5</u>	<u>-5.8</u>	<u>-5.9</u>
3	<u>-7.7</u>	<u>-7.1</u>	<u>-9.3</u>	<u>-7.5</u>	<u>-5.8</u>	<u>-5.5</u>
4	<u>-7.7</u>	<u>-7.1</u>	<u>-9.2</u>	<u>-7.5</u>	<u>-5.7</u>	<u>-5.4</u>
5	<u>-7.6</u>	<u>-6.9</u>	<u>-9.1</u>	<u>-7.4</u>	<u>-5.7</u>	<u>-5.4</u>
6	<u>-7.5</u>	<u>-6.9</u>	<u>-9.1</u>	<u>-7.3</u>	<u>-5.7</u>	<u>-5.4</u>
7	<u>-7.2</u>	<u>-6.9</u>	<u>-8.9</u>	<u>-7.3</u>	<u>-5.7</u>	<u>-5.3</u>

interactions. Molecular docking of cytochrome c with L-37 shows the maximum number of interactions dominated by conventional hydrogen bonds, carbon-H bonds and pi-donor H bonds, while few  $\pi$ - $\pi$  and arene -  $\pi$  interactions are also seen (Figure 3.92 A, B, C, D). On the other hand, the oligomer Es-37 shows only six types of interactions with cytochrome c, (Figure 3.93 A, B, C, D). The dominant interactions are hydrogen bonds, C-H and alkyl interactions. For the protein p53, the oligomer L-37 shows four dominant hydrogen bonds (Figure 3.94 A, B, C, D) while the oligomer Es-37 shows twelve interactions with protein residues, which consist of hydrogen bonds (8), carbon-hydrogen bonds (1) and unfavourable positive-positive interactions (Figure 3.95 A, B, C, D).

**Table 3.3: Bonding interactions of L-37 and Es-37 oligomers with amino acid residues of Bcl-2, cytochrome c, and p53**

LIGAND	Protein (Pdb id)	Hydrogen bonding interactions with Amino acid Residues
	Bcl-2 (5jsn)	ASP D-87, ASP D-3, LYS B-5

<b>L-37</b>	Cytochrome c (5z62)	PHE-D:33, LEU-D:35, ARG-F:112, SER-M:28, TYR-A:260, TYR-A:261
	p53(4mzi)	SER-A:260, ARG-A:267, ARG-A:158, ASP-A:207, TYR-A :205
<b>Es-37</b>	Bcl-2 (5jsn)	ASN-A:192, ASN-B:17, LYS-D:103, ARG-B:67
	Cytochrome c (5z62)	SER-D:97, ARG-A:480, SER-M:28
	p53 (4mzi)	LYS-A:139, ASN-A:239, THR-A:140, CYS-A:227, GLN-A:136, MET-A:243, LYS-A:235, ARG-A:196

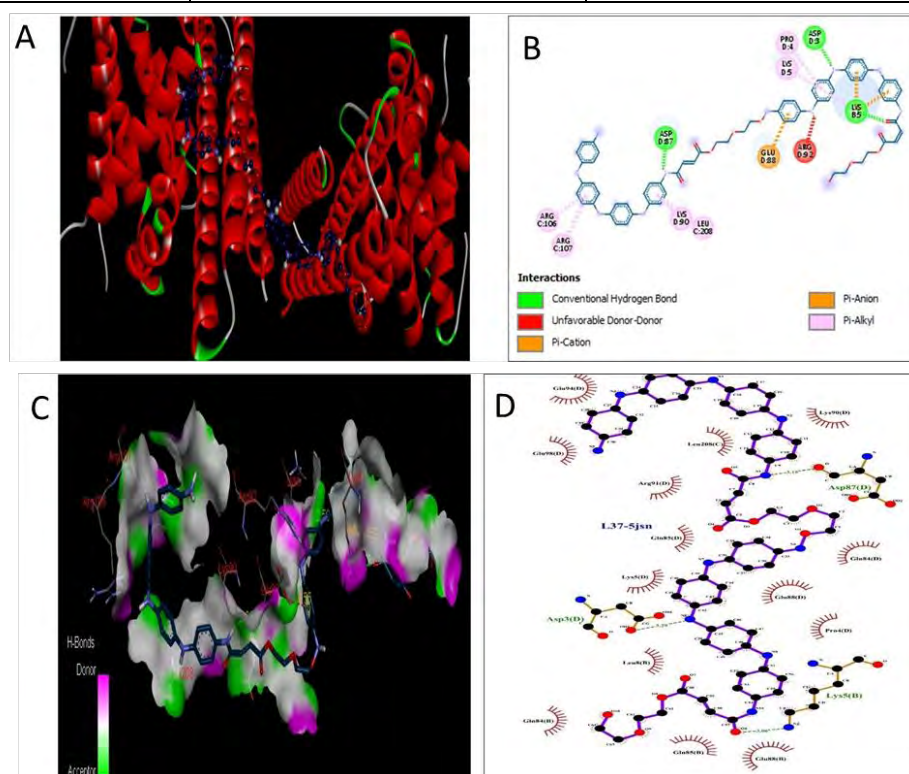


Figure 3. 90 Molecular docking of L-37 with Bcl-2. (A) 3D structure of interactions of target protein Bcl-2 (PDB id: 5jsn) with L-37 oligomer (blue) (B) 2D Ligplot of Bcl-2 interactions with L-37 (C) Hydrogen bonding between Bcl-2 and L-37 (D) Other types of interaction between Bcl-2 and L-37 in the 2D Ligplot. The color bar in (C) indicates the strength of the H-bonds

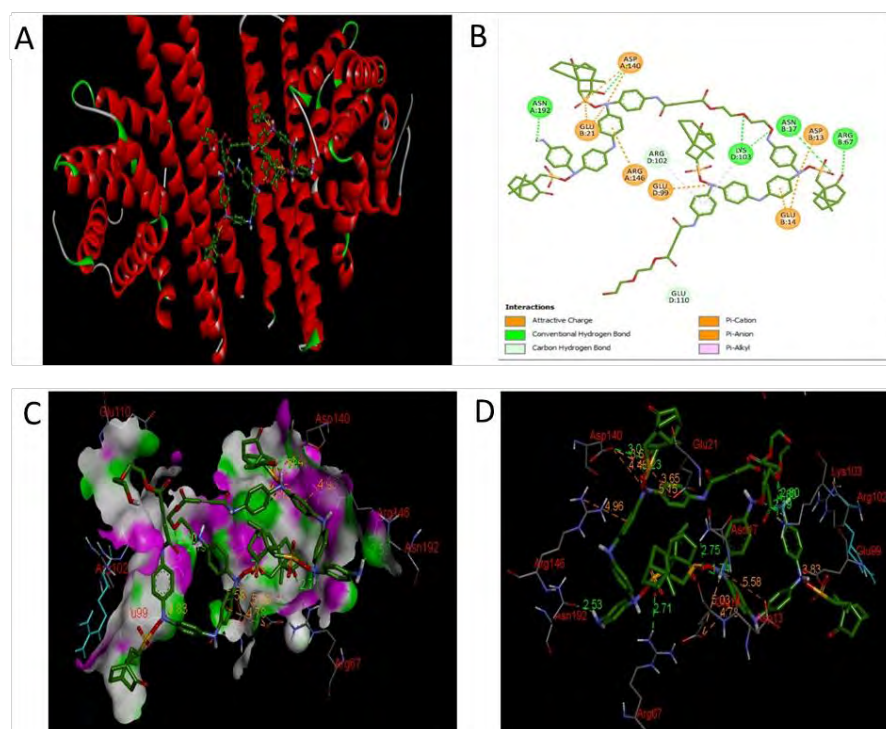


Figure 3.91 Molecular docking of Es-37 with Bcl-2. (A) 3D structure of interactions of target protein Bcl-2 (PDB id: 5jsn) with Es-37 oligomer (green) (B) 2D Ligplot of Bcl-2 interactions with Es-37 (C) Hydrogen bonding between Bcl-2 and Es-37 (cyan) (D) 3D view of different type of interactions between Bcl-2 and Es-37 with corresponding distances

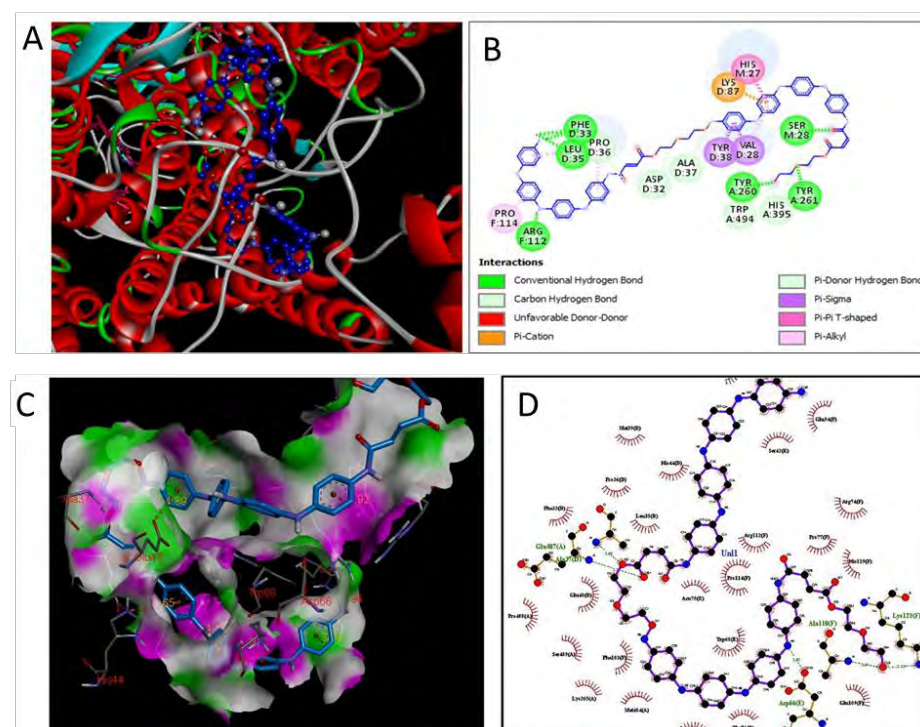


Figure 3.92 Molecular docking of L-37 with Cytochrome c. (A) 3D structure of interactions of target protein cytochrome c (PDB id: 5z62) with L-37 oligomer (blue) (B) 2D Ligplot of protein interactions with L-37 (C) Hydrogen bonding between cytochrome c and L-37 (D) Other types of interaction between cytochrome c and L-37 in the 2D Ligplot

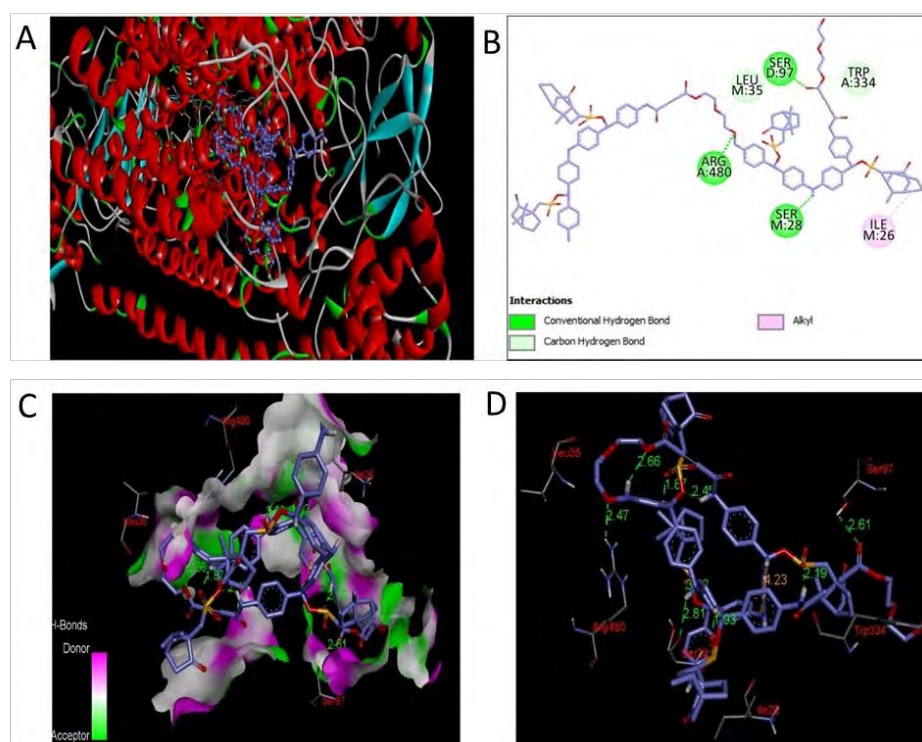


Figure 3.93 Molecular docking of Es-37 with cytochrome c (A) 3D structure of interactions of target protein cytochrome c (PDB id: 5z62) with Es-37 oligomer (blue) (B) 2D Ligplot of protein interactions with Es-37 (C) Hydrogen bonding between cytochrome c and Es-37 (blue) (D) 3D view of different type of interactions between cytochrome c and Es-37 with corresponding distances

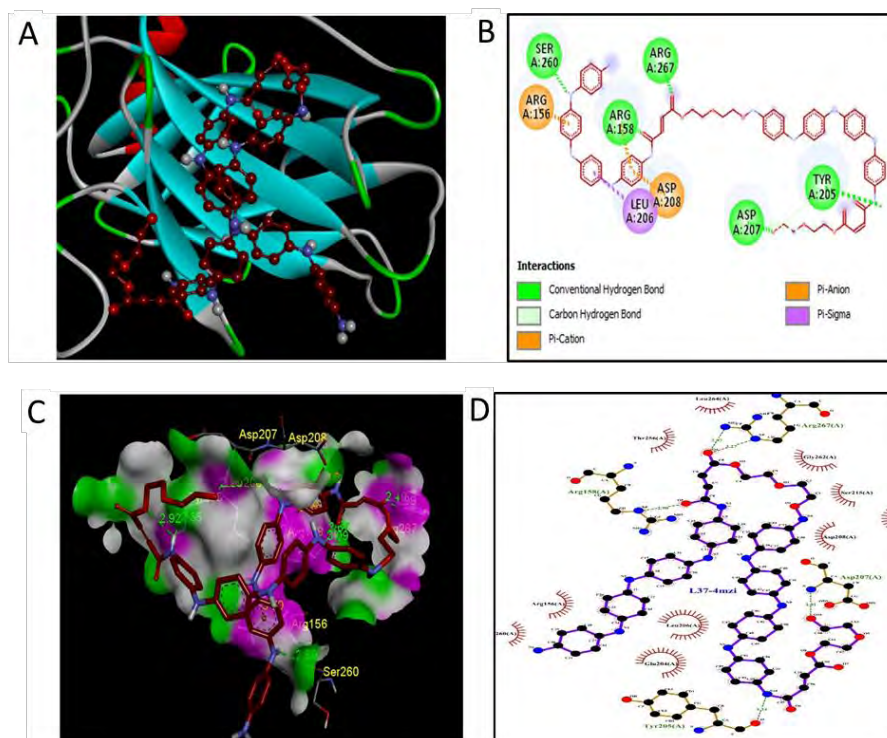


Figure 3.94 Molecular docking of L-37 with p53 (A) 3D structure of interactions of target protein p53 (PDB id: 4mzi) with L-37 oligomer (red) (B) 2D Ligplot of protein interactions



with L-37 (C) Hydrogen bonding between p53 and L-37 (red) (D) Other types of interaction between p53 and L-37 in the 2D Ligplot

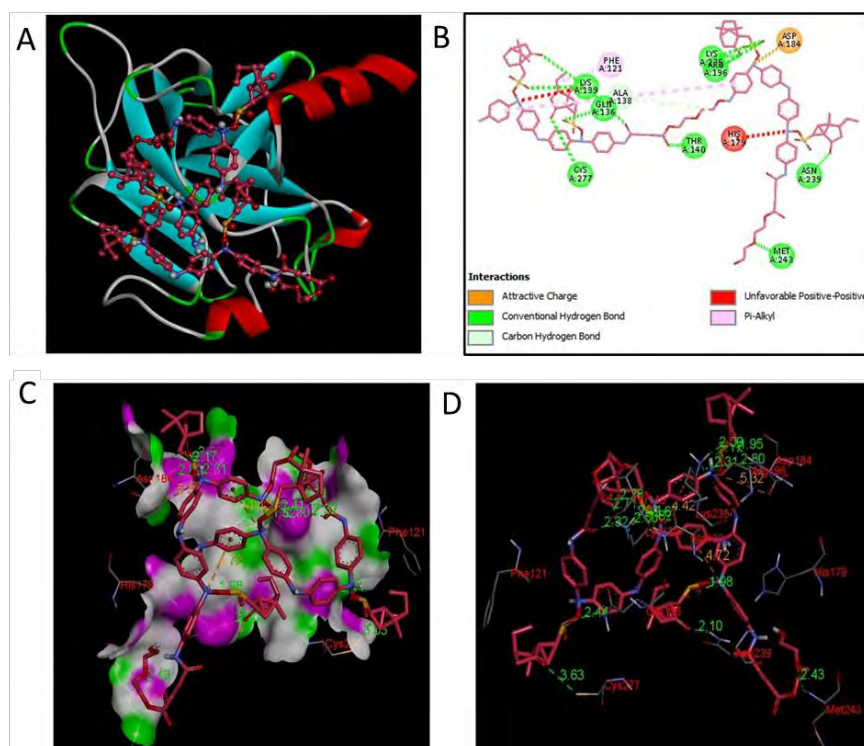


Figure 3.95 Molecular docking of Es-37 with p53 (A) 3D structure of interactions of target protein p53 (PDB id: 4mzi) with Es-37 oligomer (red) (B) 2D Ligplot of protein interactions with Es-37 (C) Hydrogen bonding between p53 and Es-37 (pink) (D) 3D view of different type of interactions between p53 and Es-37 with corresponding distances.

### 3.23 Molecular dynamic simulation analysis

The conformational dynamics and configuration stability of the proteins with docked synthetic polymers were probed by MD simulation run of 100-ns. The resulted trajectories were subjected to analysis of root mean square deviations (RMSD) of backbone and ligands, and root mean square fluctuations (RMSF). All these structural evaluations are illustrated below in figure 3.96 A. Calculation of RMSD for C $\alpha$  atoms of proteins was done in order to elucidate the geometric variations between the superimposed frames achieved by MD simulation.

### 3.24 RMSD and RMSF analysis for stability and flexibility prediction

RMSD analysis was conducted to analyze the stability of all six systems. The research also highlighted the firmness of L-37 and Es-37 (docked polymers) inside the active site pocket of the target proteins p53, Bcl-2, and cytochrome c. RMSD explained that the net RMSD was determined to be within the range of 1-10 Å for all three L-37 systems, validating that L-37-cytochrome c and L-37-p53 systems were stable while L-

37-Bcl-2 was highly unstable. In the case of the L-37-Bcl-2 complex, the net RMSD was found 10.0 Å. For L-37-Bcl-2 complex, snapshots taken at different production run intervals revealed that the observed larger fluctuations in the RMSD were due to conformational changes caused by the movement of the polymer (figure 3.96 B).

It was observed that at 4ns the polymer moved away from the initial docked conformation and after 10ns it returned to its original position. Again, at 11ns, 60ns, and 72ns a significant rise in RMSD was observed because of the mobility of the polymer. On the contrary, we noted that the net RMSD in the case of L-37-cytochrome c complex was 2.8 Å, and the system remained stable during the simulation runtime except for some minor structural changes due to ligand-induced movements in the configuration of the protein loops. These structural moves were noted to assist in adequately adapting the Es-37 or L-37 inside the pocket, making strong interactions and forming a stable complex. The mean RMSD of the L-37-p53 complex was 1.9 Å. While in case of Es-37, RMSD for all 3 systems was calculated to be within the range of 1-15 Å validating that Es-37-cytochrome c and Es-37-p53 systems were stable. Es-37-cytochrome c and Es-37-p53 complex revealed high stability and showed a net RMSD score of 2.9 Å and 2.2 Å, respectively. Es-37-Bcl-2 complex showed a mean RMSD of 15.9 Å. The docked complex of Bcl-2-Es-37 also showed more significant fluctuations over the first 11-14ns; a rapid rise was observed at 60ns and 72ns, respectively. The superimposition of snapshots extracted at mentioned intervals revealed that this instability was because of a repositioning of the Es-37 (figure 3.96 C). The mean RMSD of both polymers showed stable conformation with cytochrome c and p53, while unstable conformation was observed with Bcl-2. Moreover, flexibility analysis of the amino acid residues of the protein was evaluated to calculate the RMSF. Amino acid residues present in the active pocket of the protein responsible for polymer binding and the stability of this binding were also assessed in this assay. Exception to L-37-cytochrome c and Es-37-cytochrome c (mean RMSF 9.7Å and 7.1Å) all the secondary components of Es-37-Bcl-2, Es-37-p53, and L-37-cytochrome c, L-37-p53 showed similar fluctuations in the range of 20 Å -34 Å and 13.3 Å -33.6 Å, respectively.

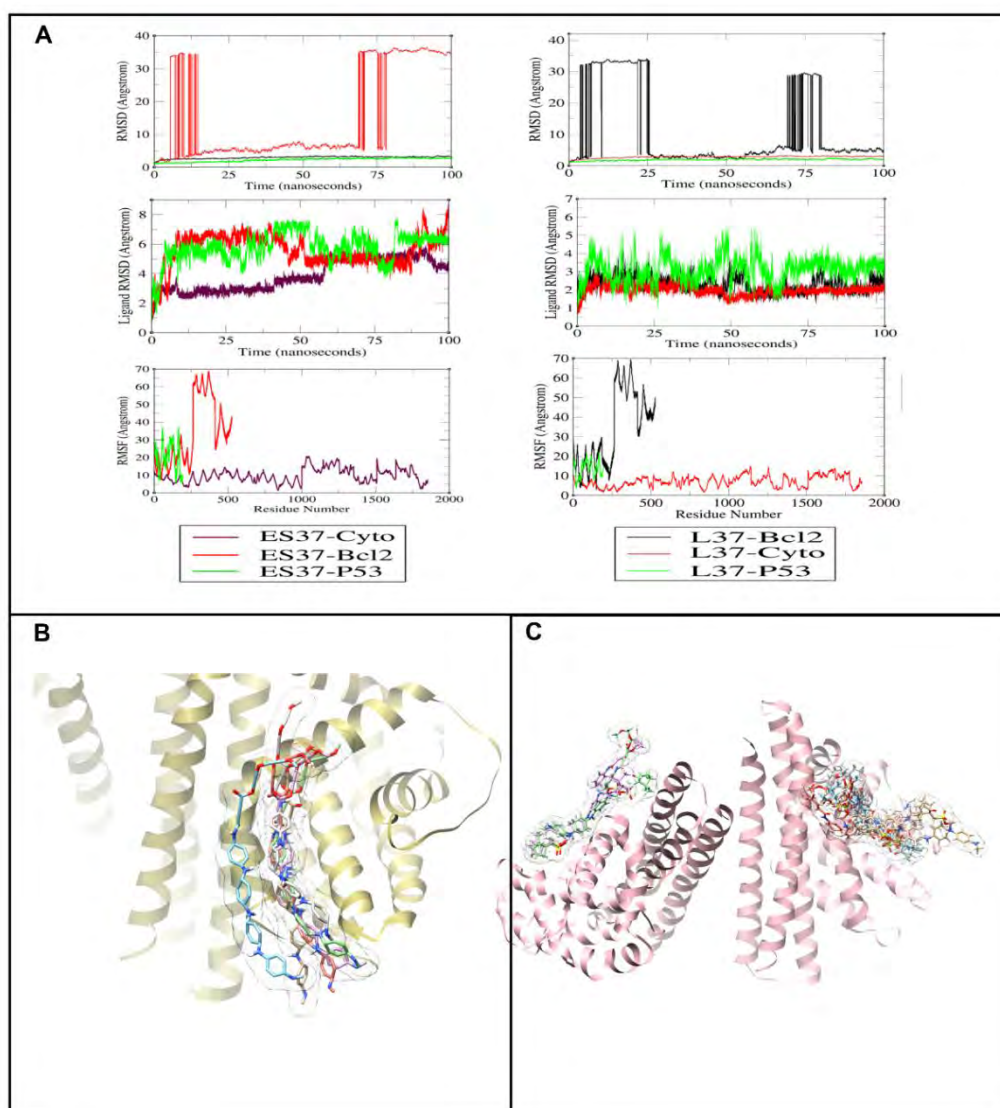


Figure 3.96 Trajectories analysis. (A) C alpha root mean square deviation and root mean square fluctuations of selected proteins and ligands (Es-37, L-37) (B) superimposition of Bcl-2-L-37 snapshots extracted at 11, 60 and 72ns, respectively (C) superimposition of Bcl-2-Es-37 snapshots extracted at 11, 60 and 72 ns, respectively

### 3.25 Es-37 and L-37 abolished BPA induced disturbed cellular architecture

An increased number of nuclei, disruption of the cellular membrane, the increased surface area of the cell, and disturbed nucleus-to-cytoplasm ratio (figure 3.97) all are the hallmarks of toxicity and apoptosis at the cellular level (Ishtiaq, Ali et al. 2021). Herein, BPA treatment significantly induced cellular toxicity by increasing the number of nuclei, %age of abnormal cells, and disrupted cellular organization in the heart tissue of the rats. However, Es-37 and L-37, as well as NAC treatment, rescued these changes, demonstrating their therapeutic and antitoxic potential against BPA-induced cellular

toxicity. We further validated these findings by Masson's trichrome staining. The BPA-administered group showed an excessive deposition of collagen (green color depicts the collagen) in the heart tissues than that of the normal control (bright red color) (Fig. 3.93). However, the Es-37 and L-37 treated groups showed less collagen deposition than the disease group. These findings indicate that Es-37 and L-37, as well as NAC (reference drug), possessed antitoxic potential by attenuating cardiac fibrosis.

### **3.26 Es-37 and L-37 abated BPA induced miRNA-15a-5p and target gene expression**

miRNAs play a pivotal role in disease initiation, progression, and treatment response via the regulation of post-transcriptional gene expression (Peng and Croce 2016). Here in the present study, BPA administration significantly upregulated miRNA-15a-5p expression in the cardiac tissue of rats. However, Es-37, L-37, and NAC treatment entirely averted miRNA-15a-5p upregulation in the presence of BPA. Notably, BPA+Es-37 treated showed more similar expression of miRNA-15a-5p to the normal and the reference groups (BPA+NAC). These findings suggest miRNA-15a-5p expression correlates with BPA-induced oxidative stress, and Es-37 acts as an antioxidant and may possess cellular toxicity (apoptosis) regulatory potential via miRNA-15a-5p-BCL2 axes (figure 3.97 J, 3.100 A). The bioinformatics software, TargetScan analysis showed that Bcl-2 is the putative target gene of miRNA-15a-5p. miRNA-15a-5p binds to a highly conserved 8 mer sequence of mRNA of target gene Bcl-2. The binding region of miRNA-15a-5p with Bcl-2 is shown in (figure 3.97N). As Bcl-2 is a potential target gene of miRNA-15a-5p, its expression was significantly downregulated in a diseased group compared to the normal control. In all treatment groups *i.e.* BPA+ NAC, BPA+ Es-37 and BPA+ L-37, Bcl-2 expression was significantly upregulated as compared to the diseased group. However, the treatment groups (BPA+Es-37 and BPA+L-37) showed higher expression of Bcl-2 as compared to the standard antioxidant reference group, which suggests the analeptic effects of synthetic tetra-aniline polymers. Expression of Bcl-2 in NAC, Es-37, and L-37 were comparable to normal control. The upregulation of miRNA-15a-5p and downregulation of Bcl-2 in the BPA administered group and the reversion of expression upon treatment with terpolymers propose that miRNA-15a-5p directly regulates the mRNA level of Bcl-2. suggesting the anti-apoptotic role of Es-37 and L-37 (figure 3.97 K, 3.100 B).

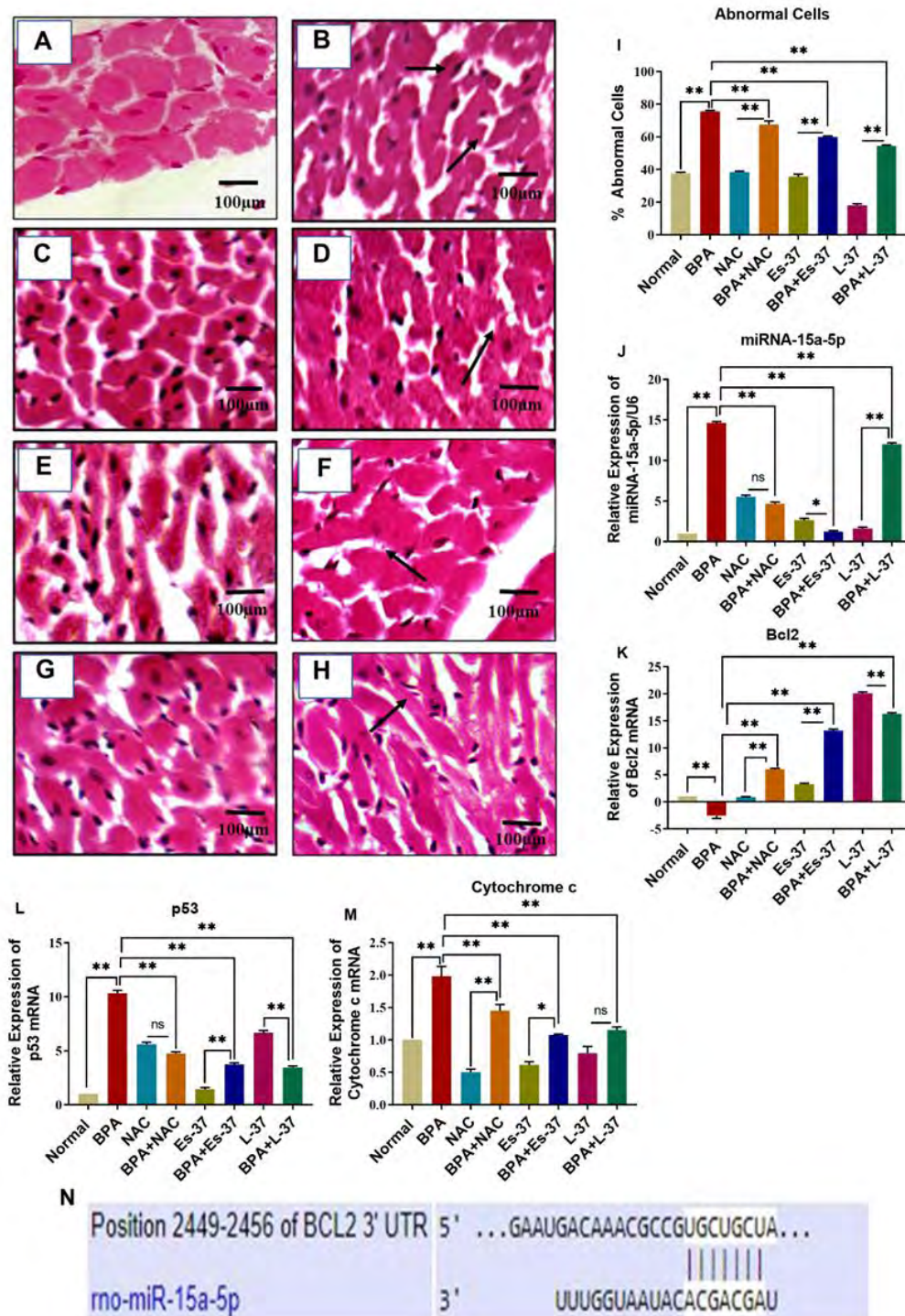


Figure 3.97 Histological analysis and relative mRNA expression. A-H; H&E staining of heart tissues; (A) normal, (B) BPA, (C) NAC, (D) BPA+NAC, (E) Es-37, (F) BPA+Es-37, (G) L-37, (H) BPA+L-37 treated heart tissues (images taken at 40X, scale bar 100 $\mu$ m), (I) % abnormal cells of heart, (J) Graphical representation of the relative expression of miRNA 15a-5p, (K) Graphical representation of the relative expression of Bcl-2 mRNA, (L) Graphical representation of the relative expression of p53 mRNA, (M) Graphical representation of the relative expression of cytochrome c mRNA, (N) Binding region of miRNA-15a-5p to 3'UTR of Bcl-2 gene (source TargetScan database), “(\*) at  $p$  value < 0.05, (\*\*) at  $p$  value < 0.01”

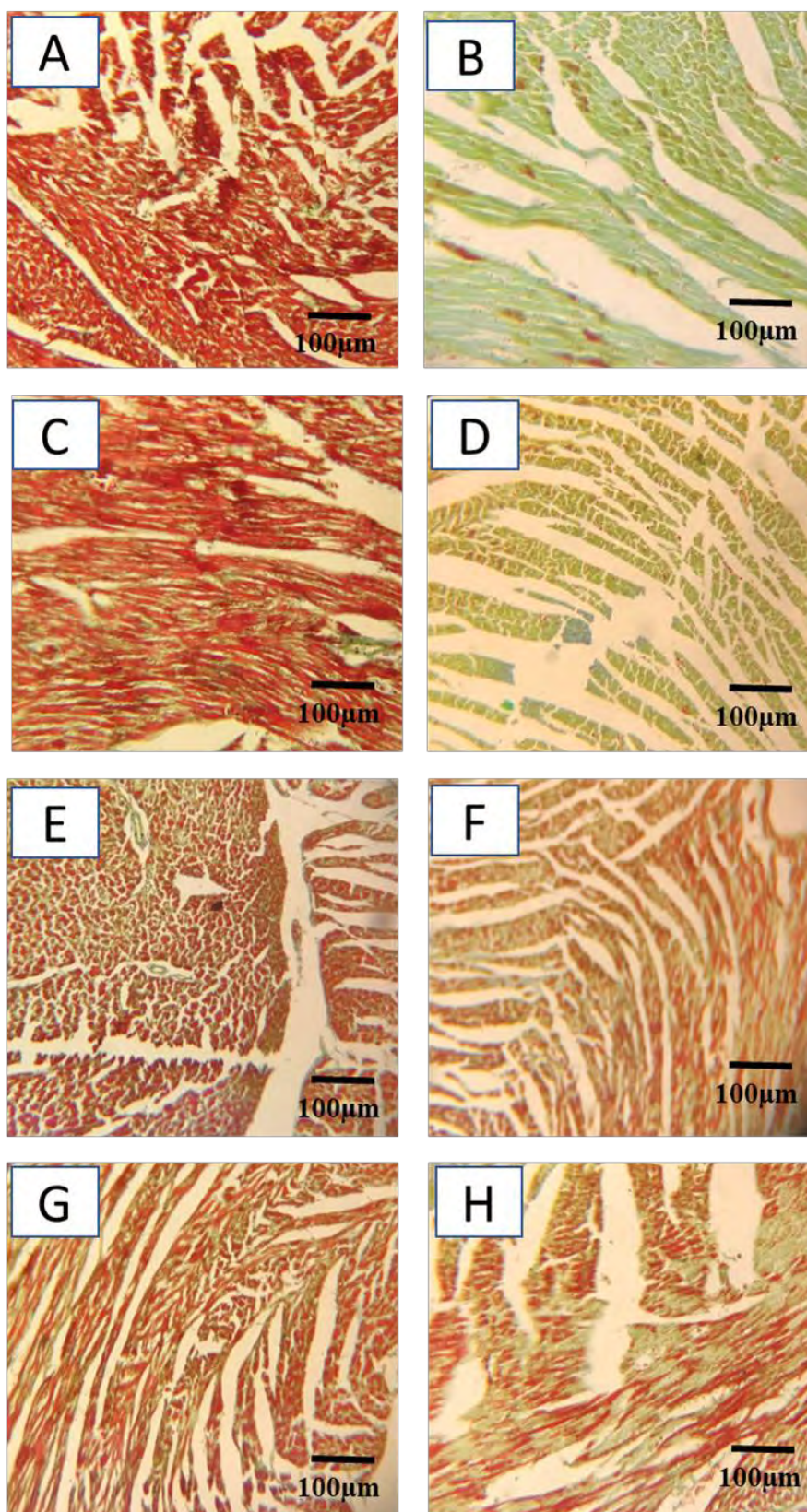


Figure 3.98 Collagen deposition analysis A-H; Representative images of Masson's Trichrome staining of heart tissues; (A) normal, (B) BPA, (C) NAC, (D) BPA+NAC, (E) Es-37, (F) BPA+Es-37, (G) L-37, (H) BPA+L-37 treated heart tissues. (The light green colour depicts the collagen deposition). Images taken at 10X magnification, scale bar 100µm

### 3.27 Es-37 and L-37 alleviated the BPA induced p53 and cytochrome c expression

The key players of apoptotic signaling pathway p53 and cytochrome c were significantly upregulated at both transcriptional and translational level in BPA administered group as compared to the control which suggests the role of BPA in apoptosis. However, upon treatment with Es-37 and L-37 in the presence of BPA significantly reduced the expression of both p53 and cytochrome c (figure 3.97 L, M, 3.99 A, B, E, F, 3.100 C, D). Interestingly the markedly reduced expression of p53 and cytochrome c in both treatment groups (BPA+Es-37 and BPA+L-37) compared to the standard antioxidant treatment group (BPA+NAC), suggests the ameliorative potential of the synthetic terpolymers.

As the phosphorylation of p53 modulates the mitochondrial linked apoptosis therefore in current study we have evaluated the expression of p-p53. the expression of p-p53 was significantly upregulated in disease group as compared to control. While, in treatment groups *i.e.* BPA+ Es-37 and BPA+ L-37 p-p53 expression was significantly downregulated, the synthetic terpolymer Es-37 showed better results than NAC and L-37 treatment groups (figure 3.99 C, D, 3.100 E, F, G). All these results highlight the anti-apoptotic potential of Es-37 and L-37; thus, these synthetic terpolymers (Es-37, and L-37) may serve as potent antioxidant and anti-cardiotoxic agents.

### 3.28 Es-37 and L-37 scavenged the BPA-generated free radicals

Free radical generation leads to the cardiac toxicity. BPA administered group showed significantly high levels of ROS and TBARs as compared to control. While, the ROS and TBARs levels were significantly decreased in treatment groups *i.e.* BPA+ NAC, BPA+ Es-37 and BPA+ L-37 as compared to BPA administered group, which shows the free radical scavenging potential of Es-37 and L-37 (figure 3.101 A, B, 3.112 A, B).

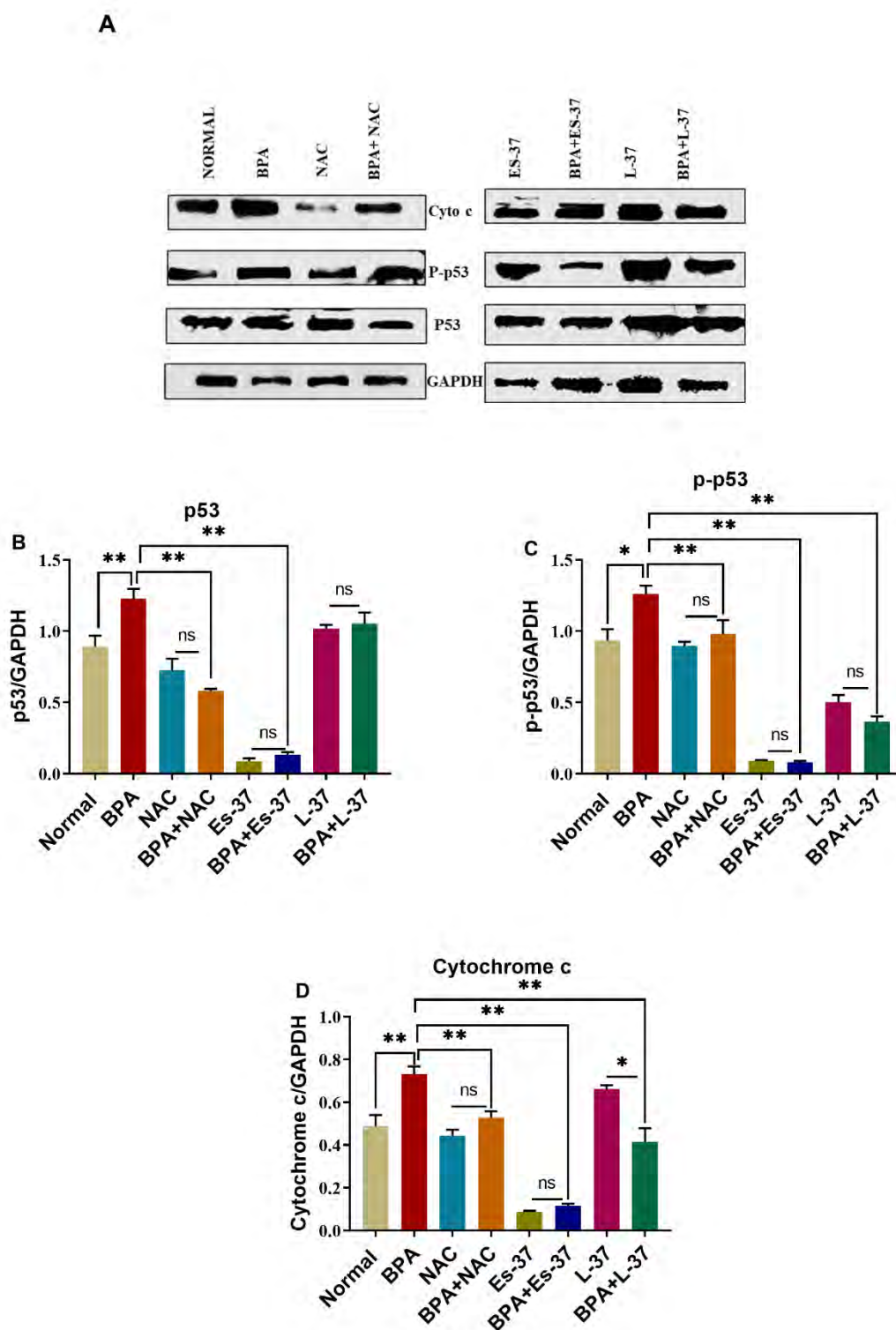


Figure 3.99 Protein expression analysis (A) Western blot of p53 protein, (B) Graphical representation of the densitometric analysis of p53 protein, (C) Western blot of p-p53 protein, (D) Graphical representation of the densitometric analysis of p-p53 protein, (E) Western blot of cytochrome c protein, (F) Graphical representation of the densitometric analysis of



cytochrome protein. GAPDH was used as loading control. “(\*) at  $p$  value  $< 0.05$ , (\*\*) at  $p$  value  $< 0.01$ ”

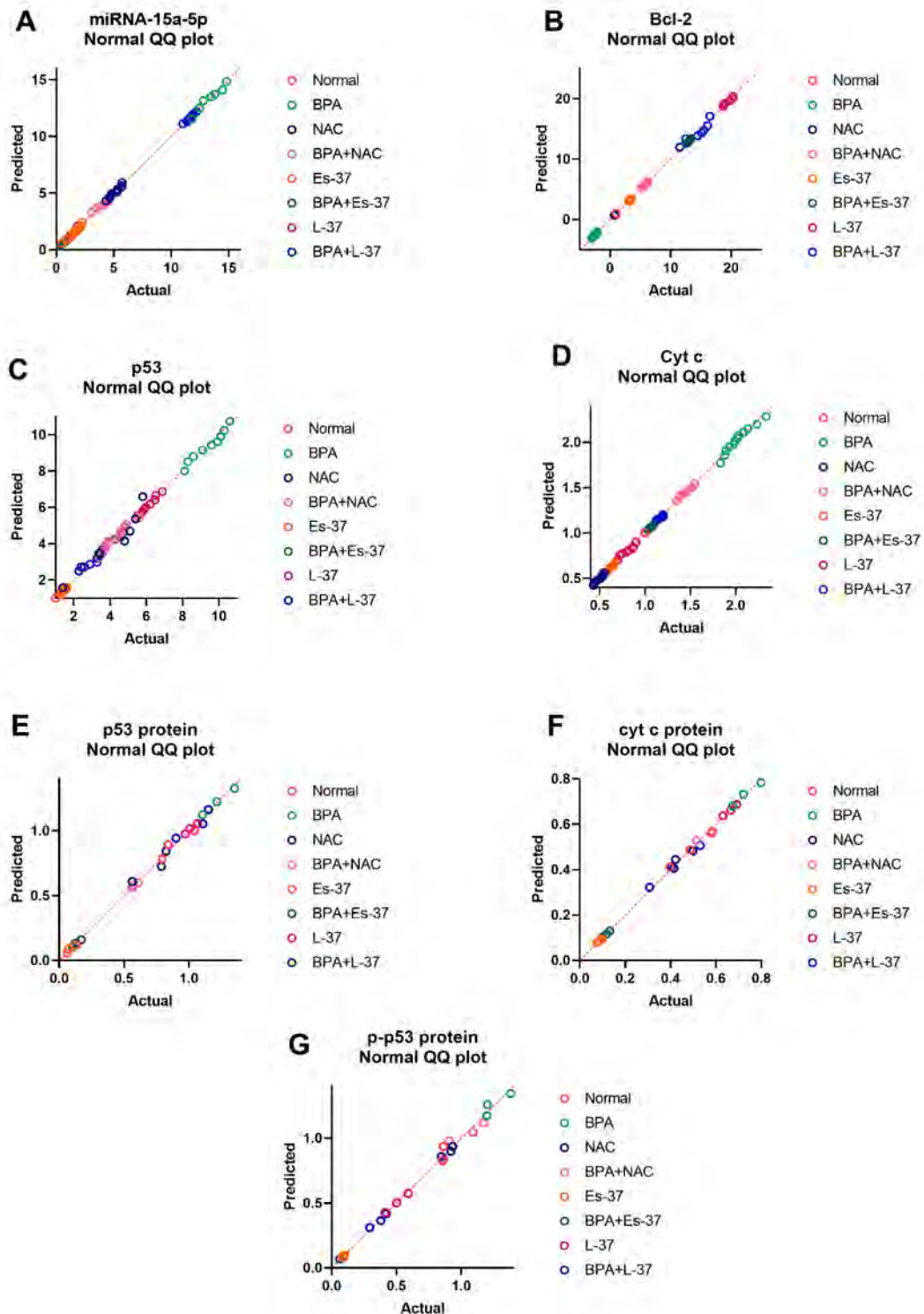


Figure 3.100 Normality curves of p53 and target genes, A miRNA-15a-5p expression, B Bcl2 mRNA expression, C p53 mRNA expression, D Cyt c mRNA expression, E p53 protein expression, F Cytochrome c protein expression, G P-p53 protein expression

### 3.29 Es-37 and L-37 enhanced the antioxidant enzyme activities

In current study, to confirm the antioxidant potential of Es-37 and L-37 different antioxidant enzyme activities were measured. SOD activity (serum and heart tissues) was significantly decreased in BPA group as compared to control. While, the activity of SOD enzyme in NAC, Es-37 and L-37 was comparable to normal control (figure 3.101 C, 3.102 C). Whereas, SOD activity was significantly increased in treatment groups *i.e.* BPA+ NAC, BPA+ Es-37 and BPA+ L-37 as compared to BPA treated group showing the greater antioxidant activity boosting potential of Es-37 and L-37. In addition, catalase (CAT) is another antioxidant enzyme, involved in scavenging cellular ROS. The catalase activity was significantly decreased in heart tissue and serum samples of disease group as compared to control. However, the activity of catalase enzyme was significantly increased in treatment groups BPA+ NAC, BPA+ Es-37 and BPA+ L-37 as compared to disease group showing the therapeutic potential of Es-37 and L-37 (figure 3.101 D, 3.102 D). Moreover, GSH activity was significantly reduced in BPA administered group as compared to the control in case of both serum and heart tissues. Whereas, in treatment groups *i.e.* BPA+ NAC, BPA+ Es-37 and BPA+ L-37, GSH activity was significantly increased as compared to disease group, indicating the antioxidant potential of Es-37 and L-37 (figure 3.101 E, 3.102 E). The POD activity in serum and heart homogenate samples was significantly decreased in BPA administered group as compared to control., While, in treatment groups *i.e.* BPA+ NAC, BPA+ Es-37 and BPA+ L-37 the APX level was significantly high as compared to diseased group (figure 3.101 F, 3.102 G). Ascorbate peroxidase level in both heart tissues and serum samples was significantly decreased in BPA administered group as compared to control. However, the treatment with Es-37 and L-37 has significantly increased the APX level in the presence of BPA suggesting the antioxidant boosting potential of these terpolymers (figure 3.101 G, 3.102 F).

### 3.30 Es-37 and L-37 normalized the BPA induced cellular damage markers

ALT and AST levels were significantly high in BPA group as compared to the control. In Es-37 and L-37 treated groups, ALT and AST levels were comparable to normal control suggesting the safer dose administration and no hepatotoxic effects of terpolymers. While, in treatment groups BPA+ NAC, BPA+ Es-37 and BPA+ L-37

significant decrease in ALT and AST levels were observed as compared to disease group (figure 3.101 H, 3.103 A, B). In addition, both triglycerides and cholesterol levels were significantly high in BPA group as compared to the control. The triglycerides and cholesterol levels in NAC, Es-37 and L-37 were comparable to normal control. While, in treatment groups *i.e.* BPA+ NAC, BPA+ Es-37 and BPA+ L-37 the triglycerides and cholesterol levels were significantly decreased as compared to diseasegroup showing the therapeutic potential of Es-37 and L-37 (figure 3.101 I, 3.103 E, F). The creatinine and uric acid levels were significantly high in BPA treated group as compared to the normal control. While, in treatment groups BPA+ NAC, BPA+ Es-37 and BPA+ L-37, creatinine and uric acid levels were significantly decreased as compared to diseased group (figure 3.101 J, 3.103 C, D). In Es-37 and L-37 treated groups, creatine and uric acid levels were comparable to control proposing that both Es-37 and L-37 have no toxic effect on renal function.

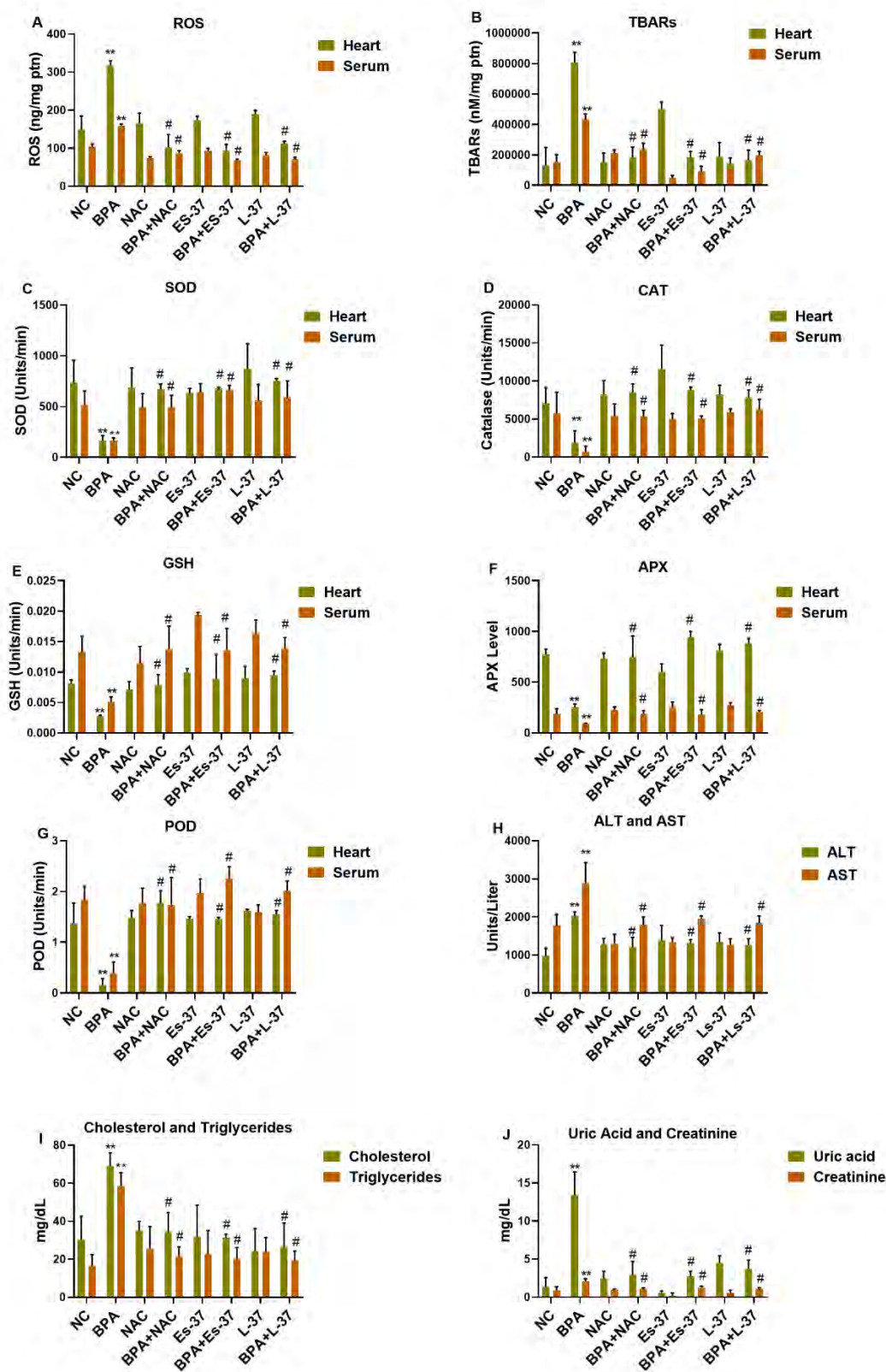


Figure 3. 101 Effect of Es-37 and L-37 on biochemical Profile (A) Estimation of ROS activity in heart and serum, (B) Estimation of TBARs level in heart and serum, (C) Estimation of SOD

activity in heart and serum, (D) Estimation of CAT activity in heart and serum, (E) Estimation of GSH activity in heart and serum, (F) Estimation of APX in heart and serum, (G) Estimation of POD activity in heart and serum, (H) Estimation of liver markers ALT and AST in serum, (I) Estimation of lipid profile cholesterol and triglycerides in serum, (J) Estimation of kidney profile uric acid and creatinine in serum “(\*\*) in comparison to normal control at  $p$  value < 0.01, (#) in comparison to disease control at  $p$  value < 0.01”

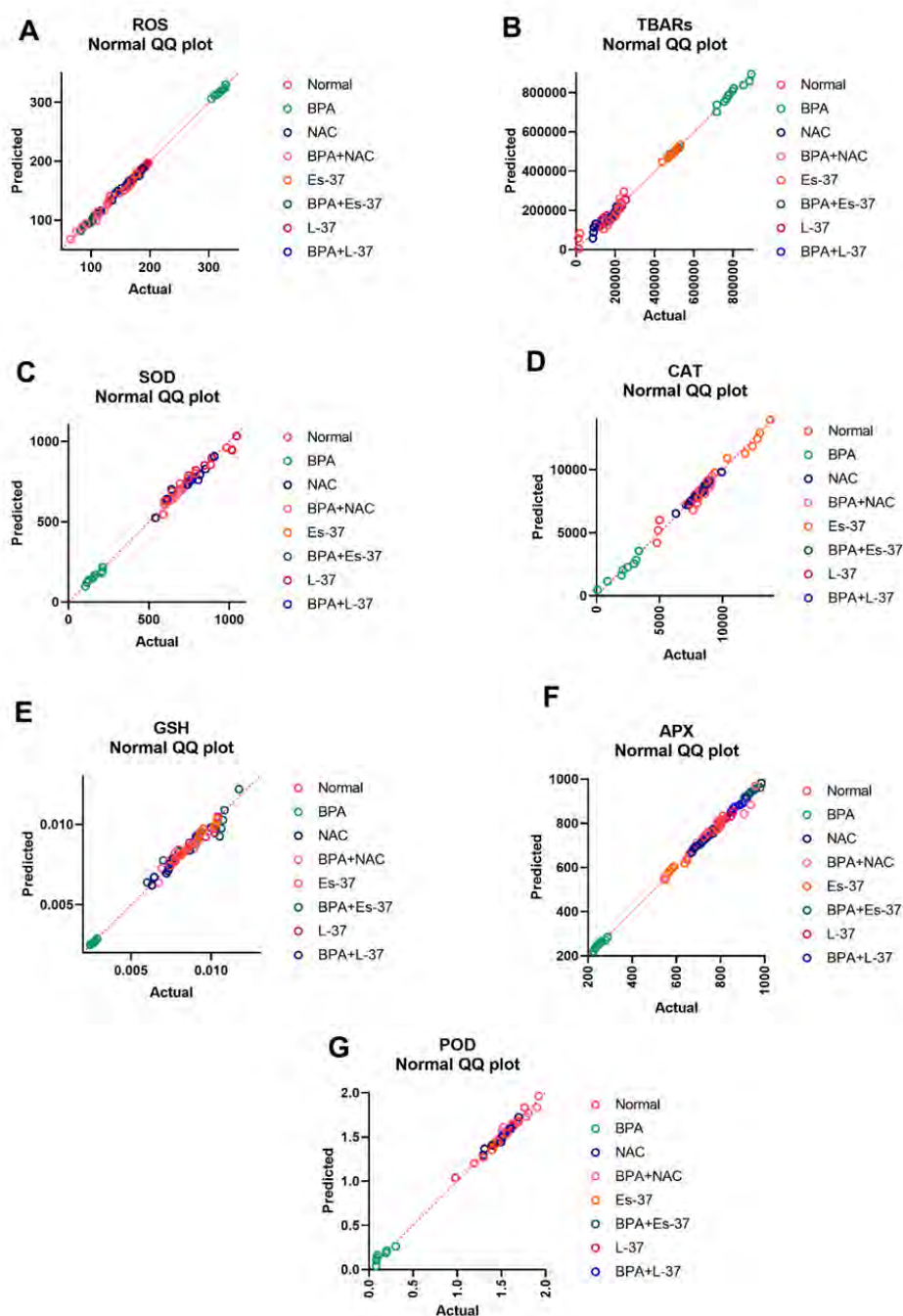


Figure 3.102 Normality curve analysis of oxidative stress markers, A Representative graph of ROS, B Normality curve of TBARs, C Normality plot of SOD, D Normality plot of CAT, E Normality plot of GSH, F Normality plot of APX, G Normality plot of POD

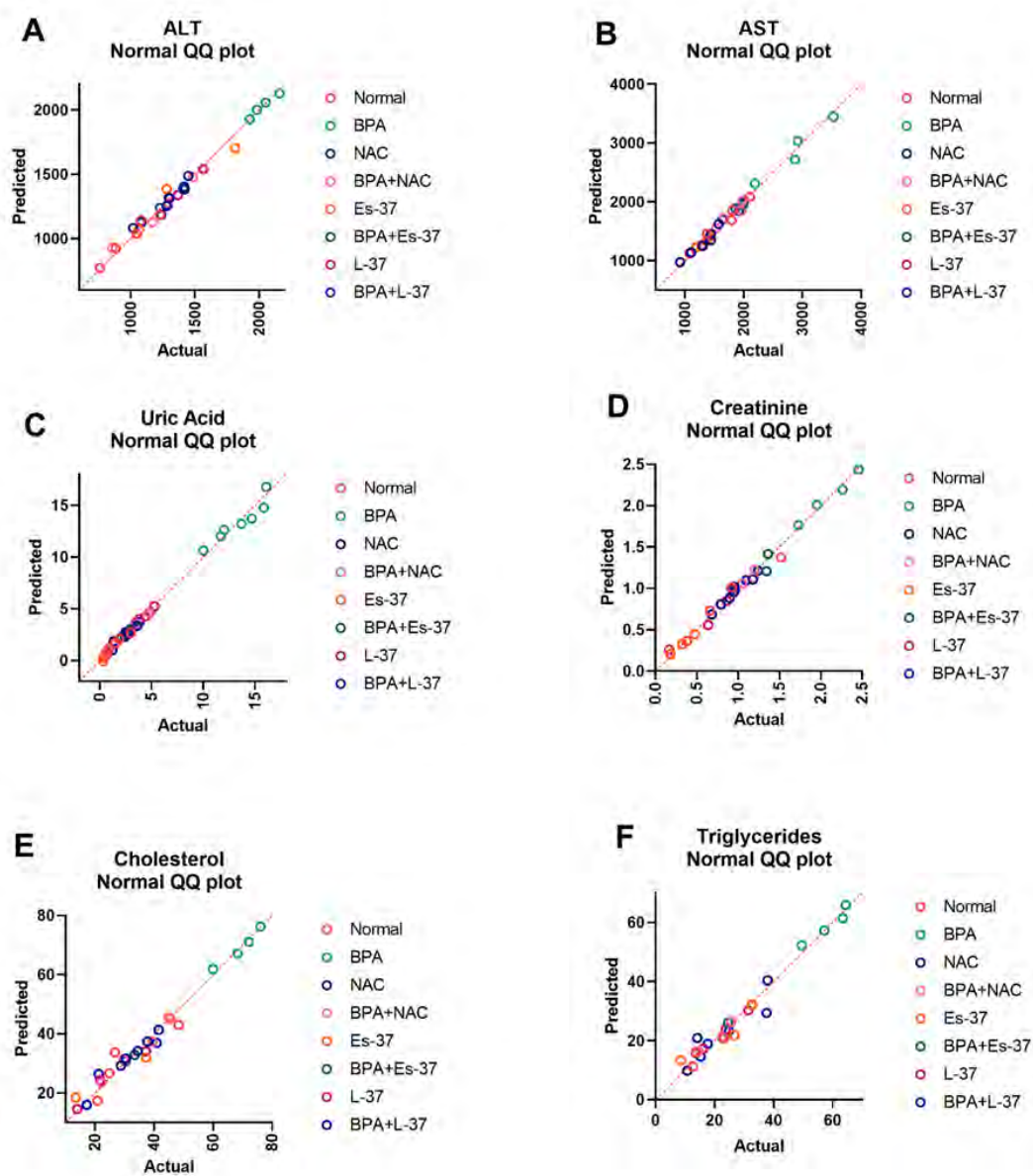


Figure 3.103 Normality curve analysis of toxicity markers, A Representative graph of normality curve of ALT, B Normality curve of AST, C Normality plot of Uric acid, D Normality plot of Creatinine, E Normality plot of Cholesterol, F Normality plot of Triglycerides

The objective of the current study was to analyze the role of BPA in the development of cardiotoxicity and the neurotoxicity. As BPA is the endocrine disruptor therefore the current study also sought to investigate the role of BPA in the breast cancer development. Breast cancer is one of the most common disorders among women and is reported as the second leading cause of cancer-related deaths worldwide.

### 3.31 Demographic and clinical characters of breast cancer patients

On the basis of age as a demographic character, breast cancer patients were classified into three subgroups ranging from 15-30 years,  $\leq 60$  years and  $\geq 60$  years, respectively. A large number (66.7%) of patients belong to age group  $\leq 60$ . Only 4.7% fall in age group ranging from 15-30, and 28.5% patients fall in the age group  $\geq 60$ . Breast cancer patients were categorized as canned food users and canned food non-users. Only 4.7% of patient was canned food user, and 95.2% were canned food non-users. Moreover, the breast cancer patients were also split into two subgroups: plastic bottle users and plastic bottle non-users. 71.4% of patients were frequent plastic bottle users, and 28.5% were plastic bottle non-users. Table 3.4 represents a comprehensive overview of different demographic and clinical characters of breast cancer patients who participated in the study.

**Table.3.4 Demographical and clinical characters of breast cancer patients**

Parameters/variables	Percentage (%)
<b>Age groups</b>	
15-30	4.7%
<60	66.7%
>60	28.5%
<b>Ethnic groups</b>	
Punjabi	71.4%
Pakhtoon	9.5%
Kashmiri	14.3%
Sindhi	4.8%
<b>Gender</b>	
Female	95.2%
Male	4.8%
<b>Family history</b>	
Sporadic	80.9%
Familial	19.0%
<b>Matrimonial status</b>	
Married	85.7%
Un-married	4.8%
Widow	9.5%
<b>Weight</b>	
Normal weight	61.9%
Under-weight	14.2%
Obese	23.8%

<b>Educational status</b>	
Illiterate	52.3%
Middle	19.0%
Matric	23.8%
Graduate	4.7%
<b>Smoking</b>	
Non-smokers	90.4%
Smokers	9.5%
<b>Lifestyle</b>	
House-wives	90.4%
Professional	9.5%
<b>Canned food</b>	
Canned food users	4.7%
Canned food non-users	95.2%
<b>Plastic bottles</b>	
Plastic bottle users	71.4%
Plastic bottle non-users	28.5%
<b>Other diseases</b>	
Heart disease	0%
Liver disease	9.5%
Lung disease	9.5%
Diabetes	14.2%
Blood pressure	38.0%
<b>Menopausal status</b>	
Pre-menopause	47.6%
Peri-menopause	4.7%
Post-menopause	47.6%
<b>Stages of breast cancer</b>	
Stage I	9.5%
Stage II	23.8%
Stage III	66.6%
Stage IV	0%
<b>Hormonal receptor status</b>	
ER+PR-HER2+	4.7%
ER+PR+HER2+	14.2%
ER-PR-HER2+	9.5%
ER+PR+HER2-	14.2%
E-cadherin+	4.7%
<b>Histological classification of breast cancer patients</b>	
DCIS	19.0%
IDC	66.6%
ILC	4.7%
<b>Biopsy side of breast tumor</b>	
Right breast	33.3%
Left breast	66.6%
Both	0%
<b>Ki67 score of breast cancer patients</b>	
Ki67 10-15%	9.5%
Ki67 16-25%	14.2%
Ki67 26-36%	9.5%
Ki67 37-50%	4.7%
<b>Tumor size of breast cancer patients</b>	
10-100mm	23.8%
110-200mm	9.5%
210-300mm	19.0%



### 3.32 Analysis of Bisphenol A (BPA) Concentration

Bisphenol A concentration was analyzed in the serum samples of healthy individuals. HPLC Agilent 1100 UV system was used for the analysis of serum samples and the chromatograms of standard, and patient samples that were obtained by HPLC are shown in figure 3.104.

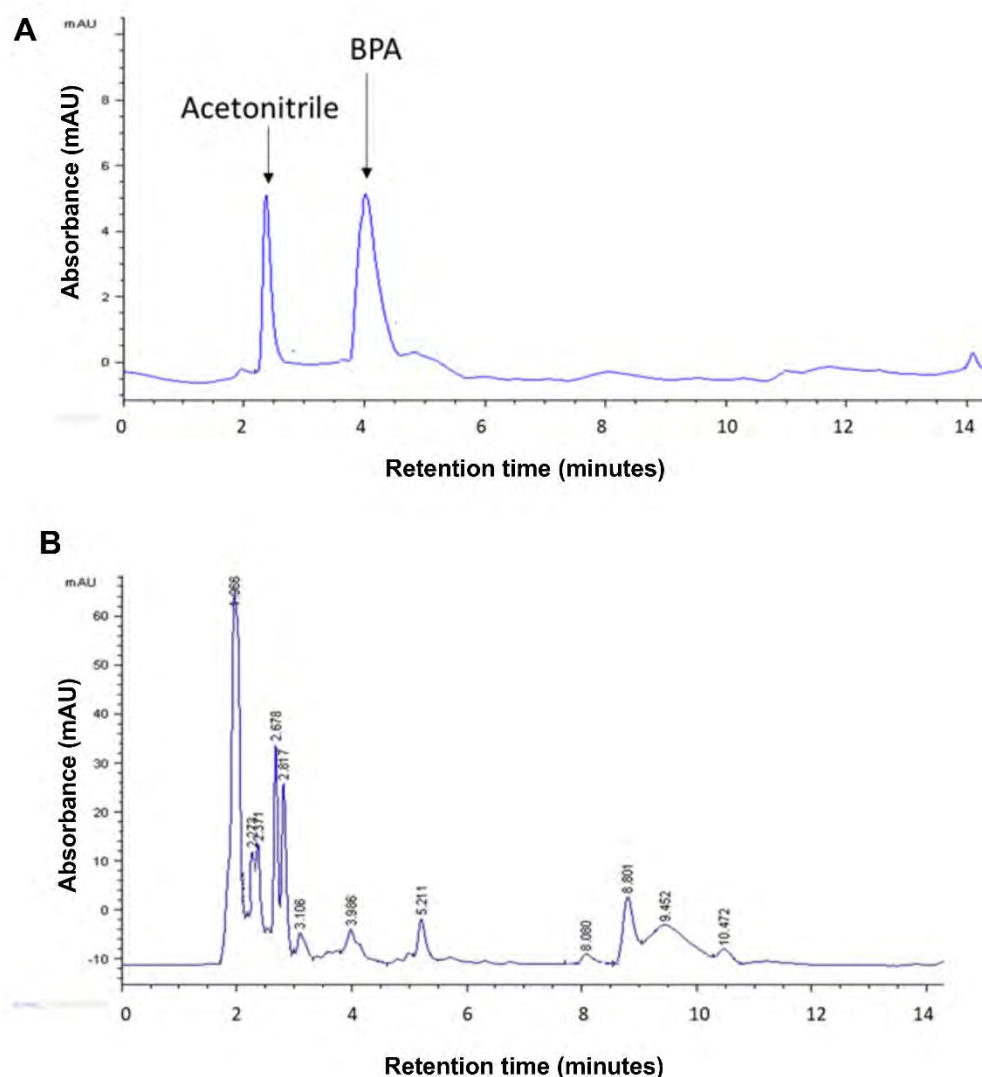


Figure 3.104. Representative images of Chromatograms; A: chromatogram of standard at 210nm; B: chromatogram of serum sample of normal individuals at 210nm

### 3.33 Redox profiling of breast cancer samples

BPA has a vital role in the generation and progression of oxidative stress. There was a significantly increased ROS level in malignant tissue samples in comparison to control tissue samples (figure 3.105 B). Malignant tissues showed significantly low levels of

superoxide dismutase (SOD) and catalase (CAT) enzymes respectively as compared to control tissues (figure 3.105 C, D).

### **3.34 Expression analysis of p53 and linked markers in breast cancer samples**

p53 is the key player of tumorigenesis in several cancers. There was about 17 folds increased activity of the p53 gene with significant value of in malignant breast tissue samples as compared to control tissue samples at mRNA level (figure 3.105 E). p53 protein expression was also analysed by western blotting. There was a significant increase in the expression of p53 protein in malignant breast tissues compared to control tissue. The upregulated level of p53 suggests the link of BPA-generated oxidative stress in breast cancer progression. In addition, the WNT1 gene expression was approximately increased by 35 folds with significant value of in malignant breast tissue samples as compared to control tissue samples at mRNA level (figure 3.105 F). ZEB1 gene expression at mRNA was nearly increased by 328 folds with significant value of in malignant tissues as compared to control tissues (figure 3.105 G).

### **3.35 Histological Analysis of Breast Cancer Tissue Samples**

The histological examination of the breast cancer tissue samples has shown the high-grade ductal carcinoma in situ (DCIS). The architectural pattern of cribriform with pagetoid spread was clearly observed. All margins of DCIS were clear, with no invasive carcinoma (figure 3.106 A). The other type of the carcinoma detected in our study was Invasive mammary carcinoma. The histological grade III out of III was observed (figure 3.106 B). The histology of male breast cancer tissue sample has shown the invasive mammary carcinoma with no particular type. The margins were clear, and extensive extra nodal extensions were discerned (figure 3.106 C). The receptor analysis showed there were only (4.7%) patients with ER+ PR- HER2+ receptor status, while (14.2%), (9.5%), (14.2%) and (4.7%) patients had ER+ PR+ HER2+ , ER- PR- HER2+, ER+ PR+ HER2- and E-cadherin+ receptor status respectively (figure 3.107 A, B).

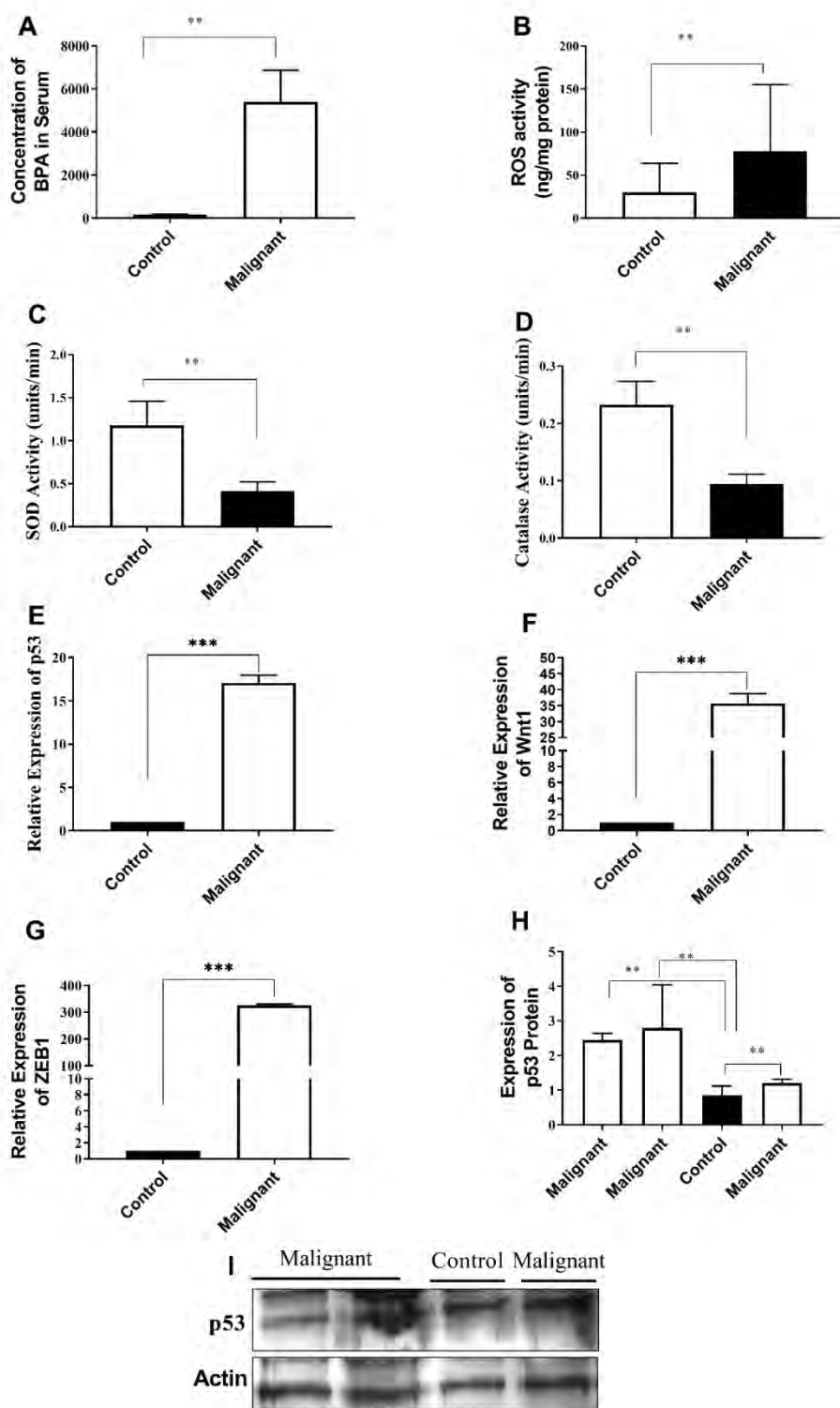


Figure 3.105 Graphical representation of BPA concentration in control and malignant breast tissue samples; B: Graphical representation of ROS activity in control and malignant breast tissue samples; C: Graphical representation of SOD activity in control and malignant breast tissue samples; D: Graphical representation of Catalase (CAT) activity in control and malignant breast tissue samples; E: Graphical representation of the relative fold activity change of p53 in control and malignant breast tissue samples; F: Graphical representation of the relative fold activity change of WNT1 in control and malignant breast tissue samples; G:

Graphical representation of the relative fold activity change of ZEB1 in control and malignant breast tissue samples; H: Graphical representation of the densitometric analysis of p53 protein in malignant and control breast tissue samples; I: Blot image of p53 and actin in malignant and control breast tissue samples. "The data was considered significant at \*\* p-value  $\leq 0.01$  or \*\*\*p-value  $\leq 0.001$ "

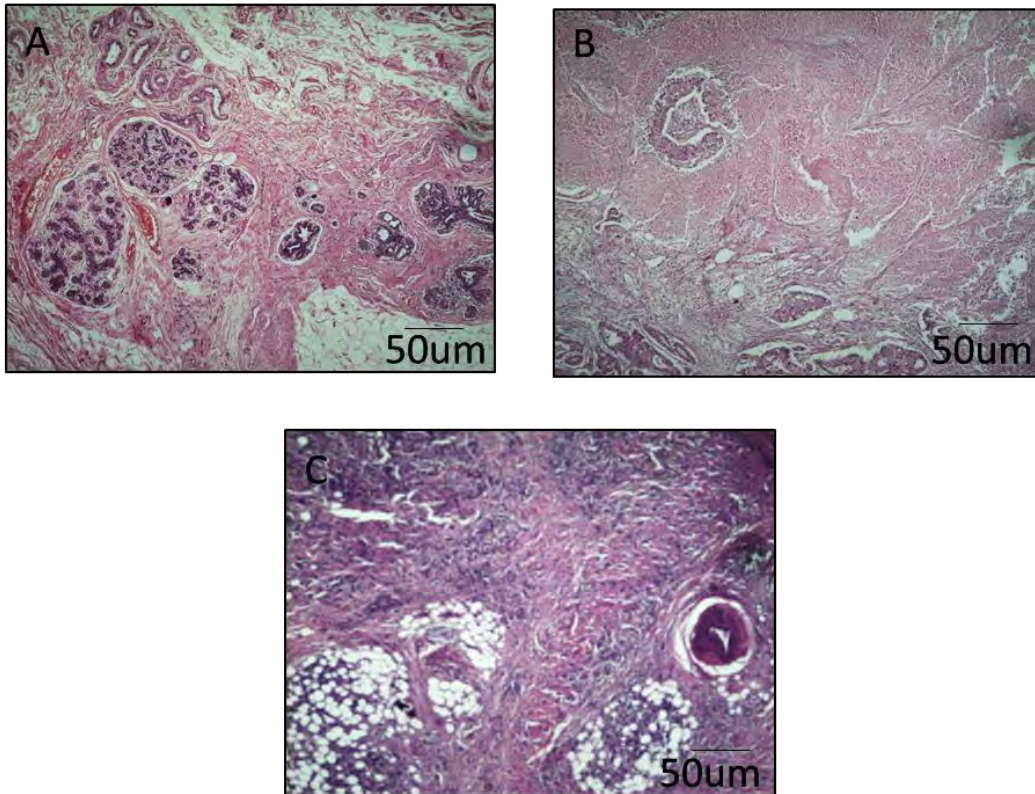


Figure 3.106 Histological analysis of breast tissue samples; A: Representative image of DCIS female breast tissue; B: Representative image of IDC female breast tissue; C: Representative image of IDC male breast tissue, (magnification: 40X, Scale bar 50µm)

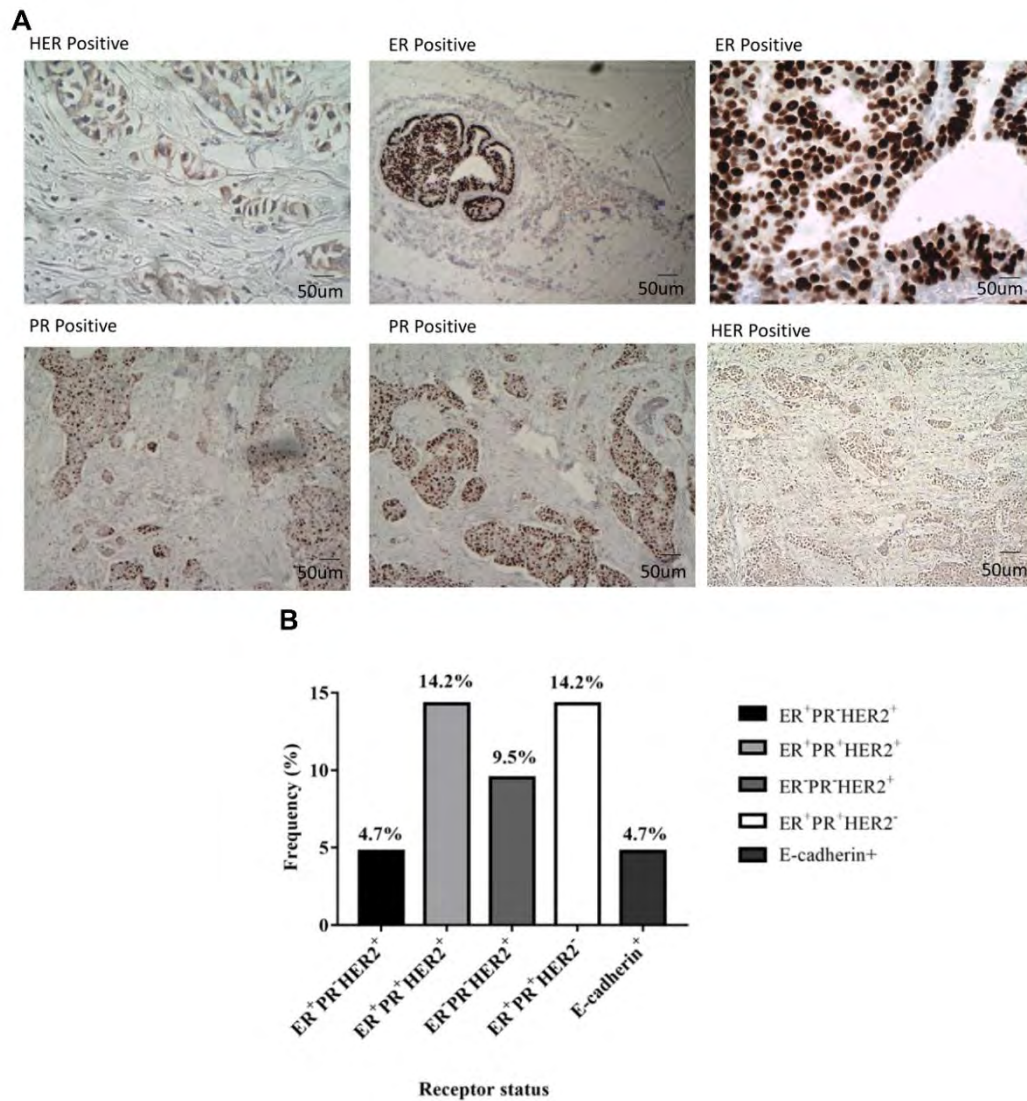


Figure 3.107. Representative images of receptor status of different breast tissue samples analysed by IHC (Magnification 40X, scale bar 50µm), B Graphical representation of the frequency distribution of receptor status of breast cancer tissue samples

#### 4. DISCUSSION

The plastic monomer, environmental toxicant, and endocrine disruptor BPA is one of the ubiquitously produced chemicals worldwide. BPA is used in the manufacturing of polycarbonate plastics and epoxy resins used in several consumer products (Vandenberg, Hauser et al. 2007). The consumption of BPA in the lining of food cans and drinking water bottles are the leading cause of BPA exposure to humans. It can cause inauspicious effects on various vital organs (Mourad and Khadrawy 2012) by enhancing the ROS generation (Gharibi, Dilmaghanian et al. 2013). Despite of the several debates and research on the toxic effects of BPA, still the investigation of the exact molecular targets is needed. Therefore, the present study aimed to delineate the molecular mechanism and tried to put forward the therapeutic strategy against BPA induced oxidative stress. The Sprague Dawley rats of average age 6-8 weeks were administered with the three different doses (100µg/kg BW, 1mg/kg BW and 10mg/kg BW) of BPA to investigate its role in cardiotoxicity and neurotoxicity *via* regulation of miRNAs and their target mitochondrial apoptosis regulators. In present study, the BPA treated group has shown the increased level of ROS and decreased antioxidant enzymes in serum as well as in tissues (heart, brain, liver, and kidney). The elevated level of TBARs has also confirmed the reactive oxygen species generation. However, the treatment with *P. integerrima* and melatonin has resulted in the decreased oxidative. The galls of *P. integerrima* contain quercetin, naringenin and 3,5,7,4'-tetrahydroxyflavanone, which attributes to its antioxidant potential (Rauf, Saleem et al. 2015, Zahoor, Zafar et al. 2018).

In current study BPA2 and BPA3 showed significant effects on rats body weight. The results of present study are in consistent with the previous studies as BPA is an endocrine disruptor which significantly increases the adipogenesis that ultimately leads to the increase in body weight (Ohlstein, Strong et al. 2014). However, the melatonin treatment group showed the reduced body weight as compared to disease groups. These results are in consistent with De Pedro et al studies, that melatonin increases the lipid mobilization and reduces the muscles glycogen stores (De Pedro, Martínez-Álvarez et al. 2008). Moreover, the methanolic extract of *P. Integerrima* significantly reduced the body weight as compared to the disease groups suggesting its analeptic potential.

The present study showed the increase in serum uric acid level, cholesterol, and triglyceride level whereas decreased HDL level of BPA treated group suggesting its potential role in organ toxicity. These dysregulated levels can cause the renal and cardiovascular complications (Diepeveen, Wetzels et al. 2008). However, the treatment with potent antioxidant melatonin and *Pistacia integerrima* has reverted the changes, manifesting the therapeutic potential of melatonin and *Pistacia integerrima*.

The hepatocytes damage leads to the release of enzymes into the blood such as ALT, AST, and ALP which indicates damage to cytosol and mitochondria (Mathuria and Verma 2008). In the current study, the elevated levels of liver markers ALT, AST, and ALP suggest hepatocytes damage. Our study has shown that in the presence of methanolic extract of *P. integerrima*, enzymes remained normal compared to BPA treated rats, proposing the beneficial role of plant extract against BPA toxicity.

BPA is the source of ROS production which can lead to oxidative stress (Gassman 2017). It modulates different signaling pathways involved in cytotoxicity, mitochondrial damage, and apoptosis (El-Beshbishy, Aly et al. 2013, Khan, Beigh et al. 2016, Faheem and Lone 2017). Herein, BPA-induced free radicals confirm the oxidative stress linked toxic effects of BPA in different organs (heart, brain, liver, kidney) of rats. Further, the decline in ROS level by *P. Integerrima* and melatonin evidenced the radical scavenging potential of *P. Integerrima* and melatonin. Interestingly, our findings depicted the decreased levels of TBARs in *P. Integerrima* and melatonin treated rats with all three doses of BPA which suggest the role of ROS in BPA generated lipid peroxidation. There is an efficient endogenous antioxidant defense mechanism in the body which neutralizes the oxidative stress (Ahangarpour, Alboghobeish et al. 2018). Since antioxidants are the scavengers of oxidative stress by preventing cellular damage and apoptosis, so antioxidant profiling (SOD, CAT, APX, POD, GSH) was done to evaluate the bridging role of depleted antioxidants in BPA induced apoptosis. *P. Integerrima* efficiently scavenged the ROS in the treatment group (10mg/kg) which suggests its strong antioxidant potential. The reduction in SOD activity at all three doses of BPA depicted the oxidative damage, as SOD is the first line of defense against oxidative stress. Both melatonin and *P. Integerrima* appreciably replenished the depleted SOD level in all the three treatment groups. SOD scavenges superoxide anion and neutralizes it into O<sub>2</sub> and H<sub>2</sub>O<sub>2</sub>, whereas the transformation of

hydrogen peroxide is catalyzed by other antioxidant enzymes catalase, APX, and peroxidase (POD) that shows the intracellular conversion of H<sub>2</sub>O<sub>2</sub> into nontoxic by-products (Dutta, Ghosh et al. 2014). In the present study, the level of CAT, APX and POD were found to be reduced in all the three doses of BPA. However, *P. Integerrima* and melatonin were potentially able to increase the antioxidant enzymes levels such as CAT, POD, and APX in all the treatment groups which suggests the beneficial role of *P. Integerrima* and melatonin in mitigating the BPA induced free radical stress. Moreover, we found decreased levels of GSH in all three doses of BPA whereas the levels were restored upon treatment with melatonin and *P. Integerrima* which is in consistent with the previous findings that depletion in GSH levels causes neuronal toxicity (Julka, Pal et al. 1992, Jagasia, Grote et al. 2005). The decreased level of antioxidant enzymes (SOD, CAT, POD, GSH and APX) in all the three doses of BPA suggests its potential role in apoptosis. Moreover, our findings suggest the antioxidant boosting potential of *P. Integerrima* and melatonin in neutralizing BPA generated oxidative stress linked apoptosis.

Disruption of cellular architecture and loss of cellular integrity are the key indicators of apoptosis (Jain, Maheshwari et al. 2009, Elmore, Dixon et al. 2016). In current study BPA treatment resulted in loss of cellular architecture along with increased percentage of abnormal cells suggesting the toxic effects of BPA on brain morphology. However, our treatment compound melatonin and *P. Integerrima* showed their ameliorative potential by normalizing the cellular architecture in all treatment group.

In an attempt to evaluate the effect of BPA on ubiquitination and p53 mediated apoptosis we have analysed the expression of Ubc13. Under normal conditions, cellular homeostasis is maintained by keeping the low levels of p53 by the process of ubiquitination. Increased Ubc13 expression inhibits p53 mediated apoptosis (Lee and Gu 2010) by lowering the p53 transcription. We have analysed the transcriptional and translational levels of Ubc13 in the heart tissues. Our results showed reduced expression of Ubc13 in Bisphenol A treated heart tissues at both RNA and protein level suggesting the role of BPA in cardiotoxicity by triggering p53 mediated apoptosis. However, the expression level of Ubc 13 was normalized in *P.integerrima* and melatonin treatment groups.



ROS disturbs several signaling pathways including MAPK/ERK, Akt/P13K, activation of p53 and thus disrupts the mitochondrial membrane potential. In present study transcriptional and translational levels of p53 expression were significantly high in BPA treated group exhibiting apoptosis which is consistent with our above-mentioned findings that lower level of Ubc13 is an indicator of apoptosis. The current study proposes that oxidative stress caused by BPA might be responsible for the dissociation of this Ubc13/p53 complex, which is in accordance with the previous study that generation of oxidative stress is responsible for dissociation of Ubc13/p53 complex by phosphorylation of p53 and activates p53 for its apoptotic function (Topisirovic, Gutierrez et al. 2009). To confirm the BPA induced p53 mediated apoptosis we have also analysed the expression of phosphorylated p53. Our results showed increased expression of phosphorylated p53 in BPA treated toxic model whereas normalized levels of phosphorylated p53 in treatment groups (*P. Integerrima* and melatonin). The previous study of Castrogiovanni et al., (2018) has also reported the role of Ser392 phosphorylated p53 in transcription independent apoptosis (Castrogiovanni, Waterschoot et al. 2018). The decreased ratio of p-p53/p53 upon treatment with *P. Integerrima* and melatonin suggest their ameliorative potential in neutralizing the cardiotoxic and neurotoxic effects of BPA.

Moreover, to investigate the role of BPA induced cardiotoxicity and neurotoxicity in p53 transcription dependent apoptosis we have analysed the expression of mitochondrial apoptosis regulatory factors PUMA and Drp1. In the present study, mitochondrial stress regulatory genes PUMA and Drp-1 mRNA level were significantly upregulated in all the three doses of BPA, which suggests the role of BPA in potential toxicity by inducing mitochondrial apoptosis. The gene expression was further confirmed by western blotting at the translational level, which further depicted the significantly increased levels of apoptotic proteins (p53, PUMA and Drp-1). PUMA acts as a proximal signaling molecule which transduces the death signal to mitochondria by recruiting Drp-1 on outer mitochondrial membrane, thus causing the membrane pore and leading to apoptosis (Yu and Zhang 2008). So, the present study suggests the role of BPA in regulating mitochondrial linked apoptosis *via* PUMA and Drp-1. The melatonin has been proven to be a potent antioxidant in overcoming oxidative stress (Ali, Mushtaq et al. 2019). The present study has also exhibited the therapeutic potential

of *P. Integerrima* and melatonin as both were able to downregulate the expression of mitochondrial stress regulators in the case of all three doses which suggests their strong antioxidant potential. The *P. Integerrima* has appreciably decreased the gene expression of mitochondrial apoptotic regulators in case of all three doses but the effect in the higher dose (10mg/kg) suggests its protective effects. USP7 is a key regulator of p53, which regulates p53 levels in both normal and pathological conditions (Brooks, Li et al. 2007). In current study, the significantly downregulated expression of USP7 was identified in both higher doses of BPA (BPA2 and BPA3) as compared to the control. However, the treatment with *P. integerrima* and melatonin showed upregulated levels of USP7. In addition to USP7, there are several other signaling modulators like ATM and CHK1 which stabilizes the p53 level in the cytosol and triggers the mitochondrial-linked apoptotic pathway (Brooks et al., 2007). Therefore, the elevated level of proapoptotic proteins by BPA administration in both heart and brain tissues arbitrates the mitochondrial-linked apoptosis.

Oxidative stress and apoptosis play a major role in the development of pathophysiological conditions that promote cell death. BPA interrupts the redox state by lipid peroxidation and alter the antioxidant level in living cells (Aydoğan, Korkmaz et al. 2008). Mitochondria is the potential target organelle of BPA toxicity in cardiac cells (Jiang, Xia et al. 2015). BPA has adverse effects on mitochondrial dysfunction and apoptosis which causes various pathological conditions. To categorically explore the pro-apoptotic effect of BPA so we have investigated the expression of cytochrome C, as the release of cytochrome C from the mitochondria is one of the distinctive feature of apoptosis (Guo, Zhao et al. 2017). We have found the increased expression of cytosolic cytochrome C in BPA treated rats. However, the expression of cytochrome C was found to be normalized upon treatment with *P. Integerrima* and melatonin (Fig. 4.103). The data suggest that *P. Integerrima* and melatonin in BPA treated model may contribute to mitigate the underlying mechanism of BPA induced cardiotoxicity and neurotoxicity.

Moreover, several studies explained that the environmental toxicants dysregulate the miRNAs expression by activating the inflammatory and oxidative stress response which may lead to various pathological conditions (De Felice, Manfellotto et al. 2015). Micro RNAs are small oligonucleotides which binds with their complementary

sequence on mRNA resulting in translation repression or degradation of mRNA (Vrijens, Bollati et al. 2015). From last two decades advances in molecular biology and emerging role of miRNA has highlighted the miRNAs as a novel biomarker for several pathophysiological processes. In current study after an excessive literature survey and bioinformatics analysis we sought to investigate the role of miRNA-214-3p and miRNA-15a-5p in BPA induced cardiotoxicity and neurotoxicity. The expression of miRNA-214-3p was found to be decreased in the BPA-administered groups (BPA2 and BPA3) which shows the antiapoptotic role of miRNA-214-3p. To the best of our knowledge, no previous study has reported the role of miRNA-214-3p in cardiotoxicity. miRNA-214 is a bifunctional micro-RNA, it has dual role in heart diseases it blocks apoptosis through PI3K/Protein kinase B signaling pathway (Zhao *et al.*, 2017). In the present study, the expression of miRNA-214-3p was normalized upon treatment with *Pistacia integerrima* even at the higher dose of BPA, suggesting the antiapoptotic potential of *P. integerrima*. To further elucidate the role of miRNA-214-3p in BPA-induced apoptosis we investigated the expression of its target genes, CDIP1, BNIP3 and PKCD. These target genes are the critical player of the mitochondrial-dependent apoptotic pathway. The expression of CDIP1 was significantly elevated in diseased suggesting that elevated expression of CDIP1 initiates apoptosis in Bax dependent manner. Our results are in consistent with the study of Namba *et al.*, (2013) that elevated expression of CDIP1 in response to stress conditions triggers apoptosis by activating mitochondrial proapoptotic machinery (Bax, caspase 8 and Bid) (Namba, Tian et al. 2013). However, the treatment group of *P. integerrima* and melatonin showed downregulated expression of CDIP1 depicting the antiapoptotic potential of both therapeutic agents.

BNIP3 is a BH3-only protein that is localized in mitochondria and involved in mitophagy. In the present study, we have analyzed the transcript level of BNIP3 in both heart and brain tissues. Expression of BNIP3 was significantly increased in both organs in the case of higher doses of BPA. However, the *P. Integerrima* and melatonin treatments were able to downregulate the levels of BNIP3 suggesting the analeptic potential of *P. Integerrima*. Wang *et al.*, 2013 have reported that BNIP3 is a downstream transcriptional target of p53 and is involved in mitochondrial dysfunction leading to cell death (Wang, Gang et al. 2013). These findings indicate that BNIP3 has

a critical role in cell apoptosis. The decreased expression of miRNA-214-3p and increased expression of its target gene BNIP3 suggest its role in the regulation of signaling cascade in BPA-induced oxidative stress-linked apoptosis.

PKC- $\delta$  is a protein kinase C family member which is an important mediator of apoptosis. In the present study, a significantly elevated level of PKC- $\delta$  was observed at the transcription level in both heart and brain tissues of BPA-treated groups (BPA2 and BPA3). However, the *P. integerrima* treatment group showed downregulated levels of PKC- $\delta$ . The increased expression level of PKC- $\delta$  demonstrates the potential involvement of PKC- $\delta$  in apoptosis induced by BPA. This is consistent with the study of Xu *et al.*, 2018 that they observed the role of PKC- $\delta$  in mediating apoptosis. In this study, we have tried to establish a correlation between miR-214-3p and PKC- $\delta$ , that downregulation of miR-214-3p enhances the activation of PKC- $\delta$  and subsequently promotes apoptosis in case of BPA-induced toxicity (Xu, Pan et al. 2019).

As previous studies have demonstrated the role of miR-15a-5p in various diseases including leukemia, hepatocellular carcinoma, lung cancer and suppress the inflammation and metastasis (Cimmino, Calin et al. 2005, Long, Jiang et al. 2016, Ni, Yang et al. 2017). To the best of our knowledge no previous study has reported the role of miRNA in cardiac apoptosis so current study was designed to explore the miRNA-15a-5p regulation in BPA induced apoptosis. In addition, the study also elucidated the therapeutic potential of *P. Integerrima* as an ameliorative agent for BPA induced apoptosis. Previously, it was reported that miRNA-15a-5p negatively regulates cell survival and promotes apoptosis (Chen, Wu et al. 2017). The expression analysis showed significantly upregulated expression of miRNA-15a-5p in disease conditions (BPA2 and BPA3). However, in melatonin treated groups the expression of miRNA-15a-5p was significantly downregulated. This alteration in expression of miRNA suggests its involvement in BPA generated oxidative stress.

In present study we have hypothesized that miR-15a-5p regulate BPA induced apoptosis, the increased expression of miRNA-15a-5p in disease group (BPA2 and BPA3) and normalized expression upon treatment with *P. Integerrima* and melatonin suggests its potential role in BPA induced oxidative stress linked apoptosis. To further confirm our hypothesis, we identified the potential target genes of miRNA-15a-5p by

using different bioinformatics tools such as TargetScan, and MiRbase. Out of multiple targets we selected the two stress responsive factors, mitofusin 2 and B-cell lymphoma 2 (Bcl-2). Mitofusin 2 under oxidative stress regulates the cell fate of cardiomyocytes (Shen, Zheng et al. 2007) and Li, Yin *et al* reported that Mfn2 maintains the myocardial energy homeostasis (Li, Yin et al. 2009). Mitofusin 2 is ubiquitously expressed and has multiple functions and mainly regulate the mitochondrial fusion. Mfn2 and Bcl-2 plays fundamental role in intrinsic mitochondrial mediated apoptosis (Bayeva, Gheorghide et al. 2013). Mfn2 is involved in mitochondrial dynamics, balance between mitochondria fusion and fission is dependent upon the Mfn2 and Drp1 respectively. In current study, the expression of Mfn2 was significantly downregulated at both transcriptional and translational level in disease groups (BPA2 and BPA3). However, the expression was found to be normalized upon treatment with melatonin and *P. Integerrima*. Moreover, the target gene Bcl-2 was also downregulated in both higher doses of BPA which reflects that the BPA has a potential to induce cardiac apoptosis by modulating the expression of antiapoptotic factors. The current study reveals that oxidative stress has elevated the levels of miR-15a-5p in BPA administered groups which leads to the mitochondrial linked apoptosis. In present study melatonin and *P. Integerrima* were used as antioxidant agent which significantly retrieved the BPA mediated oxidative stress and enhanced the expression of antiapoptotic Bcl-2 and Mfn2 genes in treatment groups. As reported previously, melatonin prevent the apoptosis by decreasing the mitochondrial transition pore permeability which ultimately inhibits the release of proapoptotic factor, cytochrome c and maintains the mitochondrial membrane potential (Andrabi, Sayeed et al. 2004). The expression level of miRNA-15a-5p was significantly decreased in treatment groups (melatonin and *P. Integerrima*) which ultimately leads to increase stability of Bcl-2 and Mfn2 mRNA. The current study suggests that melatonin and *P. integerrima* maintain the expression of Mfn2 and Bcl-2 at mRNA level by downregulating the level of miR-15a-5p. Interestingly, the expression of miR-15a-5p was significantly reduced in *P. Integerrima* treated group as compared to the disease group even at the higher dose of BPA, suggesting the more effective response of *P. Integerrima* in mitigating the toxic effects of BPA. The mRNA expression data was further strengthened by western blot analysis. Protein expression of miRNA-15a-5p target genes, Mfn2 and Bcl-2 was significantly downregulated in BPA administered group (BPA2 and BPA3). In treatment groups, the expression was

upregulated as compared to disease group (BPA2, BPA3). Previous studies have shown that under cellular stress when Mfn2 is downregulated, Drp1 leads to increase the mitochondrial fission (Estaquier and Arnoult 2007). During mitochondrial fission Drp1 assist the release of cytochrome c and cause the fragmentation of mitochondria, which ultimately induces the apoptosis in cells (Estaquier and Arnoult 2007). Decreased Mfn2 enhances the mitochondrial fission and ROS production that promotes apoptosis in cardiac cells (Tang, Tao et al. 2017). Bcl-2 is a regulator of apoptosis, it plays a central role in apoptosis by inhibiting the pro-apoptotic member of Bcl-2 family. Under stress conditions multiple factors regulate protein expression. During cellular stress c-Jun N-terminal kinase is activated which phosphorylates Bcl-2 and inhibits its functional activities. To confirm the phosphorylation status of Bcl2 western blotting was performed. The increased expression of P-Bcl2 in disease group (BPA2 and BPA3) establish a link between BPA induced oxidative stress and mitochondrial apoptosis. The increased P-Bcl2/Bcl2 and Bax/Bcl2 are the hallmarks of apoptosis, therefore the increased ratio of P-Bcl2/Bcl2 and Bax/Bcl2 in BPA administered group (BPA2 and BPA3) confirms the role of BPA in oxidative stress induced mitochondrial linked apoptosis. However, the treatment with *P. Integerrima* and melatonin were able to normalize the ratio suggesting the antiapoptotic potential of the therapeutic agents.

In this study we proposed that Bcl-2 plays a survival role by inhibiting the BPA induced oxidative stress mediated apoptosis. Previous studies have reported that BH3 only proteins (Bim, PUMA, Noxa, Bad, Bik, Bid, Bmf, Hrk) sense the stress stimuli and promote the apoptosis by neutralizing and engaging the antiapoptotic Bcl2 and indirectly activate the Bax/Bak which ultimately causes cardiac apoptosis (Adams and Cory 2007). In current study the expression of Bax was significantly upregulated in BPA administered groups suggesting its toxic potential. However, the treatment with *P. Integerrima* and melatonin showed the significantly reduced expression. To further confirm the role of role of BPA in apoptosis the Bax/Bcl2 and P-Bcl2/Bcl2 ratios were also analyzed (Fig. 4.108). The upregulated expression of p53 and its associated downstream apoptotic signalling modulators, dysregulated levels of miRNA-15a-5p, miRNA-214-3p and their target genes confirms our hypothesis that oxidative stress generated by BPA is involved in mitochondrial linked apoptosis.

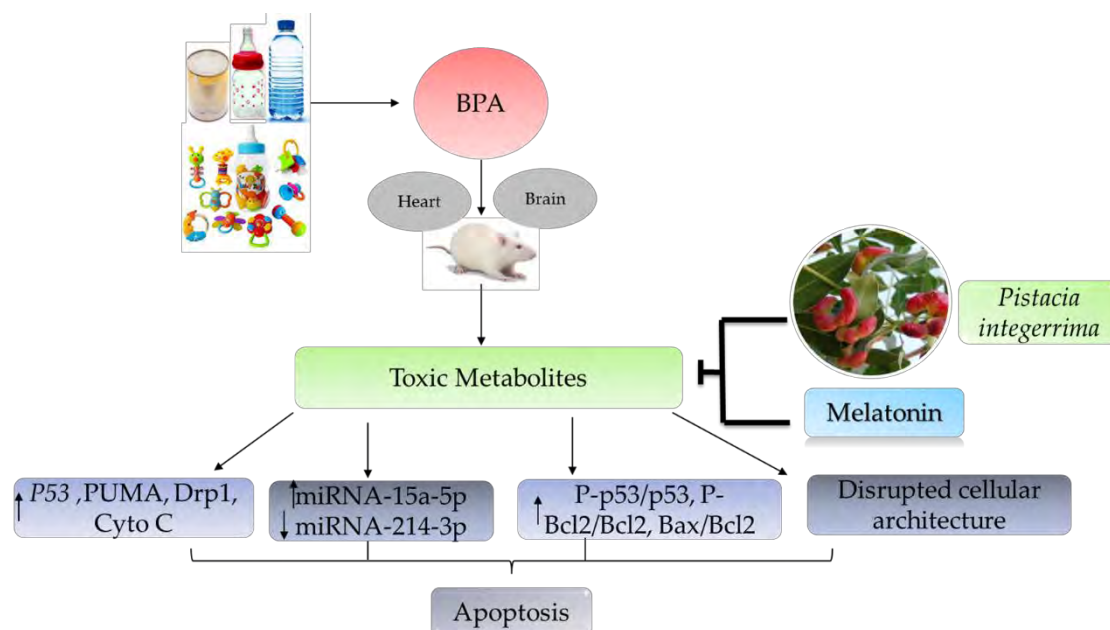


Figure 4.108 Schematic illustration of therapeutic potential of *Pistacia integerrima*

Molecular modelling techniques provide two- and three-dimensional pictures of interactions between Es-37 and L-37 and target proteins. The structural properties of the ligand are crucial in defining the binding modes with the target protein in a docked complex. The binding affinities and interactions between two synthetic terpolymers (L-37 and Es-37) were studied herein with three proteins (Bcl-2, cytochrome c, and p53). The oligomeric structures of the Es-37 and L-37 were considered in molecular docking to minimize computation cost and time. In the case of Bcl-2, L-37 showed hydrogen bonding with the active site of Asp D87, Asp D3, and Lys B5 only, while the Es-37 showed hydrogen bonding interactions with Asn A192, Asn B17, Lys D103, and Arg B67. Also observed were some minor binding interactions, such as pi anion and pi-cation type weak interactions between Bcl-2 and the oligomers of L-37 and Es-37. In the case of the docked complex of cytochrome c and L-37, multiple hydrogen bonds were found with the protein residues of Phe D33, Leu D35, Arg F112, Ser M28, Tyr A260 and Tyr A261, as shown in Table 2. Similarly, the oligomer Es-37 also indicated the presence of four hydrogen bonds with Ser D97, Arg A480 and Ser M28 in cytochrome c, along with minor C-H bonds and weak alkyl interactions. In the case of the protein p53, its docked complex with the oligomer L-37 showed hydrogen bonds with Ser A260, Arg A267, Arg A158, Asp A207, Tyr A205. On the other hand, Es-37 shows some unfavorable positive-positive interactions along with significant hydrogen

bonds with Lys A139, Asn A239, Thr A140, Cys A277, Gln-A136, Met A243, Lys A235 and Arg A196. The docking results conclude that the polymer L-37 showed greater binding affinity with the three receptors, particularly with cytochrome c. MD simulations have also been conducted to refine and validate the docking results at the atomic level. Analysis of trajectories revealed that in case of Bcl-2, both Es-37 and L-37 undergo conformational changes. This conformational instability was caused because of the repositioning of terpolymers.

Oxidative profiling among different experimental groups showed that BPA increases the ROS and TBARs level in heart tissues of the diseased model which cause oxidative damage as described in (Kovacic 2010, Ishtiaq, Bakhtiar et al. 2020). Current results suggest the role of BPA in cardiac toxicity via ROS-stimulated signaling pathways. Moreover, treatment with NAC significantly eliminated the BPA-mediated oxidative stress responses which is in accordance with Baky et al (2009) (Baky, Mohamed et al. 2009, Elsayed, Elkomy et al. 2021). Similar results were obtained in the case of Es-37 and L-37 which suggests that Es-37 and L-37 have strong radical scavenging activity against BPA-generated ROS. The elevated ROS is scavenged by first line of defence antioxidant enzymes SOD and CAT (Sirisha and Manohar 2013, Ishtiaq, Bakhtiar et al. 2020). The current study showed a significant decrease in SOD, CAT, APX, GSH and POD level in case of serum and heart tissues of diseased model as discussed by Kovacic and Morgan in (Kovacic 2010, Morgan, El-Ballal et al. 2014). However, the treatment group with NAC showed significant improvement in oxidative enzymes activity compared to the diseased model. These results are consistent with the results of (Aboubakr, Elmahdy et al. , Baky, Mohamed et al. 2009, Ali, Mushtaq et al. 2019, Elsayed, Elkomy et al. 2021). However, synthetic terpolymers treatment groups (BPA+Es-37 and BPA+L-37) showed better antioxidant enzymes level than NAC proposing Es-37 and L-37 as good antioxidant against ROS generated in response to BPA. In our previous study, both Es-37 and L-37 have also showed antioxidant potential in in-vitro analysis. Results of renal function analysis showed a marked increase in serum creatinine and uric acid level in diseased model as also analyzed by (Sirisha and Manohar 2013) while upon treatment with NAC significant decrease in serum creatinine and uric acid level was observed. We obtained similar results in case of treatment with Es-37 and L-37. The lipid and liver profiling results showed marked



increase in serum cholesterol, triglyceride, ALT and AST level in diseased group respectively (Mahdavinia, Alizadeh et al. 2019). While upon treatment with NAC, these levels were significantly reduced. Results were consistent with the study of (Korou et al., 2010). Es-37 and L-37 showed similar pattern with respect to NAC treatment.

To find out the expression of apoptotic markers at transcription and translational level, qRT-PCR and western blot analysis was performed. Results showed a significant increase in p53 and phosphorylated p53 protein expression in heart tissues of BPA treated model suggesting the role of BPA in apoptosis via oxidative stress mediated p53 expression. Similar upregulation of p53 was observed in studies by (Macip, Igarashi et al. 2003, Nakamura, Matoba et al. 2012), suggesting BPA's role in apoptosis. However, antioxidant treatment of NAC showed significant decrease in p53 and phosphorylated p53 protein expression while treatment with Es-37 showed more marked results with respect to NAC and L-37 treatment groups suggesting the anti-apoptotic role of Es-37 by neutralizing the BPA induced oxidative stress in heart.

The present study showed that under oxidative stress cytochrome c expression was upregulated in heart tissues. These results were consistent with the previous literature (Wu, Yan et al. 2009). Whereas NAC treatment has remarkably reduced the protein expression of cytochrome c in heart. Treatment with Es-37 and Ls 37 showed more pronounced effects in comparison to NAC. mRNA expression of cytochrome c in heart was also analyzed. Results showed marked upregulation of cytochrome c mRNA in diseased (BPA administered) rat model. The results obtained were consistent with the research (Hildeman, Mitchell et al. 2003). Upon treatment with NAC mRNA expression of cytochrome c was markedly reduced as described in (Wang, Li et al. 2018). Moreover, the treatment with ES-37 and L-37 has also shown the downregulated expression of cytochrome c. The Es-37 has shown distinctly downregulated expression of cytochrome c at both transcriptional and translational level suggesting its more therapeutic potential.

Bcl-2 plays a crucial role in maintaining mitochondrial integrity. It is an anti-apoptotic factor, that inhibits apoptosis by binding to apoptotic markers BAK and BAX. Our results showed a significant decrease in mRNA expression of Bcl-2 gene in case of the diseased group. A similar anti-apoptotic role of Bcl-2 was previously documented (El-Shorbagy, Eissa et al. 2019). The current results suggest that Bcl-2 being anti-apoptotic

is attenuated by BPA-induced ROS. mRNA level of Bcl-2 was significantly upregulated in the treatment group of NAC and similar results have been previously documented in (Wang, Li et al. 2018). Es-37 and L-37 showed more marked results with respect to NAC. However, the Es-37 has behaved more potently. Previous studies have reported that pro-survival Bcl-2 can prevent cytochrome c release, hence caspase-9 activation ultimately leads to cell survival. Therefore, based on our results i.e. increased level of cytochrome c and phosphorylated p53 in diseased model we propose the role of BPA in apoptosis (Cory and Adams 2002). Current study has also been proceeded for micro-RNA analysis. As no previous studies have reported the role of miRNA-15a-5p in toxicity. In this study we delineated the interplay of Bcl-2 and miRNA-15a-5p, to elucidate how BPA is involved in toxicity at the molecular level. A significant increase in miRNA-15a-5p was observed in the diseased group. Overexpression of miRNA-15a-5p in diseased rat model confirms its role in BPA-generated oxidative stress-induced cardiac toxicity ultimately leading to apoptosis. Its expression level was markedly reduced in the treatment group of NAC and L-37. However, the treatment with Es-37 has shown more cogent effects. In our current study miRNA-15a-5p is nullifying the anti-apoptotic behaviour of Bcl-2, therefore involved in promoting BPA-induced apoptosis. The role of miRNA-15a-5p in BPA-mediated apoptosis is a novel finding of the current study. It negatively regulates Bcl-2 expression and promotes apoptosis (Cimmino, Calin et al. 2005). Results of the histological analysis showed that cell surface area of cardiomyocytes was markedly altered in BPA treated group i.e. blurring of borders, loss of cellular architecture, flatter of cardiomyocytes cell surface as compared to normal which is inconsistent with the previous studies (Sheikh Abdul Kadir, Rasidi et al. 2017). Treatment with NAC has reduced the effects of oxidative stress by decreasing the surface area of cardiomyocytes as compared to BPA treated group (Xu, Chen et al. 2004). However, the treatment with Es-37 and L-37 has shown analeptic effects. The excessive deposition of collagen in the extracellular matrix within the heart is termed as cardiac fibrosis (Cowling, Kupsky et al. 2019). Previous study has reported that BPA exposure can leads to liver fibrosis (Elswefy, Abdallah et al. 2016). The results of the Masson's trichome staining showed the excessive deposition of collagen in the BPA administered heart tissues which confirms cardiac fibrosis. However the treatment with antioxidant

NAC, Es-37 and L-37 showed a marked reduction in the cardiac fibrosis suggesting the therapeutic potential of the synthetic compounds (Fig. 4.109).

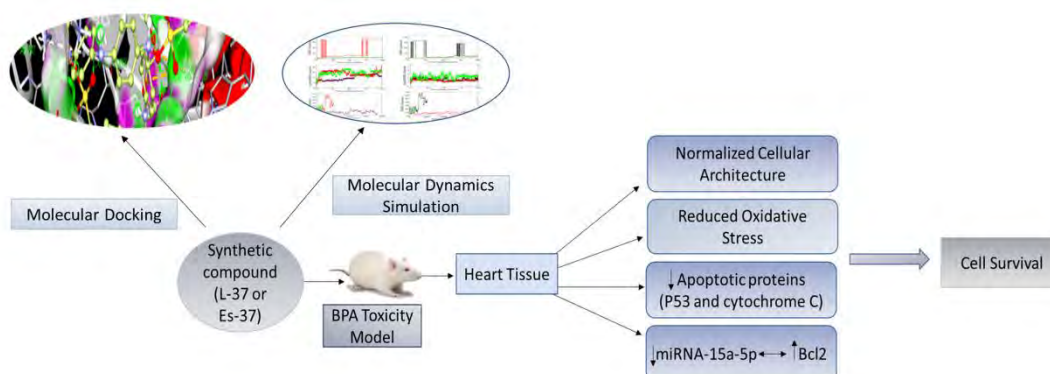


Figure 4.109 Schematic diagram illustrating the therapeutic potential of synthetic compounds

Breast cancer is one of the most common disorders among women and is reported as the second leading cause of cancer-related deaths worldwide (Heer, Harper et al. 2020, Anderson, Ilbawi et al. 2021). The results of the current study have shown the role of BPA in the progression of breast cancer through oxidative stress. In the current study, the data of canned food and plastic bottle users was recorded to find the contribution of bisphenol A (BPA) in breast cancer development. The results of current study showed that the large number (95.2%) of patients were canned food non-users and 4.7% were canned food users while in the case of plastic bottles 71.4% of patients were using plastic bottles for drinking water. The lower percentage of canned food users in our data might be due to the socio-economic status of the patients. Hence, data from plastic bottle users exhibit that BPA can be a potential agent for the development of breast cancer malignancies among women.

Data of breast cancer stages depicted that a large number (66.7%) of patients were at stage III of tumor, which is comparable to the study of (Asif, Sultana et al. 2014) demonstrating that the prevalence of stage III breast cancer is more in Pakistani young women. Receptor status shows ER+ and PR+ status of breast cancer is commonly diagnosed among the Pakistani population and is cognate to the study of (Faheem, Mahmood et al. 2012). Histological data classification of breast cancer patients revealed that a large number of patients had invasive ductal carcinoma (IDC) while 19.0% and

4.7% of patients were diagnosed with ductal carcinoma in situ (DCIS) and invasive lobular carcinoma (ILC), respectively, suggesting that invasive ductal carcinoma is the most common subtype of breast cancer diagnosed in young Pakistani women.

In the current study, BPA level in the serum samples of breast cancer patients increased significantly ( $p \leq 0.01$ ) as compared to the control which confirmed our hypothesis that BPA may be an emerging risk factor of breast cancer progression among the Pakistani population. Different histological subtypes of breast cancer, such as ductal carcinoma in situ (DCIS) and invasive ductal carcinoma (IDC) were evaluated from breast cancer tissue samples.

There was a significant increase of ROS level in malignant breast tissues as compared to control tissues and the level of SOD and CAT anti-oxidant enzymes was significantly low in malignant breast cancer tissues as compared to control tissues. These results confirmed the role of BPA-generated oxidative stress in breast cancer malignancy. This data complies with the previous studies that oxidative stress plays role in the progression of breast cancer (Hassan, Elobeid et al. 2012, Longhitano, Forte et al. 2022).

In the present study, p53 expression was significantly increased in malignant breast tissues at both transcriptional and translational levels. BPA dysregulates the p53 expression in breast cancer through the activation of several signalling pathways such as Akt/Pi3k, mTOR and JAK-STAT pathways that leads towards the survival of cancer cells (Gao, Yang et al. 2015, Murata and Kang 2018, Lloyd, Morse et al. 2019). Moreover, the expression of WNT1 was significantly increased in malignant breast tissues by 35 folds. Prior studies have demonstrated the role of BPA in the regulation of WNT4 gene expression in breast cancer (Ayyanan, Laribi et al. 2011). However, in this current study for the first time, we have analysed the role of BPA in the upregulation of WNT1 gene expression in breast cancer tissues. The upregulation of p53 and WNT1 in the breast cancer samples suggests the possible oncogenic potential of BPA. In addition, ZEB1 gene expression at the mRNA level was increased in malignant breast tissues by 328 folds with a significance value of ( $p \leq 0.01$ ). ZEB1 gene is involved in breast cancer proliferation by epithelial to mesenchymal transition (EMT) mechanism (Baranwal and Alahari 2009, Wu, Zhong et al. 2020, Longhitano, Forte et al. 2022). However, no data was available for the role of BPA in regulation of Breast

cancer via ZEB1. The present study proposes that higher level of BPA and increased expression of p53 mediated ZEB1 and WNT-1 expression may play a role in the pathogenesis of breast cancer (Fig. 4.110).

Keeping in view the findings of the current research, it is concluded that exposure to BPA is the potential source of breast cancer progression among the studied cohort. BPA generates oxidative stress and leads to tumorigenic activities in breast tissues. It is a preliminary study in which we have highlighted the cross-talk between p53, WNT1 and ZEB1 pathways in BPA-generated oxidative stress linked breast cancer, which may open new horizons of research for the development of future therapeutic strategies.

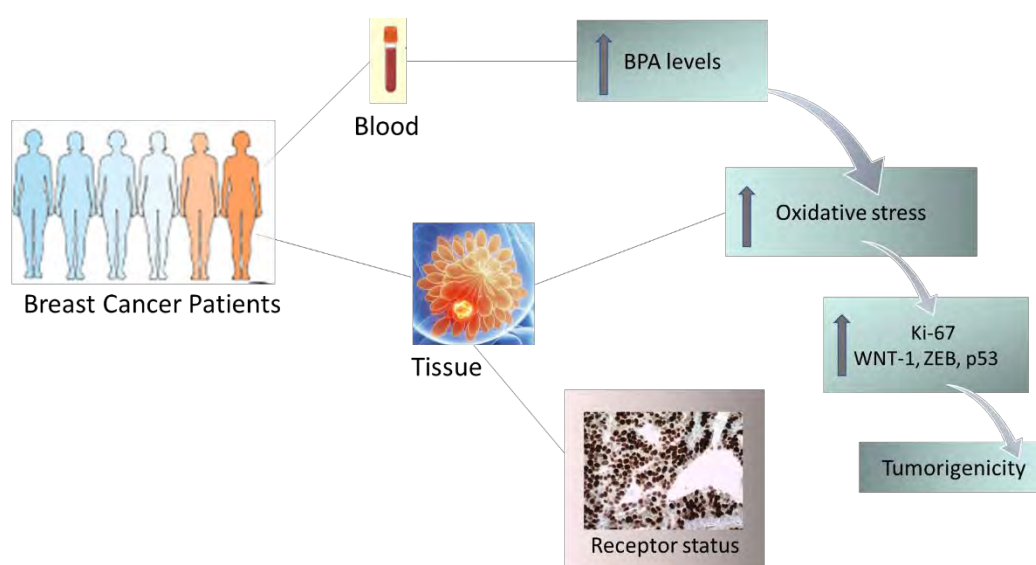


Figure 4.110 Schematic illustration of role of BPA in breast cancer

### Conclusion and Future Perspective

The current study proposed that oxidative stress caused by BPA which is an environmental toxicant might be responsible for the upregulation of p53 and its downstream signaling modulators of apoptosis such as PUMA and Drp-1. Moreover, in current study we sought to investigate the expression of p-p53 to further confirm the p53 mediated apoptosis as the phosphorylation at Ser392 transduces the mitochondrial linked apoptosis. We found the increased expression of p-p53 in all three doses of BPA whereas the treatment with melatonin has shown the profoundly reduced expression of p-p53. The findings of the present study could present new insights into molecular mechanisms by which BPA exerts its neurotoxic effects as well as its target



---

**Publications**

- **Ishtiaq, A.**, Ali, T., Bakhtiar, A., Bibi, R., Bibi, K., Mushtaq, I., ... & Murtaza, I. (2021). Melatonin abated Bisphenol A-induced neurotoxicity via p53/PUMA/Drp-1 signaling. *Environmental Science and Pollution Research*, 28, 17789-17801. <https://doi.org/10.1007/s11356-020-12129-5>.
- **Ishtiaq, A.**, Bakhtiar, A., Silas, E., Saeed, J., Ajmal, S., Mushtaq, I., ... & Murtaza, I. (2020). Pistacia integerrima alleviated Bisphenol A induced toxicity through Ubc13/p53 signalling. *Molecular Biology Reports*, 47, 6545-6559. <https://doi.org/10.1007/s11033-020-05706-x>.
- **Ishtiaq, A.**, Nasrullah, M. A., Khan, J. S., Malik, S., Tareen, U., Anees, M., ... & Murtaza, I. (2023). A cohort study investigating the role of Bisphenol A in the molecular pathogenesis of breast cancer. *Journal of Cancer Research and Clinical Oncology*. <https://doi.org/1-11.10.1007/s00432-023-05247-3>.
- Shaheen, S., Liaqat, F., Qamar, S., Murtaza, I., Rasheed, A., **Ishtiaq, A.**, & Akhter, Z. (2023). Single crystal structure of nitro terminated Azo Schiff base: DNA binding, antioxidant, enzyme inhibitory and photo-isomerization investigation. *Journal of Molecular Structure*, 1284, 135376.
- Jan, M. I., Khan, R. A., Ahmad, I., Khan, N., Urooj, K., Shah, A. U. H. A., Ali T., **Ishtiaq, A.**, ... & Murthy, H. C. (2022). C-reactive protein and high-sensitive cardiac troponins correlate with oxidative stress in valvular heart disease patients. *Oxidative Medicine and Cellular Longevity*, 2022.
- Khan, M., Patujo, J., Mushtaq, I., **Ishtiaq, A.**, Tahir, M. N., Bibi, S., ... & Murtaza, I. (2022). Anti-diabetic potential, crystal structure, molecular docking, DFT, and optical-electrochemical studies of new dimethyl and diethyl carbamoyl-N, N'-disubstituted based thioureas. *Journal of Molecular Structure*, 1253, 132207.
- Mushtaq, I., Bashir, Z., Sarwar, M., Arshad, M., **Ishtiaq, A.**, Khan, W., ... & Murtaza, I. (2021). N-acetyl cysteine, selenium, and ascorbic acid rescue diabetic cardiac hypertrophy via mitochondrial-associated redox regulators. *Molecules*, 26(23), 7285.

- 
- Ali, T., **Ishtiaq, A.**, Mushtaq, I., Ayaz, N., Jan, M. I., Khan, W., ... & Murtaza, I. (2021). *Mentha longifolia* alleviates exogenous serotonin-induced diabetic hypoglycemia and relieves renal toxicity via ROS regulation. *Plant Foods for Human Nutrition*, 76, 501-506.
  - Mushtaq, I., **Ishtiaq, A.**, Ali, T., Jan, M. I., & Murtaza, I. (2020). An Overview of Non-coding RNAs and Cardiovascular System. *Non-coding RNAs in Cardiovascular Diseases*, 3-45.
  - Jan, M. I., Ali, T., **Ishtiaq, A.**, Mushtaq, I., & Murtaza, I. (2020). Prospective advances in non-coding RNAs investigation. *Non-coding RNAs in Cardiovascular Diseases*, 385-426.
  - Naeem, A., **Ishtiaq, A.**, & Murtaza, I. (2023). miRNAs as a Therapeutic Target for Vascular Dysfunction in Diabetes. *Metabolism-Clinical and Experimental*, 142. (proceedings)
  - Hussain, K., **Ishtiaq, A.**, Mushtaq, I., & Murtaza, I. (2023). Profiling of Targeted miRNAs (8-nt) for the Genes Involved in Type 2 Diabetes Mellitus and Cardiac Hypertrophy. *Molecular Biology*, 1-8.
  - Azhar, I., **Ishtiaq, A.**, & Murtaza, I. (2022). Investigating the Micromnas as Key Regulator in Diabetic Cardiomyopathy. *American Heart Journal*, 254, 239. (proceedings)
  - Karim, S., **Ishtiaq, A.**, & Murtaza, I. (2022). Mirnas as Potential Diagnostic Tool for Diabetes-Linked Myocardial Infarction. *American Heart Journal*, 254, 239-240. (proceedings)
  - **Ishtiaq, A.**, Mushtaq, I., & Murtaza, I. (2022). miRNAs and Endothelin: A potential nexus in the roadmap for diabetes linked cardiac complications therapeutic strategy. *Metabolism-Clinical and Experimental*, 128. (proceedings)
  - Murtaza, I., Mushtaq, I., & **Ishtiaq, A.** (2022). Development of Cardiac specific Neurohormonal based diagnostic marker for Diabetes linked cardiac failure. *Metabolism-Clinical and Experimental*, 128. (proceedings)
  - AKRAM, N., Shahzor, Z., Mushtaq, I., **Ishtiaq, A.**, Hussain, K., & Murtaza, I. (2021). MicroRNAs in molecular technology to address global diseases bench to bedside research. *Avrupa Bilim ve Teknoloji Dergisi*, (28), 1492-1500.
-



- Naeem, T., Ali, T., Mushtaq, I., **Ishtiaq, A.**, & Murtaza, I. (2020). Cross talk of serum elements, cardiac and liver enzymes in patients with HCV chronic hepatitis and hepatocellular carcinoma in Pakistani population. *NUST Journal of Natural Sciences*, 5(1), 16-24.
- Jan, M. I., Khan, R. A., Sultan, A., Ullah, A., **Ishtiaq, A.**, & Murtaza, I. (2019). Analysis of NT-proBNP and uric acid due to left ventricle hypertrophy in the patients of aortic valve disease. *Pakistan Journal of Medical Sciences*, 35(1), 183.
- **Ishtiaq, A.**, Mushtaq, I., Rehman, H., Mushtaq, I., ... & Murtaza, I. Tetra aniline-based polymers alleviate Bisphenol A-induced oxidative stress by regulating p53/Bcl-2 nexus. *Environmental Science and Pollution Research* (Submitted)

## 5. REFERENCES

(2022). "WHO ", from <https://www.who.int/news/item/04-04-2022-billions-of-people-still-breathe-unhealthy-air-new-who-data>.

Aboubakr, M., A. M. Elmahdy, S. Taima, M. A. Emam, A. Farag, M. Alkafafy, A. M. Said and A. Soliman "Protective Effects of N Acetylcysteine and Vitamin E against Acrylamide-induced Neurotoxicity in Rats."

Aboul Ezz, H. S., Y. A. Khadrawy and I. M. Mourad (2015). "The effect of bisphenol A on some oxidative stress parameters and acetylcholinesterase activity in the heart of male albino rats." *Cytotechnology* **67**(1): 145-155.

Acuña-Castroviejo, D., G. Escames, C. Venegas, M. E. Díaz-Casado, E. Lima-Cabello, L. C. López, S. Rosales-Corral, D.-X. Tan and R. J. Reiter (2014). "Extrapineal melatonin: sources, regulation, and potential functions." *Cellular and molecular life sciences* **71**(16): 2997-3025.

Adam-Vizi, V. (2005). "Production of reactive oxygen species in brain mitochondria: contribution by electron transport chain and non-electron transport chain sources." *Antioxidants & redox signaling* **7**(9-10): 1140-1149.

Adams, J. M. and S. Cory (2007). "Bcl-2-regulated apoptosis: mechanism and therapeutic potential." *Current opinion in immunology* **19**(5): 488-496.

Adlam, V. J., J. C. Harrison, C. M. Porteous, A. M. James, R. A. Smith, M. P. Murphy and I. A. Sammut (2005). "Targeting an antioxidant to mitochondria decreases cardiac ischemia-reperfusion injury." *The FASEB Journal* **19**(9): 1088-1095.

Ahangarpour, A., S. Alboghobeish, A. Oroojan and M. Dehghani (2018). "Mice pancreatic islets protection from oxidative stress induced by single-walled carbon nanotubes through naringin." *Human & experimental toxicology* **37**(12): 1268-1281.

Ahmad, N. S., M. Farman, M. H. Najmi, K. B. Mian and A. Hasan (2008). "Pharmacological basis for use of Pistacia integerrima leaves in hyperuricemia and gout." *Journal of ethnopharmacology* **117**(3): 478-482.

Ahmad, N. S., A. Waheed, M. Farman and A. Qayyum (2010). "Analgesic and anti-inflammatory effects of Pistacia integerrima extracts in mice." *Journal of ethnopharmacology* **129**(2): 250-253.

Ali, T., I. Mushtaq, S. Maryam, A. Farhan, K. Saba, M. I. Jan, A. Sultan, M. Anees, B. Duygu and S. Hamera (2019). "Interplay of N acetyl cysteine and melatonin in regulating oxidative stress-induced cardiac hypertrophic factors and microRNAs." *Archives of biochemistry and biophysics* **661**: 56-65.

Ali, T., H. Waheed, F. Shaheen, M. Mahmud, Q. Javed and I. Murtaza (2015). "Increased endogenous serotonin level in diabetic conditions may lead to cardiac valvulopathy via reactive oxygen species regulation." *Biologia* **70**(2): 273-278.

Almeida, S., A. Raposo, M. Almeida-González and C. Carrascosa (2018). "Bisphenol A: Food exposure and impact on human health." *Comprehensive Reviews in Food Science and Food Safety* **17**(6): 1503-1517.

Alonso-Magdalena, P., A. B. Ropero, S. Soriano, M. García-Arévalo, C. Ripoll, E. Fuentes, I. Quesada and Á. Nadal (2012). "Bisphenol-A acts as a potent estrogen via non-classical estrogen triggered pathways." *Molecular and cellular endocrinology* **355**(2): 201-207.

Amin, A. F., O. M. Shaaban and M. A. Bediawy (2008). "N-acetyl cysteine for treatment of recurrent unexplained pregnancy loss." *Reproductive biomedicine online* **17**(5): 722-726.

Andersen, P. L., H. Zhou, L. Pastushok, T. Moraes, S. McKenna, B. Ziola, M. J. Ellison, V. M. Dixit and W. Xiao (2005). "Distinct regulation of Ubc13 functions by the two ubiquitin-conjugating enzyme variants Mms2 and Uev1A." *The Journal of cell biology* **170**(5): 745-755.

- Anderson, B. O., A. M. Ilbawi, E. Fidarova, E. Weiderpass, L. Stevens, M. Abdel-Wahab and B. Mikkelsen (2021). "The Global Breast Cancer Initiative: a strategic collaboration to strengthen health care for non-communicable diseases." *The Lancet Oncology* **22**(5): 578-581.
- Andrabi, S. A., I. Sayeed, D. Siemen, G. Wolf and T. F. Horn (2004). "Direct inhibition of the mitochondrial permeability transition pore: a possible mechanism responsible for anti-apoptotic effects of melatonin." *The FASEB journal* **18**(7): 869-871.
- Anilkumar, U. and J. H. Prehn (2014). "Anti-apoptotic BCL-2 family proteins in acute neural injury." *Frontiers in cellular neuroscience* **8**: 281.
- Anjum, S., S. Rahman, M. Kaur, F. Ahmad, H. Rashid, R. A. Ansari and S. Raisuddin (2011). "Melatonin ameliorates bisphenol A-induced biochemical toxicity in testicular mitochondria of mouse." *Food and chemical Toxicology* **49**(11): 2849-2854.
- Annual Cancer Registry Report.
- Aristiawan, Y., N. Aryana, D. Putri and D. Styarini (2015). "Analytical Method Development for Bisphenol a in Tuna by Using High Performance Liquid Chromatography-UV." *Procedia Chemistry* **16**: 202-208.
- Asano, S., J. D. Tune and G. M. Dick (2010). "Bisphenol A activates Maxi-K (KCa1. 1) channels in coronary smooth muscle." *British journal of pharmacology* **160**(1): 160-170.
- Asif, H. M., S. Sultana, N. Akhtar, J. U. Rehman and R. U. Rehman (2014). "Prevalence, risk factors and disease knowledge of breast cancer in Pakistan." *Asian Pac J Cancer Prev* **15**(11): 4411-4416.
- Atkinson, A. and D. Roy (1995). "In vitro conversion of environmental estrogenic chemical bisphenol A to DNA binding metabolite (s)." *Biochemical and biophysical research communications* **210**(2): 424-433.
- Augustyniak, A., G. Bartosz, A. Čipak, G. Duburs, L. U. Horáková, W. Łuczaj, M. Majekova, A. D. Odysseos, L. Rackova and E. Skrzydlewska (2010). "Natural and synthetic antioxidants: an updated overview." *Free radical research* **44**(10): 1216-1262.
- Aydoğan, M., A. Korkmaz, N. Barlas and D. Kolankaya (2008). "The effect of vitamin C on bisphenol A, nonylphenol and octylphenol induced brain damages of male rats." *Toxicology* **249**(1): 35-39.
- Ayyanan, A., O. Laribi, S. Schuepbach-Mallepell, C. Schrick, M. Gutierrez, T. Tanos, G. Lefebvre, J. Rougemont, Ö. Yalcin-Ozuysal and C. Brisken (2011). "Perinatal exposure to bisphenol a increases adult mammary gland progesterone response and cell number." *Molecular Endocrinology* **25**(11): 1915-1923.
- Bahar, E., H. Kim and H. Yoon (2016). "ER stress-mediated signaling: Action potential and Ca<sup>2+</sup> as key players." *International journal of molecular sciences* **17**(9): 1558.
- Baky, N. A., A. M. Mohamed and L. Faddah (2009). "Protective effect of N-acetyl cysteine and/or pro vitamin A against monosodium glutamate-induced cardiopathy in rats." *Journal of Pharmacology and Toxicology* **4**(5): 178-193.
- Balasubramani, S. G., G. P. Chen, S. Coriani, M. Diedenhofen, M. S. Frank, Y. J. Franzke, F. Furche, R. Grotjahn, M. E. Harding and C. Hättig (2020). "TURBOMOLE: Modular program suite for ab initio quantum-chemical and condensed-matter simulations." *The Journal of chemical physics* **152**(18).
- Baranwal, S. and S. K. Alahari (2009). "Molecular mechanisms controlling E-cadherin expression in breast cancer." *Biochemical and biophysical research communications* **384**(1): 6-11.
- Baskerville, S. and D. P. Bartel (2005). "Microarray profiling of microRNAs reveals frequent coexpression with neighboring miRNAs and host genes." *Rna* **11**(3): 241-247.
- Batista, T. M., P. Alonso-Magdalena, E. Vieira, M. E. C. Amaral, C. R. Cederroth, S. Nef, I. Quesada, E. M. Carneiro and A. Nadal (2012). "Short-term treatment with bisphenol-A leads to metabolic abnormalities in adult male mice." *PloS one* **7**(3): e33814.
- Bats, C., L. Groc and D. Choquet (2007). "The interaction between Stargazin and PSD-95 regulates AMPA receptor surface trafficking." *Neuron* **53**(5): 719-734.

- Bauersachs, J., A. Bouloumié, D. Fraccarollo, K. Hu, R. Busse and G. Ertl (1999). "Endothelial dysfunction in chronic myocardial infarction despite increased vascular endothelial nitric oxide synthase and soluble guanylate cyclase expression: role of enhanced vascular superoxide production." *Circulation* **100**(3): 292-298.
- Bavarsad Shahripour, R., M. R. Harrigan and A. V. Alexandrov (2014). "N-acetylcysteine (NAC) in neurological disorders: mechanisms of action and therapeutic opportunities." *Brain and behavior* **4**(2): 108-122.
- Bayeva, M., M. Gheorghide and H. Ardehali (2013). "Mitochondria as a therapeutic target in heart failure." *Journal of the American College of Cardiology* **61**(6): 599-610.
- Ben-Jonathan, N. (2019). *Endocrine Disrupting Chemicals and Breast Cancer: The Saga of Bisphenol A. Estrogen Receptor and Breast Cancer*, Springer: 343-377.
- Benleulmi-Chaachoua, A., L. Chen, K. Sokolina, V. Wong, I. Jurisica, M. B. Emerit, M. Darmon, A. Espin, I. Stajlar and P. Tafelmeyer (2016). "Protein interactome mining defines melatonin MT 1 receptors as integral component of presynaptic protein complexes of neurons." *Journal of pineal research* **60**(1): 95-108.
- Berezikov, E. and R. H. Plasterk (2005). "Camels and zebrafish, viruses and cancer: a microRNA update." *Human molecular genetics* **14**(suppl\_2): R183-R190.
- Bhaskaran, M. and M. Mohan (2014). "MicroRNAs: history, biogenesis, and their evolving role in animal development and disease." *Veterinary pathology* **51**(4): 759-774.
- Bibi, Y., M. Zia and A. Qayyum (2015). "An overview of Pistacia integerrima a medicinal plant species: Ethnobotany, biological activities and phytochemistry." *Pakistan journal of pharmaceutical sciences* **28**(3): 1009-1013.
- Bild, A. H., G. Yao, J. T. Chang, Q. Wang, A. Potti, D. Chasse, M.-B. Joshi, D. Harpole, J. M. Lancaster and A. Berchuck (2006). "Oncogenic pathway signatures in human cancers as a guide to targeted therapies." *Nature* **439**(7074): 353-357.
- Bilen, J., N. Liu and N. M. Bonini (2006). "A new role for microRNA pathways: modulation of degeneration induced by pathogenic human disease proteins." *Cell Cycle* **5**(24): 2835-2838.
- Bindhumol, V., K. Chitra and P. Mathur (2003). "Bisphenol A induces reactive oxygen species generation in the liver of male rats." *Toxicology* **188**(2-3): 117-124.
- Birnbaum, L. S. and S. E. Fenton (2003). "Cancer and developmental exposure to endocrine disruptors." *Environmental health perspectives* **111**(4): 389-394.
- Biswas, R. K. and A. Kapoor (2005). "Age at menarche and menopause among Saharia women—A primitive tribe of Madhya Pradesh." *The Anthropologist* **7**(2): 1-5.
- Boland, M. L., A. H. Chourasia and K. F. Macleod (2013). "Mitochondrial dysfunction in cancer." *Frontiers in oncology* **3**: 292.
- Bolli, A., P. Bulzomi, P. Galluzzo, F. Acconcia and M. Marino (2010). "Bisphenol A impairs estradiol-induced protective effects against DLD-1 colon cancer cell growth." *IUBMB life* **62**(9): 684-687.
- Bostjancic, E. and D. Glavac (2008). "Importance of microRNAs in skin morphogenesis and diseases." *Acta dermatovenerologica Alpina, Pannonica, et Adriatica* **17**(3): 95-102.
- Bouskine, A., M. Nebout, F. Brücker-Davis, M. Benahmed and P. Fenichel (2009). "Low doses of bisphenol A promote human seminoma cell proliferation by activating PKA and PKG via a membrane G-protein-coupled estrogen receptor." *Environmental health perspectives* **117**(7): 1053-1058.
- Bray, F., J. Ferlay, I. Soerjomataram, R. L. Siegel, L. A. Torre and A. Jemal (2018). "Global cancer statistics 2018: GLOBOCAN estimates of incidence and mortality worldwide for 36 cancers in 185 countries." *CA: a cancer journal for clinicians* **68**(6): 394-424.
- Brooks, C., M. Li, M. Hu, Y. Shi and W. Gu (2007). "The p53-Mdm2-HAUSP complex is involved in p53 stabilization by HAUSP." *Oncogene* **26**(51): 7262-7266.

- Brooks, C., Q. Wei, L. Feng, G. Dong, Y. Tao, L. Mei, Z.-J. Xie and Z. Dong (2007). "Bak regulates mitochondrial morphology and pathology during apoptosis by interacting with mitofusins." *Proceedings of the National Academy of Sciences* **104**(28): 11649-11654.
- Brooks, C. L. and W. Gu (2006). "p53 ubiquitination: Mdm2 and beyond." *Molecular cell* **21**(3): 307-315.
- Brooks, C. L. and W. Gu (2011). "p53 regulation by ubiquitin." *FEBS letters* **585**(18): 2803-2809.
- Brown, L., P. P. Ongusaha, H. G. Kim, S. Nuti, A. Mandinova, J. W. Lee, R. Khosravi-Far, S. A. Aaronson and S. W. Lee (2007). "CDIP, a novel pro-apoptotic gene, regulates TNF $\alpha$ -mediated apoptosis in a p53-dependent manner." *The EMBO journal* **26**(14): 3410-3422.
- Bruno, K. A., J. E. Mathews, A. L. Yang, J. A. Frisancho, A. J. Scott, H. D. Greyner, F. A. Molina, M. S. Greenaway, G. M. Cooper and A. Bucek (2019). "BPA alters estrogen receptor expression in the heart after viral infection activating cardiac mast cells and T cells leading to perimyocarditis and fibrosis." *Frontiers in endocrinology* **10**: 598.
- Burton, T. R. and S. B. Gibson (2009). "The role of Bcl-2 family member BNIP3 in cell death and disease: NIPping at the heels of cell death." *Cell Death & Differentiation* **16**(4): 515-523.
- Cao, H., W. Yu, X. Li, J. Wang, S. Gao, N. E. Holton, S. Eliason, T. Sharp and B. A. Amendt (2016). "A new plasmid-based microRNA inhibitor system that inhibits microRNA families in transgenic mice and cells: a potential new therapeutic reagent." *Gene therapy* **23**(6): 527-542.
- Cao, L.-Y., X.-M. Ren, C.-H. Li, J. Zhang, W.-P. Qin, Y. Yang, B. Wan and L.-H. Guo (2017). "Bisphenol AF and bisphenol B exert higher estrogenic effects than bisphenol A via G protein-coupled estrogen receptor pathway." *Environmental science & technology* **51**(19): 11423-11430.
- Cardiff, R. D., C. H. Miller and R. J. Munn (2014). "Manual hematoxylin and eosin staining of mouse tissue sections." *Cold Spring Harbor Protocols* **2014**(6): pdb. prot073411.
- Care, A., D. Catalucci, F. Felicetti, D. Bonci, A. Addario, P. Gallo, M.-L. Bang, P. Segnalini, Y. Gu and N. D. Dalton (2007). "MicroRNA-133 controls cardiac hypertrophy." *Nature medicine* **13**(5): 613-618.
- Case, D., D. Cerutti, T. Cheateham, T. Darden, R. Duke, T. Giese, H. Gohlke, A. Goetz, D. Greene and N. Homeyer (2016). "others, AMBER16 Package, Univ." *California, San Fr.*
- Castilla-Llorente, V., L. Spraggon, M. Okamura, S. Naseeruddin, M. Adamow, S. Qamar and J. Liu (2012). "Mammalian GW220/TNGW1 is essential for the formation of GW/P bodies containing miRISC." *J Cell Biol* **198**(4): 529-544.
- Castrogiovanni, C., B. Waterschoot, O. De Backer and P. Dumont (2018). "Serine 392 phosphorylation modulates p53 mitochondrial translocation and transcription-independent apoptosis." *Cell Death & Differentiation* **25**(1): 190-203.
- Cervený, K. L., Y. Tamura, Z. Zhang, R. E. Jensen and H. Sesaki (2007). "Regulation of mitochondrial fusion and division." *Trends in cell biology* **17**(11): 563-569.
- Chan, D. C. (2006). "Dissecting mitochondrial fusion." *Developmental cell* **11**(5): 592-594.
- Chan, D. C. (2006). "Mitochondria: dynamic organelles in disease, aging, and development." *Cell* **125**(7): 1241-1252.
- Chandira, R. M., M. Prabakaran, B. Jaykar, B. Venkateswarlu and P. Palanisamy (2019). "BRCA mutation: A review of breast cancer." *Journal of Drug Delivery and Therapeutics* **9**(4): 750-758.
- Chaurasia, V., S. Pal and B. Tiwari (2018). "Prediction of benign and malignant breast cancer using data mining techniques." *Journal of Algorithms & Computational Technology* **12**(2): 119-126.
- Chen, D., D. Wu, K. Shao, B. Ye, J. Huang and Y. Gao (2017). "MiR-15a-5p negatively regulates cell survival and metastasis by targeting CXCL10 in chronic myeloid leukemia." *American journal of translational research* **9**(9): 4308.
- Chen, J.-F., E. M. Mandel, J. M. Thomson, Q. Wu, T. E. Callis, S. M. Hammond, F. L. Conlon and D.-Z. Wang (2006). "The role of microRNA-1 and microRNA-133 in skeletal muscle proliferation and differentiation." *Nature genetics* **38**(2): 228-233.

- Chen, J., X. Qin, S. Zhong, S. Chen, W. Su and Y. Liu (2018). "Characterization of Curcumin/Cyclodextrin Polymer Inclusion Complex and Investigation on Its Antioxidant and Antiproliferative Activities." Molecules **23**(5): 1179.
- Chen, Y. and G. W. Dorn (2013). "PINK1-phosphorylated mitofusin 2 is a Parkin receptor for culling damaged mitochondria." Science **340**(6131): 471-475.
- Chen, Z., C. C. Chua, Y.-S. Ho, R. C. Hamdy and B. H. Chua (2001). "Overexpression of Bcl-2 attenuates apoptosis and protects against myocardial I/R injury in transgenic mice." American Journal of Physiology-Heart and Circulatory Physiology **280**(5): H2313-H2320.
- Cheng, A. M., M. W. Byrom, J. Shelton and L. P. Ford (2005). "Antisense inhibition of human miRNAs and indications for an involvement of miRNA in cell growth and apoptosis." Nucleic acids research **33**(4): 1290-1297.
- Chipuk, J. E. and D. R. Green (2009). "PUMA cooperates with direct activator proteins to promote mitochondrial outer membrane permeabilization and apoptosis." Cell cycle **8**(17): 2692-2696.
- Choi, E., M.-J. Cha and K.-C. Hwang (2014). "Roles of calcium regulating microRNAs in cardiac ischemia-reperfusion injury." Cells **3**(3): 899-913.
- Chu, P.-Y., F.-W. Hu, C.-C. Yu, L.-L. Tsai, C.-H. Yu, B.-C. Wu, Y.-W. Chen, P.-I. Huang and W.-L. Lo (2013). "Epithelial–mesenchymal transition transcription factor ZEB1/ZEB2 co-expression predicts poor prognosis and maintains tumor-initiating properties in head and neck cancer." Oral oncology **49**(1): 34-41.
- Cimmino, A., G. A. Calin, M. Fabbri, M. V. Iorio, M. Ferracin, M. Shimizu, S. E. Wojcik, R. I. Aqeilan, S. Zupo and M. Dono (2005). "miR-15 and miR-16 induce apoptosis by targeting BCL2." Proceedings of the National Academy of Sciences **102**(39): 13944-13949.
- ČIPAK GAŠPAROVIĆ, A., T. Lovaković and N. Žarković (2010). "Oxidative stress and antioxidants: biological response modifiers of oxidative homeostasis in cancer." Periodicum biologorum **112**(4): 433-439.
- Claus, S. P., H. Guillou and S. Ellero-Simatos (2017). "The gut microbiota: a major player in the toxicity of environmental pollutants?" NPJ Biofilms and Microbiomes **3**: 17001.
- Constantinou, S. J., R. M. Pace, A. Stangl, L. M. Nagy and T. A. Williams (2016). "Wnt repertoire and developmental expression patterns in the crustacean *Thamnocephalus platyurus*." Evolution & development **18**(5-6): 324-341.
- Corsten, M., R. Dennert, S. Jochems, T. Kuznetsova, D. Wagner, J. Staessen, L. Hofstra, S. Heymans and B. Schroen (2010). "Circulating microRNA-208b and miR-499 reflect myocardial damage in cardiovascular disease." EUROPEAN HEART JOURNAL **31**: 75-75.
- Cory, S. and J. M. Adams (2002). "The Bcl2 family: regulators of the cellular life-or-death switch." Nature Reviews Cancer **2**(9): 647-656.
- Cowling, R. T., D. Kupsky, A. M. Kahn, L. B. Daniels and B. H. Greenberg (2019). "Mechanisms of cardiac collagen deposition in experimental models and human disease." Translational Research **209**: 138-155.
- Dakshayani, K., P. Subramanian, T. Manivasagam, M. M. Essa and S. Manoharan (2005). "Melatonin modulates the oxidant-antioxidant imbalance during N-nitrosodiethylamine induced hepatocarcinogenesis in rats." Journal of pharmacy & pharmaceutical sciences: a publication of the Canadian Society for Pharmaceutical Sciences, Societe canadienne des sciences pharmaceutiques **8**(2): 316-321.
- De Felice, B., F. Manfellotto, A. Palumbo, J. Troisi, F. Zullo, C. Di Carlo, A. D. S. Sardo, N. De Stefano, U. Ferbo and M. Guida (2015). "Genome–wide microRNA expression profiling in placentas from pregnant women exposed to BPA." BMC medical genomics **8**(1): 56.
- De Pedro, N., R. M. Martínez-Álvarez and M. J. Delgado (2008). "Melatonin reduces body weight in goldfish (*Carassius auratus*): effects on metabolic resources and some feeding regulators." Journal of pineal research **45**(1): 32-39.

- Denli, A. M., B. B. Tops, R. H. Plasterk, R. F. Ketting and G. J. Hannon (2004). "Processing of primary microRNAs by the Microprocessor complex." *Nature* **432**(7014): 231.
- Deutschmann, A., M. Hans, R. Meyer, H. Häberlein and D. Swandulla (2013). "Bisphenol A inhibits voltage-activated Ca<sup>2+</sup> channels in vitro: mechanisms and structural requirements." *Molecular pharmacology* **83**(2): 501-511.
- Diamanti-Kandarakis, E., J.-P. Bourguignon, L. C. Giudice, R. Hauser, G. S. Prins, A. M. Soto, R. T. Zoeller and A. C. Gore (2009). "Endocrine-disrupting chemicals: an Endocrine Society scientific statement." *Endocrine reviews* **30**(4): 293-342.
- Diepeveen, S., J. Wetzels, H. Bilo, L. Van Tits and A. Stalenhoef (2008). "Cholesterol in end-stage renal disease: the good, the bad or the ugly." *Neth J Med* **66**(2): 53-61.
- Din, S., M. Mason, M. Völkers, B. Johnson, C. T. Cottage, Z. Wang, A. Y. Joyo, P. Quijada, P. Erhardt and N. S. Magnuson (2013). "Pim-1 preserves mitochondrial morphology by inhibiting dynamin-related protein 1 translocation." *Proceedings of the National Academy of Sciences* **110**(15): 5969-5974.
- Dodds, E. C. and W. Lawson (1936). "Synthetic strogenic agents without the phenanthrene nucleus." *Nature* **137**(3476): 996.
- Draganov, D. I., D. A. Markham, D. Beyer, J. M. Waechter Jr, S. S. Dimond, R. A. Budinsky, R. N. Shiotsuka, S. A. Snyder, K. D. Ehman and S. G. Hentges (2015). "Extensive metabolism and route-dependent pharmacokinetics of bisphenol A (BPA) in neonatal mice following oral or subcutaneous administration." *Toxicology* **333**: 168-178.
- Du, Y., J. Li, T. Xu, D.-D. Zhou, L. Zhang and X. Wang (2017). "MicroRNA-145 induces apoptosis of glioma cells by targeting BNIP3 and Notch signaling." *Oncotarget* **8**(37): 61510.
- Dubois-Deruy, E., V. Peugnet, A. Turkieh and F. Pinet (2020). "Oxidative stress in cardiovascular diseases." *Antioxidants* **9**(9): 864.
- Dutta, M., D. Ghosh, A. K. Ghosh, G. Bose, A. Chattopadhyay, S. Rudra, M. Dey, A. Bandyopadhyay, S. K. Pattari and S. Mallick (2014). "High fat diet aggravates arsenic induced oxidative stress in rat heart and liver." *Food and Chemical Toxicology* **66**: 262-277.
- Eger, A., K. Aigner, S. Sonderegger, B. Dampier, S. Oehler, M. Schreiber, G. Berx, A. Cano, H. Beug and R. Foisner (2005). "DeltaEF1 is a transcriptional repressor of E-cadherin and regulates epithelial plasticity in breast cancer cells." *Oncogene* **24**(14): 2375.
- Eggemann, H., A. Ignatov, B. J. Smith, U. Altmann, G. von Minckwitz, F. W. Röhl, M. Jahn and S.-D. Costa (2013). "Adjuvant therapy with tamoxifen compared to aromatase inhibitors for 257 male breast cancer patients." *Breast cancer research and treatment* **137**: 465-470.
- Eisenberg, I., M. S. Alexander and L. M. Kunkel (2009). "miRNAs in normal and diseased skeletal muscle." *Journal of cellular and molecular medicine* **13**(1): 2-11.
- Eisenberg, I., A. Eran, I. Nishino, M. Moggio, C. Lamperti, A. A. Amato, H. G. Lidov, P. B. Kang, K. N. North and S. Mitrani-Rosenbaum (2007). "Distinctive patterns of microRNA expression in primary muscular disorders." *Proceedings of the National Academy of Sciences* **104**(43): 17016-17021.
- El-Beshbishy, H. A., H. A. Aly and M. El-Shafey (2013). "Lipoic acid mitigates bisphenol A-induced testicular mitochondrial toxicity in rats." *Toxicology and industrial health* **29**(10): 875-887.
- El-Shorbagy, H. M., S. M. Eissa, S. Sabet and A. A. El-Ghor (2019). "Apoptosis and oxidative stress as relevant mechanisms of antitumor activity and genotoxicity of ZnO-NPs alone and in combination with N-acetyl cysteine in tumor-bearing mice." *International Journal of Nanomedicine* **14**: 3911.
- Elgindy, E. A., A. M. El-Huseiny, M. I. Mostafa, A. M. Gaballah and T. A. Ahmed (2010). "N-acetyl cysteine: could it be an effective adjuvant therapy in ICSI cycles? A preliminary study." *Reproductive biomedicine online* **20**(6): 789-796.
- Ellahi, M. and M. ur Rashid (2017). "The Toxic Effects BPA on Fetuses, Infants, and Children." *Bisphenol A: Exposure and Health Risks*: 143.

- Elmore, S. A., D. Dixon, J. R. Hailey, T. Harada, R. A. Herbert, R. R. Maronpot, T. Nolte, J. E. Rehg, S. Rittinghausen and T. J. Rosol (2016). "Recommendations from the INHAND apoptosis/necrosis working group." *Toxicologic pathology* **44**(2): 173-188.
- Elsayed, A., A. Elkomy, R. Elkammar, G. Youssef, E. Y. Abdelhiee, W. Abdo, S. E. Fadl, A. Soliman and M. Aboubakr (2021). "Synergistic protective effects of lycopene and N-acetylcysteine against cisplatin-induced hepatorenal toxicity in rats." *Scientific Reports* **11**(1): 13979.
- Elswefy, S. E. S., F. R. Abdallah, H. H. Atteia, A. S. Wahba and R. A. Hasan (2016). "Inflammation, oxidative stress and apoptosis cascade implications in bisphenol A-induced liver fibrosis in male rats." *International journal of experimental pathology* **97**(5): 369-379.
- Estaquier, J. and D. Arnoult (2007). "Inhibiting Drp1-mediated mitochondrial fission selectively prevents the release of cytochrome c during apoptosis." *Cell Death & Differentiation* **14**(6): 1086-1094.
- Faheem, M. and K. P. Lone (2017). "Oxidative stress and histopathologic biomarkers of exposure to bisphenol-A in the freshwater fish, *Ctenopharyngodon idella*." *Brazilian Journal of Pharmaceutical Sciences* **53**(3).
- Faheem, M., H. Mahmood, M. Khurram, U. Qasim and J. Irfan (2012). "Estrogen receptor, progesterone receptor, and Her 2 Neu positivity and its association with tumour characteristics and menopausal status in a breast cancer cohort from northern Pakistan." *Ecancermedalscience* **6**.
- Faivre, E. J. and C. A. Lange (2007). "Progesterone receptors upregulate Wnt-1 to induce epidermal growth factor receptor transactivation and c-Src-dependent sustained activation of Erk1/2 mitogen-activated protein kinase in breast cancer cells." *Molecular and cellular biology* **27**(2): 466-480.
- Fayyad, U., G. Piatetsky-Shapiro and P. Smyth (1996). "From data mining to knowledge discovery in databases." *AI magazine* **17**(3): 37-37.
- Feller, S. E., Y. Zhang, R. W. Pastor and B. R. Brooks (1995). "Constant pressure molecular dynamics simulation: the Langevin piston method." *The Journal of chemical physics* **103**(11): 4613-4621.
- Fernandez, S. and J. Russo (2010). "Estrogen and xenoestrogens in breast cancer." *Toxicologic pathology* **38**(1): 110-122.
- Fichtlscherer, S., S. De Rosa, H. Fox, T. Schwietz, A. Fischer, C. Liebetrau, M. Weber, C. W. Hamm, T. Röxe and M. Müller-Ardogan (2010). "Circulating microRNAs in patients with coronary artery disease." *Circulation research* **107**(5): 677-684.
- Finnerty, J. R., W.-X. Wang, S. S. Hébert, B. R. Wilfred, G. Mao and P. T. Nelson (2010). "The miR-15/107 group of microRNA genes: evolutionary biology, cellular functions, and roles in human diseases." *Journal of molecular biology* **402**(3): 491-509.
- Flint, S., T. Markle, S. Thompson and E. Wallace (2012). "Bisphenol A exposure, effects, and policy: a wildlife perspective." *Journal of environmental management* **104**: 19-34.
- Fu, X., J. Xu, R. Zhang and J. Yu (2020). "The association between environmental endocrine disruptors and cardiovascular diseases: A systematic review and meta-analysis." *Environmental research* **187**: 109464.
- Galloway, C. A., H. Lee and Y. Yoon (2012). "Mitochondrial morphology—emerging role in bioenergetics." *Free Radical Biology and Medicine* **53**(12): 2218-2228.
- Gao, H., B.-J. Yang, N. Li, L.-M. Feng, X.-Y. Shi, W.-H. Zhao and S.-J. Liu (2015). "Bisphenol A and hormone-associated cancers: current progress and perspectives." *Medicine* **94**(1).
- Gao, P., X. Zhang and P. Zhang (2017). "miRNA-214 ameliorates neuronal apoptosis in an experimental rat stroke model by targeting Bax." *Int J Clin Exp Med* **10**(4): 6293-6302.
- Gao, X., Q. Liang, Y. Chen and H.-S. Wang (2013). "Molecular mechanisms underlying the rapid arrhythmogenic action of bisphenol A in female rat hearts." *Endocrinology* **154**(12): 4607-4617.



- Gao, X. and H.-S. Wang (2014). "Impact of bisphenol A on the cardiovascular system—Epidemiological and experimental evidence and molecular mechanisms." International journal of environmental research and public health **11**(8): 8399-8413.
- Garrido, M., M. Terron and A. Rodriguez (2013). "Chrononutrition against oxidative stress in aging." Oxidative medicine and cellular longevity **2013**.
- Gassman, N. R. (2017). "Induction of oxidative stress by bisphenol A and its pleiotropic effects." Environmental and molecular mutagenesis **58**(2): 60-71.
- Geens, T., D. Aerts, C. Berthot, J.-P. Bourguignon, L. Goeyens, P. Lecomte, G. Maghuin-Rogister, A.-M. Pironnet, L. Pussemier and M.-L. Scippo (2012). "A review of dietary and non-dietary exposure to bisphenol-A." Food and chemical toxicology **50**(10): 3725-3740.
- Gharibi, S., A. Dilmaghani, P. Sadighara, R. M. N. Fard, A. Erfanmanesh, T. Mohajerfar and T. Farkhondeh (2013). "The effect of bisphenol a on oxidative stress indices and pathological changes in the brain of chicken embryos." World Appl Sci J **26**: 345-351.
- Ginsburg, O., F. Bray, M. P. Coleman, V. Vanderpuye, A. Eniu, S. R. Kotha, M. Sarker, T. T. Huong, C. Allemani and A. Dvaladze (2017). "The global burden of women's cancers: a grand challenge in global health." The Lancet **389**(10071): 847-860.
- Giordano, S. H., D. S. Cohen, A. U. Buzdar, G. Perkins and G. N. Hortobagyi (2004). "Breast carcinoma in men: a population-based study." Cancer: Interdisciplinary International Journal of the American Cancer Society **101**(1): 51-57.
- Gore, A. C., V. A. Chappell, S. E. Fenton, J. A. Flaws, A. Nadal, G. S. Prins, J. Toppari and R. T. Zoeller (2015). "EDC-2: the Endocrine Society's second scientific statement on endocrine-disrupting chemicals." Endocrine reviews **36**(6): E1-E150.
- Guarnotta, V., R. Amodei, F. Frasca, A. Aversa and C. Giordano (2022). "Impact of Chemical Endocrine Disruptors and Hormone Modulators on the Endocrine System." International Journal of Molecular Sciences **23**(10): 5710.
- Guo, J., M.-H. Zhao, K.-T. Shin, Y.-J. Niu, Y.-D. Ahn, N.-H. Kim and X.-S. Cui (2017). "The possible molecular mechanisms of bisphenol A action on porcine early embryonic development." Scientific reports **7**(1): 1-9.
- Gupta, M. K., C. Halley, Z.-H. Duan, J. Lappe, J. Viterna, S. Jana, K. Augoff, M. L. Mohan, N. T. Vasudevan and J. Na (2013). "miRNA-548c: a specific signature in circulating PBMCs from dilated cardiomyopathy patients." Journal of molecular and cellular cardiology **62**: 131-141.
- Hajnóczky, G., G. Csordás, S. Das, C. Garcia-Perez, M. Saotome, S. S. Roy and M. Yi (2006). "Mitochondrial calcium signalling and cell death: approaches for assessing the role of mitochondrial Ca<sup>2+</sup> uptake in apoptosis." Cell calcium **40**(5-6): 553-560.
- Hall, A., N. Burke, R. Dongworth and D. Hausenloy (2014). "Mitochondrial fusion and fission proteins: novel therapeutic targets for combating cardiovascular disease." British journal of pharmacology **171**(8): 1890-1906.
- Hanioka, N., T. Naito and S. Narimatsu (2008). "Human UDP-glucuronosyltransferase isoforms involved in bisphenol A glucuronidation." Chemosphere **74**(1): 33-36.
- Hardeland, R. (2005). "Antioxidative protection by melatonin." Endocrine **27**(2): 119-130.
- Hardeland, R., S. Pandi-Perumal and D. P. Cardinali (2006). "Melatonin." The international journal of biochemistry & cell biology **38**(3): 313-316.
- Hardwick, J. M. and L. Soane (2013). "Multiple functions of BCL-2 family proteins." Cold Spring Harbor perspectives in biology **5**(2): a008722.
- Hashmi, A. A., S. Aijaz, S. M. Khan, R. Mahboob, M. Irfan, N. I. Zafar, M. Nisar, M. Siddiqui, M. M. Edhi and N. Faridi (2018). "Prognostic parameters of luminal A and luminal B intrinsic breast cancer subtypes of Pakistani patients." World journal of surgical oncology **16**: 1-6.
- Hassan, Z. K., M. A. Eloheid, P. Virk, S. A. Omer, M. ElAmin, M. H. Daghestani and E. M. AlOlayan (2012). "Bisphenol A induces hepatotoxicity through oxidative stress in rat model." Oxidative medicine and cellular longevity **2012**.

- Hayashi, I., Y. Morishita, K. Imai, M. Nakamura, K. Nakachi and T. Hayashi (2007). "High-throughput spectrophotometric assay of reactive oxygen species in serum." Mutation Research/Genetic Toxicology and Environmental Mutagenesis **631**(1): 55-61.
- He, B., J. Xiao, A.-J. Ren, Y.-F. Zhang, H. Zhang, M. Chen, B. Xie, X.-G. Gao and Y.-W. Wang (2011). "Role of miR-1 and miR-133a in myocardial ischemic postconditioning." Journal of biomedical science **18**(1): 22.
- He, M., Z. Xiang, L. Xu, Y. Duan, F. Li and J. Chen (2019). "Lipopolysaccharide induces human olfactory ensheathing glial apoptosis by promoting mitochondrial dysfunction and activating the JNK-Bnip3-Bax pathway." Cell Stress and Chaperones **24**(1): 91-104.
- Heer, E., A. Harper, N. Escandor, H. Sung, V. McCormack and M. M. Fidler-Benaoudia (2020). "Global burden and trends in premenopausal and postmenopausal breast cancer: a population-based study." The Lancet Global Health **8**(8): e1027-e1037.
- Heymes, C., J. K. Bendall, P. Ratajczak, A. C. Cave, J.-L. Samuel, G. Hasenfuss and A. M. Shah (2003). "Increased myocardial NADPH oxidase activity in human heart failure." Journal of the American College of Cardiology **41**(12): 2164-2171.
- Hildeman, D. A., T. Mitchell, B. Aronow, S. Wojciechowski, J. Kappler and P. Marrack (2003). "Control of Bcl-2 expression by reactive oxygen species." Proceedings of the National Academy of Sciences **100**(25): 15035-15040.
- Hu, W., Z. Ma, S. Jiang, C. Fan, C. Deng, X. Yan, S. Di, J. Lv, R. J. Reiter and Y. Yang (2016). "Melatonin: the dawning of a treatment for fibrosis?" Journal of pineal research **60**(2): 121-131.
- Huang, E., R. Liu and Y. Chu (2015). "miRNA-15a/16: As tumor suppressors and more." Future oncology **11**(16): 2351-2363.
- Huelsmann, R. D., C. Will and E. Carasek (2021). "Determination of bisphenol A: Old problem, recent creative solutions based on novel materials." Journal of Separation Science **44**(6): 1148-1173.
- Hussain, F., S. M. Shah and H. Sher (2007). "Traditional resource evaluation of some plants of Mastuj, District Chitral, Pakistan." Pakistan Journal of Botany (Pakistan).
- Iacobazzi, D., M. Suleiman, M. Ghorbel, S. George, M. Caputo and R. Tulloh (2016). "Cellular and molecular basis of RV hypertrophy in congenital heart disease." Heart **102**(1): 12-17.
- Ishige, K., M. Tanaka, M. Arakawa, H. Saito and Y. Ito (2005). "Distinct nuclear factor- $\kappa$ B/Rel proteins have opposing modulatory effects in glutamate-induced cell death in HT22 cells." Neurochemistry international **47**(8): 545-555.
- Ishtiaq, A., T. Ali, A. Bakhtiar, R. Bibi, K. Bibi, I. Mushtaq, S. Li, W. Khan, U. Khan, R. A. Anis, M. Anees, A. Sultan and I. Murtaza (2021). "Melatonin abated Bisphenol A-induced neurotoxicity via p53/PUMA/Drp-1 signaling." Environ Sci Pollut Res Int.
- Ishtiaq, A., A. Bakhtiar, E. Silas, J. Saeed, S. Ajmal, I. Mushtaq, T. Ali, H. M. Wahedi, W. Khan, U. Khan, M. Anees, A. Sultan and I. Murtaza (2020). "Pistacia integerrima alleviated Bisphenol A induced toxicity through Ubc13/p53 signalling." Mol Biol Rep.
- Islam, M., H. Ahmad, A. Rashid, A. Razzaq, N. Akhtar and I. Khan (2006). "Weeds and medicinal plants of Shawar valley, district Swat." Pak. J. Weed Sci. Res **12**(1-2): 83-86.
- Iwakuma, T. and G. Lozano (2003). "MDM2, an introduction." Molecular Cancer Research **1**(14): 993-1000.
- Izaguirre, J. A., D. P. Catarello, J. M. Wozniak and R. D. Skeel (2001). "Langevin stabilization of molecular dynamics." The Journal of chemical physics **114**(5): 2090-2098.
- Jabeen, E., N. K. Janjua, S. Ahmed, I. Murtaza, T. Ali and S. Hameed (2017). "Radical scavenging propensity of Cu<sup>2+</sup>, Fe<sup>3+</sup> complexes of flavonoids and in-vivo radical scavenging by Fe<sup>3+</sup>-primuletin." Spectrochimica Acta Part A: Molecular and Biomolecular Spectroscopy **171**: 432-438.
- Jagasia, R., P. Grote, B. Westermann and B. Conradt (2005). "DRP-1-mediated mitochondrial fragmentation during EGL-1-induced cell death in *C. elegans*." Nature **433**(7027): 754-760.

- Jain, A., V. Maheshwari, K. Alam, G. Mehdi and S. Sharma (2009). "Apoptosis in premalignant and malignant squamous cell lesions of the oral cavity: A light microscopic study." Indian Journal of Pathology and Microbiology **52**(2): 164.
- Jalal, N., A. R. Surendranath, J. L. Pathak, S. Yu and C. Y. Chung (2018). "Bisphenol A (BPA) the mighty and the mutagenic." Toxicology reports **5**: 76-84.
- Jamil, S., S. Ahmad and J. Akhtar (2002). "Pistacia integerrima Stewart ex Brandis: a review." Hamdard Medicus (Pakistan).
- Jan, M. I., R. A. Khan, T. Ali, M. Bilal, L. Bo, A. Sajid, A. Malik, N. Urehman, N. Waseem and J. Nawab (2017). "Interplay of mitochondria apoptosis regulatory factors and microRNAs in valvular heart disease." Archives of biochemistry and biophysics **633**: 50-57.
- Jang, M. H., H. J. Kim, E. J. Kim, Y. R. Chung and S. Y. Park (2015). "Expression of epithelial-mesenchymal transition-related markers in triple-negative breast cancer: ZEB1 as a potential biomarker for poor clinical outcome." Human pathology **46**(9): 1267-1274.
- Jeng, P. S., A. Inoue-Yamauchi, J. J. Hsieh and E. H. Cheng (2018). "BH3-dependent and independent activation of BAX and BAK in mitochondrial apoptosis." Current opinion in physiology **3**: 71-81.
- Jiang, Y., W. Xia, J. Yang, Y. Zhu, H. Chang, J. Liu, W. Huo, B. Xu, X. Chen and Y. Li (2015). "BPA-induced DNA hypermethylation of the master mitochondrial gene PGC-1 $\alpha$  contributes to cardiomyopathy in male rats." Toxicology **329**: 21-31.
- Jin, Q., R. Li, N. Hu, T. Xin, P. Zhu, S. Hu, S. Ma, H. Zhu, J. Ren and H. Zhou (2018). "DUSP1 alleviates cardiac ischemia/reperfusion injury by suppressing the Mff-required mitochondrial fission and Bnip3-related mitophagy via the JNK pathways." Redox biology **14**: 576-587.
- Jockers, R., P. Delagrangue, M. L. Dubocovich, R. P. Markus, N. Renault, G. Tosini, E. Cecon and D. P. Zlotos (2016). "Update on melatonin receptors: IUPHAR Review 20." British journal of pharmacology **173**(18): 2702-2725.
- Julka, D., R. Pal and K. Gill (1992). "Neurotoxicity of dichlorvos: effect on antioxidant defense system in the rat central nervous system." Experimental and molecular pathology **56**(2): 144-152.
- Kabuto, H., M. Amakawa and T. Shishibori (2004). "Exposure to bisphenol A during embryonic/fetal life and infancy increases oxidative injury and causes underdevelopment of the brain and testis in mice." Life sciences **74**(24): 2931-2940.
- Kabuto, H., S. Hasuike, N. Minagawa and T. Shishibori (2003). "Effects of bisphenol A on the metabolisms of active oxygen species in mouse tissues." Environmental research **93**(1): 31-35.
- Kalmar, B. and L. Greensmith (2009). "Induction of heat shock proteins for protection against oxidative stress." Advanced drug delivery reviews **61**(4): 310-318.
- Kantheridis, P., B. Wang, R. M. Carew and H. Y. Lan (2011). "Diabetes complications: the microRNA perspective." Diabetes **60**(7): 1832-1837.
- Karbowski, M., K. L. Norris, M. M. Cleland, S.-Y. Jeong and R. J. Youle (2006). "Role of Bax and Bak in mitochondrial morphogenesis." Nature **443**(7112): 658.
- Kashatus, J. A., A. Nascimento, L. J. Myers, A. Sher, F. L. Byrne, K. L. Hoehn, C. M. Counter and D. F. Kashatus (2015). "Erk2 phosphorylation of Drp1 promotes mitochondrial fission and MAPK-driven tumor growth." Molecular cell **57**(3): 537-551.
- Khan, S., S. Beigh, B. P. Chaudhari, S. Sharma, S. Aliul Hasan Abdi, S. Ahmad, F. Ahmad, S. Parvez and S. Raisuddin (2016). "Mitochondrial dysfunction induced by Bisphenol A is a factor of its hepatotoxicity in rats." Environmental toxicology **31**(12): 1922-1934.
- Khuwaja, G. A. and A. Abu-Rezq (2004). "Bimodal breast cancer classification system." Pattern analysis and applications **7**: 235-242.
- Kitchens, C. S., B. A. Konkle and C. M. Kessler (2013). Consultative Hemostasis and Thrombosis: Expert Consult-Online and Print, Elsevier Health Sciences.

- Komander, D., M. J. Clague and S. Urbé (2009). "Breaking the chains: structure and function of the deubiquitinases." Nature reviews Molecular cell biology **10**(8): 550-563.
- Korde, L. A., J. A. Zujewski, L. Kamin, S. Giordano, S. Domchek, W. F. Anderson, J. M. Bartlett, K. Gelmon, Z. Nahleh and J. Bergh (2010). "Multidisciplinary meeting on male breast cancer: summary and research recommendations." Journal of clinical oncology **28**(12): 2114.
- Kovacic, P. (2010). "How safe is bisphenol A? Fundamentals of toxicity: metabolism, electron transfer and oxidative stress." Med Hypotheses **75**(1): 1-4.
- Kovacic, P. (2010). How safe is bisphenol A? Fundamentals of toxicity: metabolism, electron transfer and oxidative stress, Elsevier.
- Kumar, D., S. Sharma, S. Verma, P. Kumar and R. K. Ambasta (2015). "Role of Wnt-p53-Nox signaling pathway in cancer development and progression." British Journal of Medicine and Medical Research **8**(8): 651-676.
- Kundakovic, M. and F. A. Champagne (2011). "Epigenetic perspective on the developmental effects of bisphenol A." Brain, behavior, and immunity **25**(6): 1084-1093.
- Laine, A., I. Topisirovic, D. Zhai, J. C. Reed, K. L. Borden and Z. e. Ronai (2006). "Regulation of p53 localization and activity by Ubc13." Molecular and cellular biology **26**(23): 8901-8913.
- Lam, J. K., M. Y. Chow, Y. Zhang and S. W. Leung (2015). "siRNA versus miRNA as therapeutics for gene silencing." Molecular Therapy-Nucleic Acids **4**: e252.
- Lane, D. P. (1992). "Cancer. p53, guardian of the genome." Nature **358**: 15-16.
- Lang, I. A., T. S. Galloway, A. Scarlett, W. E. Henley, M. Depledge, R. B. Wallace and D. Melzer (2008). "Association of urinary bisphenol A concentration with medical disorders and laboratory abnormalities in adults." Jama **300**(11): 1303-1310.
- Laskowski, R. A. and M. B. Swindells (2011). LigPlot+: multiple ligand–protein interaction diagrams for drug discovery, ACS Publications.
- Lee, H. J., S. Chattopadhyay, E.-Y. Gong, R. S. Ahn and K. Lee (2003). "Antiandrogenic effects of bisphenol A and nonylphenol on the function of androgen receptor." Toxicological Sciences **75**(1): 40-46.
- Lee, J. and W. Gu (2010). "The multiple levels of regulation by p53 ubiquitination." Cell Death & Differentiation **17**(1): 86-92.
- Lee, R. C., R. L. Feinbaum and V. Ambros (1993). "The C. elegans heterochronic gene lin-4 encodes small RNAs with antisense complementarity to lin-14." cell **75**(5): 843-854.
- Lee, S.-J., D.-C. Kim, B.-H. Choi, H. Ha and K.-T. Kim (2006). "Regulation of p53 by activated protein kinase C- $\delta$  during nitric oxide-induced dopaminergic cell death." Journal of Biological Chemistry **281**(4): 2215-2224.
- Lee, S., K. Suk, I. K. Kim, I. S. Jang, J. W. Park, V. J. Johnson, T. K. Kwon, B. J. Choi and S. H. Kim (2008). "Signaling pathways of bisphenol A–induced apoptosis in hippocampal neuronal cells: Role of calcium-induced reactive oxygen species, mitogen-activated protein kinases, and nuclear factor- $\kappa$ B." Journal of neuroscience research **86**(13): 2932-2942.
- Lee, Y., H.-Y. Lee, R. A. Hanna and Å. B. Gustafsson (2011). "Mitochondrial autophagy by Bnip3 involves Drp1-mediated mitochondrial fission and recruitment of Parkin in cardiac myocytes." American journal of physiology-heart and circulatory physiology **301**(5): H1924-H1931.
- Lee, Y. M., M. J. Seong, J. W. Lee, Y. K. Lee, T. M. Kim, S.-Y. Nam, D. J. Kim, Y. W. Yun, T. S. Kim and S. Y. Han (2007). "Estrogen receptor independent neurotoxic mechanism of bisphenol A, an environmental estrogen." Journal of veterinary science **8**(1): 27-38.
- Lemak, A. and N. Balabaev (1994). "On the Berendsen thermostat." Molecular Simulation **13**(3): 177-187.
- Lendeckel, L.-Q. M. R. R. "W Tuschl T 2001 Identification of novel genes coding for small expressed RNAs." Science **294**(853858): 10.1126.
- Lerner, A. B., J. D. Case and R. V. Heinzelman (1959). "Structure of melatonin1." Journal of the American Chemical Society **81**(22): 6084-6085.

- Li, T., X. Liu, L. Jiang, J. Manfredi, S. Zha and W. Gu (2016). "Loss of p53-mediated cell-cycle arrest, senescence and apoptosis promotes genomic instability and premature aging." Oncotarget **7**(11): 11838.
- Li, Y., R. Yin, J. Liu, P. Wang, S. Wu, J. Luo, O. Zhelyabovska and Q. Yang (2009). "Peroxisome proliferator-activated receptor  $\delta$  regulates mitofusin 2 expression in the heart." Journal of molecular and cellular cardiology **46**(6): 876-882.
- Liesa, M., B. Borda-d'Água, G. Medina-Gómez, C. J. Lelliott, J. C. Paz, M. Rojo, M. Palacín, A. Vidal-Puig and A. Zorzano (2008). "Mitochondrial fusion is increased by the nuclear coactivator PGC-1 $\beta$ ." PloS one **3**(10): e3613.
- Liu, J., P. Yu, W. Qian, Y. Li, J. Zhao, F. Huan, J. Wang and H. Xiao (2013). "Perinatal bisphenol A exposure and adult glucose homeostasis: identifying critical windows of exposure." PloS one **8**(5): e64143.
- Liu, X., M. Zhao, J. Wang, B. Yang and Y. Jiang (2008). "Antioxidant activity of methanolic extract of emblica fruit (*Phyllanthus emblica* L.) from six regions in China." Journal of food composition and Analysis **21**(3): 219-228.
- Lloyd, V., M. Morse, B. Purakal, J. Parker, P. Benard, M. Crone, S. Pfiffner, M. Szmyd and S. Dinda (2019). "Hormone-like effects of bisphenol A on p53 and estrogen receptor alpha in breast cancer cells." BioResearch Open Access **8**(1): 169-184.
- Lobo, V., A. Patil, A. Phatak and N. Chandra (2010). "Free radicals, antioxidants and functional foods: Impact on human health." Pharmacognosy reviews **4**(8): 118.
- Long, J., C. Jiang, B. Liu, S. Fang and M. Kuang (2016). "MicroRNA-15a-5p suppresses cancer proliferation and division in human hepatocellular carcinoma by targeting BDNF." Tumor Biology **37**(5): 5821-5828.
- Longhitano, L., S. Forte, L. Orlando, S. Grasso, A. Barbato, N. Vicario, R. Parenti, P. Fontana, A. M. Amorini and G. Lazzarino (2022). "The crosstalk between GPR81/IGFBP6 promotes breast cancer progression by modulating lactate metabolism and oxidative stress." Antioxidants **11**(2): 275.
- Lorenzen, J. M., S. Batkai and T. Thum (2013). "Regulation of cardiac and renal ischemia–reperfusion injury by microRNAs." Free Radical Biology and Medicine **64**: 78-84.
- Losón, O. C., Z. Song, H. Chen and D. C. Chan (2013). "Fis1, Mff, MiD49, and MiD51 mediate Drp1 recruitment in mitochondrial fission." Molecular biology of the cell **24**(5): 659-667.
- Lu, Z., Y. Miao, I. Muhammad, E. Tian, W. Hu, J. Wang, B. Wang, R. Li and J. Li (2017). "Colistin-induced autophagy and apoptosis involves the JNK-Bcl2-Bax signaling pathway and JNK-p53-ROS positive feedback loop in PC-12 cells." Chemico-Biological Interactions **277**: 62-73.
- Lund, E., S. Güttinger, A. Calado, J. E. Dahlberg and U. Kutay (2004). "Nuclear export of microRNA precursors." science **303**(5654): 95-98.
- Luo, G., R. Wei, R. Niu, C. Wang and J. Wang (2013). "Pubertal exposure to Bisphenol A increases anxiety-like behavior and decreases acetylcholinesterase activity of hippocampus in adult male mice." Food and chemical toxicology **60**: 177-180.
- Ma, Z., C. Chen, P. Tang, H. Zhang, J. Yue and Z. Yu (2017). "BNIP3 induces apoptosis and protective autophagy under hypoxia in esophageal squamous cell carcinoma cell lines: BNIP3 regulates cell death." Diseases of the Esophagus **30**(9).
- Macip, S., M. Igarashi, P. Berggren, J. Yu, S. W. Lee and S. A. Aaronson (2003). "Influence of induced reactive oxygen species in p53-mediated cell fate decisions." Molecular and cellular biology **23**(23): 8576-8585.
- MacKay, H. and A. Abizaid (2018). "A plurality of molecular targets: The receptor ecosystem for bisphenol-A (BPA)." Hormones and behavior **101**: 59-67.
- Mahdavinia, M., S. Alizadeh, A. R. Vanani, M. A. Dehghani, M. Shirani, M. Alipour, H. A. Shahmohammadi and S. R. Asl (2019). "Effects of quercetin on bisphenol A-induced mitochondrial toxicity in rat liver." Iranian Journal of Basic Medical Sciences **22**(5): 499.

- Mahmood, S., T. F. Rana and M. Ahmad (2006). "Common determinants of Ca breast-a case control study in Lahore." *Annals of King Edward Medical University* **12**(2).
- Maier, J. A., C. Martinez, K. Kasavajhala, L. Wickstrom, K. E. Hauser and C. Simmerling (2015). "ff14SB: improving the accuracy of protein side chain and backbone parameters from ff99SB." *Journal of chemical theory and computation* **11**(8): 3696-3713.
- Majidinia, M., R. J. Reiter, S. K. Shakouri, I. Mohebbi, M. Rastegar, M. Kaviani, S. G. Darband, R. Jahanban-Esfahlan, S. M. Nabavi and B. Yousefi (2018). "The multiple functions of melatonin in regenerative medicine." *Ageing research reviews* **45**: 33-52.
- Malkin, D., F. P. Li, L. C. Strong, J. F. Fraumeni, C. E. Nelson, D. H. Kim, J. Kassel, M. A. Gryka, F. Z. Bischoff and M. A. Tainsky (1990). "Germ line p53 mutations in a familial syndrome of breast cancer, sarcomas, and other neoplasms." *Science* **250**(4985): 1233-1238.
- Mamoona, M., A. K. Mir, A. Mushtaq, S. Nighat, N. A. Sidra, T. Kanwal, T. Saira, M. Tehmeena, A. Madhia and B. Shazia (2011). "Foliar epidermal anatomy of some ethnobotanically important species of wild edible fruits of northern Pakistan." *Journal of Medicinal Plants Research* **5**(24): 5873-5880.
- Manavitehrani, I., A. Fathi, H. Badr, S. Daly, A. Negahi Shirazi and F. Dehghani (2016). "Biomedical applications of biodegradable polyesters." *Polymers* **8**(1): 20.
- Marchenko, N. D., S. Wolff, S. Erster, K. Becker and U. M. Moll (2007). "Monoubiquitylation promotes mitochondrial p53 translocation." *The EMBO journal* **26**(4): 923-934.
- Mathuria, N. and R. J. Verma (2008). "Ameliorative effect of curcumin on aflatoxin-induced toxicity in serum of mice." *Acta Pol. Pharm* **65**(3): 339-343.
- Matsuzawa, A. and H. Ichijo (2005). "Stress-responsive protein kinases in redox-regulated apoptosis signaling." *Antioxidants & redox signaling* **7**(3-4): 472-481.
- Mattison, D. R., N. Karyakina, M. Goodman and J. S. LaKind (2014). "Pharmaco- and toxicokinetics of selected exogenous and endogenous estrogens: a review of the data and identification of knowledge gaps." *Critical reviews in toxicology* **44**(8): 696-724.
- McCarthy, J. J. and K. A. Esser (2007). "MicroRNA-1 and microRNA-133a expression are decreased during skeletal muscle hypertrophy." *Journal of applied physiology* **102**(1): 306-313.
- Melzer, D., N. J. Osborne, W. E. Henley, R. Cipelli, A. Young, C. Money, P. McCormack, R. Luben, K.-T. Khaw and N. J. Wareham (2012). "Urinary bisphenol A concentration and risk of future coronary artery disease in apparently healthy men and women." *Circulation* **125**(12): 1482-1490.
- Michaela, P., K. Mária, H. Silvia and L. Lúbia (2014). "Bisphenol A differently inhibits Ca V 3.1, Ca V 3.2 and Ca V 3.3 calcium channels." *Naunyn-Schmiedeberg's archives of pharmacology* **387**(2): 153-163.
- Midoro-Horiuti, T. and R. M. Goldblum (2017). "The effects of early low dose exposures to the Environmental Estrogen Bisphenol A on the Development of Childhood Asthma."
- Mieszkowski, M. (2006). "Cancer-A biophysicist's point of view." *Digital Recordings* **4**: 15.
- Ming, L., P. Wang, A. Bank, J. Yu and L. Zhang (2006). "PUMA dissociates Bax and BCL-XL to induce apoptosis in colon cancer cells." *Journal of Biological Chemistry* **281**(23): 16034-16042.
- Misra, M. K., M. Sarwat, P. Bhakuni, R. Tuteja and N. Tuteja (2009). "Oxidative stress and ischemic myocardial syndromes." *Medical Science Monitor* **15**(10): RA209-RA219.
- Modi, G., V. Pillay and Y. E. Choonara (2010). "Advances in the treatment of neurodegenerative disorders employing nanotechnology." *Annals of the New York Academy of Sciences* **1184**(1): 154-172.
- Mohapatra, D., S. Brar, R. Tyagi and R. Surampalli (2010). "Physico-chemical pre-treatment and biotransformation of wastewater and wastewater Sludge—Fate of bisphenol A." *Chemosphere* **78**(8): 923-941.
- Mokhtari, V., P. Afsharian, M. Shahhoseini, S. M. Kalantar and A. Moini (2017). "A review on various uses of N-acetyl cysteine." *Cell Journal (Yakhteh)* **19**(1): 11.
- Moore, M. N. (2019). "Environmental health impacts of natural and man-made chemicals."

- Morgan, A. M., S. S. El-Ballal, B. E. El-Bialy and N. B. El-Borai (2014). "Studies on the potential protective effect of cinnamon against bisphenol A-and octylphenol-induced oxidative stress in male albino rats." *Toxicology reports* **1**: 92-101.
- Mourad, I. M. and Y. A. Khadrawy (2012). "The sensitivity of liver, kidney and testis of rats to oxidative stress induced by different doses of bisphenol A." *Life* **50**: 19.
- Murata, M. and J.-H. Kang (2018). "Bisphenol A (BPA) and cell signaling pathways." *Biotechnology advances* **36**(1): 311-327.
- Nair, S., S. Suresh, A. Kaniyassery, P. Jaya and J. Abraham (2018). "A review on melatonin action as therapeutic agent in cancer." *Frontiers in Biology* **13**(3): 180-189.
- Nakamura, H., S. Matoba, E. Iwai-Kanai, M. Kimata, A. Hoshino, M. Nakaoka, M. Katamura, Y. Okawa, M. Ariyoshi and Y. Mita (2012). "p53 promotes cardiac dysfunction in diabetic mellitus caused by excessive mitochondrial respiration-mediated reactive oxygen species generation and lipid accumulation." *Circulation: heart failure* **5**(1): 106-115.
- Nakao, T., E. Akiyama, H. Kakutani, A. Mizuno, O. Aozasa, Y. Akai and S. Ohta (2015). "Levels of tetrabromobisphenol A, tribromobisphenol A, dibromobisphenol A, monobromobisphenol A, and bisphenol A in Japanese breast milk." *Chemical research in toxicology* **28**(4): 722-728.
- Namba, T., F. Tian, K. Chu, S.-Y. Hwang, K. W. Yoon, S. Byun, M. Hiraki, A. Mandinova and S. W. Lee (2013). "CDIP1-BAP31 complex transduces apoptotic signals from endoplasmic reticulum to mitochondria under endoplasmic reticulum stress." *Cell reports* **5**(2): 331-339.
- Naseem Saud, A., F. Muhammad, N. Muzammil Hasan, M. Kouser Bashir and H. Aurangzeb (2006). "Activity of polyphenolic plant extracts as scavengers of free radicals and inhibitors of xanthine oxidase."
- Ni, D., Z. Yang, J. Teng, Y. Cheng and Z. Zhu (2017). "MicroRNA-15a-5p Suppresses Proliferation and Metastasis by Directly Targeting of Nf- $\kappa$ B1 in Human Lung Cancer Cells." *Journal of Biomaterials and Tissue Engineering* **7**(4): 302-309.
- Nielsen, C. B., N. Shomron, R. Sandberg, E. Hornstein, J. Kitzman and C. B. Burge (2007). "Determinants of targeting by endogenous and exogenous microRNAs and siRNAs." *Rna* **13**(11): 1894-1910.
- Nishio, N., W. Taniguchi, Y. Sugimura, N. Takiguchi, M. Yamanaka, Y. Kiyoyuki, H. Yamada, N. Miyazaki, M. Yoshida and T. Nakatsuka (2013). "Reactive oxygen species enhance excitatory synaptic transmission in rat spinal dorsal horn neurons by activating TRPA1 and TRPV1 channels." *Neuroscience* **247**: 201-212.
- Nosarka, A. (2017). "The plastics portal." *South African Food Review* **44**(6): 37-37.
- Nosjean, O., M. Ferro, F. Cogé, P. Beauverger, J.-M. Henlin, F. Lefoulon, J.-L. Fauchere, P. Delagrangé, E. Canet and J. A. Boutin (2000). "Identification of the Melatonin-binding Site MT 3 as the Quinone Reductase 2." *Journal of Biological Chemistry* **275**(40): 31311-31317.
- Nusse, R. and H. E. Varmus (1982). "Many tumors induced by the mouse mammary tumor virus contain a provirus integrated in the same region of the host genome." *Cell* **31**(1): 99-109.
- O'Reilly, A. O., E. Eberhardt, C. Weidner, C. Alzheimer, B. Wallace and A. Lampert (2012). "Bisphenol A binds to the local anesthetic receptor site to block the human cardiac sodium channel." *PLoS One* **7**(7): e41667.
- Ohlstein, J. F., A. L. Strong, J. A. McLachlan, J. M. Gimble, M. E. Burow and B. A. Bunnell (2014). "Bisphenol A enhances adipogenic differentiation of human adipose stromal/stem cells." *Journal of molecular endocrinology* **53**(3): 345.
- Okada, H., T. Tokunaga, X. Liu, S. Takayanagi, A. Matsushima and Y. Shimohigashi (2007). "Direct evidence revealing structural elements essential for the high binding ability of bisphenol A to human estrogen-related receptor- $\gamma$ ." *Environmental health perspectives* **116**(1): 32-38.
- Olsen, C. M., E. T. Meussen-Elholm, M. Samuelsen, J. A. Holme and J. K. Hongslo (2003). "Effects of the environmental oestrogens bisphenol A, tetrachlorobisphenol A, tetrabromobisphenol A, 4-hydroxybiphenyl and 4, 4'-dihydroxybiphenyl on oestrogen receptor binding, cell proliferation

- and regulation of oestrogen sensitive proteins in the human breast cancer cell line MCF-7." *Pharmacology & toxicology* **92**(4): 180-188.
- Orwa, C., A. Mutua, R. Kindt, R. Jamnadass and A. Simons (2009). "Agroforestry Database: a tree reference and selection guide. Version 4." *Agroforestry Database: a tree reference and selection guide. Version 4*.
- Özen, S. and Ş. Darcan (2011). "Effects of environmental endocrine disruptors on pubertal development." *Journal of clinical research in pediatric endocrinology* **3**(1): 1.
- Pallepati, P. and D. Averill-Bates (2010). "Mild thermotolerance induced at 40 C increases antioxidants and protects HeLa cells against mitochondrial apoptosis induced by hydrogen peroxide: role of p53." *Archives of biochemistry and biophysics* **495**(2): 97-111.
- Pant, S. and S. Samant (2010). "Ethnobotanical observations in the Mornaula reserve forest of Komoun, West Himalaya, India." *Ethnobotanical leaflets* **2010**(2): 8.
- Papanicolaou, K. N., R. J. Khairallah, G. A. Ngoh, A. Chikando, I. Luptak, K. M. O'Shea, D. D. Riley, J. J. Lugus, W. S. Colucci and W. J. Lederer (2011). "Mitofusin-2 maintains mitochondrial structure and contributes to stress-induced permeability transition in cardiac myocytes." *Molecular and cellular biology* **31**(6): 1309-1328.
- Parker, B. and S. Sukumar (2003). "Distant metastasis in breast cancer: molecular mechanisms and therapeutic targets." *Cancer biology & therapy* **2**(1): 13-22.
- Paul, P., A. Chakraborty, D. Sarkar, M. Langthasa, M. Rahman, M. Bari, R. S. Singha, A. K. Malakar and S. Chakraborty (2018). "Interplay between miRNAs and human diseases." *Journal of cellular physiology* **233**(3): 2007-2018.
- Peng, C., W. Rao, L. Zhang, K. Wang, H. Hui, L. Wang, N. Su, P. Luo, Y.-I. Hao and Y. Tu (2015). "Mitofusin 2 ameliorates hypoxia-induced apoptosis via mitochondrial function and signaling pathways." *The international journal of biochemistry & cell biology* **69**: 29-40.
- Peng, Y. and C. M. Croce (2016). "The role of MicroRNAs in human cancer." *Signal transduction and targeted therapy* **1**(1): 1-9.
- Pérez, M. J. and R. A. Quintanilla (2017). "Development or disease: duality of the mitochondrial permeability transition pore." *Developmental biology* **426**(1): 1-7.
- Peters, A., W. Ingman, W. D. Tilley and L. Butler (2011). "Differential effects of exogenous androgen and an androgen receptor antagonist in the peri- and postpubertal murine mammary gland." *Endocrinology* **152**(10): 3728-3737.
- Petroski, M. D., X. Zhou, G. Dong, S. Daniel-Issakani, D. G. Payan and J. Huang (2007). "Substrate modification with lysine 63-linked ubiquitin chains through the UBC13-UEV1A ubiquitin-conjugating enzyme." *Journal of Biological Chemistry* **282**(41): 29936-29945.
- Pettersen, E. F., T. D. Goddard, C. C. Huang, G. S. Couch, D. M. Greenblatt, E. C. Meng and T. E. Ferrin (2004). "UCSF Chimera—a visualization system for exploratory research and analysis." *Journal of computational chemistry* **25**(13): 1605-1612.
- Pfaffl, M. W., G. W. Horgan and L. Dempfle (2002). "Relative expression software tool (REST©) for group-wise comparison and statistical analysis of relative expression results in real-time PCR." *Nucleic acids research* **30**(9): e36-e36.
- Poliseno, L., A. Tuccoli, L. Mariani, M. Evangelista, L. Citti, K. Woods, A. Mercatanti, S. Hammond and G. Rainaldi (2006). "MicroRNAs modulate the angiogenic properties of HUVECs." *Blood* **108**(9): 3068-3071.
- Posnack, N. G. (2021). "Cardiac toxicity from bisphenol A: Are electrophysiology and calcium handling perturbations dose-dependent?" *Toxicology and applied pharmacology* **431**: 115740.
- Posnack, N. G. (2021). "Plastics and cardiovascular disease." *Nature Reviews Cardiology* **18**(2): 69-70.
- Qipshidze, N., N. Tyagi, N. Metreveli, D. Lominadze and S. C. Tyagi (2011). "Autophagy mechanism of right ventricular remodeling in murine model of pulmonary artery constriction." *American Journal of Physiology-Heart and Circulatory Physiology* **302**(3): H688-H696.



- Rajak, S., S. Raza, A. Tewari and R. A. Sinha (2021). "Environmental Toxicants and NAFLD: A Neglected yet Significant Relationship." Digestive Diseases and Sciences: 1-11.
- Ramos, J. G., J. Varayoud, L. Kass, H. Rodríguez, L. Costabel, M. n. Muñoz-de-Toro and E. H. Luque (2003). "Bisphenol A induces both transient and permanent histofunctional alterations of the hypothalamic-pituitary-gonadal axis in prenatally exposed male rats." Endocrinology **144**(7): 3206-3215.
- Rauf, A., M. Saleem, G. Uddin, B. S. Siddiqui, H. Khan, M. Raza, S. Z. Hamid, A. Khan, F. Maione and N. Mascolo (2015). "Phosphodiesterase-1 inhibitory activity of two flavonoids isolated from *Pistacia integerrima* JL stewart galls." Evidence-Based Complementary and Alternative Medicine **2015**.
- Rebolledo-Solleiro, D., L. C. Flores and H. Solleiro-Villavicencio (2021). "Impact of BPA on behavior, neurodevelopment and neurodegeneration." Frontiers in bioscience **26**: 363-400.
- Reddy, K. B. (2015). "MicroRNA (miRNA) in cancer." Cancer cell international **15**(1): 38.
- Redza-Dutordoir, M. and D. A. Averill-Bates (2016). "Activation of apoptosis signalling pathways by reactive oxygen species." Biochimica et Biophysica Acta (BBA)-Molecular Cell Research **1863**(12): 2977-2992.
- Reiter, R. J., J. C. Mayo, D. X. Tan, R. M. Sainz, M. Alatorre-Jimenez and L. Qin (2016). "Melatonin as an antioxidant: under promises but over delivers." Journal of pineal research **61**(3): 253-278.
- Rice-Evans, C. A. and A. T. Diplock (1993). "Current status of antioxidant therapy." Free Radical Biology and Medicine **15**(1): 77-96.
- Riffo-Campos, Á. L., I. Riquelme and P. Brebi-Mieville (2016). "Tools for sequence-based miRNA target prediction: what to choose?" International journal of molecular sciences **17**(12): 1987.
- Roe, D. R. and T. E. Cheatham III (2013). "PTRAJ and CPPTRAJ: software for processing and analysis of molecular dynamics trajectory data." Journal of chemical theory and computation **9**(7): 3084-3095.
- Rubin, B. S. (2011). "Bisphenol A: an endocrine disruptor with widespread exposure and multiple effects." The Journal of steroid biochemistry and molecular biology **127**(1-2): 27-34.
- Ryu, D.-Y., M. Rahman and M.-G. Pang (2017). "Determination of Highly Sensitive Biological Cell Model Systems to Screen BPA-Related Health Hazards Using Pathway Studio." International journal of molecular sciences **18**(9): 1909.
- Sanchez, A. P. and K. Sharma (2009). "Transcription factors in the pathogenesis of diabetic nephropathy." Expert reviews in molecular medicine **11**.
- Schönfelder, G., W. Wittfoht, H. Hopp, C. E. Talsness, M. Paul and I. Chahoud (2002). "Parent bisphenol A accumulation in the human maternal-fetal-placental unit." Environmental health perspectives **110**(11): A703-A707.
- Schug, T. T., A. Janesick, B. Blumberg and J. J. Heindel (2011). "Endocrine disrupting chemicals and disease susceptibility." The Journal of steroid biochemistry and molecular biology **127**(3-5): 204-215.
- Schwarz, D. S., G. Hutvagner, T. Du, Z. Xu, N. Aronin and P. D. Zamore (2003). "Asymmetry in the assembly of the RNAi enzyme complex." Cell **115**(2): 199-208.
- Sewerynek, E., M. Abe, R. J. Reiter, L. R. Barlow-Walden, L. Chen, T. J. McCabe, L. J. Roman and B. Diaz-Lopez (1995). "Melatonin administration prevents lipopolysaccharide-induced oxidative damage in phenobarbital-treated animals." Journal of cellular biochemistry **58**(4): 436-444.
- Shafiq, u. R., I. Muhammad, M. Naveed, A. Farhat, A. C. Kamran and I. Muhammad (2011). "Evaluation of the stem bark of *Pistacia integerrima* Stew ex Brandis for its antimicrobial and phytotoxic activities." African Journal of Pharmacy and Pharmacology **5**(8): 1170-1174.
- Shahin, A. Y., I. Hassanin, A. M. Ismail, J. S. Kruessel and J. Hirchenhain (2009). "Effect of oral N-acetyl cysteine on recurrent preterm labor following treatment for bacterial vaginosis." International Journal of Gynecology & Obstetrics **104**(1): 44-48.

- Shan, Z.-X., Q.-X. Lin, C.-Y. Deng, J.-N. Zhu, L.-P. Mai, J.-L. Liu, Y.-H. Fu, X.-Y. Liu, Y.-X. Li and Y.-Y. Zhang (2010). "miR-1/miR-206 regulate Hsp60 expression contributing to glucose-mediated apoptosis in cardiomyocytes." FEBS letters **584**(16): 3592-3600.
- Sharif-Askari, E., A. Alam, E. Rhéaume, P. J. Beresford, C. Scotto, K. Sharma, D. Lee, W. E. DeWolf, M. E. Nuttall and J. Lieberman (2001). "Direct cleavage of the human DNA fragmentation factor-45 by granzyme B induces caspase-activated DNase release and DNA fragmentation." The EMBO journal **20**(12): 3101-3113.
- Sharma, G. N., R. Dave, J. Sanadya, P. Sharma and K. Sharma (2010). "Various types and management of breast cancer: an overview." Journal of advanced pharmaceutical technology & research **1**(2): 109-126.
- Sharma, K. and D. A. Kass (2014). "Heart failure with preserved ejection fraction: mechanisms, clinical features, and therapies." Circulation research **115**(1): 79-96.
- Sheikh Abdul Kadir, S., Z. Rasidi, N. Hanafi, R. Kamaludin, S. Ab. Rahim, R. Siran and M. Othman (2017). "17P Endocrine disrupting chemicals, bisphenol A alters cardiomyocytes beating rate and cell morphology." Annals of Oncology **28**(suppl\_10): mdx652. 016.
- Sheikhpour, M., L. Barani and A. Kasaeian (2017). "Biomimetics in drug delivery systems: a critical review." Journal of Controlled Release **253**: 97-109.
- Shen, T., M. Zheng, C. Cao, C. Chen, J. Tang, W. Zhang, H. Cheng, K.-H. Chen and R.-P. Xiao (2007). "Mitofusin-2 is a major determinant of oxidative stress-mediated heart muscle cell apoptosis." Journal of Biological Chemistry **282**(32): 23354-23361.
- Sheridan, C. and S. J. Martin (2010). "Mitochondrial fission/fusion dynamics and apoptosis." Mitochondrion **10**(6): 640-648.
- Shi, H., N. Noguchi and E. Niki (1999). "Comparative study on dynamics of antioxidative action of  $\alpha$ -tocopheryl hydroquinone, ubiquinol, and  $\alpha$ -tocopherol against lipid peroxidation." Free Radical Biology and Medicine **27**(3-4): 334-346.
- Shilo, S., S. Roy, S. Khanna and C. K. Sen (2007). "MicroRNA in cutaneous wound healing: a new paradigm." DNA and cell biology **26**(4): 227-237.
- Shirani, M., S. Alizadeh, M. Mahdavinia and M. A. Dehghani (2019). "The ameliorative effect of quercetin on bisphenol A-induced toxicity in mitochondria isolated from rats." Environmental Science and Pollution Research **26**(8): 7688-7696.
- Shuaib, M., K. Ali, U. Zeb, F. Hussain, M. A. Zeb, S. Hussain and F. Hussain (2017). "Evaluation of Pistacia integririma; an important plant." Inter J of Biosciences **11**(5): 412-442.
- Siegel, R. L., K. D. Miller and A. Jemal (2015). "Cancer statistics, 2015." CA: a cancer journal for clinicians **65**(1): 5-29.
- Sigal, A. and V. Rotter (2000). "Oncogenic mutations of the p53 tumor suppressor: the demons of the guardian of the genome." Cancer research **60**(24): 6788-6793.
- Sirisha, C. V. N. and R. M. Manohar (2013). "Study of antioxidant enzymes superoxide dismutase and glutathione peroxidase levels in tobacco chewers and smokers: A pilot study." Journal of cancer research and therapeutics **9**(2): 210.
- Siu, W. P., P. B. Pun, C. Latchoumycandane and U. A. Boelsterli (2008). "Bax-mediated mitochondrial outer membrane permeabilization (MOMP), distinct from the mitochondrial permeability transition, is a key mechanism in diclofenac-induced hepatocyte injury: Multiple protective roles of cyclosporin A." Toxicol Appl Pharmacol **227**(3): 451-461.
- SJ, S. (2000). "Pathology of invasive breast cancer." Diseases of the Breast.
- Sohail, S. and S. N. Alam (2007). "Breast cancer in Pakistan-awareness and early detection."
- Son, G. and J. Han (2018). "Roles of mitochondria in neuronal development." BMB reports **51**(11): 549.
- Song, M. S., L. Salmena, A. Carracedo, A. Egia, F. Lo-Coco, J. Teruya-Feldstein and P. P. Pandolfi (2008). "The deubiquitinylation and localization of PTEN are regulated by a HAUSP-PML network." Nature **455**(7214): 813-817.

- Soriano, F. X., M. Liesa, D. Bach, D. C. Chan, M. Palacín and A. Zorzano (2006). "Evidence for a mitochondrial regulatory pathway defined by peroxisome proliferator-activated receptor-γ coactivator-1α, estrogen-related receptor-α, and mitofusin 2." *Diabetes* **55**(6): 1783-1791.
- Soriano, S., C. Ripoll, P. Alonso-Magdalena, E. Fuentes, I. Quesada, A. Nadal and J. Martínez-Pinna (2016). "Effects of bisphenol A on ion channels: experimental evidence and molecular mechanisms." *Steroids* **111**: 12-20.
- Spurdle, A. B., F. J. Couch, M. T. Parsons, L. McGuffog, D. Barrowdale, M. K. Bolla, Q. Wang, S. Healey, R. K. Schmutzler and B. Wappenschmidt (2014). "Refined histopathological predictors of BRCA1 and BRCA2 mutation status: a large-scale analysis of breast cancer characteristics from the BCAC, CIMBA, and ENIGMA consortia." *Breast Cancer Research* **16**: 1-16.
- Srinivasan, V., R. Zakaria, Z. Othman, E. C. Lauterbach and D. Acuña-Castroviejo (2012). "Agomelatine in depressive disorders: its novel mechanisms of action." *The Journal of neuropsychiatry and clinical neurosciences* **24**(3): 290-308.
- Strassburg, C., A. Strassburg, S. Kneip, A. Barut, R. Tukey, B. Rodeck and M. Manns (2002). "Developmental aspects of human hepatic drug glucuronidation in young children and adults." *Gut* **50**(2): 259-265.
- Suárez, Y., C. Fernández-Hernando, J. S. Pober and W. C. Sessa (2007). "Dicer dependent microRNAs regulate gene expression and functions in human endothelial cells." *Circulation research* **100**(8): 1164-1173.
- Suthar, H., R. Verma, S. Patel and Y. Jasrai (2014). "Green tea potentially ameliorates bisphenol A-induced oxidative stress: an in vitro and in silico study." *Biochemistry research international* **2014**.
- Szabo, G. and S. Bala (2013). "MicroRNAs in liver disease." *Nature reviews Gastroenterology & hepatology* **10**(9): 542.
- Tan, D.-X. (1993). "Melatonin: a potent, endogenous hydroxyl radical scavenger." *Endocr j* **1**: 57-60.
- Tanaka, A., M. M. Cleland, S. Xu, D. P. Narendra, D.-F. Suen, M. Karbowski and R. J. Youle (2010). "Proteasome and p97 mediate mitophagy and degradation of mitofusins induced by Parkin." *The Journal of cell biology* **191**(7): 1367-1380.
- Tang, H., A. Tao, J. Song, Q. Liu, H. Wang and T. Rui (2017). "Doxorubicin-induced cardiomyocyte apoptosis: Role of mitofusin 2." *The international journal of biochemistry & cell biology* **88**: 55-59.
- Tang, X., G. Tang and S. Özcan (2008). "Role of microRNAs in diabetes." *Biochimica Et Biophysica Acta (BBA)-Gene Regulatory Mechanisms* **1779**(11): 697-701.
- Tardiolo, G., P. Bramanti and E. Mazzon (2018). "Overview on the effects of N-acetylcysteine in neurodegenerative diseases." *Molecules* **23**(12): 3305.
- Tarocco, A., N. Carocchia, G. Morciano, M. R. Wieckowski, G. Ancora, G. Garani and P. Pinton (2019). "Melatonin as a master regulator of cell death and inflammation: molecular mechanisms and clinical implications for newborn care." *Cell death & disease* **10**(4): 1-12.
- Thayer, K. A., D. R. Doerge, D. Hunt, S. H. Schurman, N. C. Twaddle, M. I. Churchwell, S. Garantzotis, G. E. Kissling, M. R. Easterling and J. R. Bucher (2015). "Pharmacokinetics of bisphenol A in humans following a single oral administration." *Environment international* **83**: 107-115.
- Tokunaga, F., S.-i. Sakata, Y. Saeki, Y. Satomi, T. Kirisako, K. Kamei, T. Nakagawa, M. Kato, S. Murata and S. Yamaoka (2009). "Involvement of linear polyubiquitylation of NEMO in NF-κB activation." *Nature cell biology* **11**(2): 123-132.
- Tomita, Y., N. Marchenko, S. Erster, A. Nemajerova, A. Dehner, C. Klein, H. Pan, H. Kessler, P. Pancoska and U. M. Moll (2006). "WT p53, but not tumor-derived mutants, bind to Bcl2 via the DNA binding domain and induce mitochondrial permeabilization." *Journal of Biological Chemistry* **281**(13): 8600-8606.

- Topisirovic, I., G. J. Gutierrez, M. Chen, E. Appella, K. L. Borden and Z. e. A. Ronai (2009). "Control of p53 multimerization by Ubc13 is JNK-regulated." Proceedings of the National Academy of Sciences **106**(31): 12676-12681.
- Topisirovic, I., G. J. Gutierrez, M. Chen, E. Appella, K. L. Borden and A. R. Ze'ev (2009). "Control of p53 multimerization by Ubc13 is JNK-regulated." Proceedings of the National Academy of Sciences **106**(31): 12676-12681.
- Trifunovic, A., A. Wredenberg, M. Falkenberg, J. N. Spelbrink, A. T. Rovio, C. E. Bruder, M. Bohlooly-Y, S. Gidlöf, A. Oldfors and R. Wibom (2004). "Premature ageing in mice expressing defective mitochondrial DNA polymerase." Nature **429**(6990): 417.
- Tsai, N.-W., Y.-T. Chang, C.-R. Huang, Y.-J. Lin, W.-C. Lin, B.-C. Cheng, C.-M. Su, Y.-F. Chiang, S.-F. Chen and C.-C. Huang (2014). "Association between oxidative stress and outcome in different subtypes of acute ischemic stroke." BioMed research international **2014**.
- Tsutsui, H., S. Kinugawa and S. Matsushima (2008). "Mitochondrial oxidative stress and dysfunction in myocardial remodelling." Cardiovascular research **81**(3): 449-456.
- Tsutsui, H., S. Kinugawa and S. Matsushima (2009). "Mitochondrial oxidative stress and dysfunction in myocardial remodelling." Cardiovascular research **81**(3): 449-456.
- Tsutsui, H., S. Kinugawa and S. Matsushima (2011). "Oxidative stress and heart failure." American journal of physiology-Heart and circulatory physiology **301**(6): H2181-H2190.
- Uddin, G., A. Rauf, T. Rehman and M. Qaisar (2011). "Phytochemical screening of Pistacia chinensis var. integerrima." Middle-East J Sci Res **7**(5): 707-711.
- Ullah, Z., R. Mehmood, M. Imran, A. Malik and R. A. Afzal (2012). "Flavonoid constituents of Pistacia integerrima." Natural Product Communications **7**(8): 1934578X1200700813.
- Urbich, C., A. Kuehbachner and S. Dimmeler (2008). "Role of microRNAs in vascular diseases, inflammation, and angiogenesis." Cardiovascular research **79**(4): 581-588.
- Van Amerongen, R. (2012). "Alternative Wnt pathways and receptors." Cold Spring Harbor perspectives in biology **4**(10): a007914.
- Van der Horst, A., A. M. de Vries-Smits, A. B. Brenkman, M. H. van Triest, N. van den Broek, F. Colland, M. M. Maurice and B. M. Burgering (2006). "FOXO4 transcriptional activity is regulated by monoubiquitination and USP7/HAUSP." Nature cell biology **8**(10): 1064-1073.
- van der Pol, A., W. H. van Gilst, A. A. Voors and P. van der Meer (2019). "Treating oxidative stress in heart failure: past, present and future." European Journal of Heart Failure **21**(4): 425-435.
- van Lith, R. and G. A. Ameer (2016). Antioxidant Polymers as Biomaterial. Oxidative Stress and Biomaterials, Elsevier: 251-296.
- Vandenberg, L. N., R. Hauser, M. Marcus, N. Olea and W. V. Welshons (2007). "Human exposure to bisphenol A (BPA)." Reproductive toxicology **24**(2): 139-177.
- Viñas, R., R. M. Goldblum and C. S. Watson (2013). "Rapid estrogenic signaling activities of the modified (chlorinated, sulfonated, and glucuronidated) endocrine disruptor bisphenol A." Endocrine Disruptors **1**(1): e25411.
- Vogelstein, B., D. Lane and A. J. Levine (2000). "Surfing the p53 network." Nature **408**(6810): 307.
- Völkel, W., M. Kiranoglu and H. Fromme (2008). "Determination of free and total bisphenol A in human urine to assess daily uptake as a basis for a valid risk assessment." Toxicology Letters **179**(3): 155-162.
- Vrijens, K., V. Bollati and T. S. Nawrot (2015). "MicroRNAs as potential signatures of environmental exposure or effect: a systematic review." Environmental health perspectives **123**(5): 399-411.
- Wade, M., Y.-C. Li and G. M. Wahl (2013). "MDM2, MDMX and p53 in oncogenesis and cancer therapy." Nature Reviews Cancer **13**(2): 83.

- Wang, C., W. Fu, C. Quan, M. Yan, C. Liu, S. Qi and K. Yang (2015). "The role of Pten/Akt signaling pathway involved in BPA-induced apoptosis of rat sertoli cells." *Environmental toxicology* **30**(7): 793-802.
- Wang, E. Y., H. Gang, Y. Aviv, R. Dhingra, V. Margulets and L. A. Kirshenbaum (2013). "p53 mediates autophagy and cell death by a mechanism contingent on Bnip3." *Hypertension* **62**(1): 70-77.
- Wang, H., Z.-h. Liu, J. Zhang, R.-P. Huang, H. Yin and Z. Dang (2020). "Human exposure of bisphenol A and its analogues: understandings from human urinary excretion data and wastewater-based epidemiology." *Environmental Science and Pollution Research* **27**(3): 3247-3256.
- Wang, J.-X., Q. Li and P.-F. Li (2009). "Apoptosis repressor with caspase recruitment domain contributes to chemotherapy resistance by abolishing mitochondrial fission mediated by dynamin-related protein-1." *Cancer Research* **69**(2): 492-500.
- Wang, J., M. Li, W. Zhang, A. Gu, J. Dong, J. Li and A. Shan (2018). "Protective effect of n-acetylcysteine against oxidative stress induced by zearalenone via mitochondrial apoptosis pathway in SIEC02 cells." *Toxins* **10**(10): 407.
- Wang, J., W. Wang, P. A. Kollman and D. A. Case (2006). "Automatic atom type and bond type perception in molecular mechanical calculations." *Journal of molecular graphics and modelling* **25**(2): 247-260.
- Wang, L., H. Erlandsen, J. Haavik, P. M. Knappskog and R. C. Stevens (2002). "Three-dimensional structure of human tryptophan hydroxylase and its implications for the biosynthesis of the neurotransmitters serotonin and melatonin." *Biochemistry* **41**(42): 12569-12574.
- Wang, P., J. Yu and L. Zhang (2007). "The nuclear function of p53 is required for PUMA-mediated apoptosis induced by DNA damage." *Proceedings of the National Academy of Sciences* **104**(10): 4054-4059.
- Wang, W.-X., R. J. Danaher, C. S. Miller, J. R. Berger, V. G. Nubia, B. S. Wilfred, J. H. Neltner, C. M. Norris and P. T. Nelson (2014). "Expression of miR-15/107 family microRNAs in human tissues and cultured rat brain cells." *Genomics, proteomics & bioinformatics* **12**(1): 19-30.
- Wang, X., T. Ha, Y. Hu, C. Lu, L. Liu, X. Zhang, R. Kao, J. Kalbfleisch, D. Williams and C. Li (2016). "MicroRNA-214 protects against hypoxia/reoxygenation induced cell damage and myocardial ischemia/reperfusion injury via suppression of PTEN and Bim1 expression." *Oncotarget* **7**(52): 86926.
- Warren, C. F., M. W. Wong-Brown and N. A. Bowden (2019). "BCL-2 family isoforms in apoptosis and cancer." *Cell death & disease* **10**(3): 1-12.
- Weigelt, B., A. Glas, L. Wessels, A. Witteveen, A. Bosma, J. Peterse and L. van't Veer (2004). "Gene expression profiles of primary breast tumors maintained in lymph node-and distant metastases." *EJC Supplements* **3**(2): 125.
- Welshons, W. V., S. C. Nagel and F. S. vom Saal (2006). "Large effects from small exposures. III. Endocrine mechanisms mediating effects of bisphenol A at levels of human exposure." *Endocrinology* **147**(6): s56-s69.
- Wen, L., L. Liu, J. Li, L. Tong, K. Zhang, Q. Zhang and C. Li (2019). "NDRG4 protects against cerebral ischemia injury by inhibiting p53-mediated apoptosis." *Brain Research Bulletin* **146**: 104-111.
- Wertz, I. E. and V. M. Dixit (2008). "Ubiquitin-mediated regulation of TNFR1 signaling." *Cytokine & growth factor reviews* **19**(3-4): 313-324.
- Wetherill, Y. B., B. T. Akingbemi, J. Kanno, J. A. McLachlan, A. Nadal, C. Sonnenschein, C. S. Watson, R. T. Zoeller and S. M. Belcher (2007). "In vitro molecular mechanisms of bisphenol A action." *Reproductive toxicology* **24**(2): 178-198.
- White, M. C., R. Gao, W. Xu, S. M. Mandal, J. G. Lim, T. K. Hazra, M. Wakamiya, S. F. Edwards, S. Raskin and H. A. Teive (2010). "Inactivation of hnRNP K by expanded intronic AUUCU repeat

- induces apoptosis via translocation of PKC $\delta$  to mitochondria in spinocerebellar ataxia 10." *PLoS genetics* **6**(6): e1000984.
- Wu, C., L. Yan, C. Depre, S. K. Dhar, Y.-T. Shen, J. Sadoshima, S. F. Vatner and D. E. Vatner (2009). "Cytochrome c oxidase III as a mechanism for apoptosis in heart failure following myocardial infarction." *American Journal of Physiology-Cell Physiology* **297**(4): C928-C934.
- Wu, H.-T., H.-T. Zhong, G.-W. Li, J.-X. Shen, Q.-Q. Ye, M.-L. Zhang and J. Liu (2020). "Oncogenic functions of the EMT-related transcription factor ZEB1 in breast cancer." *Journal of translational medicine* **18**(1): 1-10.
- Wu, L. and J. G. Belasco (2008). "Let me count the ways: mechanisms of gene regulation by miRNAs and siRNAs." *Molecular cell* **29**(1): 1-7.
- Xu, C., Y. Lu, Z. Pan, W. Chu, X. Luo, H. Lin, J. Xiao, H. Shan, Z. Wang and B. Yang (2007). "The muscle-specific microRNAs miR-1 and miR-133 produce opposing effects on apoptosis by targeting HSP60, HSP70 and caspase-9 in cardiomyocytes." *Journal of cell science* **120**(17): 3045-3052.
- Xu, F.-P., M.-S. Chen, Y.-Z. Wang, Q. Yi, S.-B. Lin, A. F. Chen and J.-D. Luo (2004). "Leptin induces hypertrophy via endothelin-1–reactive oxygen species pathway in cultured neonatal rat cardiomyocytes." *Circulation* **110**(10): 1269-1275.
- Xu, X., J. Pan, H. Li, X. Li, F. Fang, D. Wu, Y. Zhou, P. Zheng, L. Xiong and D. Zhang (2019). "Atg7 mediates renal tubular cell apoptosis in vancomycin nephrotoxicity through activation of PKC- $\delta$ ." *The FASEB Journal* **33**(3): 4513-4524.
- Yan, S., Y. Chen, M. Dong, W. Song, S. M. Belcher and H.-S. Wang (2011). "Bisphenol A and 17 $\beta$ -estradiol promote arrhythmia in the female heart via alteration of calcium handling." *PloS one* **6**(9): e25455.
- Yang, O., H. L. Kim, J.-I. Weon and Y. R. Seo (2015). "Endocrine-disrupting chemicals: review of toxicological mechanisms using molecular pathway analysis." *Journal of cancer prevention* **20**(1): 12.
- Yang, S. and G. Lian (2020). "ROS and diseases: Role in metabolism and energy supply." *Molecular and cellular biochemistry* **467**(1): 1-12.
- Ye, X. and R. A. Weinberg (2015). "Epithelial–mesenchymal plasticity: a central regulator of cancer progression." *Trends in cell biology* **25**(11): 675-686.
- Ye, Y., J. R. Perez-Polo, J. Qian and Y. Birnbaum (2011). "The role of microRNA in modulating myocardial ischemia-reperfusion injury." *Physiological genomics* **43**(10): 534-542.
- Yoshida, K. and Y. Miki (2010). "The cell death machinery governed by the p53 tumor suppressor in response to DNA damage." *Cancer science* **101**(4): 831-835.
- Yu, J., Z. Wang, K. W. Kinzler, B. Vogelstein and L. Zhang (2003). "PUMA mediates the apoptotic response to p53 in colorectal cancer cells." *Proceedings of the National Academy of Sciences* **100**(4): 1931-1936.
- Yu, J. and L. Zhang (2008). "PUMA, a potent killer with or without p53." *Oncogene* **27**(1): S71-S83.
- Zahoor, M., R. Zafar and N. U. Rahman (2018). "Isolation and identification of phenolic antioxidants from Pistacia integerrima gall and their anticholine esterase activities." *Heliyon* **4**(12): e01007.
- Zavadil, J., M. Narasimhan, M. Blumenberg and R. J. Schneider (2007). "Transforming growth factor- $\beta$  and microRNA: mRNA regulatory networks in epithelial plasticity." *Cells Tissues Organs* **185**(1-3): 157-161.
- Zhang, B., X. Pan, G. P. Cobb and T. A. Anderson (2007). "microRNAs as oncogenes and tumor suppressors." *Developmental biology* **302**(1): 1-12.
- Zhang, P., Y. Sun and L. Ma (2015). "ZEB1: at the crossroads of epithelial-mesenchymal transition, metastasis and therapy resistance." *Cell cycle* **14**(4): 481-487.

- Zhang, Y.-F., C. Shan, Y. Wang, L.-L. Qian, D.-D. Jia, Y.-F. Zhang, X.-D. Hao and H.-M. Xu (2020). "Cardiovascular toxicity and mechanism of bisphenol A and emerging risk of bisphenol S." *Science of the Total Environment* **723**: 137952.
- Zhao, M., L. Xia and G.-Q. Chen (2012). "Protein kinase cδ in apoptosis: a brief overview." *Archivum immunologiae et therapiae experimentalis* **60**(5): 361-372.
- Zhao, T., X. Tang, C. S. Umeshappa, H. Ma, H. Gao, Y. Deng, A. Freywald and J. Xiang (2016). "Simulated Microgravity Promotes Cell Apoptosis Through Suppressing Uev1A/TICAM/TRAF/NF-κB-Regulated Anti-Apoptosis and p53/PCNA-and ATM/ATR-Chk1/2-Controlled DNA-Damage Response Pathways." *Journal of cellular biochemistry* **117**(9): 2138-2148.
- Zhao, Y., E. Samal and D. Srivastava (2005). "Serum response factor regulates a muscle-specific microRNA that targets Hand2 during cardiogenesis." *Nature* **436**(7048): 214-220.
- Zhou, Y., Z. Wang, M. Xia, S. Zhuang, X. Gong, J. Pan, C. Li, R. Fan, Q. Pang and S. Lu (2017). "Neurotoxicity of low bisphenol A (BPA) exposure for young male mice: Implications for children exposed to environmental levels of BPA." *Environmental Pollution* **229**: 40-48.
- Zoeller, R. T., T. R. Brown, L. L. Doan, A. C. Gore, N. Skakkebaek, A. Soto, T. Woodruff and F. Vom Saal (2012). "Endocrine-disrupting chemicals and public health protection: a statement of principles from The Endocrine Society." *Endocrinology* **153**(9): 4097-4110.

## Turnitin Originality Report

ELUCIDATION OF UNDERLYING MOLECULAR MECHANISMS INVOLVED IN  
BISPHENOL A INDUCED CARDIOTOXICITY AND NEUROTOXICITY by Ayesha  
Ishtiaq .



From PhD (PhD DRSMML)

- Processed on 21-Aug-2023 08:51 PKT
- ID: 2148664973
- Word Count: 39283

## Similarity Index

15%

## Similarity by Source

Internet Sources:

10%

Publications:

11%

Student Papers:

1%

  
**Focal Person (Turnitin)**  
**Quaid-i-Azam University**  
**Islamabad**

## sources:

- 1 1% match (Internet from 12-Aug-2022)  
<https://www.pubfacts.com/author/%20Anees/2>
- 2 < 1% match (Internet from 21-Dec-2022)  
<https://www.mdpi.com/1420-3049/26/23/7285/htm>
- 3 < 1% match (Internet from 15-Aug-2022)  
<https://www.mdpi.com/1467-3045/44/8/249/htm>
- 4 < 1% match (Internet from 12-Jul-2023)  
<https://WWW.MDPI.COM/2218-273X/9/1/16>
- 5 < 1% match (Internet from 01-Oct-2022)  
<https://www.mdpi.com/2073-4409/8/7/760/htm>
- 6 < 1% match (Internet from 24-Dec-2021)  
<https://www.mdpi.com/2072-6694/12/9/2425/html>
- 7 < 1% match (Internet from 02-Oct-2019)  
<https://www.mdpi.com/1422-0067/20/12/3029/htm>
- 8 < 1% match (Internet from 30-Jan-2020)  
<https://www.mdpi.com/2073-4409/9/1/147/html>
- 9 < 1% match (Internet from 25-May-2022)  
<https://www.mdpi.com/2073-4409/11/10/1690/htm>
- 10 < 1% match (Internet from 19-Oct-2022)  
<https://www.mdpi.com/2072-6694/13/17/4390/htm>
- 11 < 1% match (Internet from 23-Apr-2023)  
<https://www.mdpi.com/1422-0067/24/2/1741>
- 12 < 1% match (Internet from 02-Mar-2020)  
<https://www.mdpi.com/1660-3397/15/5/143/html>
- 13 < 1% match (Internet from 31-May-2023)  
<https://www.mdpi.com/1999-4915/15/5/1050>
- 14 < 1% match (Internet from 14-Oct-2022)  
<https://www.mdpi.com/2079-4991/10/5/898/htm>

  
**PROFESSOR**  
Department of Biochemistry  
Quaid-i-Azam University, Islamabad





## *Pistacia integerrima* alleviated Bisphenol A induced toxicity through Ubc13/p53 signalling

Ayesha Ihtilal<sup>1</sup>, Atia Bahittar<sup>1</sup>, Erica Sitas<sup>2</sup>, Inesria Saadi<sup>1</sup>, Siba Ajmal<sup>1</sup>, Iram Mushtaq<sup>3</sup>, Taher Ad<sup>4</sup>, Hussain M. Waleed<sup>5</sup>, Wajiba Khan<sup>6</sup>, Uzma Khan<sup>6</sup>, Mariam Amjad<sup>6</sup>, Anesha Sultan<sup>6</sup>, Iram Murtaza<sup>7</sup>

Received: 24 January 2020 / Accepted: 2 August 2020  
© Springer Science + Business Media B.V. 2020

### Abstract

Exposure to environmental toxicants such as Bisphenol A (BPA) has raised serious health concerns globally particularly in developing countries. It is ubiquitously used in the manufacturing of canned food and drinking bottles. BPA generated reactive oxygen species can lead to several diseases including cardiovascularity. However, the endpoints stimulated in BPA cardiotoxicity yet need to be investigated. The current study was aimed to investigate the underlying molecular pathways which may contribute in revealing the protective effects of *Pistacia integerrima* against BPA induced oxidative stress. The dose of 100 µg/kg BW of BPA, 200 mg/kg BW *P. integerrima*, and 4 mg/kg BW melatonin was administered to Sprague-Dawley rats. Present marks of western blotting and qRT-PCR showed the increased expression of p53, PUMA and Dep1, while downregulation of Ubc13 in heart tissues of BPA treated group whereas the levels were reversed upon treatment with *P. integerrima*. The role of BPA in heart tissue apoptosis was further confirmed by the increased level of p-p53, cytochrome C and disrupted cellular architecture whereas the *P. integerrima* has shown its ameliorative potential by mitigating the adverse effects of BPA. Moreover, the oxidant, antioxidant, lipid and liver markers profile has also revealed the therapeutic potential of *P. integerrima* by maintaining the levels in the normal range. However, melatonin has also manifested the normalized expression of apoptotic markers, biochemical markers, and tissue architecture. Conclusively, the data suggest that *P. integerrima* may be a potential candidate for the treatment of BPA induced toxicity by normalizing the oxidative stress through Ubc13/p53 pathway.

**Electronic supplementary material** The online version of this article (<https://doi.org/10.1007/s10240-020-1004-4>) contains supplementary material, which is available to authorized users.

✉ Ines Murtaza  
inesm199@uoi.edu.pk

<sup>1</sup> Signal Transduction Lab, Department of Biochemistry, Faculty of Biological Sciences, Quaid-i-Azam University, H-8, Islamabad 45320, Pakistan

<sup>2</sup> Department of Biological Sciences, National University of Medical Sciences, F-7/3 H-8, Islamabad 45500, Pakistan

<sup>3</sup> Department of Biochemistry, COMSATS University, Islamabad, Abbottabad Campus, Abbottabad, Pakistan

<sup>4</sup> Faculty of Biological Sciences, Theraa University, Marouf, KFE, Pakistan

<sup>5</sup> Department of Biochemistry, Faculty of Biological Sciences, Quaid-i-Azam University, Islamabad 45320, Pakistan

Published online: 21 August 2020





## Melatonin abated Bisphenol A-induced neurotoxicity via p53/PUMA/Drp-1 signaling

Ayesha Ishaq<sup>1</sup> · Tahir Ali<sup>1,2</sup> · Athia Kahkhar<sup>1</sup> · Rubina Bibi<sup>1</sup> · Kiran Bibi<sup>1</sup> · Iram Muhsin<sup>1</sup> · Shupeng Li<sup>3</sup> · Waqar Khan<sup>4</sup> · Uzma Khan<sup>5</sup> · Rifat Ayesha Aris<sup>6</sup> · Mariam Anwar<sup>7</sup> · Amosa Sulhan<sup>8</sup> · Iram Nurhaza<sup>9</sup>

Received: 31 May 2020 / Accepted: 13 December 2020

© The Author(s), under exclusive license to Springer-Verlag GmbH, part of Springer Nature 2021

### Abstract

Bisphenol A (BPA), an endocrine disruptor, is widely used in the manufacture of different daily life products. Accumulating evidence supports the association between the increasing incidence of neurodegenerative diseases and the BPA level in the environment. In the present study, we aimed to evaluate the neuroprotective role of melatonin against BPA-induced mitochondrial dysfunction-mediated apoptosis in the brain. Hence, adult Sprague-Dawley rats were administered (subcutaneously) with BPA (100 µg/kg BW, 1 mg/kg BW, and 10 mg/kg BW) and melatonin (4 mg/kg BW) for 16 days. Our results showed BPA exposure significantly increased the oxidative stress as demonstrated by increased free radicals (ROS), TBARS level, disrupted cellular architecture, and decreased antioxidant enzymes including SOD, CAT, APX, POD, and GSH levels. Additionally, BPA treatment increased the expression of PUMA, p53, and Drp-1 resulting in apoptosis in the brain tissue of rats. However, melatonin treatment significantly abated BPA-induced toxic effects by scavenging ROS, boosting antioxidant enzyme activities, and interestingly, averted brain apoptosis by normalizing p53, PUMA, and Drp-1 expressions at both transcriptional and translational level. Moreover, the brain tissue histology also revealed the therapeutic potential of melatonin by normalizing the cellular architecture. Conclusively, our finding suggests that melatonin could avert oxidative stress and mitochondrial dysfunction-linked apoptosis, producing its neuroprotective potential against BPA-induced toxicity.

**Keywords** BPA · Melatonin · Neurotoxicity · p53 · Mitochondrial dysfunction · Oxidative stress

### Introduction

Bisphenol A (BPA) is a synthetic chemical produced in large volumes worldwide. BPA is released from the commercial products including food cans, food containers, water containers, plastic water bottles, and baby bottles, and enters into the food enhancing the chances of BPA exposure to humans (Harris-Estrada et al. 2014; Fattore and Cirillo 2018). The most commonly consumed isobutylene of Bisphenol A molecule Bisphenol-o-oxymene, BPA glycidic acid, 4-methyl-2, and 4-hex (p-hydroxyphenyl) pent-3-ene. These metabolites are the source of reactive oxygen species (ROS). Increased cellular levels of ROS cause damage to macromolecules, cell membranes, and organelles, which ultimately leads to the activation of cell death processes such as apoptosis (Radu-Domulea and Averil-Bates 2016). BPA-induced ROS over-whelms the antioxidant defense system that leads to oxidative stress, which in turn participates in the pathogenesis of numerous diseases including diabetes, thyroid oxidative damage, reproductive disorders, and neurological abnormalities.

Responsible Editor: Mohamed M. Abd-Elgawad.

Iram Muhsin  
iamuhsin@spau.edu.pk

<sup>1</sup> Signal Transduction Laboratory, Department of Biochemistry, Faculty of Biological Sciences, Quaid-e-Azam University, Islamabad-45320, Pakistan

<sup>2</sup> State Key Laboratory of Deep-sea Geochemistry, School of Chemical Biology and Biotechnology, Peking University Shenzhen Graduate School, Shenzhen, China

<sup>3</sup> Department of Biotechnology, CHINA STATE UNIVERSITY, Shenzhen Campus, Shenzhen, P.R. China

<sup>4</sup> Faculty of Biological Sciences, Huzhou University, Huzhou, K.P.S., Pakistan

<sup>5</sup> Institute of Theoretical and Mathematical Sciences, The University of Lahore, Islamabad Campus, Islamabad, Pakistan

<sup>6</sup> Department of Biochemistry, Faculty of Biological Sciences, Quaid-e-Azam University, Islamabad-45320, Pakistan

Published online: 03 January 2021

Springer



## A cohort study investigating the role of Bisphenol A in the molecular pathogenesis of breast cancer

Ayesha Ishaq<sup>1</sup> · Maryam Ayyat Nasrullah<sup>2</sup> · Jahangir Sarwar Khan<sup>2</sup> · Sani Malik<sup>2</sup> · Usman Taseer<sup>3</sup> · Mariam Anwar<sup>4</sup> · Anousha Sultan<sup>5</sup> · Iram Murazaq<sup>6</sup>

Received: 28 May 2021 / Accepted: 23 August 2021  
© The Author(s), under exclusive license to Springer-Verlag GmbH Germany, part of Springer Nature 2022

### Abstract

**Background** Breast cancer is an abnormal division of breast cells. Bisphenol A (BPA), an environmental toxicant, is identified as an emerging risk factor for breast cancer development. However, to the best of our knowledge, no previous study has investigated the BPA levels in breast cancer patients in Pakistan. The present study sought to explore the role of BPA in tumor growth among the Pakistani population.

**Methods** The levels of BPA were analyzed in the serum samples of breast cancer patients and controls by using HPLC. To elucidate the role of BPA in tumor formation, events in breast tissue different biochemical assays along with expression analysis of tumor markers were performed.

**Results** The level of BPA in the serum samples of breast cancer patients was significantly higher than controls. Histological analysis of breast cancer tissue samples revealed distinct subtypes of tumor such as ductal carcinoma in situ (DCIS) and invasive ductal carcinoma (IDC). There was a significant increase in ROS level while a significant decrease in the levels of superoxide dismutase (SOD) and catalase (CAT) enzymes in malignant breast tissue samples as compared to control tissue samples. We found upregulated expression of p53, ZEB1 and WNT1 genes in mRNA level in malignant breast tissue samples by 13 folds, 78 folds and 25 folds respectively. p53 protein expression in malignant breast tissue sample was also enhanced at the transcriptional level.

**Conclusion** Current findings suggest a relationship between BPA and the progression of breast cancer among the Pakistani population.

**Keywords** Bisphenol A · Pakistan · Environmental toxicant · Breast cancer · Oxidative stress

### Abbreviations

BPA	Bisphenol A	SOD	Superoxide dismutase
EDC	Endocrine-disrupting chemical	CAT	Catalase
DCIS	Ductal carcinoma in situ	ROS	Reactive oxygen species
IDC	Invasive ductal carcinoma	ZEB1	Zinc finger E-box binding protein 1
		EMT	Epithelial to mesenchymal transition
		EPA	Environmental protection agency
		WWF	World Wide Fund for nature
		HPLC	High-performance liquid chromatography

- ✉ Ayesha Ishaq  
ayesha@pcr.edu.pk
- Mariam Ayyat Nasrullah  
mariam@pcr.edu.pk
- Iram Murazaq  
iram@pcr.edu.pk

- <sup>1</sup> Serum Toxicology Laboratory, Department of Biochemistry, Quaid-i-Azam University Islamabad, Islamabad 45320, Pakistan
- <sup>2</sup> Karolinkh Medical University, Karolinkh, Pakistan
- <sup>3</sup> Department of Biochemistry, Quaid-i-Azam University Islamabad, Islamabad 45320, Pakistan

### Introduction

Breast cancer is considered as a complex pathogenesis and multiplication of cells in the breast tissue (Khanjari and Akbari 2019). Breast cancer has now taken over lung cancer as the most frequently detected form of cancer among women worldwide (Sung et al. 2021). In 2020, approximately 2,200,000 (2.2 million) new cases of female breast